IDENTIFICATION AND CHARACTERIZATION OF LAYILIN, A TALIN-BINDING TRANSMEMBRANE PROTEIN

MARK LEE BOROWSKY

A.B. HARVARD UNIVERSITY, 1989

SUBMITTED TO THE DEPARTMENT OF BIOLOGY IN PARTIAL FULFILLMENT OF THE REQUIREMENTS FOR THE DEGREE OF

DOCTOR OF PHILOSOPHY

AT THE
MASSACHUSETTS INSTITUTE OF TECHNOLOGY

FEBRUARY 1999

SIGNATURE OF AUTHOR: _____
DEPARTMENT OF BIOLOGY
NOVEMBER 13, 1998

CERTIFIED BY: _____
RICHARD O. HYNES
PROFESSOR OF BIOLOGY
THESIS SUPERVISOR

ACCEPTED BY: _____
ALAN GROSSMAN
GRADUATE COMMITTEE CHAIRPERSON
DEPARTMENT OF BIOLOGY

IDENTIFICATION AND CHARACTERIZATION OF LAYILIN, A TALIN-BINDING TRANSMEMBRANE PROTEIN

MARK LEE BOROWSKY

SUBMITTED TO THE DEPARTMENT OF BIOLOGY ON NOVEMBER 13, 1998 IN PARTIAL FULFILLMENT OF THE REQUIREMENTS FOR THE DEGREE OF DOCTOR OF PHILOSOPHY

Abstract

This thesis explores the function of the conserved amino-terminal domain of the cytoskeletal protein talin. This domain of talin is homologous with the band 4.1 superfamily of membrane-cytoskeleton linking proteins. Chapter 2 describes the discovery and initial characterization of a cell-surface protein that I have named layilin. This protein binds to the amino-terminal domain of talin, confirming the decade-old hypothesis that this region of talin contains a membrane binding site. In addition, this discovery enhances the structure-function parallels between talin and other band 4.1 family members. Data show that layilin colocalizes with talin in membrane ruffles, suggesting that layilin anchors talin, and, indirectly, actin, to the plasma membrane in ruffles. The layilin extracellular domain is significantly homologous with C-type lectins, suggesting that layilin may function similarly to selectins or lectin endocytic receptors. The layilin cytoplasmic domain contains three repeated motifs not yet found in other proteins. Two of these motifs form a 10 amino acid talin-binding site, and layilin and FAK bind to overlapping sites within talin's amino-terminal domain. Furthermore, binding between layilin and radixin, another member of the band 4.1 superfamily, is shown. I report an association between talin's amino-terminal domain and focal adhesion kinase (FAK), a signaling molecule involved in cell motility. In chapter 3 my efforts to uncover the function of layilin through dominant-negative and antisense approaches are reported. I believe the discovery of layilin and FAK as talin binding partners represents a signficant advance in our understanding of talin as a membrane-cytoskeleton linker with implications for both cell motility and signaling.

Thesis Supervisor: Richard O. Hynes
Title: Professor of Biology

ACKNOWLEDGEMENTS

I thank my wife Leila for her love, support, and encouragement during my graduate training. Her patience has been an example, her sacrifices an inspiration, and her tolerance of late nights in the lab no longer necessary, I hope. I also wish to express my thanks to my son Jonathan, who arrived just in time to restore my perspective.

Thanks also to my parents, Radine and Ben Borowsky whose unconditional love, enthusiasm, and support have been essential to my progress. I am also appreciative of the love, support, and interest in my work shown by Helen and Bob Haddad.

Thanks to Richard Hynes for guiding and encouraging me during the past 6 years, for providing an excellent training environment, and for giving me the freedom to pursue my (sometimes foolish) ideas.

I wish to acknowledge the contribution of my thesis committee members to the course of this work.

Thanks to all the members of the Hynes' lab. Many have advanced this work, taught me valuable lessons, and made the lab a fun and intellectually-stimulating place to work, especially Grant Wheeler, Laird Bloom, Ed Clark, Mike DiPersio, Gene Huh, Jane Trevithick, and Colleen Leslie.

I also express my gratitude to Etchell Cordero with whom it has been a pleasure to collaborate. My thanks to Frank Solomon for his friendship, advice on science, careers in science, and life.

Among my many congenial classmates, I want to acknowledge friends whose company has made the journey particularly worthwhile: Adam Grancell, Matt and Monicia Elrod-Erickson, Mark Metzstein, and Gillian Stanfield.

Chapter 1

Introduction

The study of cell shape, motility and adhesion is essential to our understanding of numerous aspects of development, physiology and disease. Changes in cell morphology are necessary for fundamental developmental steps such as gastrulation and organogenesis. A fundamental immune function, phagocytosis, requires dramatic changes in cell shape, and normal blood clotting involves platelet shape change (Hartwig and Stossel, 1976; Fox, 1993). Both cell adhesion and motility participate in immunity, development and tumor metastasis (Hynes, 1987; Hynes and Lander, 1992; Lauffenburger and Horwitz, 1996). Moreover, cell adhesion, like shape change, is necessary for hemostasis. Defects in keratinocyte adhesion can lead to a variety of skin blistering diseases (DiPersio et al., 1997; Fuchs and Cleveland, 1998). These cellular behaviors depend on the particular molecules that interface the cell with relevant environmental cues such as extracellular matrix, adjacent cells, or foreign particles. These specialized receptors, in turn, interact with the underlying cytoskeleton which effects requisite architectural changes (Luna and Hitt, 1992). Several parameters of the actin cytoskeleton can be modulated, including net polymerization, extent of crosslinking, and association with membranes (Ayscough, 1998). How actin regulatory proteins coordinate to create various desired cytoskeletal (and hence cellular) structures is not yet known.

This thesis is concerned with the mechanism by which one actin-binding protein, talin, mediates association of F-actin with the plasma membrane. My investigations into talin function have been guided by an understanding of other membrane-actin linkages. In particular, I have been influenced by advances in knowledge of the band 4.1 superfamily of proteins. Talin contains a domain weakly homologous with band 4.1 superfamily members and has an overall structure analogous with this group of proteins. In addition, progress in dissecting the molecular interactions in focal adhesions (or focal contacts), one site of talin subcellular localization, has necessarily affected my thinking on membrane cytoskeleton associations. As such, this introduction reviews briefly recent advances in erythrocyte membrane-cytoskeleton junctions, the site of action of band 4.1, and also relates relevant results regarding ezrin, radixin, and moesin, members of the band 4.1 superfamily. I conclude with an overview of focal contact assembly and a detailed summary of talin structure and function.

The band 4.1 superfamily

The erythrocyte has long been a model for studying membrane cytoskeleton due to the ease of obtaining large numbers of red blood cells (RBCs) and the relatively small number of proteins in purified RBC cytoskeletons. This paradigm has further impact due to the sequence homology between a major element of the RBC cytoskeleton, band 4.1, and several other cytoskeleton-associated proteins (Rees et al., 1990). Motifs in other RBC cytoskeletal elements, particularly spectrin and ankyrin, recur in other proteins as well (Bennett, 1992; Pascual et al., 1997). It remains to be seen how broadly lessons learned from this system can be applied. The band 4.1 superfamily includes talin, ezrin/radixin/moesin (the ERM family), merlin, EM10, and two protein tyrosine phosphatases (Gould et al., 1989; Frosch et al., 1991; Funayama et al., 1991; Gu et al., 1991; Lankes and Furthmayr, 1991; Yang and Tonks, 1991; Rouleau et al., 1993; Trofatter et al., 1993). These proteins are related by sequence homology in their amino-terminal domains, which corresponds to the 30 kD domain of band 4.1 (Rees et al., 1990).

Band 4.1 and the erythrocyte cytoskeleton

Recent work on the erythrocyte membrane-cytoskeleton linkage offers new insights into the nature and mechanism of membrane-cytoskeleton attachments. The erythrocyte plasma membrane is supported by a cytoskeleton consisting of spectrin tetramers connected to the erythrocyte plasma membrane by two known means (reviewed in Bennett and Gilligan, 1993). Ankyrin binds spectrin near the middle of the tetramer and associates with the cytoplasmic domain of the anion exchanger (band 3) in the membrane (Bennett and Stenbuck, 1979). Ankyrin can also bind to cytoplasmic sequences of the sodium-potassium ATPase and of CD44, a hyaluronic acid receptor (Nelson and Veshnock, 1987; Kalomiris and Bourguignon, 1988). The ends of the spectrin tetramer are bound by band 4.1, which in turn binds the cytoplasmic domain of one or more glycophorin isoforms in the red cell membrane (Anderson and Lovrien, 1984). Spectrin tetramer ends also associate with short actin filaments which are thought to serve as a hub connecting several spectrin tetramers (Bennett and Gilligan, 1993). Deficiencies in protein 4.1, glycophorin, and other components of this spectrin cytoskeleton result in abnormally shaped and fragile erythrocytes (Tchernia et al., 1981; Agre et al., 1985).

Band 4.1 participates in several interesting protein-protein interactions which contribute to erythrocyte morphology. Based on the observation that binding of exogenous lectins to glycophorins blocks erythrocyte shape changes, it was hypothesized that glycophorins were linked to the red blood cell cytoskeleton (Anderson and Lovrien, 1981). Binding of protein 4.1 to inside-out erythrocyte membranes and to purified glycophorin C confirmed that such an association was possible, and the finding that anti-glycophorin antibodies significantly inhibited band 4.1 binding to RBC membranes indicates that glycophorin C is the major membrane binding site for band 4.1 (Anderson and Lovrien, 1984; Anderson and Marchesi, 1985; Workman and Low, 1998). This association was found to be mediated by a 30 kD amino-terminal proteolytic fragment of band 4.1 and 17 membrane-proximal amino acids in the glycophorin cytoplasmic domain (Hemming et al., 1995; Marfatia et al., 1995). Mutation of three basic residues found at the junction between the transmembrane and cytoplasmic domains in glycophorin blocks binding to band 4.1 (Marfatia et al., 1995). Phospholipids are able to regulate this interaction, as binding between band 4.1 and glycophorin is enhanced in the presence of polyphosphoinositols (Anderson and Marchesi, 1985).

Membrane-associated guanylate kinase (MAGUK) proteins also bind to both glycophorin C and band 4.1, possibly forming a ternary complex (Lue et al., 1994; Marfatia et al., 1994). MAGUK proteins typically contain one or more PDZ motifs, an SH3 domain, and a domain homologous with guanylate kinase catalytic domains. PDZ motifs can bind to extreme carboxy-terminal residues in the cytoplasmic domains of some membrane proteins, while SH3 domains bind to proline-rich sequences (Ren et al., 1993; Saras and Heldin, 1996). At present, the role of the putative guanylate kinase domain in formation of the erythrocyte cytoskeleton is unclear. Studies have delineated binding interfaces between band 4.1 and two MAGUK proteins: p55, and the product of the human homolog of the *Drosophila* tumor suppressor gene *discs large* (hdlg). The conserved 30 kD domain of band 4.1 binds to short runs of basic amino acids found in p55 and hdlg (Lue et al., 1994; Marfatia et al., 1994; Marfatia et al., 1995; Lue et al., 1996). The p55 PDZ domain binds to the C-terminal sequence YFI in the glycophorin cytoplasmic domain (Marfatia et al., 1997). Although the PDZ domains of hdlg were not able to bind glycophorin C, they were shown to bind to the cytoplasmic domain of the Shaker-type potassium channel (Marfatia et al., 1996; Marfatia et al., 1997). This raises the possibility that band 4.1 can bind indirectly through hdlg to this ion channel; the association of band 4.1

superfamily members with ion channels and exchangers appears to be an emerging theme for this group of proteins. The discovery that PDZ-containing protein CASK binds to band 4.1 and to the cytoplasmic domain of syndecan-2, a heparan sulfate proteoglycan, suggests that PDZ domain proteins may associate with band 4.1 in diverse membrane-cytoskeleton assemblies (Cohen et al., 1998; Hsueh et al., 1998). A second PDZ-containing protein has been reported to bind the carboxy-terminal YFA motif in syndecans (Grootjans et al., 1997). A PDZ domain protein also has been found to bind merlin and ERM family members (discussed below; Reczek et al., 1997; Murthy et al., 1998)

Band 4.1 can bind to the cytoplasmic domain of the erythrocyte anion exchanger (Pasternack et al., 1985). Binding between purified proteins has been demonstrated, and binding of band 4.1 to RBC membranes can be blocked by antibodies to the anion exchanger cytoplasmic domain (Pasternack et al., 1985, for contradictory results see Workman and Low, 1998). A five amino acid motif (LRRRY) in the anion exchanger cytoplasmic domain was found to bind a 5 amino acid motif bearing complementary charges (LEEDY) in the band 4.1 30 kD domain (Jöns and Drenckhahn, 1992). Disruption of band 4.1-anion exchanger complexes by IRRRY peptides leads to increased rigidity in resealed ghosts (An et al., 1996). Perhaps band 4.1 binding to the anion exchanger competes spectrin-ankyrin complexes from the same membrane-binding sites, resulting in a qualitatively different cytoskeleton. Alternatively, the ratio of membrane attachment of the central domain of spectrin (i.e. through ankyrin) to membrane attachment of spectrin ends (i.e. through band 4.1) may affect erythrocyte cytoskeleton rigidity. Band 4.1 also may regulate other ankyrin-membrane interactions as binding of ankyrin to CD44 is inhibited if band 4.1 is prebound to CD44 (Nunomura et al., 1997).

The ERM family

Three closely related band 4.1 superfamily members form the ezrin/radixin/moesin family of proteins. While the biological functions of this family of proteins have not been precisely determined, the biochemical role of these proteins as membrane-cytoskeleton linkers is supported by increasing evidence. The family consists of the three proteins which give their names to the family (ezrin, radixin, and moesin), and will be discussed along with merlin, the product of the neurofibromatosis type II tumor suppressor gene (Bretscher, 1983; Tsukita et al.,

1989; Lankes and Furthmayr, 1991; Rouleau et al., 1993; Trofatter et al., 1993; Edwards et al., 1994). These proteins are related by high homology in their amino-terminal 300 amino acids and significant, but lower homology in the remaining carboxy-terminal sequences (Takeuchi et al., 1994a). Based on the similarity of their N-terminal domains to the membrane-binding domain of band 4.1, this domain was proposed to contain membrane binding activity, while the C-terminal sequences are predicted to be rich in α-helix (Rees et al., 1990; Funayama et al., 1991; Lankes and Furthmayr, 1991). This overall structure is quite similar to that of talin (discussed below, and figure 1-4A). ERM proteins are believed to contribute to the structure of cortical actin cytoskeleton. Ezrin was originally identified as a component of isolated microvilli, and radixin was purified from liver adherens junctions (Bretscher, 1983; Tsukita et al., 1989). In addition, ezrin, radixin, and moesin have been detected in cortical structures such as microvilli, membrane ruffles, cleavage furrows, growth cones, and the erythrocyte marginal band (Bretscher, 1983; Birgbauer and Solomon, 1989; Goslin et al., 1989; Tsukita et al., 1989; Berryman et al., 1993; Franck et al., 1993; Henry et al., 1995). The NF2 tumor suppressor protein, merlin, also localizes in peripheral actin structures (den Bakker et al., 1995; Gonzalez-Agosti et al., 1996; Xu et al., 1998).

ERM function

Several studies have addressed directly the functions of ERM proteins. Ezrin, radixin, and moesin were selectively depleted from cells by treatment with antisense oligonucleotides specific for each protein. Cell-substrate adhesion was disrupted when adherent cells were cultured with a mixture of antisense oligonucleotides such that cells had very little ezrin, radixin or moesin (as assessed by western blotting). Antisense suppression of radixin, and to a lesser extent ezrin, inhibited *de novo* adhesion and spreading of cells, while cells with reduced amounts of moesin adhered and spread normally. Similarly, cell-cell adhesion was reduced in cells lacking ezrin or radixin, but not moesin. In the absence of all three proteins, thymoma cells lost prominent membrane elaborations (mostly microvilli and ruffles;Takeuchi et al., 1994b). This antisense study demonstrated a specific effect of each antisense oligonucleotide on the levels of ezrin, radixin, and moesin; nonspecific effects of oligonucleotides were controlled for with equal levels of appropriate sense oligonucleotides. While reports differ on the presence of these three proteins in focal contacts, these effects on cell-substrate adhesion

strongly suggest ERM proteins play either a direct or indirect role in both establishing and maintaining cell-substratum adhesion. A potential role for ERMs in adhesion-associated cytoskeletal change was revealed by Mackay et al. (1997) who found that purified moesin, but not radixin or ezrin, can restore rho-dependent stress fiber and focal contact formation to detergent-extracted cells. Similarly, ablation of ezrin by micro chromophore assisted laser inactivation (micro CALI) results in collapse of membrane ruffles and disruption of cell-matrix adhesion (Lamb et al., 1997). Transfection of ezrin was found to alter T-cell morphology by stimulating the formation of uropods; this corresponded with sensitivity of the T-cells to lysis by natural killer cells (Helander et al., 1996). Endogenous ezrin, radixin, and moesin are concentrated in uropods where they colocalize with several cell-cell adhesion molecules, (ICAM-1,2,3, CD43, and CD44), which may recruit NK or other lymphocytes to damaged tissues (Yonemura et al., 1993; Tsukita et al., 1994; del Pozo et al., 1995; Sainio et al., 1997; Legg and Isacke, 1998; Serrador et al., 1998). Interestingly, the myosin ATPase inhibitor butanedione monoxime blocks uropod formation, suggesting that this process may require contraction (del Pozo et al., 1995; Serrador et al., 1998).

ERM protein-protein interactions

The role of ERM proteins as membrane-cytoskeleton linkers is supported by observed binding between ERMs and the cytoplasmic domains of cell adhesion molecules. CD44 was found to be the major protein coimmunoprecipitating with ezrin, radixin, and moesin from surface-labeled extracts of baby hamster kidney cells, and chimeric membrane proteins containing the CD44, CD43, or ICAM-2 cytoplasmic domain were also coimmunoprecipitated with ERMs (Tsukita et al., 1994; Yonemura et al., 1998). Endogenous CD43 also coimmunoprecipitates with ezrin and moesin (Serrador et al., 1998). GST fusion proteins containing the cytoplasmic domains of these receptors are also able to bind ezrin, radixin and moesin *in vitro* (Hirao et al., 1996; Legg and Isacke, 1998; Serrador et al., 1998; Yonemura et al., 1998). The binding sites for ERM proteins were mapped to short runs of basic amino acids found at the junction of the transmembrane and cytoplasmic domains in CD43, CD44 and ICAM-2 (Legg and Isacke, 1998; Yonemura et al., 1998). The significance of these binding sites is unclear, however, as one study found that the membrane-proximal basic amino acids were required for colocalization with ERMs of chimeric receptors bearing CD43, CD44 and

ICAM-2 cytoplasmic domain, but in another study, mutation of this binding site in the context of full length CD44 had no effect on either its subcellular localization or on that of ERM proteins (Legg and Isacke, 1998). It is indeed difficult to account for any degree of specificity of binding between ERM proteins and membrane-apposed basic residues as such motifs are common in transmembrane proteins. In chapter 2, an alternative mechanism of binding between radixin and a membrane protein is presented.

Consistent with the analogy drawn from band 4.1, the membrane binding interface in ERM proteins is localized in the amino-terminal region homologous with band 4.1. Transfection of individual ezrin domains revealed that the N-terminal domain associates with the plasma membrane, and the C-terminal domain binds cytoskeleton (Algrain et al., 1993). Hirao et al. (1996) found that the purified N- but not C-terminal domain of moesin was sufficient for binding to a GST-CD44 cytoplasmic domain fusion protein. Several other proteins have been reported to bind ERM amino-terminal domains. One of the most provocative findings is the interaction of the Na^+/H^+ exchanger regulatory factor (NHE-RF) with ezrin, radixin, moesin, and merlin N-terminal domains (Reczek et al., 1997; Murthy et al., 1998). This protein was discovered by virtue of its ability to bind to and confer protein kinase A regulation on the Na^+/H^+ exchangers NHE1 and NHE3 (Weinman et al., 1993; Weinman et al., 1995; Yun et al., 1997). NHE-RF colocalizes with ERMs in cortical actin structures in cells and tissues (Reczek et al., 1997; Murthy et al., 1998). NHE-RF may bridge ERMs and NHE1, serving indirectly as a membrane docking site for ERMs, although colocalization of NHE1 with ERMs has not been documented. Perhaps the association of band 4.1 with the erythrocyte anion exchanger is enhanced by a similar accessory protein. The guanine dissociation inhibitor for rho, rhoGDI, also binds the N-terminal domain of ERMs, and this association can activate rho signaling (Hirao et al., 1996; Takahashi et al., 1997). Myosin light chain phosphatase has also been reported to bind moesin N-terminal domain and dephosphorylate one or more sites in the moesin C-terminal domain (Fukata et al., 1998). Potential consequences of ERM phosphorylation will be discussed below.

The carboxy-terminal domains of ezrin, radixin and moesin have been found to bind to F-actin, consistent with the observed colocalization of this ERM fragment with actin filaments in living cells (Algrain et al., 1993; Gary and Bretscher, 1995; Henry et al., 1995; Turunen et al., 1994). The carboxy-terminal domain of merlin, which lacks the consensus actin-binding

domain present in ezrin, radixin, and moesin, binds spectrin in a yeast two-hybrid assay (Scoles et al., 1998). If this observation is confirmed, merlin would share amino-terminal domain binding partners with ezrin, radixin, and moesin and carboxy-terminal binding partners with band 4.1, underscoring the modular nature of these interactions.

Regulation of ERMs

The amino- and carboxy-terminal domains of ERM proteins interact with each other, providing a means to regulate binding of ERMs to their varied partners. This type of regulation was suggested by the observation that co-expression of N- and C-terminal domains of ezrin together in cells inhibits the elaboration of actin-rich cell processes induced by misexpression of the C-terminus alone (Martin et al., 1995). Similar actin-rich structures were seen in cells overexpressing radixin C-terminal domain; the inability of overexpressed full-length radixin to stimulate such processes suggests that the amino-terminal domain can exert influence over the carboxy-terminal domain (Henry et al., 1995). In addition, Henry et al. (1995) found that overexpressed radixin C-terminal domain can disrupt cytokinesis whereas full length radixin does not. This regulation can be attributed to binding between N- and C-terminal domains, which has been demonstrated with purified fragments *in vitro* (Gary and Bretscher, 1995; Magendantz et al., 1995). Just as the above misexpression experiments, as well as *in vitro* actin binding assays, demonstrate regulation of carboxy-terminal binding activities by amino-terminal domains, additional studies reveal the regulation of amino-terminal binding activities by carboxy-terminal sequences. Competitive binding experiments indicate that association of NHE-RF or ezrin C-terminal domain with ezrin's N-terminal domain is mutually exclusive (Reczek and Bretscher, 1998). The same appears to be true for the interaction of radixin with NHE-RF (E. Cordero and F. Solomon, personal communication).

Association between ERM N- and C-terminal domains, and hence their availability for binding to appropriate interactors, may be regulated by two mechanisms. Inositol phospholipids enhance the association of intact ezrin, radixin and moesin with the CD44 cytoplasmic domain at physiological salt concentrations, but do not increase CD44 binding to N-terminal domains (Hirao et al., 1996). Binding of full-length radixin to NHE-RF is also increased in the presence of acidic phospholipids (E.Cordero and F. Solomon, personal

communication). Phospholipid-regulated binding of radixin with another membrane protein is described in chapter 2. These effects may result from phospholipid inhibition of binding between radixin N- and C-terminal domains (E.Cordero and F. Solomon, personal communication). Evidence for a phospholipid-regulated intradomain interaction within the radixin N-terminal domain also exists (E.Cordero and F. Solomon, personal communication). Alternatively, ERM interdomain interactions may be regulated by phosphorylation. Phosphorylation of a C-terminal threonine residue in ezrin, radixin, and moesin blocks interaction of the N- and C-terminal domains, exposing the C-terminal actin binding site (Matsui et al., 1998). This observation is consistent with reported regulation of ERM subcellular localization in response to phosphorylation (Bretscher, 1989; Shaw et al., 1998). Constitutively active rho drives ERM proteins into cortical actin structures such as microvilli, while treatment of cells with C3 toxin, which inactivates rho, blocks LPA-stimulated relocation of ERM proteins into these structures (Kotani et al., 1997; Shaw et al., 1998). Rho-kinase may mediate the effect of rho on ERM localization by phosphorylating the C-terminal threonine, potentiating interactions of N- and C-terminal domains with their respective binding partners (Matsui et al., 1998). Protein kinase C-θ also has been shown to phosphorylate this threonine in the presence of inositol phospholipids (Pietromonaco et al., 1998). The actions of rho-kinase may be countered by myosin light chain phosphatase, which can dephosphorylate rho-kinase-phosphorylated moesin *in vitro* (Fukata et al., 1998). Identification of the PIP-binding site, and mutagenesis of it and the C-terminal threonine may clarify the physiological roles of these potential regulatory mechanisms.

Overall, ERMs appear to behave much as does band 4.1, binding membrane proteins through their amino-terminal domains and cytoskeleton with their carboxy-terminal domains. They can bind cytoplasmic domains of membrane proteins directly, and potentially indirectly through NHE-RF. The latter interaction, like the hdlg-glycophorin interaction, might be mediated by PDZ modules. Moreover, the binding between these cytoskeleton proteins and their membrane docking sites is enhanced by phospholipids.

Focal contacts as a model membrane-cytoskeleton linkage

Focal contacts (or focal adhesions) contain protein complexes which connect actin cytoskeleton to extracellular matrix. The physiological significance of focal adhesions is

controversial because they are rarely seen *in vivo*. Structures which resemble focal contacts somewhat have been reported in tendon cells of the myotendonous junction (Damsky et al., 1985; Tidball et al., 1986; Turner et al., 1991). In contrast, focal contacts are found in a wide range of cell types when grown in culture. These data are best interpreted to mean that focal contacts are formed in cells experiencing mechanical tension (Burridge, 1981). Tendon cells experience physical stress in the course of their normal function, whereas cells cultured *in vitro* tend to pull against a solid support – typically glass or plastic. A growing body of data supports the view that the components of focal contacts are the genuine mediators of actin-ECM linkages *in vivo,* and that focal contacts are an exaggerated form of an *in vivo* structure resulting from the physical conditions of tissue culture. Hence the protein complexes linking membrane and cytoskeleton may be the same regardless of the size of the contact zone. In living tissue, cell-matrix contacts may be diffusely arrayed over all of the surfaces of the cell which are in contact with the substrate. In cultured cells, "focal complexes" – punctate clusters of focal contact proteins which are smaller than focal contacts – may be a better approximation of *in vivo* cell matrix adhesions (Hotchin and Hall, 1995; Nobes and Hall, 1995; Clark et al., 1998). These small clusters of adhesions become aggregated into large, dash-shaped structures (i.e. focal contacts) by an unknown mechanism. As actin filaments are bundled into stress fibers, adhesion complexes at their termini may be drawn together into patches. Some evidence supports the proposal that this occurs as the result of myosin-driven F-actin contraction, although the existence of focal contacts in the absence of detectable clustering of F-actin into bundles (also known as stress fibers) has not been reconciled with this point of view (Burridge and Chrzanowska-Wodnicka, 1996; Chrzanowska-Wodnicka and Burridge, 1996).

In cultured cells, actin cytoskeleton and focal contacts are disrupted by oncogenic transformation; hence, it is hoped that study of these structures will impact cancer biology (Pollack et al., 1975). Indeed, it is possible that the normal role for one of the most actively studied proto-oncogenes, c-src, may be in regulating cell spreading (Rohrschneider and Rosok, 1983; Kaplan et al., 1995). Moreover, transfection of various transformed cell lines with focal contact proteins can restore cells to an untransformed phenotype (Ali et al., 1977; Giancotti and Ruoslahti, 1990; Rodriguez Fernandez et al., 1992). Understanding the etiology of stress fibers and focal contacts will likely advance our knowledge of actin dynamics and cytoskeletal

morphogenesis. Absent insight into the origins of these *in vitro* structures, we can study focal contact components and their interactions with each other, the membrane, matrix, and cytoskeleton as a way to inform our understanding of membrane-cytoskeleton associations in general.

Focal contacts coincide with the ends of stress fibers and align with fibrils of extracellular matrix proteins. Extracellular matrix supports focal contact formation, reflecting the ubiquitous presence of integrins, the major class of ECM receptors, in focal contacts. Binding between integrins and their ligands is likely responsible for the close apposition between the plasma membrane and the substratum seen in focal contacts. One member of the syndecan family, a class of integral membrane proteins, syndecan-4, is reported to be in focal contacts (Woods and Couchman, 1994). Syndecans are capable of binding to heparin-binding domains of some ECM molecules, but a requirement for these heparan-sulfate proteoglycans in cell adhesion has not been demonstrated (Saunders and Bernfield, 1988). The other protein components in focal contacts are typically divided into two groups, cytoskeleton-associated proteins and signaling molecules. This reflects the two known biological functions of cell adhesion: providing physical integrity to tissues and regulating diverse aspects of cell physiology. However, reports of binding between signaling and cytoskeletal proteins blur this distinction, and our lack of knowledge about the function of many focal contact proteins makes their classification according to such a scheme somewhat arbitrary. Most likely, adhesive signaling acts proximally to regulate membrane-cytoskeleton linkages and distally to modulate gene expression, cell cycle, and apoptosis.

Getting hitched

The physical connection between integrins and actin may be achieved in several ways through associations among numerous actin-binding proteins present in focal contacts. Integrin cytoplasmic domains can bind *in vitro* to talin and α-actinin, both of which can bind directly to F-actin (Burridge and Feramisco, 1981; Horwitz et al., 1986; Muguruma et al., 1990; Otey et al., 1990). In addition, talin and α-actinin have both been reported to bind to vinculin, which can bind to F-actin and tensin, yet another actin-binding protein (Burridge and Mangeat, 1984; Wachsstock et al., 1987; Johnson and Craig, 1995a). Thus two potential ways to link integrins to the actin cytoskeleton are integrin-talin-vinculin-tensin-actin (with the

potential for direct links to actin by talin and vinculin as well) and integrin-α-actinin-actin. These models are not mutually exclusive, and still other ways to link actin to the membrane in focal contacts may yet be discovered.

Regulation of vinculin-talin and vinculin-actin binding is an interesting example of how signaling metabolites can alter cytoskeletal structure. Phosphatidyl-inositol-phosphates (PI-4-P and PI-4,5-P_2) stimulate the interconversion of vinculin between two binding states (Johnson and Craig, 1994; Johnson and Craig, 1995a; Johnson and Craig, 1995b; Gilmore and Burridge, 1996). In the absence of phospholipid, vinculin exhibits little F-actin or talin binding, whereas, in the presence of acidic phospholipids, vinculin readily binds these cytoskeletal partners. These binding activities were inversely correlated with intramolecular association between vinculin's N- and C-terminal domains. Vinculin's N-terminal domain alone exhibited high levels of talin binding independent of phospholipid and the C-terminal domain bound F-actin readily even in the absence of polyphosphoinositides (Gilmore and Burridge, 1996). Excess N- or C-terminal domain competes with talin and actin for binding to the other half of vinculin. The classical second messenger PI-4,5-P_2, generally thought of as a precursor (via the action of phospholipase C) of diacyl-glycerol and IP_3 (which mobilize intracellular Ca^{2+} and activate PKC) is here used as a trigger to cause directly a conformational change in a cytoskeletal protein. This mode of regulation is analogous to that described above for ERMs.

Less is known about the specific contributions many other focal contact proteins. Members of the ezrin/radixin/moesin family have been detected in focal contacts, and a role for them in cell-matrix adhesion is suggested by the inhibitory effect of antisense ERM oligonucleotides on cell adhesion (Sato et al., 1992; Takeuchi et al., 1994b). Two additional cytoskeleton-associated proteins found in focal contacts, mammalian enabled (MENA) and vasodilator-stimulated phosphoprotein (VASP) may stimulate actin polymerization either directly or through associations with profilin (Reinhard et al., 1992; Reinhard et al., 1995; Gertler et al., 1996). Taken together, the proteins found in focal contacts constitute a multiprotein mechanism with biochemical properties necessary to stimulate the formation of F-actin filaments and to link them to the plasma membrane. These properties can account for the ability of actin cytoskeleton to confer mechanical stability on tissues.

Three focal contact proteins which at present might be classified as either structural or signaling contain LIM domains. Zyxin was identified as the antigen recognized by a

nonimmune antiserum which stains focal contacts, and it was subsequently found to bind α-actinin in gel overlay experiments (Crawford and Beckerle, 1991; Pavalko and Burridge, 1991; Crawford et al., 1992; Sadler et al., 1992). Fragments of zyxin can translocate to the nucleus, raising the intriguing possibility that this, and perhaps other LIM-domain proteins, relay signals by shuttling directly from focal contacts to the nucleus (Nix and Beckerle, 1997). Zyxin and another focal contact protein, cysteine-rich protein (CRP) associate through their LIM domains (Sadler et al., 1992). No specific biological function has been demonstrated for paxillin, the most studied LIM-domain protein in focal contacts (Turner et al., 1990; Turner and Miller, 1994). Paxillin binds numerous focal contact proteins including vinculin and talin and is a candidate substrate for FAK (Turner and Miller, 1994; Hildebrand et al., 1995; Salgia et al., 1995). Paxillin tyrosine phosphorylation increases in parallel with FAK kinase activity after cells adhere to integrin ligands (Burridge et al., 1992). LIM domain 3 is required for efficient focal contact targeting of this protein, but no binding partners have been found for paxillin's LIM domains (Brown et al., 1996). Binding sites for vinculin, FAK and talin map outside of the LIM domains (Salgia et al., 1995; Brown et al., 1996). Paxillin is tyrosine phosphorylated, and may therefore bind to SH2 domains of numerous proteins; since it also can bind to several other focal contact proteins, it has been suggested that paxillin acts as an adaptor linking focal contact proteins with signaling pathways.

Adhesion and signaling

The complex topic of cell-matrix adhesion and signal transduction has been divided into regulation of adhesion ("inside-out" signaling) and signaling by adhesion ("outside-in" signaling; Hynes, 1992). A diverse array of signaling proteins have been found in focal contacts or have been shown to bind to focal contact proteins *in vitro*. Although many candidate protein players have been identified, the precise pathways effecting adhesion-stimulated cellular responses (outside-in signaling) have not been determined. Candidate signaling molecules in focal adhesions include FAK, src, protein kinase C (PKC), and integrin-linked kinase (ILK; Rohrschneider and Rosok, 1983; Jaken et al., 1989; Schaller et al., 1992; Kaplan et al., 1994; Hannigan et al., 1996). The regulatory (p85) subunit of PI-3 K and $p130^{CAS}$ are known to associate with FAK but have not been shown to be present in focal contacts (Chen and Guan, 1994; Polte and Hanks, 1997). Significant effort has focussed on

finding signaling molecules that associate with integrin cytoplasmic domains. ILK was discovered in a two-hybrid screen using the β1-integrin cytoplasmic domain as a probe to screen a Hela cDNA library (Hannigan et al., 1996). ILK exhibits serine/threonine kinase activity *in vitro*; its physiological role in integrin adhesion remains to be elucidated. At least one isoform of PKC can be seen in focal contacts, but the role of PKC in cell-matrix adhesion is not known (Jaken et al., 1989). This is interesting in light of the reported interaction between β1-integrin cytoplasmic domain and receptor for activated C kinase (RACK; Liliental and Chang, 1998).

Adhesion signaling produces an array of biochemical and/or physiological responses in various cell types. Of particular interest in recent years is the observation that integrin signaling can activate the well-studied ras-MAP kinase mitogenic signaling pathway (Schlaepfer et al., 1994; Chen et al., 1994; Miyamoto et al., 1995b). It has been proposed that this signaling accounts for at least part of the adhesion requirement for cell division. Anchorage dependent growth also may result from integrin-stimulated transcription of immediate-early genes (Dike and Farmer, 1988; Guadagno and Assoian, 1991; Guadagno et al., 1993; Assoian, 1997). Integrin signaling can increase PIP_2 levels, providing a substrate for phospholipase C, thereby potentiating growth factor receptor pathways (McNamee et al., 1993; Chong et al., 1994). Integrins synergize with growth factor signaling in other, less well characterized ways, to enhance MAPK activation (Clark and Hynes, 1997). The precise points at which adhesive-signaling feeds into this and other signaling pathways have not been determined; more interestingly, the integrin-proximal signaling molecules have not been conclusively identified.

A substantial body of evidence has accumulated supporting the role of integrin-associated membrane proteins in cell signaling. Lateral binding between integrin alpha chains and several integral membrane proteins has been demonstrated (Berditchevski et al., 1995; Berditchevski et al., 1996; Wary et al., 1996; Berditchevski et al., 1997b). These may in turn effect integrin signaling by binding to cytosolic signaling molecules. Tetraspan superfamily proteins can mediate the association of PI-4 K with a subset of alpha integrins (Berditchevski et al., 1997a). Likewise a caveolin-1/integrin complex appears to stimulate fyn-mediated MAPK activation (Wary et al., 1998). Interestingly, caveolin-1 associates with a distinct spectrum of alpha integrin chains (α_1 and α_5) than do tetraspan proteins (α_3 and α_6), raising the

possibility that specificity of integrin signaling results from integrins binding to diverse integral membrane partners.

Src and FAK

Schlaepfer and colleagues (1994) have proposed that FAK and src cooperate during integrin-mediated stimulation of the ras/MAPK mitogenic signaling cascade. In this model, src binds to phosphorylated Y397 of FAK subsequent to FAK activation and autophosphorylation. Src then phosphorylates multiple additional sites on FAK, including binding sites for GRB2 and PI-3 K. The GRB2/FAK complex binds to the guanine nucleotide exchange factor Sos, which catalyses the conversion of ras-GDP to activated ras-GTP, thereby stimulating this signaling pathway (Schlaepfer et al., 1994). This signaling mechanism is extremely similar to that proposed for FAK-stimulated cell motility (discussed below), diverging in the choice of FAK binding partners and the events that follow (summarized in figure 1-1). Both pathways could be triggered by a single mechanism for FAK activation. Although binding to integrin cytoplasmic domains is not sufficient to recruit FAK to focal adhesions, it is possible that this interaction causes a change in FAK conformation, exposing the kinase domain and/or Y397, leading to FAK activation. Consistent with this view is the observation that clustering of β1-integrin or its cytoplasmic domain is sufficient to stimulate FAK phosphorylation (Kornberg et al., 1991; Akiyama et al., 1994).

Signaling through src and FAK also illustrates the extent to which signaling and cytoskeletal assembly are intertwined. The observation that fibroblasts transformed with v-src had disorganized actin cytoskeleton and rounded morphology first implicated src in membrane-cytoskeletal linkages (McClain et al., 1978). The activating mutation Y527F is sufficient to cause translocation of c-src from endosomal membranes to focal adhesions (Kaplan et al., 1994). A fragment containing only the src myristylation site and SH3 domain is concentrated in focal contacts, suggesting that in intact src, targeting information is masked by C-terminal regulatory domains (Kaplan et al., 1994). FAK and src also cooperate in the deployment of new membrane extensions both during cell spreading (which involves radially symmetric membrane extensions) and in cell migration (which requires directed membrane extension). The src SH2 domain binds to the major autophosphorylation site in FAK, Y397 (Xing et al., 1994). Fibroblasts derived from src -/- embryos exhibit delayed cell spreading; the defect is

most pronounced immediately after initial cell adhesion (Kaplan et al., 1995). Presumably other src family members compensate, albeit less efficiently, allowing the src-deficient cells to spread with reduced kinetics. Transfected src restores normal spreading kinetics to these cells. Interestingly, kinase-dead src or src lacking the kinase domain altogether can each rescue the spreading phenotype of src-null cells (Kaplan et al., 1995).

Focal adhesion kinase is a protein tyrosine kinase present in focal contacts. FAK is phosphorylated on tyrosine after integrin-mediated adhesion, treatment of cells with neuropeptides, and in cells transformed by v-src (Guan et al., 1991; Kornberg et al., 1991; Guan and Shalloway, 1992; Hanks et al., 1992; Kornberg et al., 1992; Schaller et al., 1992; Zachary et al., 1992; Zachary et al., 1993). Src and fyn appear to be responsible for phosphorylation of FAK, and both are capable of binding to FAK through their SH2 domains (Xing et al., 1994; Thomas et al., 1995). Phosphorylated FAK also binds to the SH2 domain of the p85 subunit of phosphatidyl-inositol-3-phosphate kinase (PI-3 K; Chen and Guan, 1994). Sequences in the amino-terminal domain of FAK can bind the β1-integrin cytoplasmic domain, but deletion of this FAK domain has no effect on its localization to focal contacts (Hildebrand et al., 1993; Parsons et al., 1994; Schaller et al., 1995). Rather, deletion of residues between 853-1012 in the carboxy-terminal domain of FAK block focal adhesion localization, and amino acids 852-1052 are sufficient to target a chimeric protein to focal contacts (Hildebrand et al., 1993; Parsons et al., 1994; Schaller et al., 1995). Deletion analyses of FAK's C-terminal domain indicate that paxillin binding and focal contact localization both map to amino acids 903-1052 while talin binding (discussed below) requires only amino acids 963-1052 (Chen et al., 1995; Hildebrand et al., 1995).

Understanding how src and FAK cooperate to stimulate cell migration may shed light on how they regulate membrane-cytoskeleton linkages. Cells made from FAK-null mouse embryos have reduced motility compared to wild-type controls (Ilic et al., 1995). In addition, microinjection of a putative dominant-negative FAK variant, FRNK (FAK-related non-kinase), reduces cell motility (Schaller et al., 1993; Gilmore and Romer, 1996). This FAK fragment, which contains the residues sufficient to target FAK to focal adhesions, appears to inhibit FAK by competing it out of focal adhesions (Richardson and Parsons, 1996; Gilmore and Romer, 1996). Conversely, overexpression of FAK in CHO cells stimulates migration *in vitro* in a src-dependent manner (Cary et al., 1996). The FAK mutant Y397F cannot bind src, and its

overexpression does not increase migration. Similarly, mutation of two prolines required for binding to the SH3 domain of $p130^{CAS}$ abrogates the effect of overexpressed FAK, as does misexpression of the $p130^{CAS}$ SH3 domain (Cary et al., 1998). While the FAK kinase domain is not required to stimulate motility in this assay, phosphorylation of FAK at Y397 is necessary, presumably to recruit src's SH2 domain (Cary et al., 1996). Kinase-dead FAK is able to function in this assay probably because it can be phosphorylated by endogenous FAK (Cary et al., 1996). The model which emerges is that after appropriate stimulus, FAK auto- or cross-phosphorylates at Y397, creating a src binding site. $p130^{CAS}$ binds to the proline-rich sequence in FAK's C-terminal domain, and src subsequently phosphorylates $p130^{CAS}$, activating other downstream events needed to increase motility (Vuori et al., 1996). The SH2/SH3 adaptor protein crk is one possible effector. Overexpression of either $p130^{CAS}$ or crk in COS cells increases migration, and co-overexpression of both further stimulates migration. This effect is dependent on Crk/$p130^{CAS}$ complex formation and is blocked by dominant negative rac, providing a potential link between src/FAK signaling and small GTPases (discussed below; Klemke et al., 1998). Elucidation of additional upstream and downstream targets should prove extremely interesting.

Rho family GTPases and the cytoskeleton

The small GTPases rho, rac and cdc42 exert a strong influence over cytoskeletal morphology as mediators of both growth factor and extracellular matrix signals. Rho stimulates stress fiber and focal contact formation, rac induces ruffles and activates rho, and cdc42 drives filopodia extension and activates rac (Ridley and Hall, 1992; Ridley et al., 1992; Hotchin and Hall, 1995; Nobes and Hall, 1995; Clark et al., 1998). While few downstream targets of cdc42 have been found, several putative effectors of rho and rac have been reported.

Two proposed targets of rho can account for many observations regarding both rho-induced and spontaneous formation of focal contacts and stress fibers (figure 1-2). First, rho has been shown to stimulate PI-4-P 5-kinase, resulting in a net increase in PI-4,5-P_2, and possibly explaining a previous report of PI-4,5-P_2 accumulation in response to integrin-mediated adhesion (McNamee et al., 1993; Chong et al., 1994). Clark and colleagues (1998) have reported that adhesion to extracellular matrix in the absence of serum stimulates focal contact and stress fiber formation in a rho-dependent manner; this strongly suggests that

adhesion through integrins is sufficient to activate rho, which could in turn stimulate PI-4-P 5-kinase. Activation of rho by adhesion is a reasonable prediction since integrin-mediated adhesion is sufficient to activate ras (Clark and Hynes, 1996). PI-4,5-P_2 can have many effects, several of which impinge on cytoskeletal assembly. One effect is to increase net F-actin by releasing actin-capping proteins such as gelsolin to create free barbed ends which are available for monomer addition (Janmey et al., 1987; Janmey and Stossel, 1987; Janmey and Stossel, 1989; Hartwig et al., 1995). Polyphosphoinositides can also activate vinculin and ERM family members for binding to actin and other proteins involved in actin-membrane linkage (discussed above). These two rho-stimulated outcomes would result in polymerization of F-actin and its association with several proteins implicated in linking it to the plasma membrane.

Another putative rho effector, rho-kinase, can stimulate focal adhesion and stress fiber assembly when its catalytic domain alone is introduced into cells (Leung et al., 1996; Matsui et al., 1996; Amano et al., 1997; Chihara et al., 1997). Three targets of rho-kinase will be considered. First, ezrin, radixin, and moesin can be phosphorylated on carboxy-terminal threonines such that an intramolecular interaction is disrupted to reveal binding sites for actin and putative membrane docking sites for ERM proteins (Fukata et al., 1998; Matsui et al., 1998). Rho-dependent phosphorylation of ERMs correlates with their translocation into actin-rich membrane projections resembling microvilli; phosphorylation- and/or PI-4,5-P_2-induced conformational changes (discussed above) in ERMs could also result in their assembly into focal contacts (Shaw et al., 1998). Rho-kinase can also phosphorylate myosin-light chain phosphatase (MLCP), inactivating it (Kimura et al., 1996). MLCP dephosphorylates myosin light chain (MLC), inhibiting myosin ATPase activity. MLC itself is a rho-kinase substrate, and phosphorylation of MLC increases myosin motor activity (Amano et al., 1996; Chihara et al., 1997). Hence the net effect of rho stimulation would be myosin activation. MLCP coimmunoprecipitates with ERM proteins and binds *in vitro* to their amino-terminal domains, suggesting a direct link between these two branches of rho-regulated cytoskeletal dynamics (Fukata et al., 1998).

The role of myosin-dependent contractility in stress fiber and focal contact formation was demonstrated through the use of pharmacological inhibitors of myosin light chain kinase (KT5926), myosin ATPase (butanedione monoxime, BDM), and the kinase inhibitor H7. Each

of these compounds blocked both serum-induced contractility and rho-induced stress fiber and focal contact formation (Chrzanowska-Wodnicka and Burridge, 1996). Rho-dependent phosphorylation of FAK and paxillin, which follows integrin-mediated adhesion, was also inhibited by these contractility inhibitors, raising the possibility that at least some integrin-mediated signals may be secondary to, or enhanced by cytoskeletal rearrangements (Chrzanowska-Wodnicka and Burridge, 1996; Clark et al., 1998).

A third protein shown to be required for rho-induced stress fiber and focal contact formation is the sodium/proton exchanger 1 (NHE1; Vexler et al., 1996; Tominaga and Barber, 1998). NHE1 can be activated as a consequence of integrin-mediated adhesion (Ingber et al., 1990). Studies with both pharmacological inhibitors of this ion exchanger and an NHE1-deficient cell line indicate that this protein is required for cytoskeletal rearrangements triggered by lysophosphatidic acid (the stress fiber inducing component in serum) and rho (Vexler et al., 1996; Tominaga and Barber, 1998). The same reagents were used to show the involvement of NHE1 in integrin-mediated adhesion and spreading (Tominaga and Barber, 1998). The authors have not unraveled the mechanism by which NHE1 acts in this process, but they have ruled out pH change as a contributing factor (Tominaga and Barber, 1998). An intriguing possibility is that NHE1 binds ERM proteins to the cell membrane indirectly through NHE-regulatory factor (NHE-RF). NHE1 has been reported to localize in focal contacts (Grinstein et al., 1993).

In sum, candidate downstream effectors of rho include numerous proteins otherwise implicated in cell-matrix adhesion. These proposed pathways can serve as an organizing principle for diverse models about regulated focal contact formation.

The finding that rac can stimulate membrane ruffling has spurred the search for both regulators and effectors of rac. A possible model integrating some suspected protein mediators is shown in figure 1-3. Among the several candidate proteins with demonstrable guanine nucleotide exchange factor (GEF) activity toward rac (including vav, dbl, trio and Tiam-1), Tiam-1 stands out as the most interesting potential player (Hart et al., 1991; Michiels et al., 1995; Debant et al., 1996; Crespo et al., 1997). Tiam-1 was discovered because its overexpression increased the invasiveness of a non-invasive T lymphoma cell line (Habets et al., 1994). Tiam-1 protein stimulates the dissociation of GDP from rac, cdc42 and rho (in descending order of efficacy) allowing each to become activated by binding GTP (Michiels et al., 1995). Misexpressed Tiam-1 induces ruffles, and this effect is blocked by coexpression of

a dominant negative rac, indicating that Tiam-1 acts through rac (Michiels et al., 1995). This presumably results from its ability to catalyze GDP/GTP exchange. Indeed, Tiam-1 lacking its dbl-homology domain, which is predicted to contain its exchange factor activity, does not induce ruffles (Michiels et al., 1997). The Tiam-1 protein has two plekstrin homology (PH) domains; PH domains in some other proteins have been shown to bind to phospholipids (Lemmon et al., 1996). The amino-terminal PH domain of Tiam-1 is required for membrane localization, whereas neither the dbl homology domain nor the PDZ motif is needed to achieve membrane association (Michiels et al., 1997). Deletion of the N-terminal PH domain blocks membrane association and abrogates ruffle-inducing activity. However, the N-terminal PH domain can be substituted by another suitable membrane-binding domain to restore ruffle induction (Michiels et al., 1997).

PI-3 kinase acts upstream of rac in several ruffling cell systems. Given the requirement for the Tiam-1 PH domain, it is possible that PI-3 K products provide a localized membrane binding site for the Tiam-1 PH domain. Studies using the pharmacological inhibitors of PI-3 K, wortmannin and LY294002, or dominant negative forms of PI-3 kinase indicate that PI-3 K is a signaling intermediate in growth factor (PDGF) and cytokine (IL2) stimulated ruffles (Wennström et al., 1994; Hooshmand-Rad et al., 1997; Arrieumerlou et al., 1998). Moreover, in most systems analyzed, these reagents suggest that PI-3 K activity is not required for ruffling induced by activated forms of rac (Hooshmand-Rad et al., 1997; Arrieumerlou et al., 1998). Since a dominant-negative form of rac blocks growth factor-, cytokine-, and activated PI-3 K-stimulated ruffling, PI-3 K has been placed between signaling receptors and rac in the ruffle signaling pathway. Using a similar approach, PI-3 K has been placed between ras and rac in ras-induced ruffling (Rodriguez-Viciana et al., 1997). These authors found that the PKC inhibitor, calphostin, blocked PI-3 K induced ruffles, but a PKC inhibitor that blocks PKC kinase activity directly had no effect. It is proposed that calphostin C, which blocks PKC by inhibiting protein-lipid binding, may inhibit ruffles in this system by blocking some other, unknown protein-lipid interaction (Rodriguez-Viciana et al., 1997). One candidate is hypothetical binding between the Tiam-1 PH domain and a D3 phosphoinositide. To date a single exception places PI-3 K downstream of rac, indicating that rac signaling pathways can vary among cell types. A rac-induced migratory phenotype in mammary epithelial cells was

found to be sensitive to the PI-3 K inhibitors wortmannin and LY294002, placing PI-3 K downstream of rac in this system (Keely et al., 1997).

As the story of upstream rac regulators has unfolded, potential rac effector molecules have emerged. Recently it was reported that LIM kinase binds F-actin and prevents its depolymerization by phosphorylating and inactivating cofilin, an actin-depolymerizing protein (Arber et al., 1998; Yang et al., 1998). Rac stimulates LIM kinase activity towards serine 3, an inhibitory site on cofilin, decreasing the rate of actin depolymerization and thereby effecting net extension of microfilaments (Arber et al., 1998; Yang et al., 1998). Kinase-dead LIM kinase inhibits rac-stimulated cofilin phosphorylation and membrane ruffling but has no effect on stress fiber formation. Indeed, overexpression of wild-type and constitutively active LIM kinase was sufficient to induce accumulation of peripheral F-actin, whereas overexpression of kinase-dead LIM kinase had no effect (Arber et al., 1998; Yang et al., 1998). Overexpression of cofilin induced changes in actin cytoskeleton which were suppressed by simultaneous overexpression of LIM kinase; a cofilin point mutant lacking the LIM kinase phosphorylation site (S3A) was not inhibited by LIM kinase (Arber et al., 1998; Yang et al., 1998). This interesting discovery is made more intriguing by the homologies present in LIM kinase: it is composed of two amino-terminal LIM domains, a PDZ domain, and a carboxy-terminal serine/threonine kinase catalytic domain (Bernard et al., 1994; Mizuno et al., 1994; Okano et al., 1995). This raises the question of binding partners for the two LIM domains and a membrane docking site for the PDZ domain. Further study of the rac/LIMK/cofilin pathway should be of interest to those studying both signal transduction mechanisms and cytoskeleton dynamics.

The role of the rac-binding protein p21-associated kinase ($p65^{PAK}$) in rac-induced cytoskeletal changes is more controversial. Sells and colleagues (1997) found that expression of an activated form of $p65^{PAK}$ induced ruffles in two cell lines, and that $p65^{PAK}$ kinase activity was neither necessary nor sufficient for this cytoskeletal change. Rather, binding to the SH2/SH3 adaptor protein Nck correlated with the ability of $p65^{PAK}$ to stimulate ruffling. Moreover, Nck- $p65^{PAK}$ association was stimulated by an activated rac allele (Sells et al., 1997). Expression of PI-3 K or activated rac caused translocation of $p65^{PAK}$ into membrane ruffles (Dharmawardhane et al., 1997). These data are suggestive of a role for $p65^{PAK}$ in ruffling. However, three other studies found that rac protein with an effector loop mutation

which either abolishes or significantly reduces binding to $p65^{PAK}$ still induces ruffling, apparently independent of $p65^{PAK}$ association (Joneson et al., 1996; Lamarche et al., 1996; Westwick et al., 1997). These results suggest that direct and stable binding between $p65^{PAK}$ and rac is not required for signaling, but they do not rule out the possibility that transient associations between rac and $p65^{PAK}$, or indirect signaling through one or more unknown intermediaries, are sufficient to induce ruffles.

Based on the phenotype of gelsolin-deficient cells, gelsolin has been proposed to mediate the effects of rac on actin cytoskeleton (Azuma et al., 1998). Cell lines derived from gelsolin-null mice fail to ruffle and migrate at half the speed of their wild-type counterparts. In addition, these cell lines and all tissues examined from the null mice have a five-fold increase in rac protein levels. Perhaps rac is upregulated in an attempt to compensate for reduced cytoskeleton remodeling efficiency. These three phenotypes are rescued by transfection of null cell lines with gelsolin cDNA. Although there is no evidence that gelsolin is a proximal target of rac signaling, these data underscore the relationship among signaling and cytoskeletal proteins.

Talin

Talin structure

Talin was identified as a minor band in partially purified smooth muscle protein preparations migrating with an apparent molecular weight of 235 kD and was found to be present in focal contacts and ruffling membranes in cultured fibroblasts (Burridge and Connell, 1983). Rotary shadowing of purified talin revealed a rod-shaped protein with a globular domain at one end (Molony et al., 1987). Proteolysis of talin yields two polypeptides, one of 190 kD, which corresponds to the elongated rod domain, and one of 47 kD, which is the globular domain (figure 1-4B; Burridge and Connell, 1983; Fox et al., 1985; Winkler et al., 1997). The 47 kD fragment contains the N-terminus of talin; the deduced amino acid sequence in this domain is homologous to the 30 kD amino-terminal domain of band 4.1, identifying talin as a member of this protein superfamily (Rees et al., 1990). The amino-terminal sequence homology is interrupted in *C. elegans* talin by two insertions and in *Dictyostelium* talin by a short deletion in this region relative to vertebrate talins, suggesting the existence of two subdomains within talin's band 4.1 homologous sequences (Hemmings et al., 1996; Moulder et

al., 1996). These subdomains may correspond to two globular lobes seen within the 47 kD fragment in one EM study (Winkler et al., 1997). The carboxy-terminal 190 kD talin fragment is predicted to consist mostly of α-helices, probably explaining the high (approximately 75%) α-helix content measured in purified talin (Molony et al., 1987; McLachlan et al., 1994).

There is some evidence to suggest that these two domains interact with each other reversibly giving rise to two talin conformations. This type of intramolecular association has been demonstrated for vinculin and ERM proteins (discussed above). Talin, like vinculin, undergoes a salt-dependent change from a principally globular to a mostly elongated rod shape (Molony et al., 1987; Winkler et al., 1997). Moreover, this conformational change is dependent on the presence of talin's amino-terminal domain as the carboxy-terminal 190 kD domain is constitutively rod-shaped in EM studies (Molony et al., 1987). The analogous intradomain interactions in vinculin and ERM proteins appear to be regulated by acidic phospholipids, and the amino-terminal domain of talin can bind lipids under some circumstances (Niggli et al., 1994; Gilmore and Burridge, 1996). In addition, lipid binding can be correlated with morphological changes. For instance, the amount of PI-4,5-P_2 that can be coimmunoprecipitated with talin is seven- to ten-fold greater in spreading platelets than in suspended platelets (Heraud et al., 1998). Purified talin protein has also been reported to have the ability to open holes in synthetic liposomes, raising the possibility that talin can directly remodel membranes (Saitoh et al., 1998). At present there is no direct evidence indicating a functional difference between the globular and elongated forms of talin or supporting the hypothesis of intramolecular binding within talin. However, this model warrants further investigation in light of these suggestive observations and the analogy with other band 4.1 superfamily members.

Talin subcellular localization

Talin is readily detected at the ends of stress fibers coincident with integrins and other focal adhesion markers by immunofluorescence. Time-lapse video studies combined with immunostaining indicate that talin is present at the distal-most edge of newly-formed membrane extensions and that it arrives in focal contacts before vinculin (DePasquale and Izzard, 1991). The authors make the interesting claim that talin at the leading edge does not appear to incorporate into nearby forming focal adhesions, but pulse labeling studies will be

required to confirm this observation (DePasquale and Izzard, 1991). Taken together, these observations suggest that talin is involved in the earliest stages of membrane-cytoskeleton junction assembly at sites of cell-matrix adhesion. A role for talin during membrane dynamics is also supported by talin's presence in peripheral ruffles of spreading fibroblasts and platelets (Burridge and Connell, 1983; Beckerle et al., 1989). Immunoelectron microscopy studies on spreading platelets shows talin to be closely apposed to the plasma membrane, on average within 40 nm, at the platelet periphery (Beckerle et al., 1989). A *Dictyostelium* talin homolog redistributes to migrating fronts within 30 seconds of induction by cAMP, where it localizes to filopodia projecting in the direction of travel (Kreitmeier et al., 1995). Protrusion of membranes around a particle during phagocytosis has been compared to cell spreading, and talin is found in phagocytic cups in macrophages surrounding particles and at sites of bacterial pathogens invading fibroblasts (Greenberg et al., 1990).

Talin localizes not only to dynamic membranes but also to sites of stable membrane-cytoskeleton associations such as focal contacts and their *in vivo* correlate, the myotendonous junction (Burridge and Connell, 1983; Tidball et al., 1986). In chicken muscle, both immunofluorescence and immunoelectron microscopy also show talin to be concentrated in digit-like processes projecting from the end of muscle cells. These EM studies indicate that in muscle, as in platelets, talin is extremely close to the plasma membrane (Tidball et al., 1986). *C. elegans* talin colocalizes with β integrin at sites of attachment of body wall muscle to the hypodermis, a structure which, like the myotendonous junction, bears the force of muscle contraction (Moulder et al., 1996). Worm accessory muscles also contain talin, although surprisingly talin was not found in any other cell types. Given the widespread distribution of talin in adherent cells of vertebrates, the absence of talin from other worm cell types may indicate that one or more additional worm talins exist, or that other proteins can substitute for talin function in worms. Talin colocalizes with integrins at the interface between T-cells and antigen-presenting cells, suggesting that in rare circumstances talin participates in cell-cell adhesion (Kupfer et al., 1986; Burn et al., 1988).

Talin's amino-terminal domain appears to be important for proper restriction of talin in focal contacts. Microinjection of fluorescently-labelled talin into fibroblasts or MDBK cells results in labeling of focal contacts (Nuckolls et al., 1990). However, microinjected C-terminal 190 kD fragment labels both focal contacts and adherens junctions at sites of cell-cell contact

in MDBK cells, indicating that the N-terminal domain is required to keep talin out of adherens junctions (Nuckolls et al., 1990). Microinjected amino-terminal domain weakly labels focal contacts, but otherwise appears distributed diffusely throughout the cytoplasm (Nuckolls et al., 1990). Thus it does not appear as if this talin domain contains strong focal contact localization determinants, but rather may act by regulating the availability of other binding sites within talin's C-terminal domain for other proteins, most likely vinculin or actin (discussed below). In these experiments, neither injected fragment had a detectable effect on cell adhesion or cytoskeletal morphology (Nuckolls et al., 1990).

Talin function

Experimental data support a role for talin in cell adhesion and dynamic reorganization of membrane-associated cytoskeleton. The localization of *Dictyostelium* talin to migrating fronts suggested that talin would be involved in these cells' motility, but the phenotype of talin-null *Dictyostelium* does not support this hypothesis. Rather, it provides evidence that talin is necessary for tight adhesion of cells to both substrates and particles. Reflection interference contrast microscopy was used to assess the distance between the cell membrane and the substratum, revealing that over most of the ventral surface, wild type cell membranes are within 50 nm of the substrate whereas talin mutant cells only approach the underlying surface to about 140 nm. The different adhesive strength was evident in that mutant but not wild-type cells were readily released from the surface by gentle pipetting (Niewöhner et al., 1997). Surprisingly, even though these mutant cells had an obvious defect in adhesion, they were able to migrate and undergo changes in cell shape normally, suggesting that even minimal adhesion provides sufficient traction for motility in *Dictyostelium*. Reduced adhesion to particles was inferred from the inability of talin mutant *Dictyostelium* to grow in shaken liquid cultures in which cells feed on co-cultured yeast or bacteria. Niewöhner et al. (1997) found that growth was improved when cultures were shaken less, thereby causing less shear stress. Talin-null *Dictyostelium* exhibit drastically reduced growth in liquid culture on *E. coli B/r* compared to wild-type *Dictyostelium* or compared to mutant grown in culture with *Salmonella minnesota R595*. The relevant difference between these two bacterial strains is their surface carbohydrate repertoire. Growth on solid media using the same food sources showed that particle engulfment and uptake was not affected in the mutant, suggesting that the defect lay

specifically in binding. In these experiments, bacterial adhesiveness was modulated by genetically altering the surface carbohydrates, hinting that this mode of talin-dependent particle adhesion may involve one or more carbohydrate-binding receptors. Moreover, a form of EDTA-sensitive *Dictyostelium* aggregation was inhibited in the talin-null cells, indicating that talin is required for some form of divalent cation-dependent adhesion. A lectin-like activity, which could depend on both cations and sugar residues, has been implicated in binding of *Dictyostelium* to *E. coli B/r* and may interact with talin in this process as well as during EDTA-sensitive aggregation (Chadwick et al., 1984).

Manipulations interfering with talin activity in vertebrate cells reveal a role for this protein in membrane dynamics. Two morphological changes in cells which probably use closely related if not identical mechanisms are spreading and migration. In each case, cells extend sheets of new membranes away from the cell body, in one case this is polarized while in the other case it is essentially radially symmetric. Talin-null embryonic stem (ES) cells fail to spread on gelatin-coated surfaces and exhibit reduced kinetics of spreading on a fibronectin matrix (Priddle et al., 1998). In addition, when these ES cells are differentiated into embryoid bodies, relatively few cells migrate out of the null-derived EBs compared with wild type. Those cell that do migrate out of talin-null EBs represent only two cell types as compared to numerous distinguishable morphological types seen with wild-type EBs. Two caveats cloud the interpretation of these results: one is that the null ES cells have significantly reduced levels of β1 integrin and somewhat reduced levels of the focal contact proteins vinculin and α-actinin, although embryoid bodies have normal amounts of β1 integrin. This may be evidence that talin either transports β1 integrin to the membrane or stabilizes it once it gets there. An analogous reduction is seen in glycophorin C in band 4.1-deficient cells (Alloisio et al., 1985; Reid et al., 1990; Chasis and Mohandas, 1992). Also troubling is the production by the null ES cells of trace but detectable amounts of a truncated talin protein which is nearly full-length, most likely starting at codon 76 (Priddle et al., 1998). Hence, these cells may be talin hypomorphs rather than nulls. In the absence of further data or a clean talin-null, these data may be considered at least suggestive of a role for talin in both spreading and migration.

Despite these potential flaws, the results from the talin knockout agree rather well with other methods used to disrupt vertebrate talin function. Injection of anti-talin antibodies into partially spread chicken embryo fibroblasts (CEFs) prevents further spreading and, in some

cases, reverses spreading that has already occurred (Nuckolls et al., 1992). Similarly, microinjected antibodies reduce migration of CEFs in an *in vitro* wound healing model (Nuckolls et al., 1992; Bolton et al., 1997). Hela cells expressing an inducible antisense talin gene exhibit a reduction in talin protein between 60-90%. These cells, like the talin-null ES cells, have reduced levels of β1 integrin, although in this case aberrantly migrating forms of both α5 and β1 integrin can be detected on SDS gels (Albigès-Rizo et al., 1995). This result suggests that talin may have a role in normal presentation of β1 integrins on the cell surface, but the apparent reduction in normal β1 integrin renders the reported spreading defect of these cells difficult to interpret (Albigès-Rizo et al., 1995).

Localized disruption of talin protein by micro CALI offers another demonstration of the role of talin in dynamic membrane extension (Sydor et al., 1996). Malachite green-conjugated antibodies directed against either talin or vinculin were loaded into chicken dorsal root ganglia neurons. During laser irradiation of growth cone leading edges, extension and retraction of filopodia was recorded. Targeting of talin resulted in cessation of all new filopodial extensions during the laser treatment, with a gradual recovery to normal rates over the subsequent five minutes (Sydor et al., 1996). The specificity of this effect was verified by inactivating vinculin in the same way; this resulted in the buckling and collapse of filopodia but caused no decrease in the rate of new filopodial formation (Sydor et al., 1996). A role for talin in filopodial extension may explain the report of talin at the front end of motile *Listeria monocytogenes*, as this pathogen causes the formation of filopodia-like cellular processes (Dold et al., 1994). Perhaps this bacterium exploits the ability of talin to reorganize the plasma membrane to facilitate its spread from cell to cell.

Defects in morphology resulting from talin down-regulation are reflected in changes in cytoskeletal morphology in the same systems. The small number of talin-null ES cells which were able to spread on a fibronectin matrix did not form focal contacts or stress fibers, although again this observation must be tempered by the knowledge that these cells also have less β1 integrin (Priddle et al., 1998). On the other hand, differentiated cells derived from talin-null embryoid bodies form normal-looking focal contacts and stress fibers, indicating that under at least some circumstances these structures can form in the absence of full-length talin. In these cells, the small quantities of truncated talin polypeptide may be adequate to support these cytoskeletal structures, obscuring an essential role for talin. Talin-null ES cells also

exhibit abnormal membrane blebbing, which could reflect weakness in the underlying membrane-associated cytoskeleton; further exploration of this phenotype is required (Priddle et al., 1998). Consistent with the phenotype of talin-null ES cells is the observation that microinjection of human foreskin fibroblasts with anti-talin antibodies disrupts stress fibers (Bolton et al., 1997). Microinjection of talin protein fragments derived from both N- and C-terminal domains have a similar effect on CEFs (Hemmings et al., 1996).

Protein-protein interactions

The molecular basis for at least some of the proposed functions of talin can be explained by interactions with other cytoskeleton-associated proteins (known binding sites are schematized in figure 1-4). Indirect evidence that talin associates with β1 integrin comes mostly from colocalization data which extends the initial observation that talin, like integrins, is found in focal contacts (Burridge and Connell, 1983). In chicken peripheral blood lymphocytes talin was found to colocalize with antibody-induced integrin caps in the presence, but not absence, of phorbol ester (Burn et al., 1988). This suggested a role for PKC regulation of this association, but further support for that hypothesis has not emerged. In NIH 3T3 fibroblasts, talin cocaps with transfected chicken β1 integrin that has been clustered with a species-specific anti-chicken integrin antibody (Lewis and Schwartz, 1995). Talin did not cocap with transfected β1 integrin that had been deleted of the carboxy-terminal 15 amino acids. Interestingly, the ability of various truncated forms of β1 integrin to recruit F-actin into clusters correlates with their ability to cocluster talin and FAK; clustering of α-actinin is insufficient to induce F-actin colocalization (Lewis and Schwartz, 1995). Independent co-capping studies reveal that recruitment of talin to sites of capped β1 integrins depends on ligand binding by integrins. Either ligand-mimicking antibodies or non-mimicking antibodies plus the ligand-derived peptide, RGD, were able to cocluster talin with integrins, but talin was not colocalized with clustered unliganded integrins (Miyamoto et al., 1995a). In this assay, talin cocapping with integrins was not affected by inhibitors of tyrosine kinases (genistein and herbimycin) or cytochalasin D, the latter result being consistent with talin's proposed role as an adaptor between integrins and actin (Miyamoto et al., 1995b). Likewise, association of *C. elegans* talin with the plasma membrane in muscle cells was dependent upon presence of wild-type worm β integrin but not vinculin (Moulder et al., 1996).

A substantial body of *in vitro* binding data has accumulated to support the biochemical association of talin with β integrins. Equilibrium gel filtration was used to detect an integrin-talin complex exhibiting a dissociation constant on the order of $7x10^{-7}M$ (Horwitz et al., 1986). This talin-integrin complex was shown to be capable of binding to vinculin or fibronectin, and the association between talin and integrins was blocked by a small peptide derived from the β1 integrin cytoplasmic domain (Horwitz et al., 1986; Tapley et al., 1989). The integrin-binding site was mapped to the talin carboxy-terminal domain (Horwitz et al., 1986). A GST-β1 integrin cytoplasmic domain fusion protein also was shown to bind to talin in cell lysates, and deletion of the C-terminal 13 amino acids abolished this association (Chen et al., 1995). Talin coimmunoprecipitates with β1 integrins in lysates of CHO cells overexpressing the integrin; this association was specific for the β1A cytoplasmic domain and was not seen with the β1B form of the cytoplasmic domain (Retta et al., 1998). Pfaff et al. (1998) found that β1A cytoplasmic domain peptides bound to intact and carboxy-terminal domain of talin, and that β1D, a muscle-specific splice form of the β1 cytoplasmic domain, bound talin about 7-fold better, whereas a β1A peptide containing the mutation Y788A and a β7 cytoplasmic domain peptide did not bind talin at all. In this assay, another actin-binding protein, filamin, bound the β1A and β7 cytoplasmic domains but not the β1D isoform, demonstrating the specificity of these interactions, and suggesting that different integrin cytoplasmic domains utilize distinct mechanisms to connect to F-actin (Pfaff et al., 1998). Knezevic et al. (1996) detected some binding of talin to β3 integrin cytoplasmic domain peptides above background binding to a scrambled peptide, which probably reflects the sequence similarity between β3 and β1A. Talin was also found to bind more convincingly to αIIb cytoplasmic domain peptides, a result which disagrees with the observations of Pfaff et al. (1998) and is best explained by differences in the two binding assays used. Pfaff et al. (1998) used dimeric peptides which were presented in a fixed orientation, potentially obscuring a talin-binding site, whereas Knezevic and colleagues (1996) coated plastic wells with peptides which were presumably monomeric, and probably resulted in randomly displayed sequences including a putative talin binding site. Resolution of this discrepancy awaits further investigations.

Whereas β1 integrin is the major known membrane binding site for talin in focal contacts, vinculin is the primary actin-associated protein which interacts with talin. Vinculin,

which consists of a globular N-terminal domain and an elongated rod C-terminal domain, is found in focal contacts as well as cell-cell junctions (Geiger, 1979; Milam, 1985). Vinculin also has been reported to bind to F-actin and the focal contact proteins paxillin, α-actinin, and VASP (Belkin and Koteliansky, 1987; Wachsstock et al., 1987; Turner et al., 1990; Johnson and Craig, 1995a; Brindle et al., 1996). The talin-vinculin interaction has been extensively documented and has been detected by gel overlay, ligand blotting, cosedimentation, coimmunoprecipitation of purified proteins, and several solid-phase binding assays (Otto, 1983; Burridge and Mangeat, 1984; Jones et al., 1989; Turner and Burridge, 1989; Nuckolls et al., 1990; Gilmore et al., 1992; Gilmore et al., 1993; Hemmings et al., 1996). These studies reveal that talin contains three separable vinculin binding sites with highest affinity of approximately 10^{-8} M, all within the carboxy-terminal talin fragment. Analysis of these three binding sites indicates that vinculin binding is neither necessary nor sufficient for focal contact targeting of talin, consistent with results obtained in vinculin-null nematodes. Similarly, two point mutants which ablate talin binding by vinculin have no effect on targeting of vinculin to focal contacts, indicating that focal contacts contain vinculin binding activities other than talin.

Binding of vinculin to talin is regulated by an interesting mechanism which has served as a model for intramolecular interactions in other proteins (discussed above). The imperfect coincidence of talin and vinculin subcellular localization gave the first hints that talin-vinculin binding was regulated. Vinculin was found at cell-cell as well as cell-matrix adhesion sites, whereas talin was found only in focal contacts (Geiger, 1979; Burridge and Connell, 1983). Similarly, capped integrins in lymphocytes induced talin colocalization but not vinculin (Burn et al., 1988). Importantly, in the absence of the vinculin carboxy-terminal domain, PI-4,5-P_2 does not increase binding of talin to vinculin amino-terminal domain, indicating that the effect of PI-4,5-P_2 on talin-vinculin binding is not mediated by talin (Gilmore and Burridge, 1996).

Three actin-binding sites have been mapped within talin, two of which are in the carboxy-terminal domain and one of which either overlaps, or is contained within, the amino-terminal talin fragment (Hemmings et al., 1996). These interactions may explain the modest increases in actin polymerization observed *in vitro* in the presence of talin (Muguruma et al., 1990; Kaufmann et al., 1991; Niggli et al., 1994). Additional protein-protein interactions of talin are of unclear physiological significance. Chen et al. (1995) observed a small amount of

FAK in talin immunoprecipitates. This may be significant given the apparent requirement for each protein during cell motility.

Regulation of talin function

Several post-translational modifications of talin have been described, but their physiological relevance is unknown. Phosphorylation on serine, threonine, and tyrosine occurs to low stoichiometry in cells transformed by the Rous sarcoma virus (RSV; Pasquale et al., 1986; DeClue and Martin, 1987). The C-terminal domain was phosphorylated on multiple sites up to about 0.07 mole phosphate/mole talin. Since only a small fraction of talin is incorporated into the cytoskeleton, it is possible that the observed low stoichiometry of modification of the entire pool reflects efficient phosphorylation of cytoskeletal talin, resulting in relevant alterations in function. A precedent for this is found in the observation that activated src preferentially associates with actin cytoskeleton in thrombin-treated platelets (Clark and Brugge, 1993). Nonetheless, talin phosphorylation is not sufficient to cause cytoskeletal rearrangements as no correlation between talin phosphorylation and cell morphology was found in CEFs transformed by partial RSV mutants (DeClue and Martin, 1987). Similarly, PDGF-stimulated talin tyrosine phosphorylation results in no change of subcellular distribution (Tidball and Spencer, 1993). Talin has been shown to be phosphorylated by PKC *in vitro* (Litchfield and Ball, 1986). Treatment of platelets with thrombin or phorbol esters and fibroblasts with phorbol esters or dibutyryl-cAMP can cause increases in total talin phosphorylation, but these modifications only sometimes correspond to changes in cytoskeletal structure (Turner et al., 1989; Beckerle, 1990; Bertagnolli et al., 1993). Perhaps talin phosphorylation represents one of several means by which cells can effect morphological changes.

Recent studies strongly suggest a role for calpain proteases in cell spreading and migration. Inhibition of calpain in NIH 3T3 cells slowed cell spreading and reduced lamellipodia extension, whereas similar treatment of CHO cells reduced migration speed by inhibiting rear retraction rates (Huttenlocher et al., 1997; Palecek et al., 1998; Potter et al., 1998). Talin is subject to limited proteolysis in cell lysates, probably through the action of calpains and thrombin, both of which can cleave talin *in vitro* (Fox et al., 1985; Beckerle et al., 1987). It has been suggested that talin proteolysis seen in thrombin-activated platelets results

from the action of thrombin post-lysis, however, rather than from physiological action of calpains as was originally proposed (Fox et al., 1985; Bertagnolli et al., 1993). Indeed, talin proteolysis does not correlate with changes in cytoskeleton in a variety of cell types (Turner et al., 1989; Tidball and Spencer, 1993). In one study, insoluble membrane-associated talin was found to be exclusively in the cleaved form, raising the possibility that the small amount of cytoskeletal talin is proteolytically processed (Tranqui and Block, 1995). In this study, however, insufficient care was taken to show that talin was digested prior to cell lysis; more careful repetition of this work could enhance its impact. The discovery that calcium-dependent protease II colocalizes with talin in focal contacts and the growing evidence that calpains are involved in remodeling actin makes the question of physiological talin proteolysis one which must be resolved (Beckerle et al., 1987). The observation that cells overexpressing calpastatin, a calpain inhibitor, have seven-fold higher levels of ezrin and two-fold greater levels of radixin and moesin than control cells, but unchanged levels of talin, suggests that ERM proteins may be more physiologically relevant calcium-dependent protease targets than is talin (Potter et al., 1998). Proteolysis of ezrin by calcium-sensitive proteases has been reported (Yao et al., 1993; Shuster and Herman, 1995).

Evidence that talin is important for membrane-cytoskeleton association, motility, spreading and adhesion, together with its band 4.1 homology motivated investigation into the band 4.1-like amino-terminal domain. Binding by this fragment of talin to the cytoplasmic domain of a membrane protein, perhaps facilitated through interaction with a PDZ-domain containing mediator, would fulfil predictions made nearly a decade ago based solely on talin's homology to band 4.1 (figure 1-5; Rees et al., 1990). This prediction is explored in this thesis.

Figure 1-1: A model for FAK in cell motility. FAK and src may use distinct adaptors to effect motility and mitogenic signaling. Details are discussed in the text.

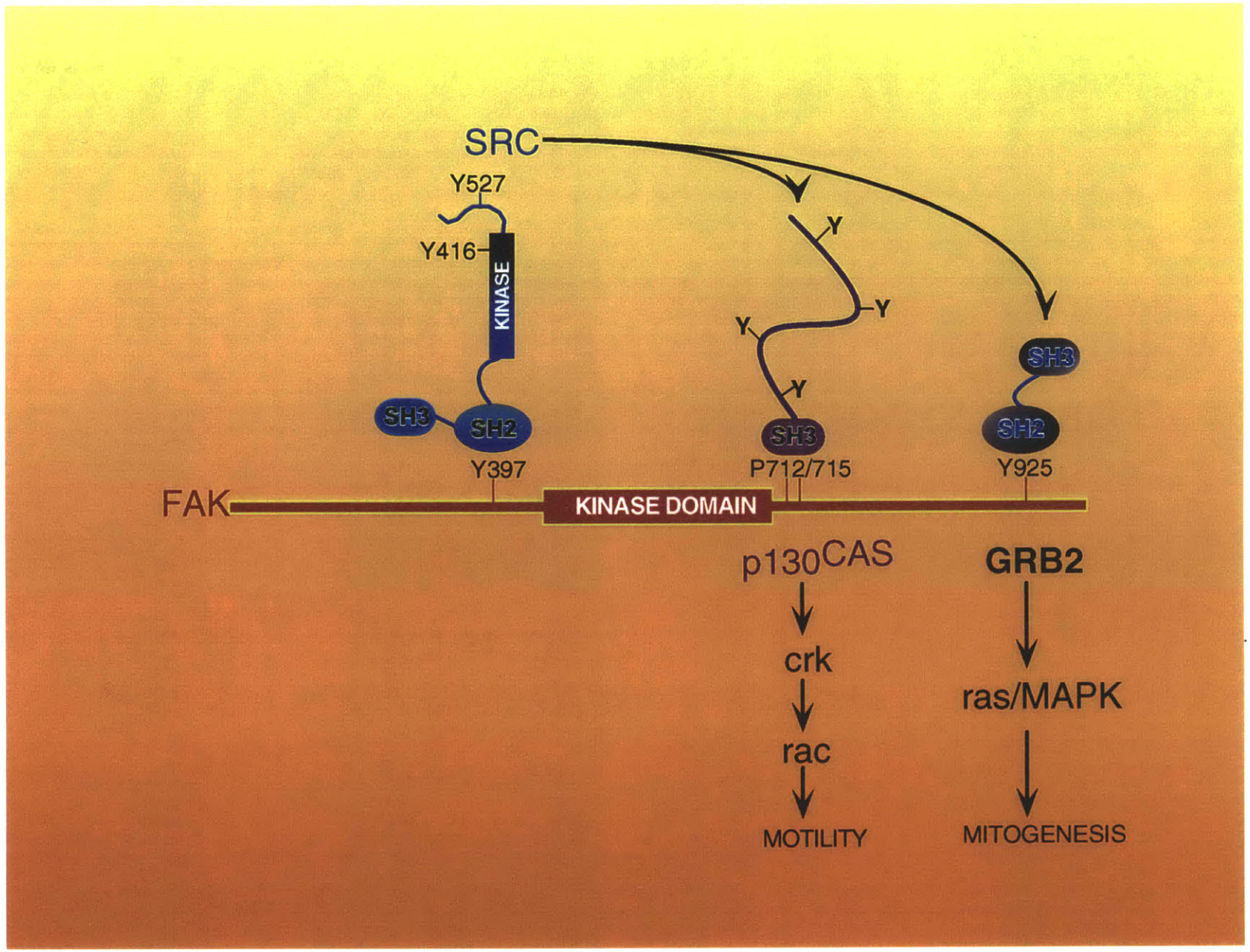
SRC
Y527
Y416
KINASE
SH3
SH2
Y397
Y
Y
Y
Y
SH3
P712/715
SH3
SH2
Y925
FAK
KINASE DOMAIN
p130CAS
crk
rac
MOTILITY
GRB2
ras/MAPK
MITOGENESIS

Figure 1-2: A model for rho-stimulated focal contact formation. The candidate effectors PI-4-P 5-kinase and rho kinase act through partially overlapping pathway to stimulate actin polymerization, membrane binding, and contraction.

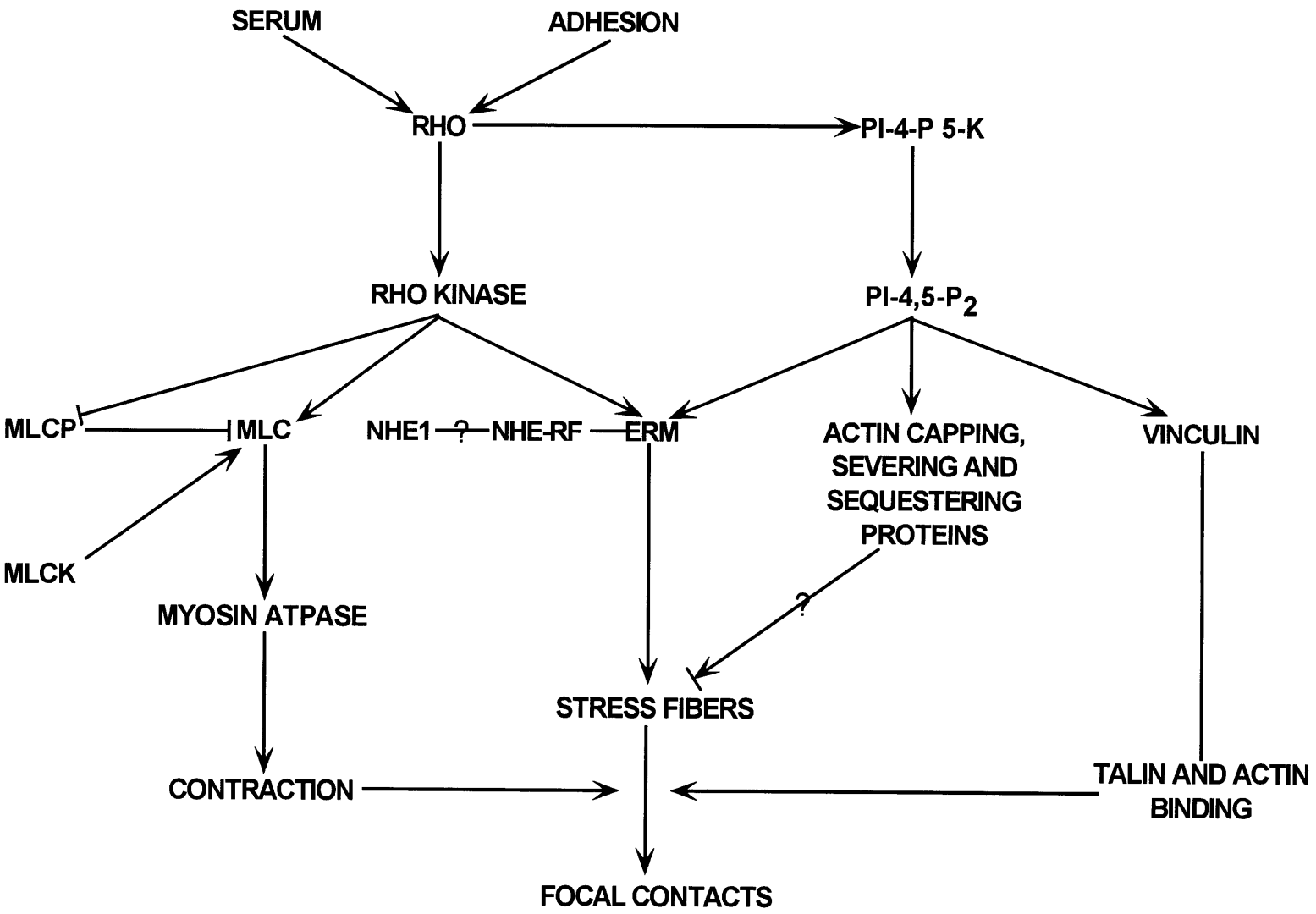
SERUM
ADHESION
RHO
PI-4-P 5-K
RHO KINASE
PI-4,5-P2
MLCP
MLC
NHE1
?
NHE-RF
ERM
ACTIN CAPPING, SEVERING AND SEQUESTERING PROTEINS
VINCULIN
MLCK
MYOSIN ATPASE
?
STRESS FIBERS
CONTRACTION
TALIN AND ACTIN BINDING
FOCAL CONTACTS

Figure 1-3: A model for rac-stimulated membrane ruffling. PI-3 kinase products may serve as membrane localization signals for rac exchange factors such as Tiam-1, dbl or vav. GTP-bound rac acts through unknown intermediates to activate LIM kinase, which increases actin polymerization by inactivating cofilin. Another candidate effector, $p65^{PAK}$, may contribute to ruffle formation directly in an unknown way, or a $p65^{PAK}$-Nck complex could recruit PI-3 kinase, amplifying the signal through positive feedback.

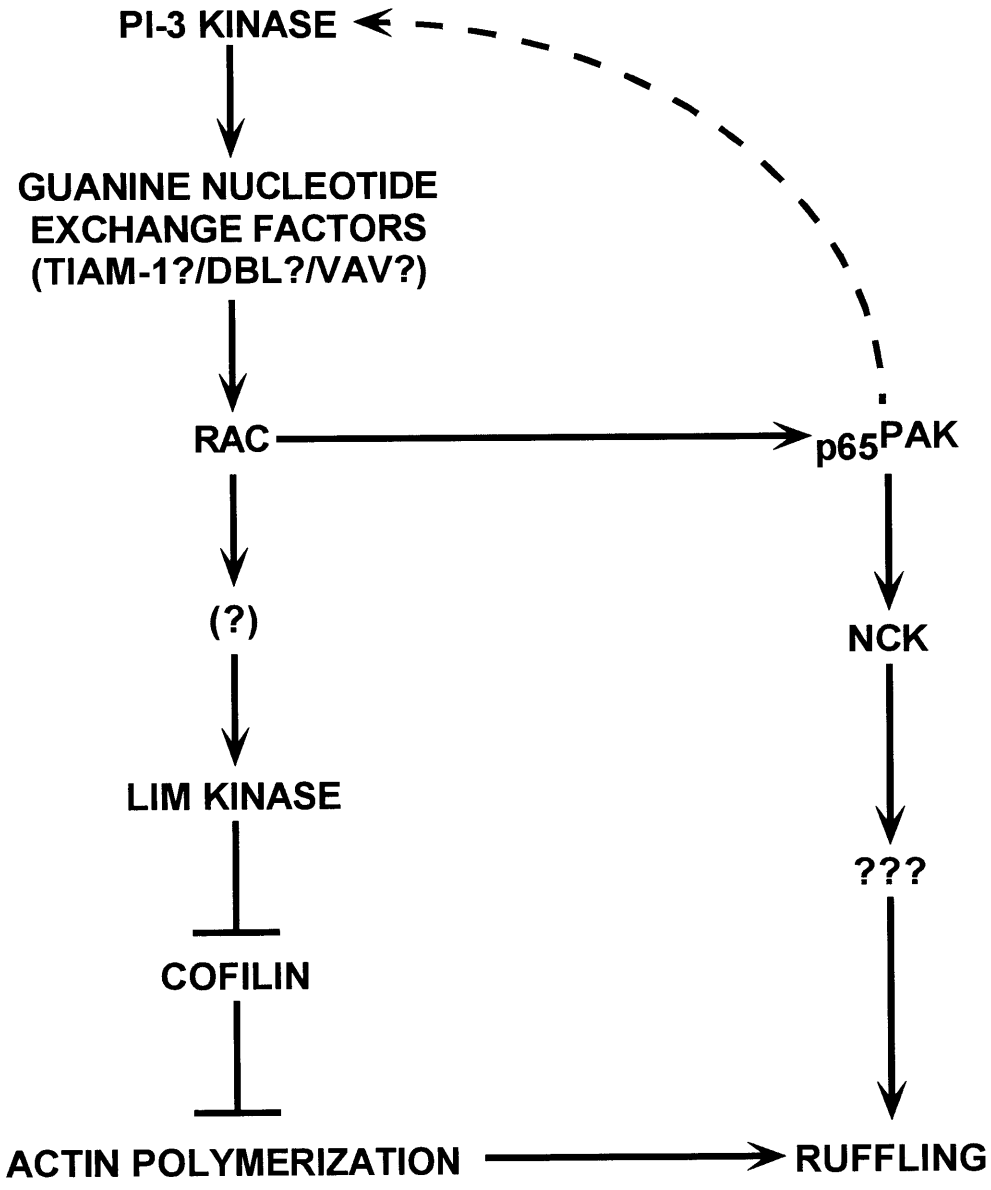
PI-3 KINASE
GUANINE NUCLEOTIDE EXCHANGE FACTORS (TIAM-1?/DBL?/VAV?)
RAC
p65PAK
(?)
NCK
LIM KINASE
???
COFILIN
ACTIN POLYMERIZATION
RUFFLING

Figure 1-4: (A) Several band 4.1 superfamily members are shown with analogous domains color-coded.

(B) Talin domain structure indicating known binding sites for cytoskeleton proteins.

A

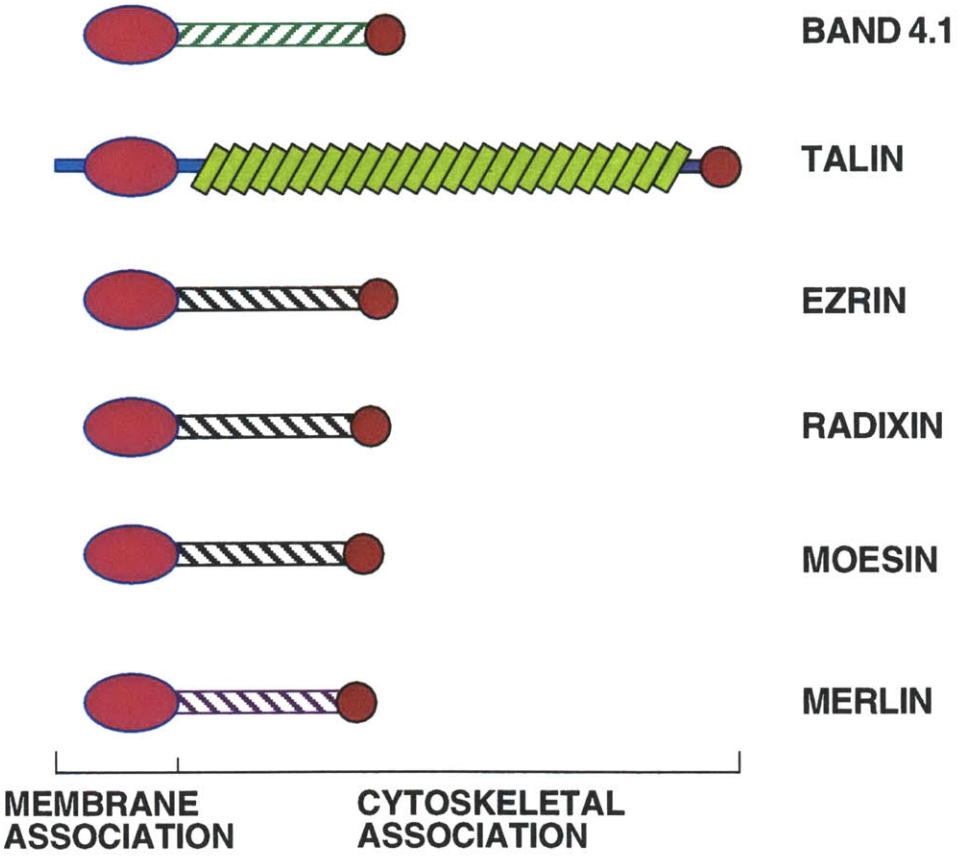
BAND 4.1
TALIN
EZRIN
RADIXIN
MOESIN
MERLIN
MEMBRANE ASSOCIATION
CYTOSKELETAL ASSOCIATION

B

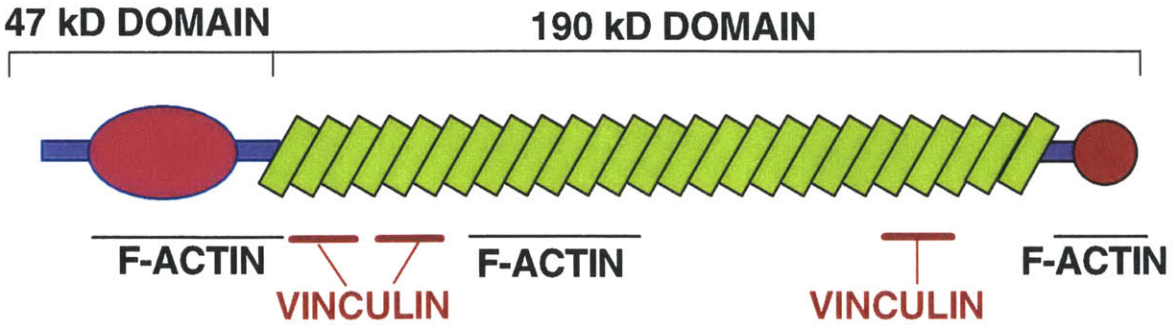
47 kD DOMAIN
190 kD DOMAIN
F-ACTIN
VINCULIN
F-ACTIN
VINCULIN
F-ACTIN

Figure 1-5: Membrane-cytoskeleton associations mediated by interaction of band 4.1 superfamily proteins with both membrane proteins and cytoskeleton. In this model, talin is shown bound to the cytoplasmic domain of integrins though talin's carboxy-terminal domain. It has been suggested that an additional membrane-binding site may exist in talin's amino-terminal domain. Several PDZ-domain-containing proteins have been found to bind to band 4.1, merlin, and members of the ERM family. Here, a hypothetical PDZ protein is shown binding both talin and its hypothetical membrane binding partner.

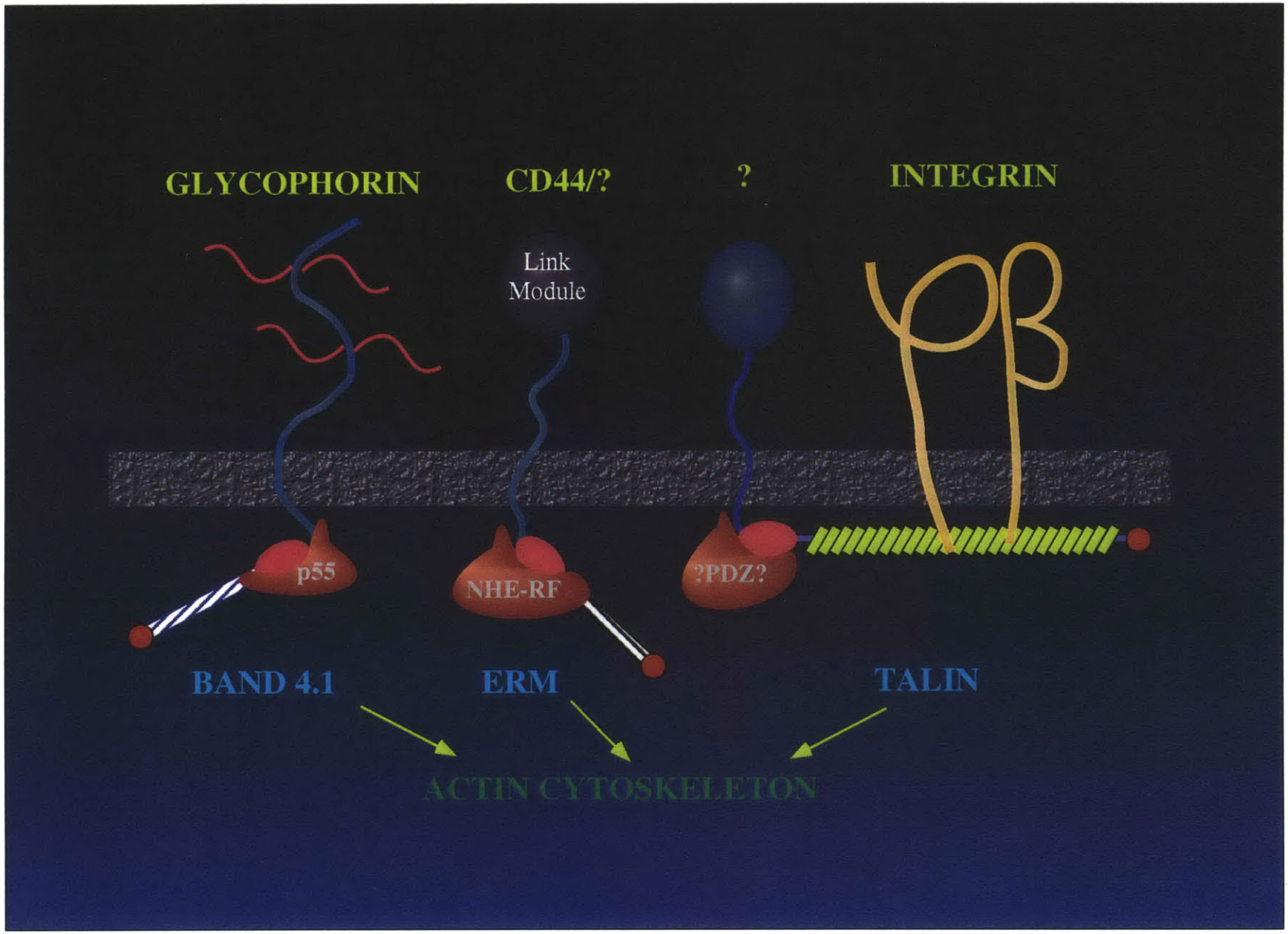
GLYCOPHORIN
CD44/?
?
INTEGRIN
Link
Module
p55
NHE-RF
?PDZ?
BAND 4.1
ERM
TALIN
ACTIN CYTOSKELETON

Chapter 2

Functions of the talin amino-terminal domain

Radixin-binding experiments described in the last section of this chapter were performed in close collaboration with Etchell Cordero and Frank Solomon (MIT). Specifically, I provided GST-layilin fusion proteins and probed the western blots, while Etchell produced the radixin fusion proteins, performed the binding steps, electrophoresed and transferred the samples. Part of this chapter has been published (Appendix B; Borowsky and Hynes, 1998).

"Don't do anything that someone else can do. Don't undertake a project unless it is manifestly important and nearly impossible...so if you succeed, you will have created a whole domain for yourself."

Edwin H. Land

Introduction

Talin's role as a membrane-cytoskeleton linker in focal contacts has been characterized in detail; a short peptide derived from the β1-integrin cytoplasmic domain can block the association of talin with integrins, and three actin-binding domains and three vinculin-binding sites have been mapped in talin (Tapley et al., 1989; Hemmings et al., 1996). Interestingly the integrin-, three vinculin-, and two of the three actin-binding sites in talin are all found within the carboxy-terminal 190 kD calpain "tail" fragment of talin (Horwitz et al., 1986; Gilmore et al., 1993; Hemmings et al., 1996). Microinjected talin tail fragment localizes to focal contacts, suggesting that the known integrin-, vinculin-, and actin-binding sites account for talin's membrane-cytoskeleton linking role in focal contacts (Nuckolls et al., 1990). In contrast, talin's role in membrane ruffles has not been elucidated, although it seems reasonable to project that, as in focal contacts, it connects F-actin to an unknown site on the plasma membrane.

While the tail fragment can account for talin's role in focal adhesions, the role of talin's 47 kD amino-terminal calpain cleavage product ("talin head", amino acids 1-435) is not known. An examination of talin protein sequence from highly divergent organisms reveals that talin's N-terminal domain is the most well conserved region within the sequence. For instance, *C. elegans* and *D. discoideum* talins are 78% and 66% similar to mouse talin within the head domain, but only 59% and 46% similar to mouse talin overall (Kreitmeier et al., 1995; Moulder et al., 1996). This highly conserved segment also contains talin's homology to band 4.1. This sequence conservation may suggest that some conserved function exists for the talin head domain, or it could mean that these proteins share a similar tertiary structure. Experimental analyses of talin head function have given somewhat mixed results. Nuckolls et al. (1990) found that a small fraction of microinjected talin 47 kD domain fragment incorporated into focal contacts while most was diffusely localized in cells; the injected protein had no effect on cytoskeletal morphology, cell spreading or adhesion. However, injected talin tail protein was targeted to focal contacts and also exhibited ectopic localization at cell-cell junctions, where full-length talin is not normally found, suggesting that talin head may enhance targeting to focal contacts or mask other binding sites within talin's tail domain (Nuckolls et al., 1992). In contrast, microinjected glutathione-S-transferase(GST)-talin 47 kD fragment colocalized with

actin filaments and disrupted stress fibers in a majority of cells (Hemmings et al., 1996). Bolton and colleagues generated two anti-talin monoclonal antibodies which, when microinjected into human foreskin fibroblasts, disrupt actin stress fibers, and when injected into chick embryo fibroblasts, significantly inhibit cell migration (Bolton et al., 1997). One of these monoclonal antibodies recognizes an epitope in the talin 47 kD fragment and the other binds a site at the extreme C-terminus of talin.

While the talin head domain appears to play an important role in cell motility and morphology, no specific mechanism has been proposed to explain these observations. Based on the sequence similarity between talin's N-terminal domain and band 4.1 Rees et al. (1990) hypothesized that the conserved talin head domain contained an additional membrane binding site for talin. Previous efforts to identify talin-head binding proteins have not produced candidates. Iodinated talin 47 kD fragment detected no bands in CEF lysates in gel overlay experiments (Nuckolls et al., 1990). Likewise, efforts to detect binding of surface-labeled or metabolically-labeled proteins to immobilized GST-talin head fusion protein were unsuccessful (DiPersio and Hynes, personal communication). Since integrins and talin colocalize in focal contacts, integrins have been considered to be a likely membrane binding site for this domain of talin. However, no β1 integrins were found to bind to columns containing GST-talin head (DiPersio and Hynes, personal communication.)

I decided to search for talin head binding proteins using a novel binding assay, the yeast two-hybrid screen, with the hope that the use of an alternative approach might be productive. In addition, to supplement prior efforts to find talin head binding partners by affinity for a GST-talin head fusion protein, I have screened material bound by a GST-talin head fusion protein for known focal contact proteins. In looking for particular proteins by western blotting, I was able to detect an interaction, not previously observed, between FAK and talin. Furthermore, in a two-hybrid screen I have identified a previously unknown type I integral membrane protein which interacts with talin head, is expressed in all adherent cell lines analyzed, and colocalizes with talin in membrane ruffles. A short motif present in the cytoplasmic domain of this protein is sufficient for talin head binding. This protein also binds at least one other member of the band 4.1 superfamily, radixin. I believe this protein represents a membrane binding site for talin in ruffles, while integrins anchor talin in focal contacts.

Materials and Methods

Yeast two-hybrid screen

Construction of plasmids: Manipulation of DNA was performed according to standard molecular biological protocols (Sambrook et al., 1989). Unless otherwise stated, restriction enzymes and DNA modifying enzymes were purchased from New England Biolabs (Beverly, MA). A pBluescript subclone of a talin cDNA encoding amino acids 1 to 435 (clone A14) was made by partially digesting a chicken talin cDNA with NcoI, digesting with PstI, and cloning the product into pBluescript SK- that had been digested with NcoI and PstI. To make the LexA fusion bait, clone A14 was digested with SacI and EcoRV, the ends polished with T4 DNA polymerase in the presence of 0.1 mM each dNTP at 11 C for 20 mins, and the appropriate fragment ligated into pEG202 that had been digested with EcoRI and rendered blunt by the action of the large fragment of DNA polymerase I in the presence of 0.2 mM each dNTP for 20' at RT (Gyuris et al., 1993). A pJG4-5 subclone of layilin lacking a cytoplasmic domain was made by inserting a synthetic oligonucleotide (2STOPS: CGGTTAATGATCATTAACCG) with two in-frame stop codons into the 3' PvuII site in the longest partial layilin cDNA isolated in the 2-hybrid screen (Gyuris et al., 1993). A pJG4-5 subclone of layilin cytoplasmic domain was made by ligating a PvuII/XhoI layilin cDNA fragment into pJG4-5 that had been digested with EcoRI, Klenow-blunted, and digested with XhoI. A plasmid encoding LexA fused to the type-II TGFβR cytoplasmic domain was the gift of Dr. R. Weinberg, MIT.

Yeast transformation: Yeast strains were cultured according to standard protocols (Guthrie and Fink, 1991). The yeast strain EGY48 (alpha, *his3*, *trp1*, *ura3-52*, lex(*leu2*)3a) was used for library screening and testing various candidate interactors (Gyuris et al., 1993). Yeast transformations were performed using a modified lithium acetate/polyethylene glycol method (Schiestl and Gietz, 1989). Briefly, yeast were grown at 30 °C to 1-2 x 10^7 cells/ml in appropriate media, pelleted at room temperature for 10 minutes at 200 x g, washed once in 50 mls of sterile distilled water, pelleted as above, and resuspended in 1 ml of sterile distilled water. Yeast were quick-spun, washed twice with 1 ml of LiTE (10 mM Tris pH 7.5, 1 mM EDTA, 100 mM lithium acetate) and resuspended in an appropriate volume of LiTE. Fifty µl of the yeast suspension was distributed to microcentrifuge tubes preloaded with 1-2 µg of each

plasmid to be transformed plus 45 μg of sheared, denatured calf thymus DNA. Three hundred μl of PEG/LiTE (10 mM Tris pH 7.5, 1 mM EDTA, 100 mM lithium acetate, 40% PEG 3350) was added to each tube and mixed by pipetting up and down. Each sample was incubated for 30 minutes at 30 C, transferred to 42 C for 20 minutes, then briefly pelleted, resuspended in 300 μl sterile water, and 50-150 μl of this suspension plated on appropriate solid growth media.

Recovery of plasmid DNA from yeast: Plasmids were recovered using a modified "bead-smash" protocol (Hoffman and Winston, 1987). Yeast from a 2 ml overnight culture were pelleted, resuspended in 50 μl STES (0.5 M NaCl, 0.2M Tris pH 7.6, 0.01M EDTA, 1% SDS) and vortexed for 1 minute in the presence of an equal volume of acid washed glass beads (Sigma G8772). Sixty μl of phenol/chloroform (1:1) were added, samples were vortexed, 150 μl additional STES added, and tubes were spun for 5 minutes at 13,000 x g. The aqueous phase was transferred to a fresh tube, extracted once with an equal volume of chloroform, ethanol precipitated in the presence of 0.3 M NaAc pH 5.2, and the pellet washed in 70% ethanol and resuspended in 40 μl of water. Alternatively, one ml of an overnight culture was pelleted, resuspended in 0.5 ml S buffer (10 mM KPO_4 pH 7.2, 10 mM EDTA, 50 mM β-ME, 50 μg/ml zymolyase), incubated for 30 minutes at 37 C, lysed with 100 μl of lysing solution (250 mM Tris pH 7.5, 25 mM EDTA, 2.5% SDS), vortexed, and incubated 30 minutes at 65 C. After 166 μl of 3M potassium acetate were added and the solution chilled on ice for 10 minutes, the samples were spun at 4 C for 10 minutes at 13,000 x g, the supernatant precipitated with 0.8 mls cold ethanol for 10 minutes on ice, the DNA pelleted by spinning as above and resuspended in 40 μl of water. Five μl of plasmid DNA were electroporated into *Escherichia coli* KC8 and selected for growth in the presence of 100 μg/ml ampicillin on minimal growth media supplemented with histidine, uracil, and leucine.

Preparation of yeast protein lysates: Yeast protein lysates were prepared using a modified "bead-smash" method (Solomon et al., 1992). One to two mls of yeast at approximately 10^7 cells/ml were spun briefly at 13,000 x g at room temperature , washed once in 1 ml PBS (137 mM NaCl, 2.7 mM KCl, 8.1 mM Na_2HPO_4, 1.5 mM KH_2PO_4, 0.9 mM $CaCl_2$, 0.5 mM $MgCl_2$)

containing protease inhibitors (1 mM PMSF, 9 TIU/ml aprotinin, 5 micrograms/ml leupeptin), and mixed with one pellet volume of glass beads and 150 ul PBS. The yeast/glass bead suspension was subjected to 5 cycles consisting of 30 seconds vigorous vortexing and 30 seconds on ice. Three hundred µl of PBS and 150 µl of 4x loading buffer were added, and samples were boiled for 10 minutes and then centrifuged for 10 minutes. The supernatants were analyzed by SDS/PAGE and western blotting.

Library screen: The two-hybrid library screen was performed as previously described using the CHO cDNA library pVPCHO (the gift of Dr. V. Prasad, Albert Einstein Medical College, Gyuris et al., 1993). EGY48 containing the LexA-talin bait and the beta-galactosidase (β-gal) reporter plasmid pSH18-34 was transformed with DNA prepared from two pools of pVPCHO library that contained approximately $7.5x10^4$ and $8.2x10^4$ recombinants. Yeast transformants were pooled, frozen in aliquots, and their plating efficiency determined. About 10^6 yeast transformants were plated on synthetic complete medium containing raffinose and galactose as carbon sources, but lacking histidine, leucine, tryptophan and uracil. Forty-eight to ninety-six hours later 244 yeast colonies were picked and assayed for blue color on medium containing X-gal (Boehringer Mannheim, Indianapolis IN). Plasmid DNA was recovered from 40 double-positive (leu^+, $lacZ^+$) colonies, and candidate interactors were sorted into 19 classes based on AluI and HaeIII restriction digestion patterns of the library inserts (Hoffman and Winston, 1987; Gyuris et al., 1993). After retesting representative interactors of each class with negative control baits, 30 of the original 40 clones were deemed worthy of further study. Based on partial sequence data these 30 candidates were determined to comprise 3 cDNAs (Epicentre PCR sequencing kit, Epicentre Technologies, Madison, WI).

Anchored PCR: Primers internal to the longest interactor cDNA recovered from pVPCHO (LECTF1: TGGACAGATGGGAGCACAT and LECTR1: GGAATTCCCCACTTTCTGAAGGGTTC) were used to screen pools of a CHO cDNA library subcloned in pcDNA I (a gift of Dr. M. Krieger, MIT) for the presence of my interactor cDNA (Guo et al., 1994). A fragment of the interactor cDNA was amplified from a positive pool using a 3' primer within the cDNA (LECTR1) and a 5' primer complementary to the T7 promoter present in the vector (T7P: TAATACGACTCACTATAGG), subcloned into

pBluescript, sequenced and found to encode an open reading frame continuous with and overlapping that in the cDNA cloned from pVPCHO. The open reading frame encoded by the PCR product completed the C-type lectin homology present in the original pVPCHO isolate, contained a suitable start codon, and so was deemed likely to be the genuine 5' end of the cDNA.

Northern analysis

Preparation of RNA: CHO RNA was prepared by acid phenol extraction as previously described (Chomczynski and Sacchi, 1987) Poly-A^+ RNA was isolated essentially as described (Bradley et al., 1988). Briefly, 20 x 15 cm dishes of nearly confluent CHO cells were trypsinized, pooled, pelleted and washed with PBS. The cells were resuspended in 20 mls of proteinase K solution (200 μg/ml proteinase K, 0.5% SDS, 100 mM NaCl, 20 mM Tris pH 7.5, 1 mM EDTA), lysed with 3 x 25 second cycles in a Polytron homogenizer (Brinkman Instruments, Waterbury NY), and incubated for 90 minutes at 37 °C. The NaCl concentration was brought to 500 mM and 200 mg of oligo dT cellulose (as a suspension in high salt buffer [0.1% SDS, 500 mM NaCl, 20 mM Tris pH 7.5, 1 mM EDTA]; Pharmacia, Piscataway NJ) was added per 10^9 cells. After mixing for 2 hours at room temperature, the oligo dT cellulose was washed twice in batch with high salt buffer, and poured as a column in a 1 ml syringe plugged at the bottom with sterile glass wool. The resulting column was washed with 10 column volumes of high salt buffer and then eluted with 4 column bed volumes of low salt buffer (0.05% SDS, 20 mM Tris pH 7.5, 1 mM EDTA). The 4 fractions were pooled, heated to 65 °C for 5 minutes, cooled on ice, brought to a final NaCl concentration of 0.5 M, and incubated with a fresh aliquot of oligo dT cellulose for 30 minutes at RT. Washes, column building, elutions, and rebinding were repeated as above twice for a total of three rounds of selection on oligo dT cellulose. On the last cycle, 4 x 300 μl fractions of poly-A^+ RNA were eluted in low salt buffer and ethanol precipitated overnight at -20 °C. RNA was pelleted, washed with 70% ethanol, and resuspended in 50 μl of diethylpyrocarbonate-treated water. Fractions were assayed by ethidium spot testing and fractions 2 and 3 appeared to contain most of the RNA at about 100 ng/μl.

Electrophoresis and transfer: One to ten micrograms of RNA was mixed with 2 volumes of loading buffer (1x MOPS, 6% formaldehyde, 40% deionized formamide), heated to 65 C for 10 minutes, cooled rapidly on ice, and run on an agarose gel (1% agarose, 1xMOPS, 6% formaldehyde). The gel was treated for 40 minutes at room temperature with 50 mM NaOH/10 mM NaCl, neutralized with 2 x 20 minute washes of 0.2 M Tris pH 7.8/18xSSC, and transferred overnight onto Hybond-N nitrocellulose (Amersham Life Sciences, Arlington Heights, IL) with 20xSSC (Alwine et al., 1977). The filter was crosslinked in a Stratagene stratalinker (Stratagene, La Jolla, CA) set on AUTO CROSSLINK, prehybridized for at least 2 hours at 57.5 C in Church-Gilbert buffer (1 mM EDTA, 500 mM $Na_2H_2PO_4$ pH 7.2, 7% SDS, 1% BSA), hybridized overnight in the same buffer containing 10^6 CPM of layilin probe, washed twice at room temperature in 2 x SSC/0.1% SDS and twice at 55C in 0.2 x SSC/0.1% SDS and then exposed on X-OMAT AR film (Kodak, Rochester NY) with an intensifying screen at -80 C.

Synthesis of probes for northern blotting: Ten ng of layilin cDNA clone B1.13 was labeled by random priming. Specifically, the DNA was denatured for 5 minutes at room temperature in 2 mg/ml $pd(N)_6$ and 100 mM NaOH, then brought to reaction conditions (0.8 mg/ml $pd(N)_6$, 40 mM NaOH, 130 mM Tris pH 7.5, 5 mM $MgCl_2$, 10 mM β-ME, 12 μM each dATP, dTTP, dGTP, and 50 μCi α-^{32}P-dCTP, 5 units Klenow fragment) and incubated at room temperature for 2 hours. Unincorporated nucleotides were removed by passing the labeling reaction mixture through a G-50 spin column (TE micro select-D, 5 Prime → 3 Prime, Inc., Boulder CO).

Preparation of polyclonal anti-layilin antisera

Conjugation of peptide antigen to Keyhole limpet hemocyanin (KLH): Conjugation of the antigen was performed using a method similar to Marcantonio and Hynes (1988). Six milligrams of KLH (20 mg/ml, Calbiochem-Behring Corp., La Jolla CA) was added in 0.3 mls to 1 ml of 10 mM KPO_4 pH 7.0 in a small beaker with stirring. Then 0.24 mls of 5 mg/ml sulfo-m-maleimidobenzo(-N-hydroxysuccinimide) ester (sulfo-MBS, Pierce, Rockford IL, in 10 mM KPO_4 pH 7.0) was added dropwise to the stirred KLH solution and then stirred for 30 minutes at room temperature. The solution was run over a G25 column (Pharmacia PD-10) as

follows. All steps were done under gravity flow. The column was equilibrated with 5 bed volumes (approx. 9 mls/bed volume) of 100 mM KPO_4 pH 6.0. Fraction number 1 was collected as the sample was run into the column. Approx. 12 x0.5 mls fractions were collected. Fractions that were blue-gray to the eye (6-8) were judged to contain the activated KLH. A synthetic oligopeptide (LC20) with the sequence CSPDRMGRSKESGWVENEIYY was purchased from the MIT Biopolymer Facility, and 21 mg of this HPLC-purified peptide was dissolved in 3 mls of PBS. Since the peptide was reported to be 75% pure, 21 mg corresponds to 15.75 mg peptide, making the solution approximately 5 mg/ml. The peptide and activated KLH were mixed in a 15 mls centrifuge tube, and the pH was adjusted with 2N NaOH until it reached approximately 7. The solution was mixed gently at room temperature for 3 hours, by which time a white precipitate had formed and the solution was cloudy. The solution was dialyzed against 2 x 4 liters of PBS at 4 C. The final preparation had a protein concentration of 3.15 mg/ml, as assayed using a Bio-rad D_C protein assay kit (Bio-rad, Hercules CA) with BSA as a standard.

Commercial production of immune sera: KLH-conjugated peptide was shipped to Covance (Denver PA) for production of antisera. Two rabbits were given intradermal implants of 0.3 mg antigen, boosted 21 days later with a subcutaneous injection of 0.3 mg antigen and then boosted every 21 days thereafter with a subcutaneous injection of 0.15 mg antigen. Rabbit 618 received a total of 5 boosts and rabbit 619 received a total of 6 boosts. Bleeds were collected 10 days following each boost and then every 2 weeks after the last boost for 4 cycles for rabbit 618 and 9 cycles for rabbit 619. Rabbit 618 produced 168 mls of serum and rabbit 619 generated 225 mls of serum.

Western blotting: Protein samples were electrophoresed on appropriate percentage SDS/PAGE gels and transferred at 4 °C for 90 minutes to Protran nitrocellulose (Schleicher and Schuell, Keene NH; Towbin et al., 1979). Filters were blocked for at least 60 minutes (room temperature) or overnight (4 °C) in blocking buffer (5% Carnation non-fat dry milk reconstituted in PBS/0.1% Tween-20). Blots were incubated either overnight at 4 °C or for 2-4 hours at room temperature with an appropriate dilution of antibody in blocking buffer. Anti-layilin antiserum was used at 1:1000. Blots were washed with PBS/0.1% Tween-20 with at

least 5 changes over 30 minutes at room temperature. Filters were incubated with appropriate HRP-conjugated secondary antibodies (Jackson Immunoresearch Labs, Inc., West Grove PA) diluted 1:2000-1:5000 in blocking buffer for 45 minutes at room temperature and then washed as above. Bands were visualized using the Renaissance chemiluminescence kit (DuPont-NEN, Boston MA) and autoluminography.

Ammonium sulfate precipitation of polyclonal antisera: Eight mls each of the E and F bleeds were pooled, spun 30 minutes at 3000 x g, and the supernatants transferred to small beakers. With all reagents at room temperature, 16 mls of a saturated solution of ammonium sulfate (pH 7.0) was added dropwise to the antiserum, with constant stirring. The mixture was transferred to 40 mls centrifuge tubes and slowly agitated overnight at 4 C. The slurry was spun and 3000 x g for 30 minutes at 4 C. The supernatant was set aside for later analysis and the pellets resuspended by pipetting up and down in 6 mls of PBS. The resuspended pellets were dialyzed overnight at 4 C against 3 changes of PBS. The dialysate was brought to a final volume of 10.5 mls with PBS and spun at 30,000 x g for 30 minutes at 4 C.

Immobilizing the peptide antigen for affinity purification: Fifteen mg of HPLC-purified LC20 peptide was dissolved in coupling buffer (100 mM Tris pH 8.0, 500 mM NaCl, 1 mM EDTA) at a final concentration of 6 mg/ml. Eight mg of DTT was dissolved in the peptide solution and the resulting solution was incubated with gentle shaking at room temperature for 72 hours to reduce the thiol group in the amino-terminal cysteine. The peptide solution was spun for 5 mins at room temperature at 13000 x g and then desalted by passage over a Sephadex G15 (Pharmacia) column with a bed volume of 20 mls. The column was equilibrated in coupling buffer and run at a flow rate of 10 mls/hour. 1.5 mls fractions were collected and assayed for peptide with a Bio-rad protein assay. Fractions 6-9 were pooled and coupled to 3.5 mls thiopropyl-Sepharose 6B (Pharmacia) prepared as follows. One gram of thiopropyl-Sepharose 6B was swollen in 200 mls degassed distilled water for one hour, washed four times with 20 mls distilled water on a sintered-glass filter, and equilibrated in degassed coupling buffer. The reduced peptide was incubated with the thiopropyl-Sepharose 6B in a 15 mls conical bottom tube with gentle mixing overnight at room temperature. The slurry was washed on a sintered-glass filter 4 times with 50 mls coupling buffer, 2 times with 50 mls blocking buffer (100 mM

sodium acetate pH 4.5), 10 times with 50 mls blocking buffer containing 1.2 mM β–ME, and 2 times with 50 mls blocking buffer. The thiopropyl-Sepharose 6B conjugated peptide (LC20) was divided into 2 aliquots of about 1.5 mls each and poured as two columns each in a 10 mls dispo column. The columns were washed with 300 mls of PBS and stored at 4 C in 0.02% azide in PBS.

Affinity purification: A thiopropyl-Sepharose 6B (Pharmacia) column with covalently-coupled LC20 was washed sequentially with 15 mls of: 10 mM Tris pH 7.5 under gravity flow, 100 mM glycine pH 2.5 at 25 mls/hour, 10 mM Tris pH 7.5 at 25 mls/hour. Ammonium sulfate-precipitated antiserum was applied to the column at 20 mls/hour. The flow rate was increased to 25 mls/hour and the eluate recirculated on the column for 30 minutes, so that the antiserum ran over the column a total of three times. On the last cycle the depleted serum was collected and saved for use as a control for the affinity-purified antiserum. The column was washed at 25 mls/hour with 30 mls of 10 mM Tris pH 7.5 and then 30 mls of 500 mM NaCl in 10 mM Tris pH 7.5. Antibody was eluted in 1.2 mls fractions with 100 mM glycine pH 2.5 into 1.5 mls microcentrifuge tubes pre-loaded with 1M Tris pH 8.0 sufficient to neutralize the glycine.

Preparation of tissue lysates

Organs dissected from an adult female mouse were washed twice with cold PBS, resuspended in an equal volume of homogenization buffer (100 mM NaCl, 10 mM Tris pH 7.5, 1 mM EDTA, 1 mM PMSF, 9 TIU/ml aprotinin, 5 micrograms/ml leupeptin) and homogenized on ice with an electric grinder (Kontes, Vineland NJ) in 1.5 ml microcentrifuge tubes. An equal volume of 2xRIPA buffer (1xRIPA: 1% Triton X-100, 1% sodium deoxycholate, 0.1% SDS, 158 mM NaCl, 10 mM Tris pH 7.5, 1 mM EGTA, 1 mM PMSF, 9 TIU/ml aprotinin, 5 micrograms/ml leupeptin) was added, samples were vortexed, incubated on ice for 60 minutes, boiled for 10 minutes, spun at 13,000 x g at 4 °C for 10 minutes, and assayed for total protein using a detergent-compatible protein assay (Bio-rad). An equal mass of each sample was analyzed by western blotting.

Avidin depletion

Three 10 cm dishes of nearly confluent CHO cells (10^7 cells) were washed with PBS, and cells were released with versene (0.02% EDTA, PBS, phenol red), pooled, washed twice with PBS, and diluted to a density of $5x10^6$/ml with PBS. The sample was divided into two parts, and DMSO containing 10 mg/ml EZ-Link sulfo-NHS-LC-biotin (Pierce) was added to one half of the sample, while DMSO alone was added to the other half, and cells were rocked gently for 60 minutes at room temperature (Isberg and Leong, 1990). Cells were washed three times with 1 ml of Tris wash buffer, lysed in 1.5 mls RIPA buffer, sheared through a 26 gauge needle to reduce viscosity, and spun for 10 minutes at 4 °C and 13,000 x g to remove insoluble debris. Two 1 ml syringes plugged with glass wool were packed with 200 µl of Immunopure Immobilized Monomeric Avidin (Pierce) poured as a 33% slurry and prepared according to the manufacturer's instructions. The columns were loaded with 200 µl of biotin-labeled or mock-labeled lysate, capped and incubated at room temperature for 76 minutes, and then PBS applied to each column as three 200 µl fractions were collected. Equal volumes of each eluted fraction were analyzed by western blotting.

Surface labeling and immunoprecipitation

RIPA lysates from surface-biotinylated CHO cells were prepared as described above. Lysate from $8x10^5$ cells was mixed with 50 µl of protein A Sepharose CL-4B (as a 1:1 slurry in RIPA buffer; Pharmacia), 1 µl of anti-layilin antiserum or control serum, and 1 mg of heat-inactivated BSA in RIPA buffer in a total volume of 450 µl. After incubation at 4 °C overnight with end-over-end mixing, the Sepharose was washed 5 times with 1 ml RIPA buffer. Each sample was divided into two parts and one part was treated with peptide: N-glycosidase F (PNGase F) according to the manufacturer's instructions (New England Biolabs). Samples were boiled for 10 minutes in 1x gel loading buffer, spun for 10 minutes at 13,000 x g at room temperature, electrophoresed on 7.5% acrylamide gels, and transferred to nitrocellulose filters. Filters were blocked overnight at 4 °C in blocking buffer (5% non-fat dry milk reconstituted in PBS/0.1% Tween-20), rinsed twice and then washed once for 5 minutes with PBS/0.1% Tween-20, incubated for 45 minutes at room temperature with HRP-streptavidin (Amersham Life Science) diluted 1:2000 in PBS/0.1% Tween-20, rinsed twice and then washed once for 15

minutes in PBS/0.1% Tween-20, followed by 5 x 10 minute washes in PBS/0.1% Tween-20. Bands were detected using chemiluminescence (DuPont-NEN).

GST fusion binding

Plasmid construction: The GST-chicken talin 1-435 fusion (GST-CT) was made by ligating a BamHI/EcoRI fragment from chicken talin clone A14 into BamHI/EcoRI digested pGEX-2T (Pharmacia). Deletions within this region of talin were made by either digesting this construct with appropriate enzymes or by generating PCR products within it. Specifically, to make GST-CT 1-94, GST-CT was cut with SphI and EcoRI, blunted with Klenow and religated. To produce GST-CT 280-435, GST-CT was cut with BglII and BamHI, blunted with Klenow and religated. To generate GST-CT 1-280, GST-CT was cut with BglII and EcoRI, blunted with Klenow and religated. To create GST-CT 187-435, GST-CT was cut with ClaI and BamHI, blunted with Klenow and religated. The insert for GST-CT 187-357 was derived from GST-CT 187-435 using PCR with a primer starting at the codon for amino acid 357 (CTR1: CGAATTCGATGTTGGTCAGGCTCC) and a primer in the vector (pGEX1: TTGCAGGGCTGGCAAGC). The insert for GST-CT 225-435 was synthesized by PCR using a primer starting at the codon for amino acid 225 (CTF1: CGGATCCGGCTCCCACCCCGTC) and a primer in the vector (pGEX2: GCTGCATGTGTCAGAGG). Each PCR product was digested with BamHI and EcoRI and ligated into BamHI, EcoRI digested pGEX-2T. In order to make the GST-layilin cytoplasmic domain fusion containing amino acids 261-374, a pBluescript subclone of layilin cDNA was made that extends from the 3' XhoII site to the 3' end of the cDNA, with the XhoII site blunted and ligated to the pBluescript EcoRV site and the 3'end of the layilin cDNA cloned into the pBluescript XhoI site. The construct was digested with EcoRI and XhoI, and the appropriate fragment was cloned into EcoRI/XhoI cut pGEX-5X-1 (Pharmacia). The GST-layilin 244-335 fusion was made by amplifying the cDNA encoding those amino acids with primers LECTF2 (GGAATTCTCAGCTGCATGTTGGGTT) and LECTR1, digesting the PCR product with EcoRI, and subcloning the fragment into EcoRI-digested, phosphatase-treated pGEX-5X-1. The GST-layilin 330-374 fusion was made by amplifying a pBluescript subclone of the layilin cDNA with a 5' primer starting with the codon for amino acid 330 (LECTF3: GGAATTCAACCCTTCAGAAAGTGGGTT) and T7P. The PCR product was digested with EcoRI and XhoI and the resulting fragment ligated into pGEX-

5X-1 which had been digested with EcoRI and XhoI. The GST-(LH23)x3 fusion was made by self-ligation of a double-stranded oligomer consisting of top strand LH23T (GATCCTTGAGAGTGGATTTGTGACCAATGACATTTATGA) and bottom strand LH23B (GATCTCATAAATGTCATTGGTCACAAATCCACTCTCAAG), digestion with BamHI and BglII, and ligation of the resulting multimerized oligomer into pGEX-5X-1 that had been digested with BamHI and treated with shrimp alkaline phosphatase(Boehringer Mannheim). All GST-talin and GST-layilin fusion protein constructs were confirmed by sequence analysis. The GST-fibronectin(FN) constructs have been described previously (Peters et al., 1995).

Protein preparation: Bacterially-expressed GST-fusion proteins were prepared essentially as described (Smith and Johnson, 1988) A saturated overnight culture of DH5α containing the plasmid of interest was diluted 1:10 in LB/AMP and grown for 3 hours with shaking at 37 C. 1 M IPTG was added to a final concentration of 1 mM and cultures were grown an additional 2 hours. Cells were harvested by centrifugation at 4 C for 5 mins at 4500x g, the pellets resuspended in 10 mls cold PBS per 200 mls culture volume, sonicated in 10 ml aliquots in a 50 mls conical bottom tube on ice for 5 mins at 0.5 seconds on/0.5 seconds off, 15% power. 1/10 vol. 10% TX-100 was added, and PMSF added to 1mM, aprotinin added to 2.2 μg/ml (9 trypsin inhibitor units/ml), and leupeptin added to 5 μg/ml. Samples were vortexed briefly and then spun at 30,000 x g for 20 mins at 4 C. The supernatant was mixed with about 250 μl of packed, preswollen glutathione agarose (Sigma, St. Louis MO) for 3 hours at either room temp or 4 C, washed four times in 10 mls PBS, and stored as a 1:1 slurry in PBS at 4 C for up to 4 weeks prior to use.

Affinity isolation: Detergent lysates of either CHO, NIL8 or their transfected derivatives were made by scraping and pooling cells, washing with Tris wash buffer (50 mM Tris pH 7.5, 150 mM NaCl, 1 mM $MgCl_2$, 1 mM $CaCl_2$) and then lysing on ice for 20 minutes with 1 ml of lysis buffer (0.1% TX-100, 0.3 M sucrose, 50 mM Tris pH 7.5, 100 mM KCl, 1 mM $CaCl_2$, 2.5 mM $MgCl_2$, 1 mM PMSF, 9 TIU/ml aprotinin, 5 micrograms/ml leupeptin) per 10^7 cells. The lysate was centrifuged at 13,000 x g for 10 minutes at 4 °C, and then precleared with 500 μl of packed glutathione-agarose (pre-equilibrated in lysis buffer) per ml of lysate for 30 minutes at 4 °C. For peptide blocking experiments, 5 mg/ml peptide in PBS was added to a final

concentration of 1 mg/ml to the cleared lysate and the mixture incubated on ice for 20 minutes. Five hundred microliters of cleared lysate were added to 50 µl of glutathione-agarose preloaded with each GST-fusion protein and rotated end-over-end for 1 hour at 4 °C. The samples were centrifuged briefly, the supernatants removed, and the glutathione-agarose pellets washed four times with 500 µl lysis buffer without detergent. The glutathione-agarose pellets were then boiled for 10 minutes in an equal volume of 1x gel loading buffer and analyzed by western blotting (Towbin et al., 1979).

Radixin-binding experiments:

All steps were performed at 4 °C. Binding of layilin in CHO cell lysates to immobilized recombinant radixin or radixin fragments was performed as described for binding to GST-CT above except that his-tagged radixin fragments (provided by Etchell Cordero) bound to nickel-Sepharose were used instead of GST-talin bound to GSH-agarose. Direct binding between recombinant radixin and layilin was detected as follows: 0.2 nmoles of his-tagged radixin (or N- or C-terminal fragments thereof) were incubated with 40 µl of a 1:1 slurry of Ni-Sepharose in buffer I (300 mM NaCl, 50 mM $NaPO_4$, 20 mM imidazole pH 8.0) for ~30 minutes in a total volume of 250 µl. The supernatant was removed, the beads were washed once with buffer I, resuspended in 225 µl, and 0.2 nmoles of GST-layilin (261-374) were added in 25 µl of PBS. After ~30 minutes, beads were washed 3 times in buffer V (300 mM NaCl, 50 mM $NaPO_4$, 40 mM imidazole pH 8.0, 10% glycerol), and bound material eluted for 10 minutes in buffer VII (300 mM NaCl, 50 mM $NaPO_4$, 250 mM imidazole pH 8.0). Samples were diluted in gel loading buffer and equal aliquots of each sample analyzed by western blotting with an antibody directed against GST. In some experiments, his-tagged radixin N-terminal domain was preincubated with 0.2, 0.4, or 2.0 nmoles of his-tagged radixin C-terminal domain, and the mixture added to beads, washed, and then mixed with layilin fusion protein as described above. To assay effects of phospholipids on radixin-layilin binding, his-tagged full-length radixin was preincubated with 15 or 50 µM of either phosphatidyl-inositol-phosphate or phosphatidyl-choline for ~30 minutes and then processed as described above for binding to GST-layilin (261-374).

Generation of cell lines expressing epitope-tagged layilin

A hemagglutinin(HA)-tagged version of layilin was made by inserting a synthetic EcoRI linker (New England Biolabs) into the 5' PvuII site in the layilin cDNA. An oligonucleotide encoding the sequence EFYPYDVPDYASPEF was ligated into the EcoRI linkered form of layilin, and this construct was confirmed by DNA sequencing (Wilson et al., 1984). The tagged layilin cDNA was transferred into the expression vector pLEN-neo and the resulting construct transfected into cells using standard calcium-phosphate protocols.

Immunofluorescence

Cells were plated on glass coverslips coated with 5 μg/ml human plasma fibronectin (Beckton Dickinson, Bedford MA), and incubated for 15 minutes to detect ruffles in spreading cells, overnight to obtain well-spread cells, or several days to achieve high cell density for *in vitro* wounding experiments. Spreading cells were stained prior to fixation and permeabilization, although identical staining patterns were observed when staining was performed on fixed and permeabilized cells. Otherwise cells were stained after fixation and permeabilization as follows. Coverslips were washed three times in PBS, fixed for 10 minutes in 4% paraformaldehyde in PBS, washed as above, permeabilized for 10 minutes in 1% Brij 99 (Fluka, Ronkonkoma NY) in PBS, washed as above, blocked with 10% normal goat serum (NGS, Vector Laboratories, Inc., Burlingame CA) in PBS for 30 minutes at 37 °C, incubated with primary antibody diluted in 10% NGS/PBS for 30 minutes at 37 °C, washed as above, incubated with fluorescently-labeled secondary antibodies (Biosource International, Camarillo CA) and fluorescently-labeled phalloidin (Sigma) as appropriate, for 30 minutes at 37 °C, washed as above, rinsed once in water and mounted in gelvatol (Monsanto, St. Louis MO) containing DABCO (Sigma) to prevent fading. For peptide blocking experiments, antibodies were preincubated on ice with an appropriate peptide at 1 mg/ml for at least 30 minutes. Antibodies were used at the following dilutions: anti-layilin, 1:200; TD77 (anti-talin), 1:100; 12CA5 (anti-HA-tag), 1:2000; secondary antibodies, 1:200, phalloidin, 1:5000. Monoclonal antibody TD77 was the gift of Dr. D.R. Critchley, University of Leicester (Bolton et al., 1997). In some experiments stained cells were viewed on a Zeiss Axiophot and immunofluorescent images were recorded on Kodak film or digitally captured with an Optronics DEI-750 CCD camera. The results of some experiments were recorded digitally on a Zeiss Axioplan 2

equipped with a Photometrix CCD camera and IPLab Spectrum software. For wounding experiments, confluent monolayers grown on fibronectin-coated coverslips were scraped under warm PBS with a rubber policeman to remove approximately half of the monolayer and returned to a 37 °C/5% CO_2 incubator for 45-90 minutes until prominent phase-dark ruffles were observed (Nuckolls et al., 1992).

Preparation of T-cells

The spleen or lymph nodes were dissected from a healthy male BALB/C mouse, and cells were dispersed mechanically by forcing the organ through a nylon mesh screen. After 2 washes in PBS + Ca/Mg, cells were resuspended in RPMI/10% fetal calf serum. Cells were spun for 20 minutes at room temperature and 1200 x g onto a lympholyte M cushion. Lymphocytes were recovered from the media/lympholyte interface, washed twice with RPMI/10% fetal calf serum, and plated in 10 mls of RPMI/10% fetal calf serum on a 10 cm plastic tissue culture dish. After 1 hour at 37 C/5% CO_2, non-adherent cells were removed and passed over a column consisting of about 1 gram of nylon wool. Non-adherent cells were eluted with RPMI/10% fetal calf serum, adjusted to 10^6/ml and cultured in the presence of 5 μg/ml concanavilin A for 48 hours. Cells were washed 4 times with RPMI/10% fetal calf serum and returned to culture in the presence of 4 ng/ml of recombinant human IL-2 for 10-12 days. Cells were plated in a small volume onto glass coverslips (which had been pre-treated with 20 μg/ml human plasma fibronectin) and incubated for 45 minutes at 37 C/5% CO_2. Samples were fixed and processed for immunofluorescence as described above.

Results

Misexpression of talin-head has cell-type specific effects

In order to elucidate the function of talin's 47 kD N-terminal fragment, NIH3T3 and CHO cells were transfected with a plasmid which constitutively expresses mouse talin head domain bearing a hemagglutinin (HA) epitope tag at its C-terminus (MT-HA). NIH3T3 cells were transfected with either MT-HA or a plasmid which expresses an HA-tagged form of radixin (HAC-RAD; Henry et al., 1995). No stable clones which expressed MT-HA were obtained in several experiments, although clones expressing tagged radixin were recovered. An appropriately sized band was detected on western blots from cells transiently transfected with MT-HA, indicating that the fusion protein is made. Cells were examined at early times after transient transfection; cells expressing MT-HA were relatively rare and always exhibited morphology of a weakly adherent cell (figure 2-1c). In contrast, mock-transfected cells or those transfected with HAC-RAD were flat. HA staining of MT-HA transfectants revealed brightly stained cells with strong signal throughout the cell (figure 2-1c). Cells expressing HAC-rad had positively stained apical membrane projections (figure 2-1b). Untransfected cells showed some faint perinuclear staining (figure 2-1a).

Whereas no NIH3T3 clones were obtained that expressed MT-HA, several stable cell lines were recovered from transfected CHO cells. In these cells, MT-HA was distributed throughout the cytoplasm with some increased staining in peripheral membrane ruffles (figure 2-1d). The establishment of cell lines stably misexpressing the talin head domain indicates that this fragment of talin does not inevitably disrupt cell adhesion or spreading. CHO cells, which are capable of growth in suspension, may be more tolerant of manipulations which disrupt cytoskeleton or adhesion than are NIH3T3 cells.

Identification of a talin-head-binding partner by a yeast two-hybrid screen

Given talin's homology to other members of the band 4.1 superfamily, Rees et al. (1990) hypothesized that talin's N-terminal domain, like those of band 4.1 and ERM proteins, would bind to an integral membrane protein. Since previous biochemical efforts to find such a talin-head-binding protein yielded no candidates, I used a LexA-based yeast two-hybrid system to find talin-head-binding proteins (Nuckolls et al., 1990; Gyuris et al., 1993). I generated a LexA-talin fusion protein containing the band 4.1 homologous region of chicken talin (amino-

acids 1-435, LexA/CT 1-435). Western analysis indicated that yeast carrying a 2μ plasmid encoding LexA/CT 1-435 express a protein of the expected size (70 kD) not expressed in the parental yeast strain or yeast expressing LexA alone (figure 2-2). This fusion protein, neither alone nor when co-expressed with the B42 acidic transcriptional activator, activated either the leu2 or β-gal reporter genes (TABLE 1, figure 2-6B, and data not shown). Based on results from a transcriptional repression assay I inferred that the LexA/CT 1-435 bait binds DNA in the nucleus (Gyuris et al., 1993, figure 2-3). In this assay, an indicator yeast strain (EGY40) exhibits inducible lacZ gene expression and β-gal activity when yeast are grown on galactose. If these yeast also express a LexA fusion protein capable of entering the nucleus and binding to LexA binding sites inserted between the promoter and start of transcription β-gal induction is inhibited. The yeast strain expressing the LexA/CT 1-435 fusion protein exhibits 4-fold lower inducibility, suggesting that the LexA/CT 1-435 bait contains a functional LexA DNA-binding domain and enters the yeast nucleus.

I screened approximately 10^6 yeast colonies representing about 10^5 cDNAs from a CHO cDNA library with this LexA-talin head bait and picked 40 colonies which displayed both leucine prototrophy and the ability to activate a lacZ reporter. After grouping the 40 cDNAs into classes based on Alu and HaeIII restriction patterns I recovered representative cDNAs from each class and retested them with LexA/CT 1-435 and a panel of four negative control LexA-fusion protein baits (LexA-max, LexA-bicoid, LexA-sec16p, LexA-TGFβR; Zervos et al., 1993; Espenshade et al., 1995). These controls were chosen because each has demonstrable DNA-binding and/or protein-protein binding activity in yeast. I recovered 30 cDNAs comprising a total of three genes which reproduced leucine prototrophy and β-gal activation when cotransformed into yeast with the talin bait but not with the negative controls (TABLE 1). Of these 3 genes, two encoded short translational fusion proteins with no homology to proteins in the GENBANK database. One of these short fusions was recovered once, and is most likely an artifact. The second was represented by four cDNA fragments with identical 5' ends; this observation suggests that all four colonies may be progeny of a single primary transformant, or alternatively, that this cDNA fragment is well represented in the library. Homology searches of GENBANK revealed this cDNA to be homologous to a ubiquitin conjugating enzyme cDNA. This interactor cDNA was fused to a sequence at the

extreme 3' untranslated region of the gene, and so it was deemed likely to be another artifact of the screen.

The remaining 25 candidate interacting sequences were overlapping fragments of a previously unidentified cDNA. Partial sequence analysis revealed that this cDNA contained a novel ORF with potentially interesting homologies. The cDNAs recovered from the yeast screen lacked 5' untranslated sequences and a start codon. The 5'-most sequences encoded part of domain homologous with C-type lectins but lacking the N-terminal extent of a complete carbohydrate recognition domain (CRD). In order to obtain additional 5' sequences, I screened pools of a pcDNA-CHO library for the presence of an internal PCR fragment of the cDNA and then cloned the 5' end of the cDNA from two positive pools using anchored PCR (Guo et al., 1994). The final assembled sequence contains a start codon embedded in a Kozak consensus and encodes a complete CRD-homologous domain (figure 2-4A). Northern analysis with probes derived from the resulting 1777 bp cDNA detected a single 1800 nucleotide (nt) band evident in CHO poly-A^+ and total RNA (figure 2-5). Upon longer exposure, a similarly-sized band is evident in total RNA prepared from NIH3T3 fibroblasts, suggesting cross-species conservation of the gene.

The cDNA contains an open reading frame predicted to encode a 374 amino acid protein of estimated molecular mass 43 kD (figure 2-4A). The protein has an amino-terminal signal sequence and predicted cleavage site typical of a secreted or transmembrane protein, a 130 amino acid domain with significant homology to C-type lectin carbohydrate-recognition domains (CRD), a 30 amino acid hydrophobic span suggestive of a transmembrane domain, and a 120 amino acid C-terminal domain containing three novel repeated motifs and two YXXΦ motifs similar to those known to allow AP-2-mediated recycling of some transmembrane proteins (von Heijne, 1986; Letourneur and Klausner, 1992; Drickamer, 1993). I named this protein *layilin* based on the sequence "LAYILI" found in its putative transmembrane domain.

Since talin is a cytosolic protein a physiologically relevant interaction between layilin and talin must be mediated by layilin's putative cytoplasmic domain. Each of the seven independent layilin cDNAs recovered and sequenced contains the cytoplasmic domain of layilin, suggesting that the layilin cytoplasmic domain is sufficient for talin binding. I confirmed this by testing the cytoplasmic domain and the extracellular and transmembrane

domains separately in the two-hybrid assay. Expression of three B42-layilin fusion proteins was confirmed by western blotting with an antibody to the HA-epitope tag (figure 2-6A). The fusion protein spanning most of the layilin extracellular domain, the transmembrane domain, and the stop-transfer sequence (amino acids 92-244) was expressed at relatively high levels, while that consisting of only the layilin cytoplasmic domain (amino acids 244-374) was expressed less well. Despite relatively low expression levels, the layilin cytoplasmic domain alone (amino acids 244-374) conferred leucine prototrophy and activated the LacZ reporter whereas the B42-fusion which contains most of layilin (amino acids 92-244), but lacks the cytoplasmic domain, did not.

A comparison of layilin's C-type lectin homologous sequences with the CRDs of two known C-type lectins is shown in figure 2-4B. Layilin contains 14/14 residues found in all carbohydrate-binding C-type lectins and an additional 18/20 highly conserved residues (Drickamer, 1993). One of the two nonconserved residues, V141, corresponds to an oxygen-containing residue which coordinates one of two calcium ions bound by some C-type lectins (Weis et al., 1991b). However, not all lectins use this calcium-binding site, and the absence of an oxygen-containing side chain at position 141 suggests that layilin lacks this second calcium-binding site (Graves et al., 1994). Interestingly, layilin contains a 5 amino acid insertion relative to the mannose-binding protein CRD (amino acids 148-152 of layilin, figure 2-4B, underline), which is of the same size and at the identical position as an insertion found in the E-selectin CRD. The inserted sequences in the E-selectin CRD form a loop which projects into the ligand-binding pocket, and mutation of these sequences disrupts selectin-mediated adhesion (arrow, figure 2-7; Graves et al., 1994). Layilin contains an additional 7 amino acid insertion adjacent to the 5 amino acid insertion which may form part of the same loop (figure 2-4B, double underline). Layilin shows approximately 40% amino acid similarity to all other CRDs examined; the presence of a selectin-like insertion raises the possibility that layilin may bind to ligand in a manner similar to selectins. Layilin also differs from other CRDs by an insertion of 7 amino acids relative to the mannose-binding protein CRD (amino acids 102-108 of layilin, figure 2-4B, broken underline). This insertion falls in sequences which form the first of four large calcium-binding loops in other CRDs and is distal to the proposed ligand-binding site (double arrow, figure 2-7).

The 45 amino acids between the CRD homology and the putative transmembrane domain are rich in negatively charged amino acids (11/45), prolines (7/45), and S/T residues which may serve as O-linked carbohydrate attachment sites (10/45). These characteristics are suggestive of an elongated stalk which serves to project the CRD away from the plasma membrane.

Potential human and pig layilin homologs present in the expressed sequence tag (EST) database indicate conservation among different species of some layilin sequence features. First, a pig EST encodes a protein that includes most of the layilin CRD (figure 2-4C). This potential homolog is 80% identical and 88% similar to hamster layilin and includes the insertions discussed above. In addition, both hamster and pig layilin sequences contain E134 and S136, residues of some value in predicting the carbohydrate specificity of CRDs (see discussion). The second candidate layilin homolog is encoded by two human ESTs and overlaps the layilin cytoplasmic domain (figure 2-4D). The 92 amino acid hypothetical human protein is 73% identical and 83% similar to hamster layilin and contains three copies of the long repeat and a single copy of each of the short cytoplasmic domain motifs. Alignment of the human and hamster cytoplasmic domains reveals that the human version lacks the C-terminal 20 amino acids, precisely those used in my peptide antigen. This may explain my inability to detect layilin protein in human cell lines with my antibody (see below).

Production of polyclonal anti-layilin antiserum

A synthetic peptide containing the C-terminal 20 residues of layilin (LC20) was coupled to keyhole limpet hemocyanin (KLH) and sent to Covance for the production of polyclonal antiserum. Serum from rabbits 618 and 619 exhibited immunoreactivity in western blotting experiments with appropriate bands in lysates from *E.coli* expressing a GST-layilin cytoplasmic domain fusion protein and so were characterized further (data not shown). Detergent lysates from CHO cells were subjected to immunoblotting with sera from both rabbits in the absence or presence of the layilin-derived peptide LC20 (figure 2-8A). No bands were detected by pre-immune sera from either rabbit (not shown). As shown, 618 sera reacted with several bands in CHO cell lysates, including two or more bands migrating at approximately 55 kD that were also recognized by serum from rabbit 619 (figure 2-8A, arrowhead). This is consistent with the predicted layilin molecular weight of 43 kD.

Moreover, these bands were competed from both sera by the LC20 peptide. Two bands recognized by 618 were not competed by the peptide, indicating that they are recognized by contaminating antibodies present in the serum. Transfection of the layilin cDNA increased the signal of the 55 kD bands recognized by both 618 and 619 but not other bands (figure 2-11A). For these reasons it was concluded that the 55 kD bands represent endogenous layilin.

The antisera were affinity purified on immobilized LC20 peptide to improve their specific signal. Panels B and C of figure 2-8 show results of affinity purification for serum from rabbits 618 and 619, respectively. The activities of the affinity purified antisera on western blots are shown in lanes 6 and 7, and the corresponding depleted sera are shown in lanes 5. Serum from rabbit 618 was efficiently depleted of reactivity with a contaminating band migrating at about 70-80 kD while the other bands were effected partially or not at all. These observations suggest that these bands cross-react with anti-layilin antibodies; no immunoreactivity was recovered in two attempts to elute antibodies from these bands. Serum from rabbit 619 exhibited specificity for the 55 kD bands similar to that seen before purification, except that background staining present throughout the lane was significantly reduced (compare lanes 3 and 6 in figure 2-8C). This general background staining was recovered in the depleted serum, as shown in lane 5 of figure 2-8C. Affinity purified 619 serum and its control depleted serum were used for all further characterization of layilin.

Layilin protein is widely expressed in cells and tissues

To find out whether layilin, like talin, is expressed in a variety of cell lines and cell types, I screened numerous cultured cell lines and mouse tissues for the presence of layilin protein. The antiserum detected an immunoreactive protein of approximately the same size as hamster layilin in several rodent cell lines tested but not in human cells (figure 2-9A). The cross-reacting band in three rat cell lines tested migrated slightly faster than the band in hamster lysates, indicating a molecular weight difference of about 4 kD (figure 2-9A). This could represent differential glycosylation (see below) or a deletion or alteration in the polypeptide itself. My inability to detect layilin-reactive protein in human cells might be explained by the sequence of the candidate human layilin homolog described above.

I found detectable levels of layilin in most of the 12 mouse tissues analyzed by western blotting (figure 2-9B). Layilin was most abundant in ovary, and readily detectable in most

other solid tissues assayed. These observations indicate that layilin, like talin, is widely expressed in adherent cell types both *in vitro* and *in vivo*.

Layilin is a glycoprotein expressed on the cell surface

The presence of a putative signal sequence and transmembrane domain suggested that layilin would be found on the cell surface. I tested this hypothesis by immunoprecipitation from surface-labeled CHO cell lysates. The anti-layilin antiserum immunoprecipitates from lysates of surface-biotinylated CHO cells a 55 kD band whose size is in good agreement with the band detected by western blotting of whole cell lysates with the same antibody (arrowhead, figure 2-10A). Similar results were obtained with NIL8 hamster fibroblasts (figure 2-12B). Peptide-depleted serum does not immunoprecipitate any surface-labeled material from biotin-labeled CHO cells, and the 55 kD band precipitated by the antiserum is competed by preincubating the affinity-purified antiserum with a layilin-derived peptide (figure 2-10A and data not shown). The surface-labeled band immunoprecipitated by anti-layilin antiserum is sensitive to treatment with PNGase F, indicating the presence of N-linked carbohydrates (figure 2-10 panel A, compare the last two lanes; Maley et al., 1989). Immunoprecipitation from the same lysate of β1 integrin indicates both effective surface-labeling and enzymatic cleavage of carbohydrate chains from β1 and associated α integrin subunits (left most lanes of figure 2-10A). The anti-HA epitope monoclonal 12CA5 immunoprecipitates a similarly sized, surface-labeled, PNGase F sensitive band from both CHO and NIL8 cells expressing HA-tagged layilin (figures 2-11B and 2-12B, and data not shown).

Western blotting of CHO cell lysates treated with PNGase F shows a shift in the mobility of the band detected by anti-layilin antiserum similar to that seen in surface-labeled material, confirming that I am observing the same band by both surface label and western blotting and indicating that most of the cellular pool of layilin is glycosylated (figure 2-10B). As a positive control I show that PNGase F efficiently trims N-linked carbohydrates from both mature and precursor forms of β1 integrin in cell lysates, as indicated by the collapse of the two forms of integrin in untreated lanes into a single, more rapidly migrating band in the treated sample (top panel of figure 2-10B). PNGase F-treated layilin migrates slightly slower than predicted based on its deduced amino acid sequence (51 kD vs. 43 kD); this discrepancy

may reflect additional post-translational modifications to layilin, such as O-linked glycosylation, or may simply result from aberrant electrophoretic migration.

I used accessibility to a membrane non-permeable biotinylation reagent to assess the proportion of total layilin present on the cell surface. A population of CHO cells was divided into two parts and one was surface-labeled with sulfo-NHS-LC-biotin while the other was subjected to the same surface-labeling protocol in parallel without addition of the biotin. Lysates made from these two samples were applied to identical columns of immobilized avidin to capture any proteins which reacted with the surface-labeling reagent, thereby depleting surface proteins from the extracts. The flow-throughs from these columns were then analyzed by western blotting for β1-integrin and layilin (figure 2-10C). The integrin control indicates that the avidin column efficiently removed all of the mature, surface-expressed β1-integrin (arrow, figure 2-10C) from the labeled lysates (lanes 2-4) without affecting the amount of precursor β1-integrin (which is not expressed on the surface, asterisk figure 2-10C). In contrast, the avidin column did not deplete either form of β1-integrin from mock-labeled lysates (figure 2-10C, lanes 5-7). By assaying the same fractions for layilin I found that the majority of layilin was depleted in the biotin-treated sample as compared to the unbiotinylated control, indicating that most layilin protein is on the cell surface (figure 2-10C, bottom panel, compare lanes 2-4 with lanes 5-7).

Layilin localization

Concurrent with production of the polyclonal antisera described above, I engineered a hemagglutinin epitope tag into the full length layilin protein to facilitate characterization of its subcellular distribution. I inserted the HA epitope in the extracellular domain immediately amino-terminal to the putative lectin domain. I reasoned that the signal sequence cleavage site was likely to be far enough away so as not to be affected by nor to result in the cleavage of the tag. CHO cells either transiently- or stably-transfected with an expression vector encoding the tagged form of layilin express the expected fusion protein. The monoclonal anti-HA antibody 12CA5 detects a cluster of bands migrating at approximately 55 kD in CHO cells transiently transfected with the construct (figure 2-11A, open arrowhead). Cells transfected in parallel with full length layilin cDNA lacking an epitope tag resemble untransfected cells on an anti-HA western blot (figure 2-11A). Probing of the same cell lysates with affinity-purified anti-

layilin antibodies reveals that CHO cells transiently transfected with DNA encoding either untagged or epitope-tagged layilin have an increased signal in bands migrating around 55 kD (solid arrowhead in figure 2-11A). This is consistent with the hypothesis that 12CA5 and the anti-layilin antibody are both detecting the same material. The bands produced by cells making HA-tagged layilin migrate slightly slower than do endogenous or transfected untagged layilin, consistent with the presence of an HA tag. Expression of particularly high levels of tagged (or untagged) layilin results in an increase in a slightly faster migrating band as well. This band corresponds to the size of PNGase F-treated layilin, and may represent unprocessed layilin precursor. Surface expression of epitope-tagged layilin is demonstrated in figure 2-11B. Immunoprecipitation from surface-biotinylated extracts of untransfected and stably-transfected CHO with antibodies against the HA tag reveal that transfected cells have high levels of HA-tagged layilin on their surface. Anti-layilin antibodies also immunoprecipitate significantly more layilin from transfectants than from untransfected controls. The material immunoprecipitated by 12CA5 also migrates slightly more slowly than does endogenous layilin, consistent with a slightly larger polypeptide. The band immunoprecipitated by anti-layilin antibodies appears to be approximately the sum of the more rapidly migrating endogenous layilin band plus the more slowly migrating HA-tagged form of the protein. Similar immunoblotting and immunoprecipation analysis of stably-transfected NIL8 hamster cells is shown in figure 2-12, indicating that proper expression of this tagged protein is not unique to CHO cells.

Immunolocalization of HA-tagged layilin in stable CHO transfectants shown in figure 2-13. Cells were plated on fibronectin-coated coverslips, allowed to spread for 50 minutes and double-labeled with 12CA5 and a polyclonal anti-talin antiserum (N681). Both antibodies stain peripheral ruffles evident around the edge of these cells (figure 2-13 panels a-c). In addition, 12CA5 gives rise to perinuclear staining similar to that seen in transiently transfected cells. The diffuse cytosolic signal evident in the talin staining is probably background. Secondary antibody produced only faint background (figure 2-13d) and anti-transferrin receptor antibodies stained the perinuclear region and gave a diffuse membrane signal (figure 2-13e). The latter control indicates that diffuse membrane expression is not sufficient to give rise to ruffle staining. These cells were subjected to similar staining after fixation in

paraformaldehyde but with varied permeabilization steps. Essentially identical staining was observed after permeabilization with NP40, Brij 99, and acetone (figure 2-14).

I also analyzed layilin subcellular distribution in NIL8 hamster fibroblasts which have a well-articulated actin cytoskeleton that has been extensively characterized (Hynes and Destree, 1978; Mautner and Hynes, 1977). To confirm the specificity of my observations, I examined the distribution of both HA-tagged and endogenous layilin. Colocalization of HA-tagged layilin with F-actin in stable NIL8 transfectants is shown in figure 2-15. Spreading cells exhibit prominent phalloidin-positive ruffles around their perimeter which also stain with 12CA5. Note the absence of 12CA5 background signal in ruffles on negative cells in the same field (for example, arrow, figure 2-15, panels a,c,e). Colocalization of HA-tagged layilin with talin in membrane ruffles is also evident in NIL8 cells shortly after plating (figure 2-15, panels b,d,f). Evidence of layilin in peripheral ruffles of spreading cells raised the possibility that layilin is present in extending membrane sheets (i.e. lamellipodia) in general. I next examined the distribution of HA-tagged layilin in NIL8 cells which had been induced to migrate in an *in vitro* wounding model. Cells were plated at high density and allowed to adhere and spread overnight, forming a confluent monolayer. Portions of the coverslip were denuded with a rubber scraper to create stripes of cells alternating with strips of the coverslip free of cells. After incubation for 45-90 minutes, the majority of cells on the edge of these "wounds" were migrating into them, with approximately 10-30% of cells exhibiting prominent phase-dark ruffles. These ruffles stained positively with the anti-HA antibody and with the affinity-purified anti-layilin antiserum (figure 2-16, panels a-c). In addition to staining ruffles, the anti-layilin antibody also stains nuclei. Examination of mitotic cells suggests the cross-reacting nuclear antigen is in chromatin.

In the experiment shown in figure 2-16, I included competing peptide to block either 12CA5 (figure 2-16, panels d-f) or the affinity-purified anti-layilin antibody (figure 2-16, panels g-i). A peptide containing the HA epitope blocked 12CA5 staining but not anti-layilin staining. Similarly, the peptide used as antigen to raise anti-layilin antisera blocked the anti-layilin signal without affecting the 12CA5 staining. In each case, staining with the other antibody confirms the presence of a layilin-containing ruffle. The combination of this experiment with western blotting and surface labeling experiments validates the specificity of the affinity-purified anti-layilin antibody.

Immunolocalization of endogenous layilin in untransfected NIL8 cells agrees well with the subcellular distribution of HA-tagged layilin. Depleted anti-layilin antiserum was used as a negative control for the affinity-pure antibody. The depleted serum gives rise to nuclear and some diffuse membrane and/or cytosolic staining but does not stain prominent phalloidin-rich ruffles (arrowheads, figure 2-17, panels a-c). In contrast, the affinity-purified antibody stains ruffles and colocalizes with phalloidin staining. The cell shown in figure 2-17 (panels d-f) is extending two lamellipodia at right angles to one another, each showing strong layilin staining at its leading edge (panel d). Phalloidin staining confirms that F-actin is also concentrated in these structures (figure 2-17f). I did not observe specific stress-fiber staining with the anti-layilin antiserum in well-spread cells exhibiting prominent stress fibers. Hence, endogenous layilin, like epitope-tagged layilin, is present at the leading edge of extending membranes. The antibody also gives rise to significant nuclear background and stains the midbody. Signals in the nucleus and the midbody are probably artifacts of the antiserum as I saw no nuclear or midbody staining with 12CA5 in cells expressing HA-tagged layilin. Furthermore, biochemical analyses, which suggest that layilin is predominantly on the cell surface, are inconsistent with the presence of significant levels of layilin in the nucleus.

Colocalization of layilin with talin in ruffles

I used double-label immunofluorescence to see whether layilin colocalizes with talin in focal contacts or membrane ruffles. Both spreading-induced and migration-driven ruffles were analyzed. I induced leading edges in NIL8 cells by scraping monolayer cultures. The resulting ruffles show strong staining with the anti-talin monoclonal TD77, confirming earlier reports of talin in ruffling membranes (figure 2-17i; Burridge and Connell, 1983; DePasquale and Izzard, 1991; Bolton et al., 1997). In the same cells, talin is also readily seen in focal contacts arrayed behind the leading edge (arrows, figure 2-17, panels h-i). Layilin staining is clearly visible in the same ruffles which contain talin but is not evident in focal contacts (arrows, figure 2-17g). The coincidence of talin and layilin staining in these cells is indicated by yellow staining in the merged image of layilin and talin immunofluorescence, while the green focal contacts confirm that talin but not layilin is found in focal contacts (figure 2-17h). Endogenous layilin also colocalized with talin in NIL8 cells allowed to adhere and spread for a short time (figure 2-17,

panels j-l). Again, talin was evident in both ruffles and nascent focal contacts whereas layilin was only present in ruffles (arrows, figure 2-17, panels j-l).

Layilin localization in polarized mouse T-cells

Several cell-cell adhesion molecules and some associated submembranous cytoskeletal proteins have been shown to polarize in cytokine activated T-cells. Under these conditions, T-cells adhere to fibronectin-coated coverslips through small but very flat leading edges and develop a dorsal protrusion termed the uropod. I found that CD43, a potential regulator of cell-cell adhesion, became concentrated in the uropod upon treatment of cells with recombinant RANTES, confirming earlier reports (figure 2-18, panel c; Serrador et al., 1998). In addition, I found that the monoclonal antibody 13H9, which can detect ezrin, radixin, moesin, and merlin, stained both the uropod and the leading edge of polarized T-cells (figure 2-18e). In contrast, anti-layilin antibody did not show appreciable uropod staining in the same cells (figure 2-18, panels d and f).

GST-talin-head fusions bind layilin and FAK

To confirm and characterize further the interaction between talin and layilin I tested the ability of several GST fusion proteins containing either talin or layilin sequences to bind layilin or talin, respectively, in detergent extracts from CHO cells. In each experiment, samples were assayed by Coomassie staining to ensure equal loading of GST fusion proteins. GST-layilin fusions containing amino acids 261-374 and 330-374 of the layilin cytoplasmic domain retained a fraction of intact talin in CHO detergent lysates whereas a GST-layilin fusion containing amino acids 244-335 and a negative control GST-fusion containing a fibronectin type III repeat (GST-FN EIIIB) did not (figure 2-19A). Moreover, the GST-layilin fusions distinguished between the full-length talin protein and a prominent proteolytic fragment present in the lysate by binding to only the full-length talin polypeptide. This fragment is probably the 190 kD C-terminal talin fragment which lacks the layilin-binding domain altogether. These observations indicate that the minimal talin binding site is within amino acids 330-374. This region of layilin includes three copies of the motif ESG(F/W)V (LH2) and two N(D/E)IY repeats (LH3), with each LH3 repeat adjacent to an LH2 repeat (figure 2-4A). Talin binds to a GST fusion protein containing 3 copies of a tandem array of the LH2+LH3

repeats found at amino acids 343-352 of layilin (figure 2-19A). In addition, a synthetic peptide (LC20) derived from the C-terminal 20 amino acids of layilin and containing one copy of the LH2+LH3 module found at amino acids 364-373, blocks binding of talin to GST-layilin 330-374 (figure 2-19A). In contrast to LC20, an unrelated peptide containing the HA epitope does not block binding of talin to the GST-layilin fusion protein (figure 2-19A). These observations confirm that talin binds layilin through one or more LH23 motif.

Acidic phospholipids have been reported to modulate binding between band 4.1 superfamily members and their membrane docking sites. I found no effect of 50 μM phosphatidyl-serine, phosphatidyl-inositol-4-phosphate (PI-4-P), or phosphatidyl-inositol-4,5-bisphosphate on talin binding to LH23 repeats (PI-4,5-P_2; figure 2-19B). As expected, there was no binding of talin to a GST-FN negative control either (figure 2-19B). Binding of vinculin to talin has also been reported to increase in the presence of PI-4-P and PI-4,5-P_2, but I saw no binding of vinculin either directly or indirectly to GST-(LH23)x3 fusion protein in the absence or presence of phospholipids (figure 2-19B). The latter result may be interpreted as a specificity control for the GST-(LH23)x3 fusion protein.

I also observed reciprocal binding of layilin to GST-talin fusions. Figure 2-20A (lower panel) shows that glutathione-agarose preloaded with a GST fusion protein containing amino acids 1-435 of talin (GST-CT 1-435), the same talin fragment used as the LexA-talin head bait, binds layilin in CHO extracts whereas glutathione-agarose loaded with equal amounts of a control GST-fibronectin fusion protein does not. The GST-CT fusion also binds HA-tagged layilin in extracts prepared from NIL8 cells expressing epitope-tagged layilin. Using the monoclonal 12CA5 to detect the epitope tag, I found that GST-talin fusions which include amino acids 280-435 can specifically retain HA-tagged layilin from a cell lysate (figure 2-20B, upper panel). A form of HA-tagged layilin lacking the cytoplasmic domain does not show binding to GST-CT above background, suggesting that this interaction is dependent on the layilin cytoplasmic domain (figure 2-20B, bottom blot).

I used this GST-talin fusion protein to determine if other focal contact proteins bound to talin head. I examined the material bound to the talin and control fibronectin GST-fusions for the presence of other focal contact proteins and found that FAK bound to talin's N-terminal domain (figure 2-20A, top blot). This confirms and extends previous reports of an interaction between FAK and talin (Chen et al., 1995; Zheng et al., 1998). I did not detect any binding of

α-actinin, tensin, tubulin, vinculin, paxillin, or β1-integrin to GST-CT 1-435 or to GST-FN EIIIB (figure 2-20C and data not shown). As specificity controls, three GST-FN type III fusions were assayed for FAK binding and found to be negative (figure 2-20C). Attempts to confirm the talin-FAK interaction by co-immunoprecipitation and two-hybrid were unsuccessful (figure A-4 and data not shown).

I used this assay to map the sequences within talin head sufficient for layilin and FAK binding (figures 2-20A and 2-20B). Layilin bound to each GST-talin fusion containing at least amino acids 280-435. FAK bound well to GST-fusions which include amino acids 186-435 and weakly to shorter fusions overlapping amino acids 225-357, including the fusion protein containing only amino acids 225-357. Hence amino acids 225-357 contain a minimal FAK-binding site, and amino acids 280-435 constitute the smallest layilin-binding site tested. The FAK-binding site maps entirely within talin's band 4.1 homologous domain, and the layilin-binding site overlaps this region while including more C-terminal talin sequences. The fact that these binding sites are distinguishable confirms the specificity of each interaction.

Interaction of layilin with radixin (in collaboration with E. Cordero and F. Solomon)

Given the sequence similarity (approximately 30%) between talin's N-terminal domain and the members of the ERM family of membrane-cytoskeleton linkers, and in light of the observation that layilin and ERMs are both found in membrane ruffles, I chose to assess the potential biochemical interaction between layilin and one member of the ERM family, radixin. In a solid-phase binding experiment parallel in design to those described in the previous section, I found that bacterially-expressed his-tagged radixin N-terminal domain (homologous with talin's N-terminal domain) was able to bind layilin in detergent extracts of CHO cells (figure 2-21A). His-tagged radixin C-terminal domain, in contrast, bears no sequence homology to talin and also does not bind layilin above background binding seen with the solid Sepharose support (figure 2-21A). Interestingly, full-length his-tagged radixin did not bind layilin in this assay either (figure 2-21A). Further *in vitro* binding studies were carried out to determine if the layilin-radixin interaction is direct. Purified bacterially-expressed GST-layilin (261-374) binds to purified bacterially-expressed his-radixin N-terminal domain but not his-radixin C-terminal or his-radixin full length proteins (figure 2-21B). Purified GST did not bind his-radixin (figure 2-21B).

Previous studies on ERM proteins suggest that they can exist in at least two conformations, one of which prevents binding of at least some ligands to the N-terminal domain (Gary and Bretscher, 1995; Magendantz et al., 1995; E. Cordero and F. Solomon, personal communication). We speculated that the layilin-binding site in the radixin N-terminal domain might be subject to such regulation. This model was tested by incubating purified his-radixin N-terminal domain and GST-layilin in the presence of increasing amounts of radixin C-terminal domain and assaying the relative amount of layilin bound. Figure 2-21C shows that increasing doses of C-terminal domain correlate with reduced binding of GST-layilin to radixin N-terminal domain. This could result from direct competition of layilin and radixin C-terminal domain for identical or nearby binding sites in radixin's N-terminal domain or it could be a secondary consequence of conformational changes within radixin's N-terminal domain brought about in the presence of the C-terminal domain.

Binding between radixin's N- and C-terminal fragments can be inhibited by acidic phospholipids. If an interaction between radixin's N- and C-domains blocks a layilin binding site, disruption of the radixin interdomain interaction should create a layilin binding site. The GST-layilin cytoplasmic domain fusion protein showed increased binding to his-tagged full length radixin in the presence of micromolar concentrations of PI-4-P (figure 2-21C). These observations support a model for layilin-radixin binding in which layilin binding is regulated by an intramolecular interaction within radixin. Furthermore, the finding that layilin can bind radixin raises the possibility of more widespread interaction of layilin with other band 4.1 family members.

Discussion

Talin was discovered as a component of focal contacts and the leading edge of migrating cells, but the molecular basis of its role in ruffles is unknown (Burridge and Connell, 1983). Similarly, the significance of talin's band 4.1 homology, initially observed when the talin cDNA was reported (Rees et al., 1990), has not been revealed. The discovery of layilin, an integral membrane protein found in ruffles, which binds to talin's band 4.1 homologous domain, confirms the hypothesis of Rees et al. that this domain of talin contains a membrane-binding site and suggests a specific function for talin in the leading edge of migrating cells as an adaptor between the membrane and F-actin. A role for talin in migration was initially suggested by its subcellular localization in ruffles and demonstrated by the inhibitory effect of microinjecting anti-talin antibodies into cells along the edge of a wound (Nuckolls et al., 1992; Bolton et al., 1997). Microinjection of a monoclonal antibody (TA205) raised against a fusion protein containing amino acids 139-433 within talin head domain also inhibits cell motility, further implicating this talin fragment in cell motility (Bolton et al., 1997). The monoclonal antibody TA205 recognizes a GST-talin fusion containing amino acids 1-186, placing the epitope between amino acids 139-186 (my unpublished observations); I have identified binding sites for both FAK and layilin adjacent to this antibody binding site which may account for its inhibitory activity (figure 2-20). Talin's role in the dynamic aspects of membrane-cytoskeletal junctions in vertebrate cells is underscored by the observation that localized disruption of talin in neuronal growth cones prevents the formation of new membrane extensions (Sydor et al., 1996). By binding to integrins and layilin, two types of transmembrane proteins with distinct subcellular distributions, talin may be able to distinguish between the relatively static membrane-cytoskeletal connections in focal contacts and the highly dynamic membrane-actin linkages in ruffles. How the talin-layilin interaction is regulated by, or contributes to, the control of membrane-cytoskeleton associations should be explored further.

Models for layilin function

Given the colocalization of layilin with talin and the observed binding between them, layilin is a good candidate for a membrane-binding site for talin in ruffles. I observe colocalization of both epitope-tagged and endogenous layilin with talin in actin-rich membrane ruffles (figures 2-13, 2-14, 2-15, and 2-17). Bacterially-expressed GST-talin fusion proteins

bound layilin in cell lysates, and, in parallel experiments, GST-layilin cytoplasmic domain fusions bound talin in cell lysates (figures 2-19 and 2-20). These results, in addition to my initial finding that talin and layilin interact in a yeast two hybrid assay, are consistent with a direct interaction between the two proteins. Moreover, direct binding between layilin and radixin was observed (figure 2-21). Layilin contains significant homology to proteins with C-type lectin activity. Carbohydrate recognition domains have been found in both type I (N-terminus extracellular) and type II (N-terminus cytoplasmic) single-pass transmembrane proteins (Drickamer and Taylor, 1993). Known type I C-type lectins fall into two functional groups: cell-cell adhesion molecules of the selectin family, and endocytic receptors such as the macrophage mannose receptor. This observation, combined with my initial characterization of the layilin protein, leads me to suggest two general models for layilin function.

In the first model layilin acts in cell migration by anchoring to the membrane talin, which in turn binds F-actin. This chain of interactions may transmit force from actin to the membrane, resulting in its characteristic deformation into ruffles. In this scenario, layilin may serve simply as a talin docking site, or it could be an early-acting adhesion molecule which binds extracellular matrix, nucleating the formation of focal contact precursors at the cell periphery. In this case layilin would be functioning analogously to selectins, which mediate transient adhesion between rolling leukocytes and the endothelium followed by tight integrin-mediated adhesion. However, whereas selectins mediate cell adhesion in specialized cells of the immune system, I hypothesize that layilin performs fundamental cell adhesion tasks common to most cells because layilin and talin are present in many different tissues (figure 2-9). Layilin would thus form transient adhesion sites between ruffles and extracellular matrix which are refined into focal contacts after integrin recruitment. This could occur in both spreading and migrating cells. Talin, which can bind both layilin and integrins, may provide continuity between the two types of cell-matrix linkages as transient layilin-containing structures mature into integrin-containing focal adhesions. Integrin extracellular matrix receptors are known to be signaling as well as adhesion receptors, and if layilin encounters matrix early in the process of cell adhesion it may also signal. The three internally-repeated motifs in the layilin cytoplasmic domain are potential binding-sites for cytoskeletal or signaling molecules in addition to talin. The conservation of these motifs in hamster and

human layilins suggests that they are of importance, and I have shown that two of these repeats form a binding-site for talin (figure 2-19).

It is interesting to note that the C-type lectin CRD is structurally homologous to another carbohydrate-binding domain, the link module (Kohda et al., 1996). Link modules are found in a variety of carbohydrate-binding proteins, including CD44, one of the proteins reported to bind to the N-terminal domain of ERMs (Tsukita et al., 1994). CD44 has also been proposed to function in cell migration and tumor metastasis (Sherman et al., 1994). It is notable that several members of the band 4.1 superfamily interact with the cytoplasmic domain of known or suspected carbohydrate-binding molecules implicated in migration and adhesion.

In a second model layilin may function as an endo- or phagocytic receptor, similar to some other C-type lectins such as the macrophage mannose receptor (Drickamer and Taylor, 1993). This model is suggested by the observation that talin is present in phagocytic cups in macrophages and at sites of uptake of some bacterial pathogens (Greenberg et al., 1990; Finlay et al., 1991; Finlay et al., 1992; Young et al., 1992; Love et al., 1998). In addition, the layilin cytoplasmic domain contains two YXXΦ motifs (YNVI, YDNM, figure 2-4A). These motifs are similar to sequences that mediate clathrin-dependent endocytosis of other membrane proteins by binding to the μ2 chain of the AP-2 adaptor complex (Ohno et al., 1995; Marks et al., 1997). Although AP-2 complexes do not bind a GST-layilin cytoplasmic domain fusion (data not shown), AP-2 complexes are not generally able to bind their targets in an affinity isolation assay (T. Kirchhausen, personal communication). Layilin may act simply by binding to and internalizing ligands bearing an appropriate carbohydrate moiety, or it may have additional functions in recruitment or stabilization of cytoskeleton in phagocytic ruffles. Alternatively, talin might stabilize a complex consisting of layilin and its bound ligand during uptake. Again I would postulate that, given its widespread expression pattern in tissues, layilin participates in some general mode of uptake not limited to macrophages or other professional phagocytes. These two models, adhesion and uptake, are not mutually exclusive.

Speculations on layilin carbohydrate binding

Although it is impossible to predict the carbohydrate specificity of a C-type lectin based solely on its amino acid sequence, some parallels between layilin and other CRDs suggest potential sugar-binding preferences for layilin. The layilin CRD shares 4/5 residues known to

form the calcium- and ligand-binding pocket in rat MBP-A (boldface, figure 2-4 panel B; Weis et al., 1992). These are layilin amino acids E134, E141, N164, and D165, which correspond to amino acids E185, E193, N205, and D206 in MBP-A. The MBP-A ligand pocket also contains N187, which is not conserved in the layilin sequence. The MBP-A ligand binding site can accommodate sugars with 2 consecutive equatorial hydroxyls stereochemically equivalent to the mannose 3' and 4' hydroxyls, accounting for all known MBP-A carbohydrate ligands (Weis et al., 1992). Glutamate 185 and N187 of MBP-A coordinate the mannose 3' OH while E193 and N205 perform the same function for the 4' OH (figure 2-7B; Weis et al., 1992). The significance of N187 is revealed by the mutant N187D, which still binds calcium but not carbohydrates (Quesenberry and Drickamer, 1992). This is presumably because the aspartate side chain can coordinate the calcium but cannot serve as a hydrogen bond donor to the mannose hydroxyl. The importance of E185 and N187 in determining ligand specificity is demonstrated further by the E185Q/N187E double mutant which mimics the sequence of galactose-binding CRDs (Drickamer, 1992). This mutant MBP binds galactose with higher affinity than it does mannose (Drickamer, 1992). While this mutant does not exhibit carbohydrate binding specificity equivalent to naturally occurring galactose-binding lectins, this experiment shows that these two amino acid positions strongly influence sugar preferences in C-type lectins. Layilin has a serine at the position equivalent to N187 of MBP-A, which, like N187, can act as both a hydrogen bond donor and acceptor. However, the serine functional group is expected to be recessed relative to an asparagine side chain in the same position since serine has one fewer carbon than does asparagine. Based on this simple model, layilin might be expected to bind to sugars topologically similar to the 3' and 4' OH of mannose, but carrying a substitution at the 3' position which extends into the opening in the binding site created by the serine.

The CRD-like domain of the FcεRII has a threonine at position 187, similar to the serine at this position in layilin. The FcεRII CRD binds Ig Fc regions independent of carbohydrate and binds to N-linked carbohydrates present on CD21 (Vercelli et al., 1989; Aubry et al., 1992; Aubry et al., 1994). This parallel underscores the possibility that this domain of layilin, despite its suggestive sequence homology, may not bind a carbohydrate ligand at all.

Implications for the band 4.1 superfamily

The band 4.1 superfamily members merlin and ezrin/radixin/moesin are present in membrane ruffles, and down regulation of ERM proteins by treatment of cells with antisense oligonucleotides results in reduced cell adhesion (Takeuchi et al., 1994b; Henry et al., 1995). This defect may be causal or may be a secondary consequence of reduced cell spreading. In collaboration with Etchell Cordero and Frank Solomon, I have found that a purified bacterially-expressed GST-layilin cytoplasmic domain fusion protein binds purified recombinant radixin head domain (figure 2-21). The scope of interactions between layilin and members of the band 4.1 superfamily has not yet been defined, but raises additional potentially interesting roles for layilin. Previous reports of binding between band 4.1 family members and membrane proteins implicate clustered basic residues as binding sites for band 4.1 and ERMs. Jöns and Drenckhahn found that band 4.1 binds to the basic sequence LRRRY in the cytoplasmic domain of the erythrocyte anion exchanger, one band 4.1 membrane docking site in red blood cells (Jöns and Drenckhahn, 1992). Marfatia and colleagues showed that mutation of three membrane-proximal basic residues in the glycophorin C cytoplasmic domain abrogates binding *in vitro* between protein 4.1 and peptides derived from glycophorin C (Hemming et al., 1995; Marfatia et al., 1995). Recently, short basic sequences in the cytoplasmic domains of CD44, CD43, and ICAM-2 were identified that appear to mediate binding to ERM proteins (Legg and Isacke, 1998; Yonemura et al., 1998). Interestingly, as shown in figure 2-19, talin binds to ten amino acids derived from two repeated motifs within the layilin cytoplasmic domain (ESGFVXNDIY). This binding site does not contain the membrane proximal or any other stretch of basic residues in layilin, demonstrating another mode of binding between band 4.1 family members and integral membrane proteins. I am collaborating with Etchell Cordero and Frank Solomon to determine if the ten amino acid talin-binding site within the layilin cytoplasmic domain is also a radixin-binding site.

The interaction of band 4.1 with glycophorin C is enhanced in the presence of poly-phosphoinositides (Anderson and Marchesi, 1985). A mechanism for this regulation is suggested by studies on ERM proteins demonstrating binding between ERM head and tail domains that is reversed in the presence of acidic phospholipids (Gary and Bretscher, 1995; Magendantz et al., 1995; Hirao et al., 1996). Radixin-layilin binding *in vitro* is subject to similar regulation (figure 2-21). Although no such regulated head-tail interaction has been

described for talin, talin's N-terminal domain has been reported to bind some phospholipids under conditions of low ionic strength (Niggli et al., 1994). In addition, talin undergoes a conformational change from a globular structure to an elongated rod in response to changes in salt concentration, which may represent a transition from a closed to an open form of the protein with different abilities to bind talin-binding partners (Molony et al., 1987; Winkler et al., 1997). I would have circumvented this mode of regulation with my recombinant LexA- and GST-fusion proteins which contain only talin head. Recent reports that ERM localization and head-tail association can be influenced by phosphorylation of ERMs suggest a potential mode of regulation that could be applied to talin and is consistent with observed talin phosphorylation (Pasquale et al., 1986; Turner et al., 1989; Beckerle, 1990; Bertagnolli et al., 1993; Tidball and Spencer, 1993; Matsui et al., 1998; Shaw et al., 1998). Moreover, radixin phosphorylation is another possible method of regulating access of layilin to radixin's N-terminal domain. It will be of interest to determine whether binding of talin to layilin or FAK is regulated by either phospholipid binding or talin phosphorylation.

In conclusion, I have uncovered novel functions for the talin head domain, analogous with those of the homologous N-terminal domains of other band 4.1 family members: the interaction with layilin in ruffles and the binding of FAK. This talin domain therefore acts both as a membrane linker and in signal transduction, while the tail of talin binds a different membrane anchor (integrins) and forms links to the cytoskeleton.

Table 1: Interaction of candidate talin-binding proteins with positive and negative controls

	LexA fusion partner									
	CT 1-435		max		TGFβRII		sec16p		bcd	
Clone	leu	βgal	leu	βgal	leu	βgal	leu	βgal	leu	βgal
A1.6	0	1	0	0	0	0	0	1	1	3
A1.10	1	0	1	0	0	0	0	0	0	0
A1.19 [b]	0	0	0	0	0	0	0	0	0	3
A1.28	3	3	0	0	0	0	0	1	0	0
A1.31	3	3	0	0	0	0	0	1	0	0
A1.36	3	3	0	0	0	0	0	0	0	1
A1.49	0	0	0	0	0	0	0	0	0	0
A1.51	2	3	0	0	0	0	1	0	0	0
A1.52	3	3	0	0	0	0	3	0	0	0
A1.53	0	0	0	0	0	0	0	0	0	0
B1.2	3	3	0	0	0	0	2	0	0	0
B1.4	3	3	0	0	0	1	0	1	0	0
B1.10	3	3	0	0	0	1	0	0	0	0
B1.19	3	3	0	0	0	0	1	1	0	0
B1.20	3	3	1	0	0	0	0	0	0	0
B1.23 [b]	1	1	0	0	0	0	0	0	0	0
B1.37	1	3	0	0	0	0	2	1	0	1
B1.51	0	0	0	0	0	0	0	0	0	0
B1.53a [a]	3	3	0	0	0	0	0	0	0	0
B1.53b [a]	0	0	0	0	0	0	0	0	0	0
B1.57	3	0	3	0	0	0	0	0	0	0
Mxi1	0	0	2	3	0	0	0	0	0	1

Yeast cotransformed with the indicated 2-hybrid primary clones (first column) and each of five control bait plasmids (top row) were patched in triplicate onto galactose/raffinose media to induce expression of the candidate interactor and scored for either leucine prototrophy (left hand columns) or blue color (right hand columns). The number of positive patches is indicated. Clones highlighted in grey were pursued further.

[a]Two plasmids were recovered from clone B1.53: plasmid a had a 1.2 kb insert while plasmid b had a 0.6 kb insert. Both plasmids were retested.

[b]These isolates were discarded because these yeast strains showed leucine prototrophy in the absence of galactose induction and did not retest positive for blue color.

Figure 2-1: Expression of talin 47 kD domain in NIH3T3 and CHO cells. NIH3T3(a-c) and CHO (d) cells were stained with the anti-HA antibody 12CA5. Cells are untransfected (a), transiently transfected with HA-radixin (b) HA-talin head (c), or stably-expressing HA-talin head (d). Bar = 10 microns.

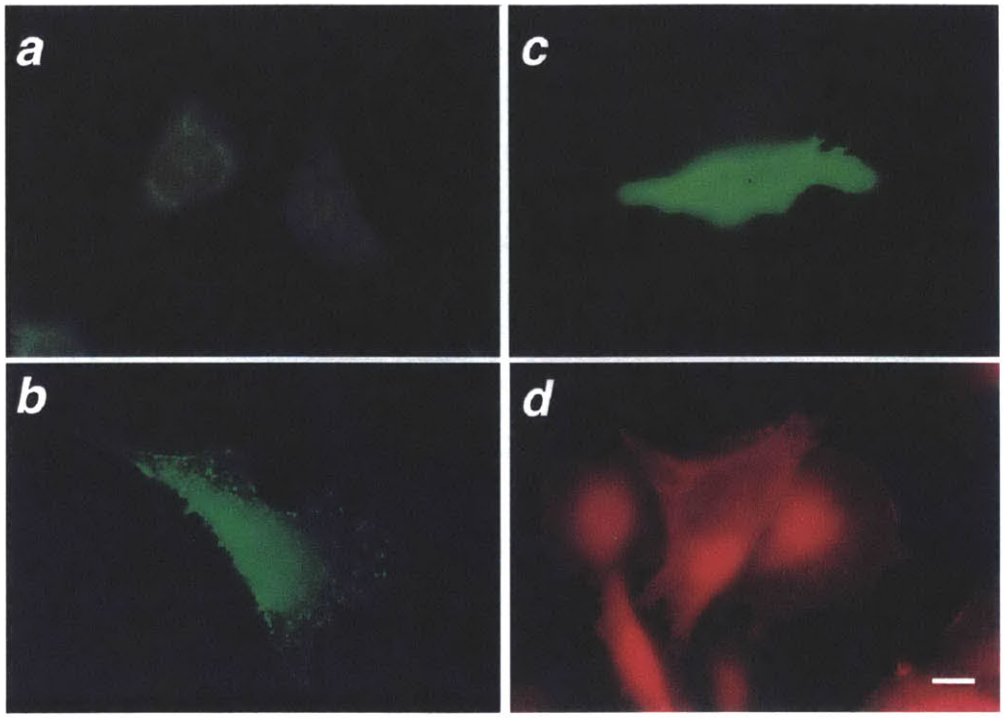
a
c
b
d

Figure 2-2: Talin head 2-hybrid bait is expressed in yeast. Anti-lexA immunoblot of lysates from parental yeast strain EGY48 and EGY48 transformed with a plasmid encoding the LexA-talin bait.

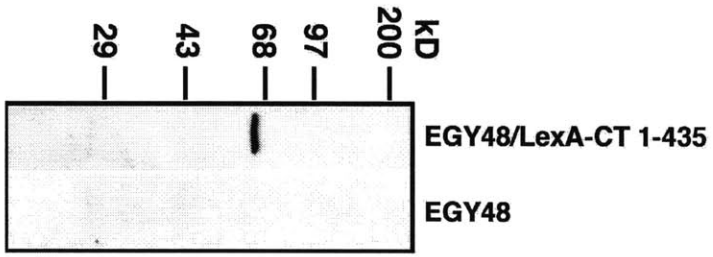
29
43
68
97
200
kD
EGY48/LexA-CT 1-435
EGY48

Figure 2-3: Quantitation of β-galactosidase activity in yeast strain EGY40 in the absence or presence of the LexA-talin bait. Comparison of LexA-CT and control strains under induced conditions shows a 4-fold repression of β-galactosidase activity in the presence of the LexA-talin fusion ($p=0.04$, student's t-test). The LexA-CT-expressing strain induces β-gal to a level 51-fold over uninduced compared to a 744-fold induction for the control strain. Each bar represents the average of three samples, and one standard deviation is indicated.

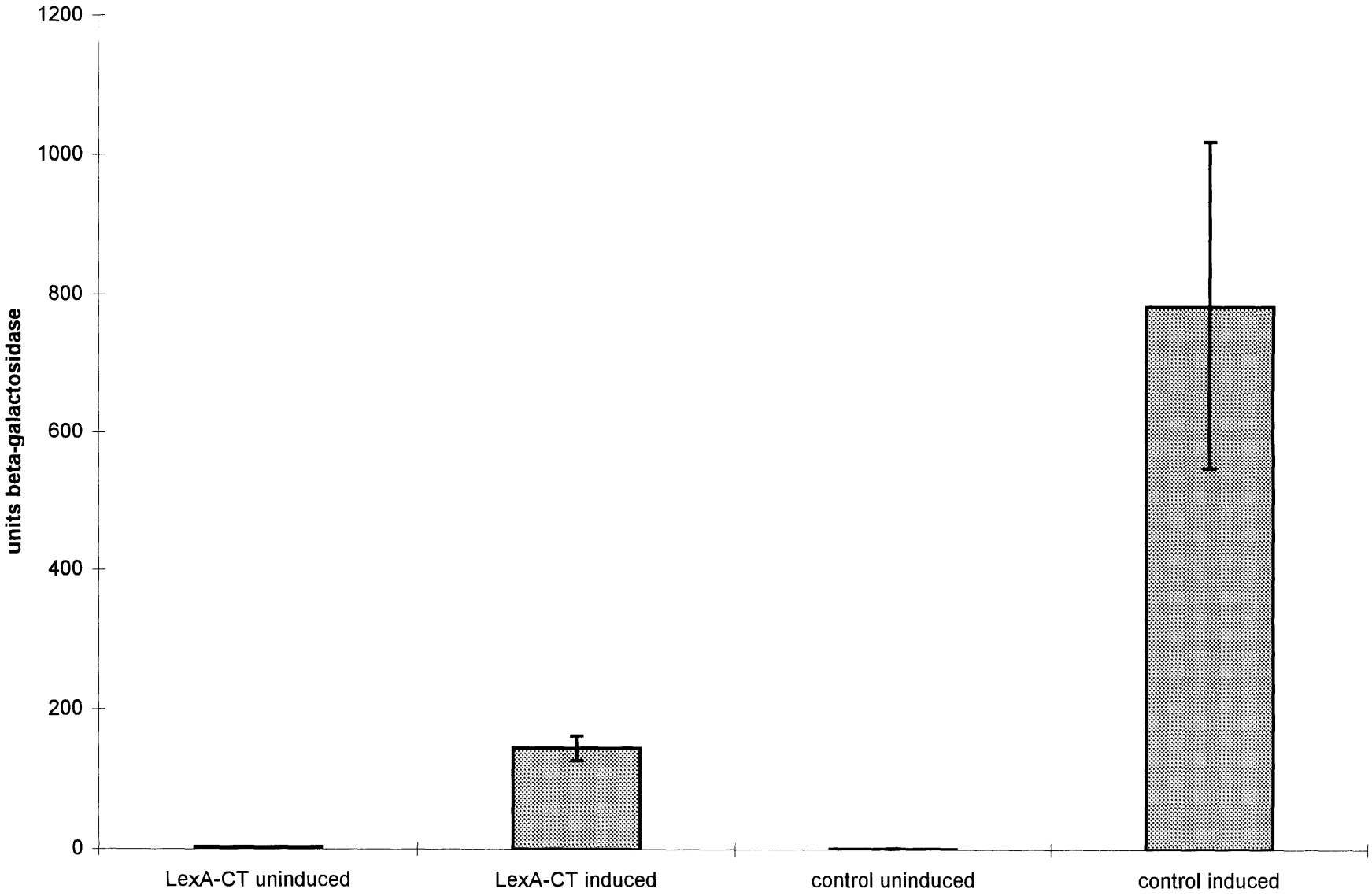
1200
1000
800
600
400
200
0
units beta-galactosidase
LexA-CT uninduced
LexA-CT induced
control uninduced
control induced

Figure 2-4: (A) The layilin cDNA and deduced amino acid sequence are shown. The signal sequence cleavage site predicted by the GCG program SIGCLEAVE is indicated with an arrow. A grey box highlights the C-type lectin homology. A single potential N-linked glycosylation site is marked with a diamond. The proposed transmembrane domain is shown in italics. Three copies of a 16-18 amino acid repeat (layilin homology 1, LH1) are shown with a broken underline. Three copies of a penta-amino acid repeat (LH2) are double underlined, and two copies of a tetra-amino acid repeat (LH3) are underlined. Two potential poly-A addition signals at the end of the cDNA are also underlined. This cDNA has been submitted to GenBank with accession number AF093673.

(B) Alignment of the carbohydrate-recognition domains from rat mannose-binding protein A, dog E-selectin, and hamster layilin. Shown at the bottom is the CRD consensus sequence derived by Drickamer (1993): single letter amino acid code indicates absolutely conserved residues; other abbreviations: O, any oxygen containing amino-acid; Z, E or Q; Θ, aliphatic; Φ, aromatic, Ω, aliphatic or aromatic residue. The alignment was performed using the GCG program PILEUP and then manually adjusted. The five amino-acid insertions found in layilin and E-selectin are underlined, a 7 amino-acid insertion unique to layilin is double underlined, a second 7 amino acid insertion is shown with a broken underline. Five amino acids which contact the mannose ligand in MBP-A are shown in boldface.

(C, D) BESTFIT alignments of putative pig (C) and human (D) homologs with hamster layilin. The hamster sequence is shown on the top line. In (C) the lectin homology is shaded, and the three insertions relative to MBP-A are underlined as in part (B) above. In part (D) internal repeats are underlined as in part (A). Asterisk, stop codon.

A

ACTAGTAACGGCCGCCAGTGTGCTCTAAAGGTGTCCTTAAGAGATGCGGCTGCCTCGGTGGCAGTTGCCCGA
ACACAGCCGCCTGTTTGCCCACTTCTCTGCCTTAGTCCCGGGGGTGTTGGGACGCACTGGAGTCCAGCA**ATGC**
M

AGCCGGGACCAGCGTTGCAGGCCGTGTTGCTGGCGGTGCTGCTGTCAGAACCACGGAGTTCGAAGGGTCGGC
Q P G P A L Q A V L L A V L L S E P R S S K G R

TGCTGAGCGGGCAGCTGGTCTGCCGGGGAGGGACTCGGAGGCCTTGCTATAAAGTCATTTACTTCCATGATG
L L S G Q L V C R G G T R R P C Y K V I Y F H D

CTTTTCAAAGACTGAACTTTGAGGAAGCCAAAGAAGCCTGCAGGAGGGATGGGGGACAGCTCGTCAGTATTG
A F Q R L N F E E A K E A C R R D G G Q L V S I

AAACAGAAGATGAGCAGAGACTGATAGAAAAATTCATTGAAAACCTCTTGGCATCTGATGGTGATTTCTGGA
E T E D E Q R L I E K F I E N L L A S D G D F W

TTGGCCTCAGGAGGCTGGAGGTGAAGCAGGTCAACAACACAGCCTGCCAGGACCTTTATGCTTGGACAGATG
I G L R R L E V K Q V N N T A C Q D L Y A W T D

GGAGCACATCACAATTTAGGAACTGGTATGTGGATGAGCCTTCTTGTGGCAGTGAGGTCTGCGTGGTGATGT
G S T S Q F R N W Y V D E P S C G S E V C V V M

ACCATCAGCCATCGGCACCACCTGGCATCGGGGGCTCATACATGTTCCAGTGGAATGACGACCGGTGCAACA
Y H Q P S A P P G I G G S Y M F Q W N D D R C N

TGAAGAACAATTTCATTTGCAAATATGCTGACGAGAAGCCAAGTACAACACCTTCTATAAGGCCTGGAGGTG
M K N N F I C K Y A D E K P S T T P S I R P G G

AAGCAACTGAGCCACCAACACCAGTACTTCCAGAAGAAACACAGAAAGAAGACACCAAAGAAACATTCAAAG
E A T E P P T P V L P E E T Q K E D T K E T F K

AAAGCAGAGAGGCTGCTTTGAATCTTGCCTACATCCTAATCCCCAGCATTCCCCTGTTCCTCTTACTAGTGG
E S R E *A A L N L A Y I L I P S I P L F L L L V*

TCACTTCAGCTGCATGTTGGGTTTGGATCTGTAGAAGAAGAAAACAAGAGCAGCCAGATCCTACCACAAAGG
***V T S A A C W V W I C* R R R K Q E Q P D P T T K**

AGCAACACACCATTTGGCCCACTCCTCACCAAGAAAACAGCCCCAACCTAGATGTTTACAATGTCATCAGAA
E Q H T I W P T P H Q E N S P N L D V Y N V I R

AACAAAGCGAAGCTGATTTAACTGAGCCCCGCCCAGACCTGAAGAACATCTCATTTCGGGTGTGTTCTAGTG
K Q S E A D L T E P R P D L K N I S F R V C S S

AAGCCCCTCCTGATGATATATCTTGTGACTATGACAACATGGCTGTGAACCCTTCAGAAAGTGGGTTTGTGA
E A P P D D I S C D Y D N M A V N P S E S G F V

CTCTGGCAAGTATGGAGAGTGGATTTGTGACCAATGACATTTATGAGTTCTCCCCTGACAGAATGGGGAGGA
T L A S M E S G F V T N D I Y E F S P D R M G R

GCAAGGAGAGTGGATGGGTGGAAAATGAAATATATTACTAAGACATATGAAAAACTGGCAAAAATGAGAAAA
S K E S G W V E N E I Y Y *

CAAAAGCAAAAGCCTCCTATTTCTCACAAGGAAAATGTTCAGAAAGTTTATGAAGATGCTCAGACCAGTTCT
TAAGGTGAGCACAGAATCTCCACAAGTTCCTACTGGGGTCCCCAAGTTCTGGTATGTATCCCTTATCCCAGA
GCCTCACCCAGCTCAGCCTTGTGAGAAGGCACCTTGCCTAGGGGCTGCCATACAGCAGACCCTCAATAACTG
TCAGCCAGTGTGCTGCAACTGATGTTCAAGGGCTGATGCTTCCAATGGTCAGGATAAAGGTGTCACCAAGGA
GTTTGGAAAGCCCGCCTCTAGGCTCCTTGCTCTCTACAGCAGCACGTGCAATCATAGAAAGACATAAACTCT
GGAATCTTCTCAAAGGCTATGTATGGAAGCCCCAGGCTGGCCTGCCCAGCAACAATTCCCATATCTTCCCCT
AGCCCAAATAAAATCCAATAAAAAAAAAAAAAAAAAAA

B

```
     MBP-A FVTNHERMPFSKVKALCSELRGTVA.IPRNAEENKAI..QEVAK....TSAFLGITDEV.........TEG
E-selectin YNASTEAMTFDEASTYCQQRYTHLVAIQNQEE.IKYLNSMFTYTPTY...YWIGIRK..........VNK
   Layilin FHDAFQRLNFEEAKEACRRDGGQLVSIETEDE.QRLIEKFIENLLASDGDFWIGLRRLEVKQVNNTACQD
 consensus Ω........Φ..Θ...C......Θ..Θ..O.E...ΩΘ..............ΦΘGΘ..............

     MBP-A QFMYVTG.GRL...TYSNWKKDEPNDHGSGEDCVTIV.....DNG.......LWNDISCQASHTAVCEFP
E-selectin KWTW.IGTQKLLTEEAKNWAPGEPNNKQNDEDCVEIYIKRDKDSG.......KWNDERCDKKKLALCYTA
   Layilin LYAWTDG.STS...QFRNWYVDEPS..CGSEVCVVMYHQPSAPPGIGGSYMFQWNDDRCNMKNNFICKYA
 consensus .Φ.Ω..G...Ω....Ω..W...ZP......EOCΘ.Ω........G........WND..C.....Ω.C...
```

C

```
EACRRDGGQLVSIETEDEQRLIEKFIENLL.....ASDGDFWIGLRRLEVKQVNNTACQD
               ..: .:|||.:::||       |||||||||:| :... ...||.|
              NSGIPKLIESMLQNLSKPGTGISDGDFWIGLWR.NGEGHTSGACPD


LYAWTDGSTSQFRNWYVDEPSCGSEVCVVMYHQPSAPPGIGGSYMFQWNDDRCNMKNNFI
||.|.||| ||:||||.|||||||| |||||||.| ||:||.|:::||||||||||:|:|
LYQWSDGSXSQYRNWYTDEPSCGSEKCVVMYHQPTANPGLGGPYLYQWNDDRCNMKHNYI


CKYADEKPSTTP
 ||..|  .|.|
XKYEPEIYPTAP
```

D

```
RRRKQEQPDPTTKEQHTIWPTPHQENSPNLDVYNVIRKQSEADLTEPRPDLKNISFRVCSSEA
     :.|||.||.||||||.|||:|||:|:||||||||||:..|.|.|||||||||||||:||
     GKPDPSTKKQHTIWPSPHQGNSPDLEVYNVIRKQSDVSLAETRPDLKNISFRVCSGEA


PPDDISCDYDNMAVNPSESGFVTLASMESGFVTNDIYEFSPDRMGRSKESGWVENEIYY*
.|||:||||||||||||||||||.|:|      |:||::
TPDDMSCDYDNMAVNPSESGFVTLVSVE.....NEIYGY*
```

Figure 2-5: Northern blot analysis of layilin expression. One or five micrograms of NIH3T3 and CHO total RNA or 1 microgram of CHO poly-A^+ RNA were analysed for layilin expression. The single transcript detected in CHO RNA is highly enriched in the poly-A^+ RNA. Upon longer exposure, several bands are evident in NIH3T3 RNA; the two most prominent comigrate with mouse rRNAs and may result from cross-reaction of the probe with rRNAs. The faint band migrating just above the 18S rRNA comigrates with the transcript in hamster RNA and may be a mouse layilin transcript. The positions of the 18S (1874 nt) and 28S (4718 nt) ribosomal RNAs are indicated for size reference.

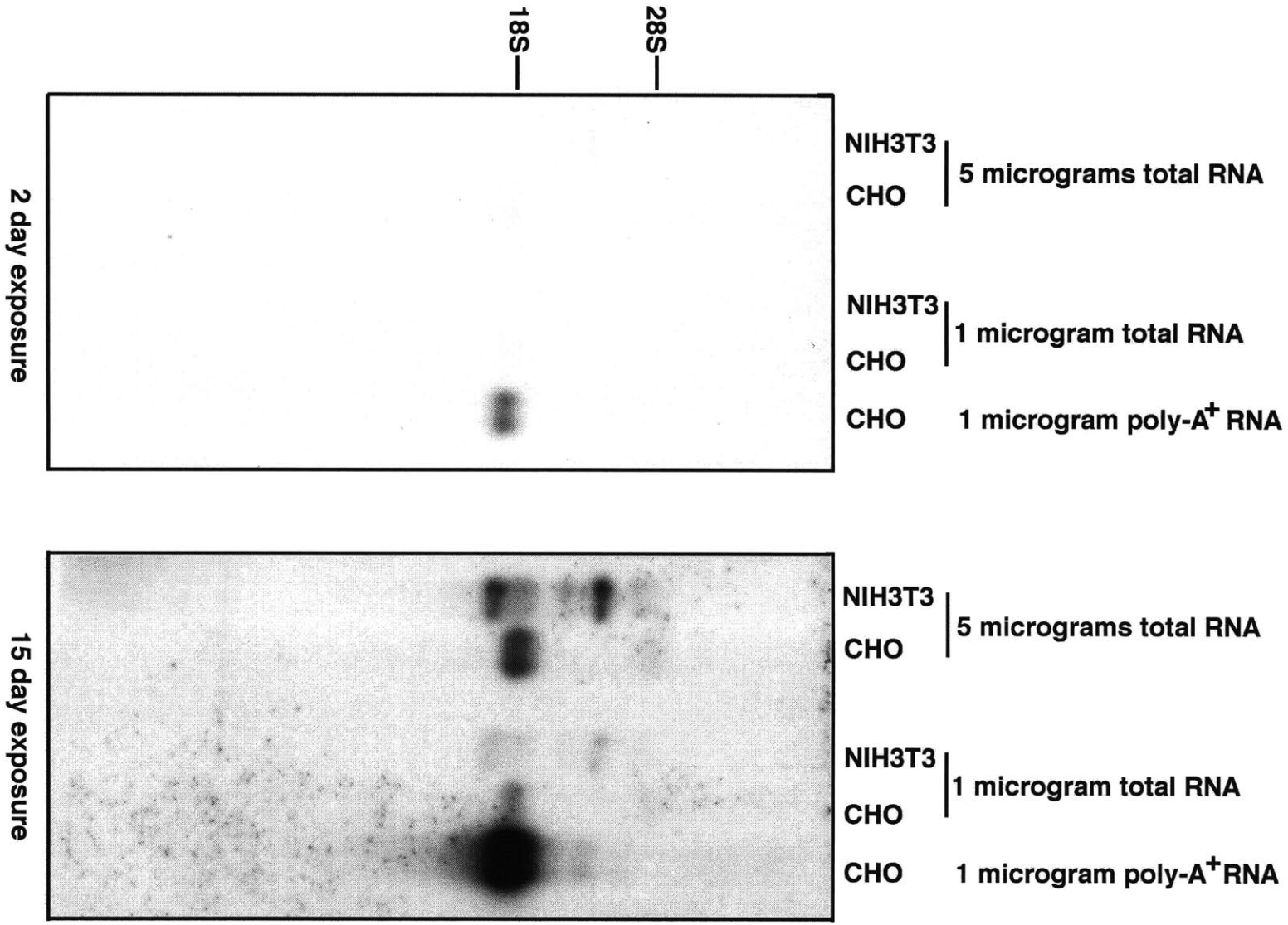
18S
28S
2 day exposure
NIH3T3
CHO
5 micrograms total RNA
NIH3T3
CHO
1 microgram total RNA
CHO
1 microgram poly-A+ RNA
15 day exposure
NIH3T3
CHO
5 micrograms total RNA
NIH3T3
CHO
1 microgram total RNA
CHO
1 microgram poly-A+RNA

Figure 2-6: (A) Anti-epitope tag immunoblot showing expression of polypeptides of the expected molecular weights for layilin cytoplasmic domain (aa 244-374), layilin (aa 92-374), and layilin lacking its cytoplasmic domain (aa 92-244). The parental yeast strain, EGY48, is included for comparison. Short and long exposures are shown to emphasize differences in expression levels of these fusion proteins. The predominant protein in each lane is of the expected size, and some degradation products are also evident, particularly in the 10 minute exposure.

(B) Growth of yeast expressing the LexA/CT 1-435 bait and fish encoding various fragments of layilin on media either lacking or supplemented with leucine. All strains grow in the presence of leucine, indicating that none of the fusion proteins are toxic to yeast. Only yeast expressing fusions containing amino acids 244-374 grow in the absence of leucine, indicating that the layilin cytoplasmic domain is both necessary and sufficient for interaction with talin amino acids 1-435 in yeast. Mxi1 and max fusion proteins are included as negative controls with talin and layilin and as a positive control together (Zervos, 1993).

A

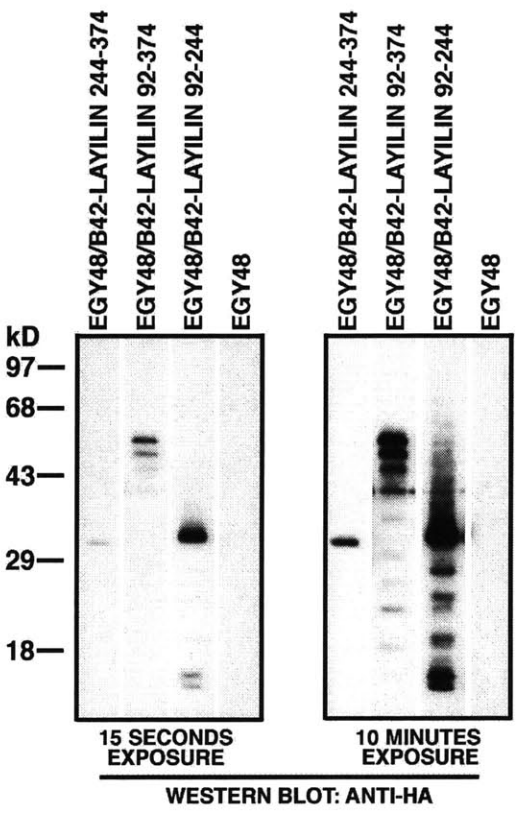

B

BAIT	FISH
CT 1-435	LAYILIN 92-374
CT 1-435	LAYILIN 92-244
CT 1-435	LAYILIN 244-374
MAX	LAYILIN 244-374
CT 1-435	MXI1
MAX	MXI1

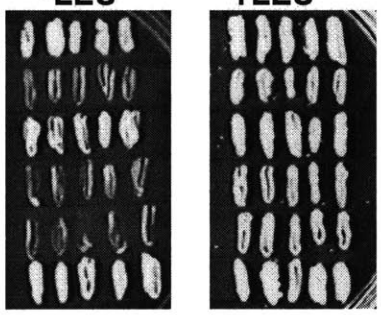

Figure 2-7: (A) Carbohydrate recognition domain structure. Three calcium ions are shown; Ca^{++} 3 is believed to be a crystal artifact. Arrow, site of 5 amino acid insertion in selectins (corresponds to underlined sequence in figure 2-4B). Double arrow, site of 7 amino acid insertion in layilin (corresponds to broken underline in figure 2-4B). Adapted from Weis (1992).

(B) Structure of the rat MBP-A ligand binding site. The 5 amino acids indicated are those shown in bold face in figure 2-4B. Adapted from Weis (1992).

A

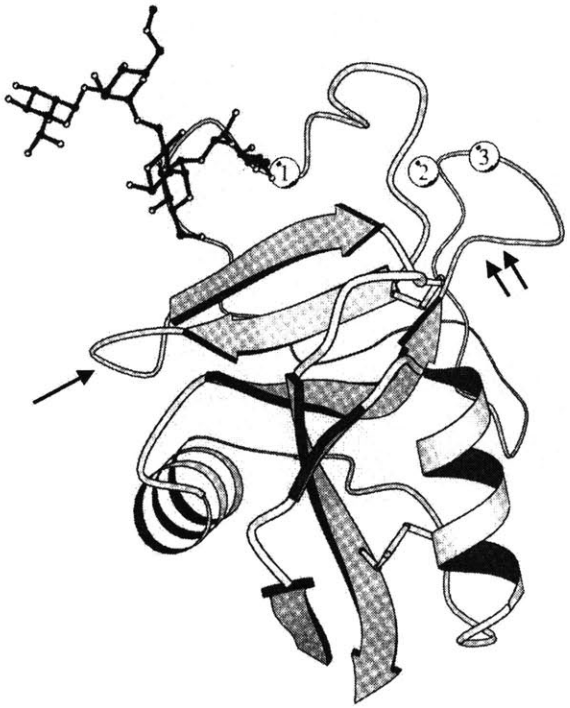

B

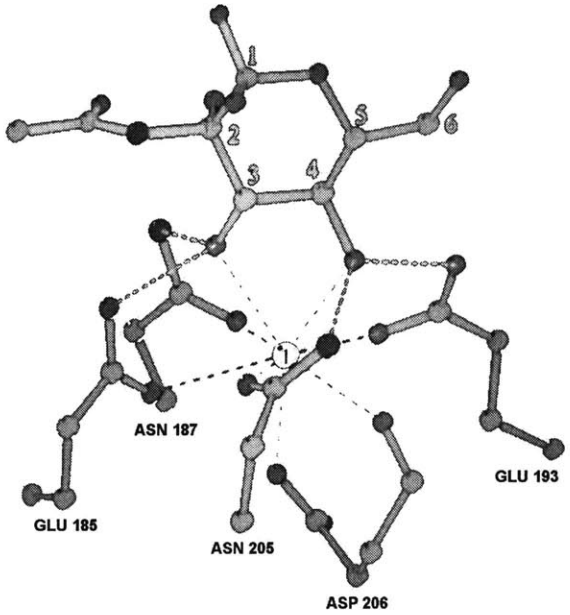

Figure 2-8: (A) Anti-layilin immunoblot of CHO cell lysates with antisera from rabbits 618 and 619. Each antiserum detects 55 kD bands which are competed in the presence of the antigen peptide (arrowhead). 618 serum also detects a number of other bands which are competed by the peptide, plus two which are not competed.
(B) Affinity purification of 618 serum. Strips from a curtain gel loaded with CHO cell lysates were probed with: lane 1, secondary antibody only; lane 2, immune serum; lane 3, ammonium sulphate-precipitated serum (dialysed to PBS); lane 4, ammonium sulphate supernatant (dialysed to PBS); lane 5, serum depleted by passage over immobilized peptide column; lane 6, affinity purified antiserum (glycine-eluted fraction 2); lane 7, affinity purified antiserum (glycine-eluted fraction 3). Arrowhead, 55 kD species recognized by both antisera.
(C) Affinity purification of 619 serum. Lanes as in (B) above.

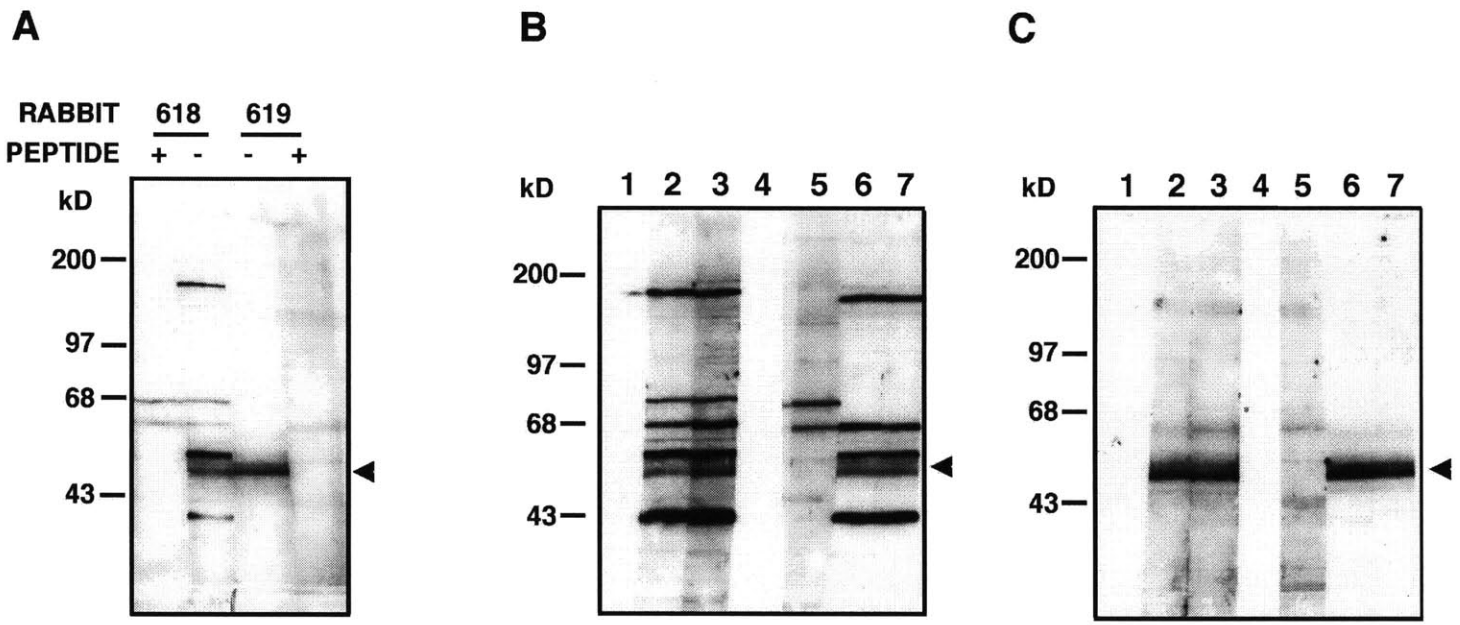
A
RABBIT 618 619
PEPTIDE + - - +
kD
200
97
68
43
B
kD 1 2 3 4 5 6 7
200
97
68
43
C
kD 1 2 3 4 5 6 7
200
97
68
43

Figure 2-9: Expression of layilin protein in cells and tissues. (A) Western blot with affinity-purified anti-layilin antiserum of mouse, rat, monkey, hamster, and human cell lines. Specifically reacting bands in rat cell lines migrate slightly faster than does the prevalent immunoreactive species in monkey, mouse and hamster cells. Abbreviations: NRK, normal rat kidney; REF, rat embryo fibroblast; BHK, baby hamster kidney. The position and size in kilodaltons of molecular weight standards are shown . Five micrograms of protein were loaded per lane.
(B) Organs were dissected from a healthy adult female mouse, homogenized and lysed in gel loading buffer. Ten micrograms of each lysate were loaded per lane and blotted for layilin. Total CHO protein is included to indicate the position of layilin .

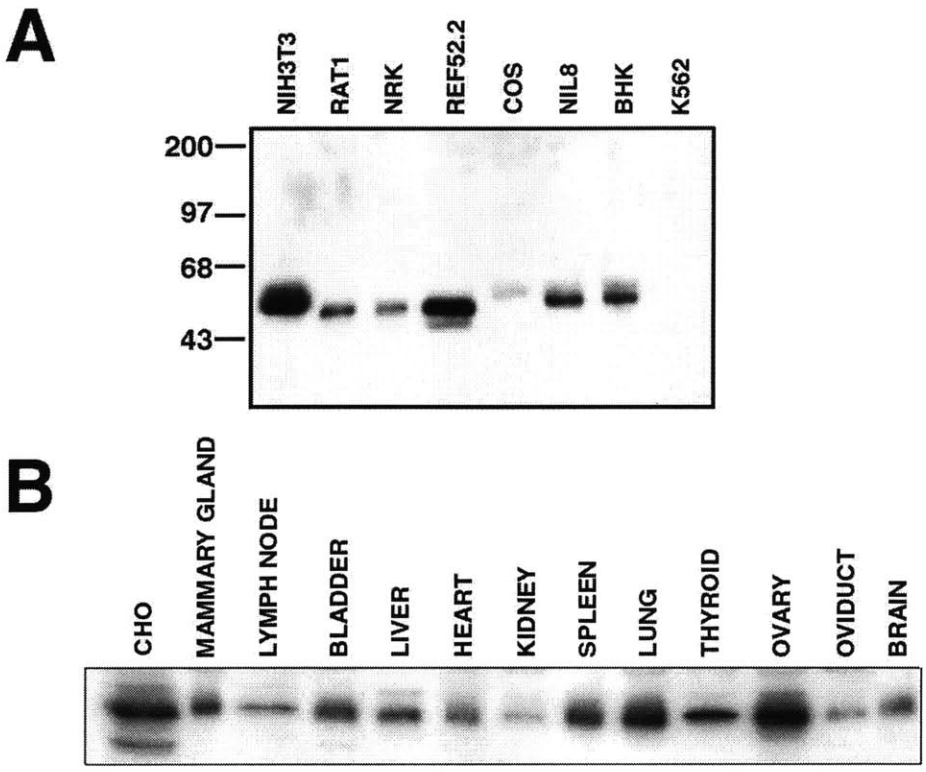
A
NIH3T3
RAT1
NRK
REF52.2
COS
NIL8
BHK
K562
200
97
68
43
B
CHO
MAMMARY GLAND
LYMPH NODE
BLADDER
LIVER
HEART
KIDNEY
SPLEEN
LUNG
THYROID
OVARY
OVIDUCT
BRAIN

Figure 2-10: Layilin is a glycoprotein expressed on the cell surface. (A) CHO cells were surface-labeled with biotin, lysed in RIPA buffer, immunoprecipitated with anti β1-integrin antiserum, peptide depleted (LAYILIN CONTROL) or affinity-purified anti-layilin antiserum (LAYILIN IMMUNE), and labeled bands detected with HRP-streptavidin. Some samples (+ lanes) were treated with PNGase F to remove N-linked carbohydrates. The position of the layilin band is marked with an arrowhead before PNGase F treatment and a small arrow after PNGase F treatment. The position and size in kilodaltons of molecular weight standards are shown .

(B) A detergent lysate of CHO cells was treated with or without PNGase F to remove N-linked sugars, western blotted and probed with anti β1-integrin or affinity purified anti-layilin antiserum. Note that essentially all the layilin and integrin present in the lysate is PNGase F-sensitive. Additional controls are included to show that the enzyme is required for the observed effect. The position and size in kilodaltons of molecular weight standards are shown . Arrowheads, untreated bands; arrows, PNGase F-treated bands; asterisk, β1-integrin precursor.

(C) Layilin is predominantly found on the cell surface. CHO cells were surface-labeled with biotin (lanes 2-4) or mock surface-labeled without biotin (lanes 5-7), lysed and passed over an avidin column to remove labeled material. The first three fractions eluted from each column (lanes 2-4 and 5-7) were analysed by western blotting for β1-integrin and layilin. When assayed for β1-integrin (top panel), the lysate (lane 1) contains two bands: the upper band (arrow) represents mature β1-integrin; the lower band (asterisk) is an intracellular precursor. Biotin selectively labels the mature (top) band without affecting the precursor form of β1 (compare lanes 2 and 5, top panel), indicating the reagent does not have access to the cells' interior. The same fractions (bottom panel) reveal that most layilin, like mature β1-integrin, is biotin-labeled (compare lanes 2 & 5, bottom panel). All lanes were loaded with equivalent fractions of the cell lysate.

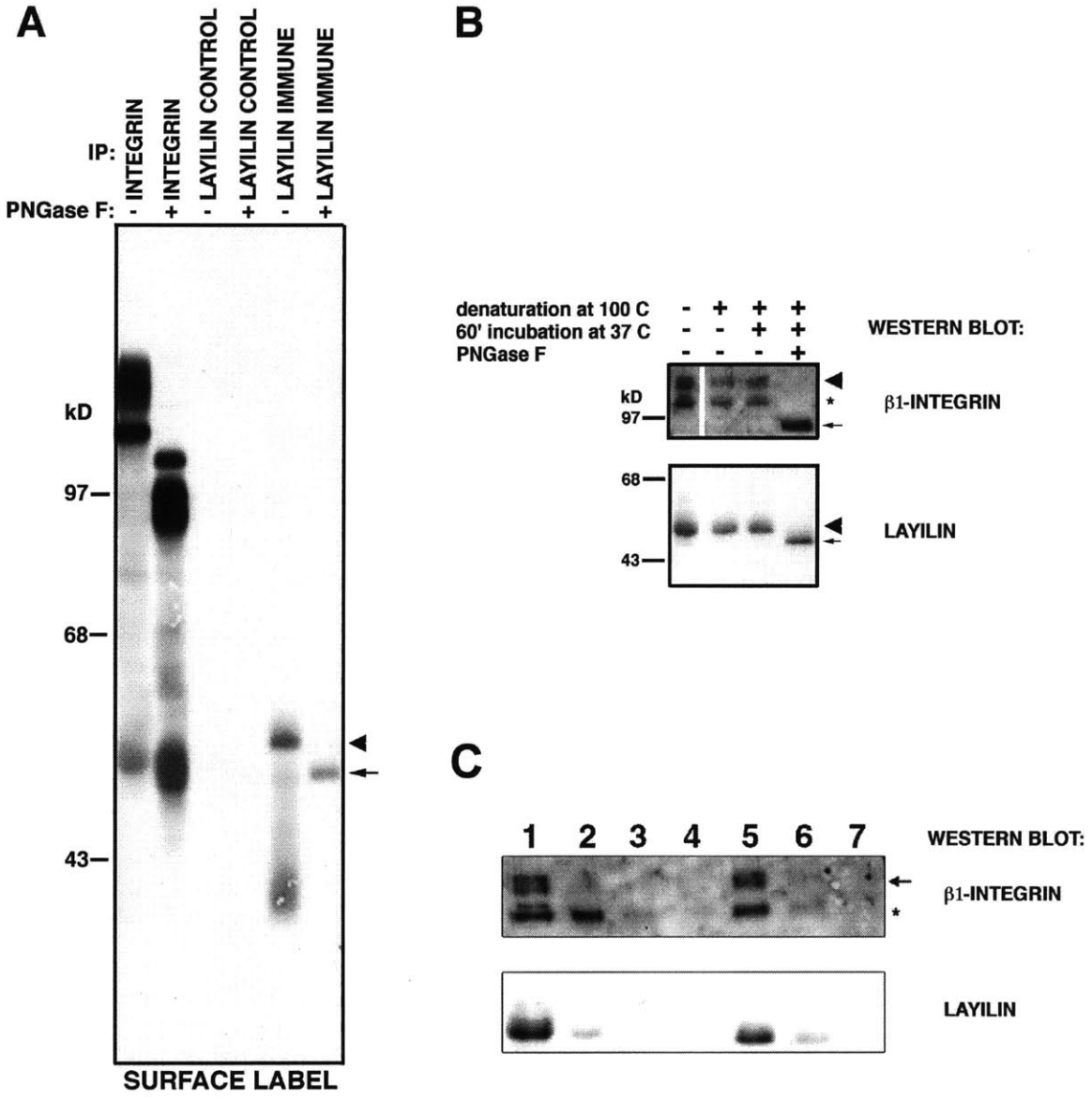
A
IP:
- INTEGRIN
+ INTEGRIN
- LAYILIN CONTROL
+ LAYILIN CONTROL
- LAYILIN IMMUNE
+ LAYILIN IMMUNE
PNGase F: - + - + - +
kD
97
68
43
SURFACE LABEL
B
denaturation at 100 C - + + +
60' incubation at 37 C - - + +
PNGase F - - - +
WESTERN BLOT:
kD
97
β1-INTEGRIN
68
43
LAYILIN
C
1 2 3 4 5 6 7
WESTERN BLOT:
β1-INTEGRIN
LAYILIN

Figure 2-11: HA-tagged layilin is expressed in and exported to the surface of CHO cells. (A) In this western blot, the anti-HA tag monoclonal 12CA5 (left panel) recognizes a set of 55 kD bands (open arrowhead) specifically in cells transfected with HA-layilin but not in cells transfected with layilin alone or untransfected cells. As a positive control for anti-HA staining, a lysate of cells transfected with HA-talin head was included; a small arrow indicates the HA-talin head band. An identical set of lanes was probed with an anti-layilin antiserum (right panel), which to reacts with a set of 55 kD bands in cells transfected with HA-layilin; this antiserum also detects a ~55 kD species in cells transfected with untagged layilin (solid arrowhead). Endogenous layilin can be seen in lanes from untransfected cells or cells transfected with HA-talin head (solid arrowhead). (B) HRP-streptavidin was used to detect surface biotinylated proteins from CHO cells or stably-transfected CHO cells which express HA-layilin. Peptide-depleted layilin antiserum (LAYILIN CONTROL) does not immunoprecipitate any surface labelled material from either cell line. In contrast, affinity-purified anti-layilin antiserum (LAYILIN IMMUNE) immunoprecipitates a 55 kD band from control untransfected cells (arrowhead) and a much broader band from HA-layilin expressing cells. The anti-HA monoclonal 12CA5 immunoprecipitates a broad band slightly above 55 kD from transfectants and nothing from untransfected controls. The material precipitated by anti-layilin from the transfected cells appears to be the sum of endogenous and HA-tagged layilin.

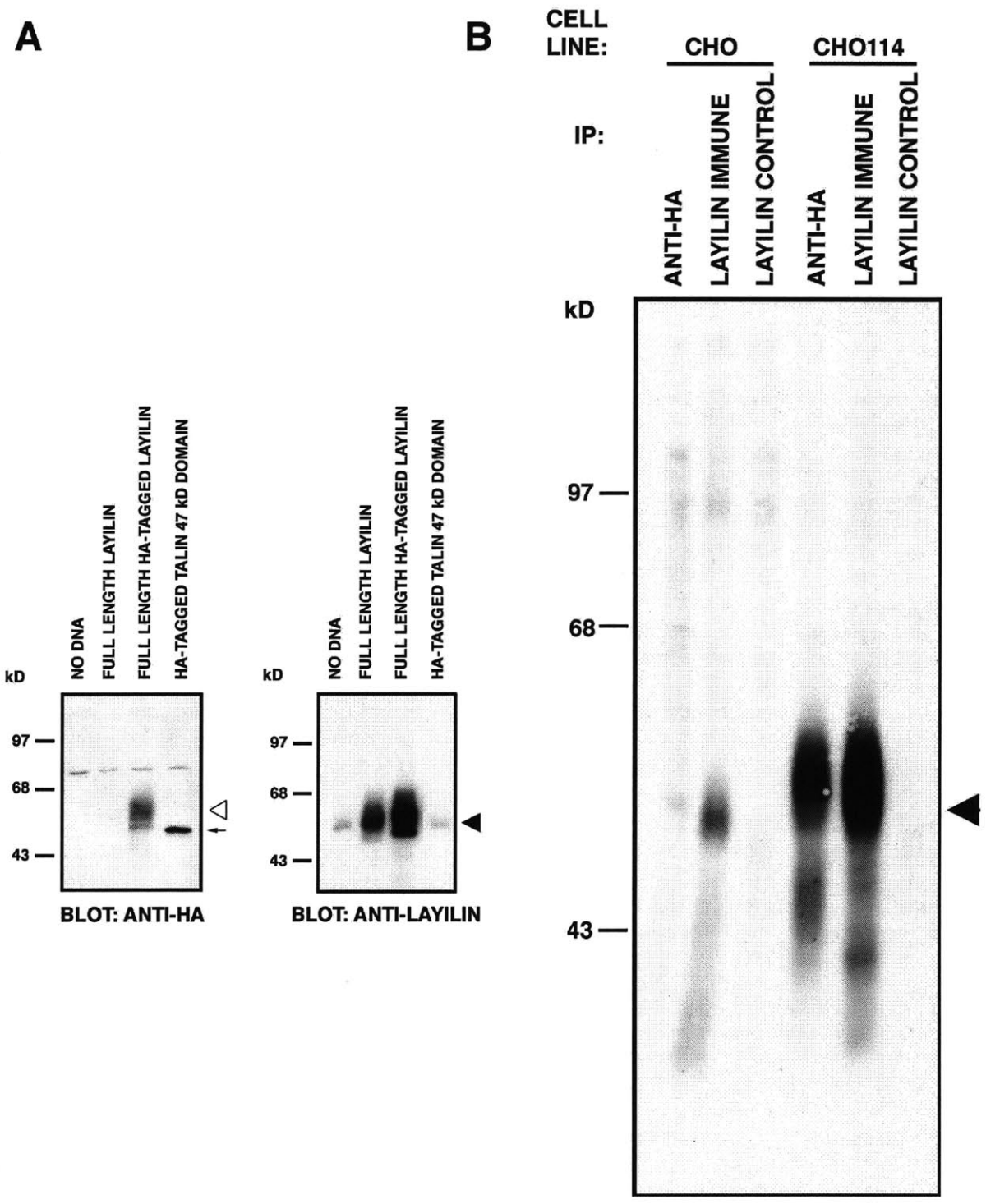
A
kD
NO DNA
FULL LENGTH LAYILIN
FULL LENGTH HA-TAGGED LAYILIN
HA-TAGGED TALIN 47 kD DOMAIN
97
68
43
BLOT: ANTI-HA
BLOT: ANTI-LAYILIN
B
CELL LINE:
CHO
CHO114
IP:
ANTI-HA
LAYILIN IMMUNE
LAYILIN CONTROL
kD
97
68
43

Figure 2-12: HA-tagged layilin is expressed in and exported to the surface of NIL8 cells.

(A) Lysates from control (NIL8) and stably-transfected NIL8 cells expressing HA-layilin (NIL114) were western blotted and probed with an anti-HA monoclonal. A band that migrates at the approximate position of endogenous layilin was detected (arrowhead) as was a contaminant seen in both untransfected and transfected cell lines (arrow).

(B) NIL8 and NIL114 cell lines were surface biotinylated and labelled material immunoprecipitated with peptide-depleted anti-layilin antiserum (LAYILIN CONTROL), affinity-purified anti-layilin antiserum (LAYILIN IMMUNE), or the anti-HA tag monoclonal 12CA5. Bands were detected with HRP-streptavidin. At 55 kD band was precipitated by the anti-layilin antibody not seen with control depleted serum (arrowhead). In addition, a prominent smear around 43 kD is present (bracket). This material is not immunoprecipitated by affinity-purified serum from rabbit 618, nor is it present in immunoprecipitates of HA-layilin from NIL114. Moreover, overexpression of HA-layilin does not lead to an increase in this material, suggesting it is not a meaningful coprecipitating band but rather a contaminant. 12CA5 immunoprecipitates a 90 kD contaminant from both untransfected NIL8 cells and from NIL114 (arrow).

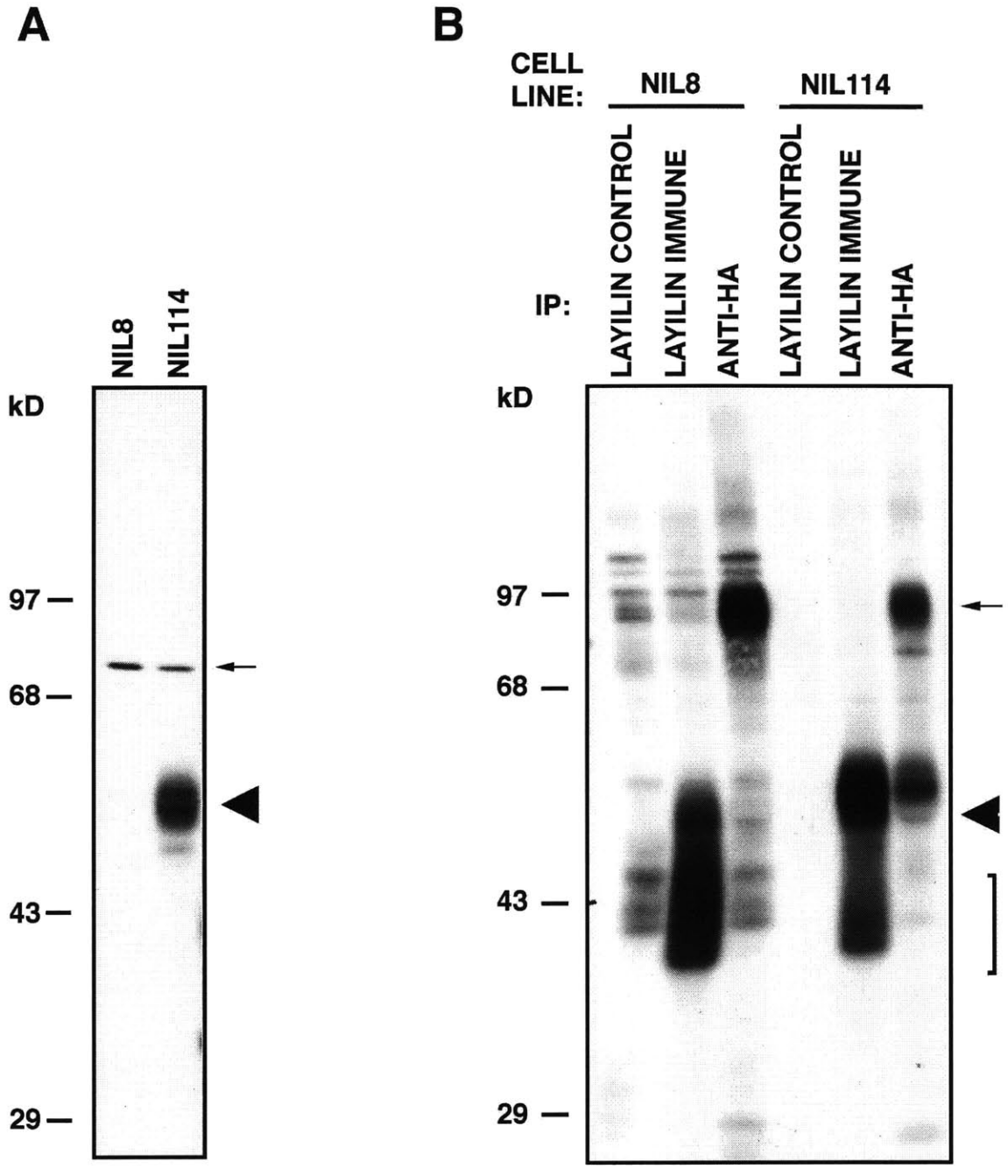
A
NIL8
NIL114
kD
97
68
43
29
B
CELL LINE:
NIL8
NIL114
IP:
LAYILIN CONTROL
LAYILIN IMMUNE
ANTI-HA
LAYILIN CONTROL
LAYILIN IMMUNE
ANTI-HA
kD
97
68
43
29

Figure 2-13: Stably-transfected CHO cells expressing HA-layilin (CHO114) were plated on FN-coated coverslips and allowed to spread for 50 minutes. Cells were stained with antibodies to (a) HA tag, (b) talin, (c) double exposure of a and b, (d) no primary antibody, (e) anti-transferrin receptor. Note coincidence of talin and HA-layilin staining in membrane ruffles around the edges of cells. Transferrin receptor staining is evident in the perinuclear region and to a lesser extent on the cell surface, similar to HA-layilin distribution; however, no transferrin receptor is found in membrane ruffles. Bar = 10 microns.

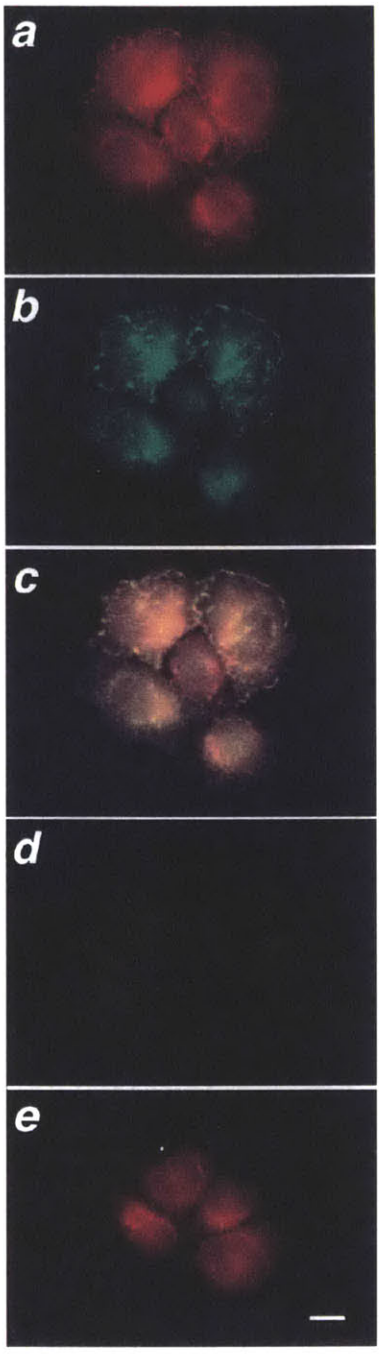
a
b
c
d
e

Figure 2-14: HA-layilin is found in ruffles of paraformaldehyde-fixed CHO114 cells immunostained after permeabilization with NP-40 (a,d), Brij 99 (b,e) or acetone (c,f). Signal for anti-HA (a-c) and anti-talin (d-f) antibodies is shown. Bar = 10 microns.

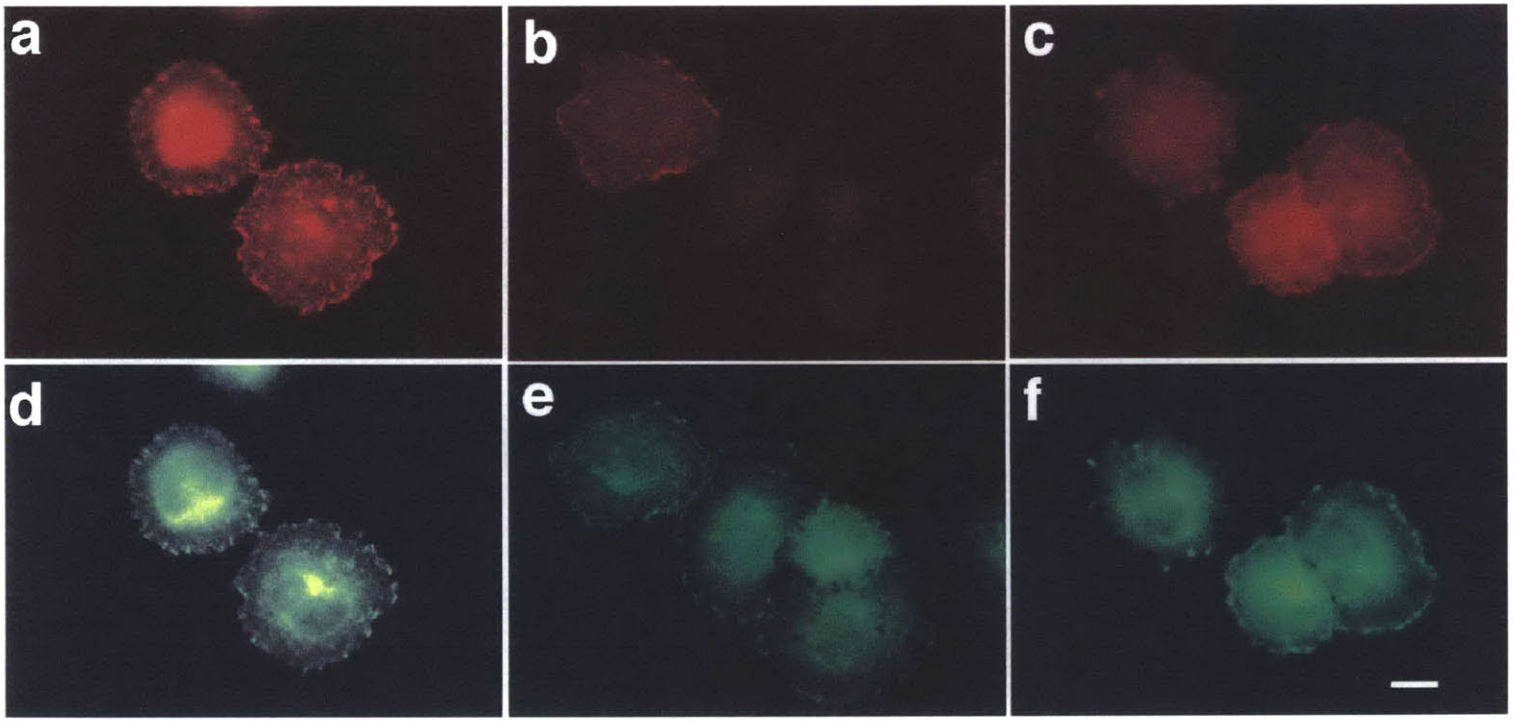
a
b
c
d
e
f

Figure 2-15: Co-localization of HA-tagged layilin with F-actin and talin in spreading NIL114 hamster cells. Cells spreading on a fibronectin matrix contain peripheral ruffles which stain for HA-layilin (a,b), phalloidin (e), and talin (f). Yellow ruffles in double exposures (c,d) show the extent of overlap of staining. Bar = 10 microns.

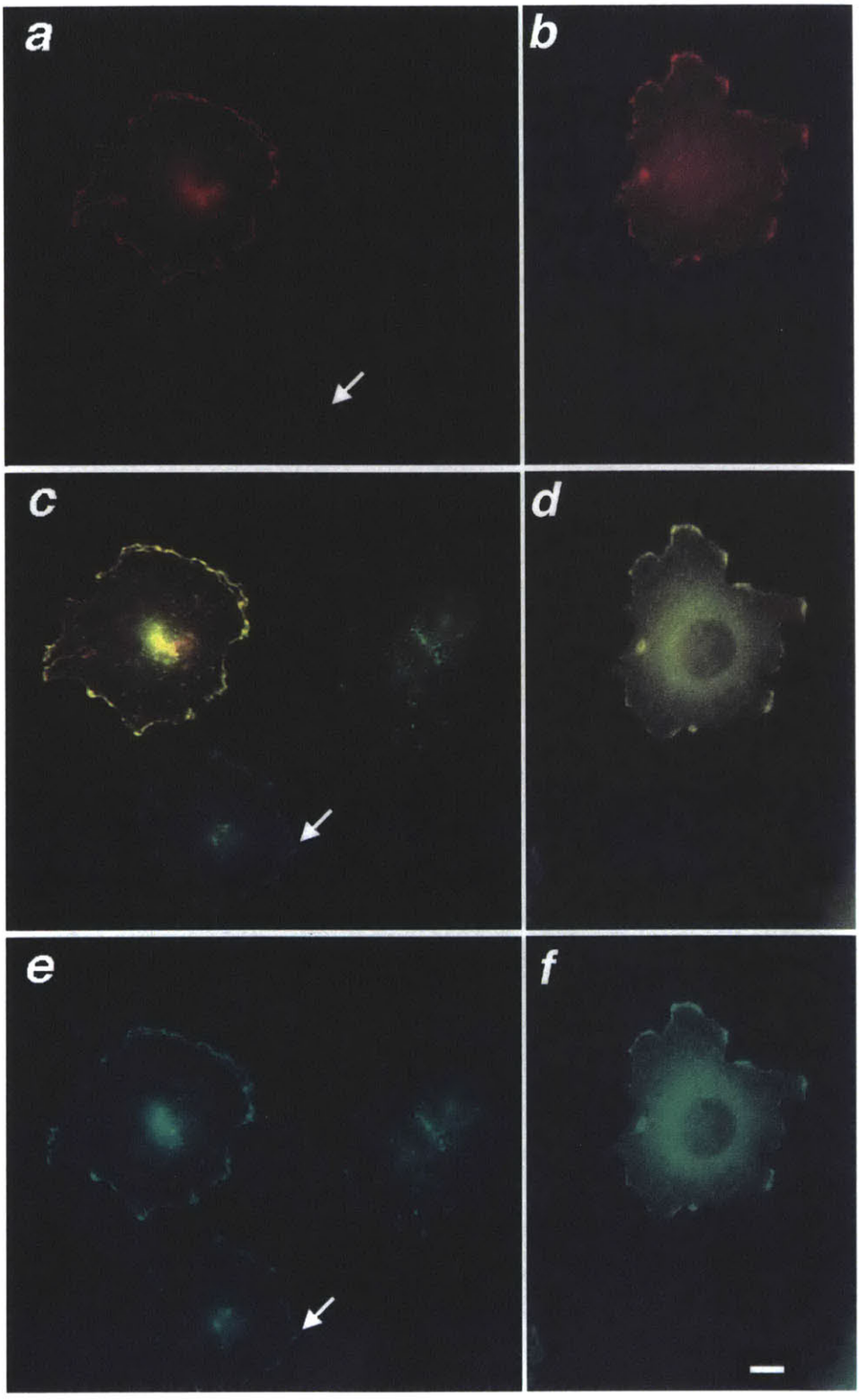
a
b
c
d
e
f

Figure 2-16: HA-layilin is present in leading edge ruffles of migrating NIL114 cells. A monolayer was wounded and cells migrating into the gap are shown stained with affinity-purified anti-layilin antiserum (a,d,g) and 12CA5 (c,f,i). Panels b, e, and h are double-exposures of 12CA5 and anti-layilin. Antibodies were incubated in the absence (a-c) or presence of competing peptides. The layilin-derived peptide LC20 competes anti-layilin staining (g) but not anti-HA tag staining (i). Conversely, an HA peptide blocks 12CA5 staining (f) but has no effect on the signal from anti-layilin antibodies (d). Bar = 10 microns.

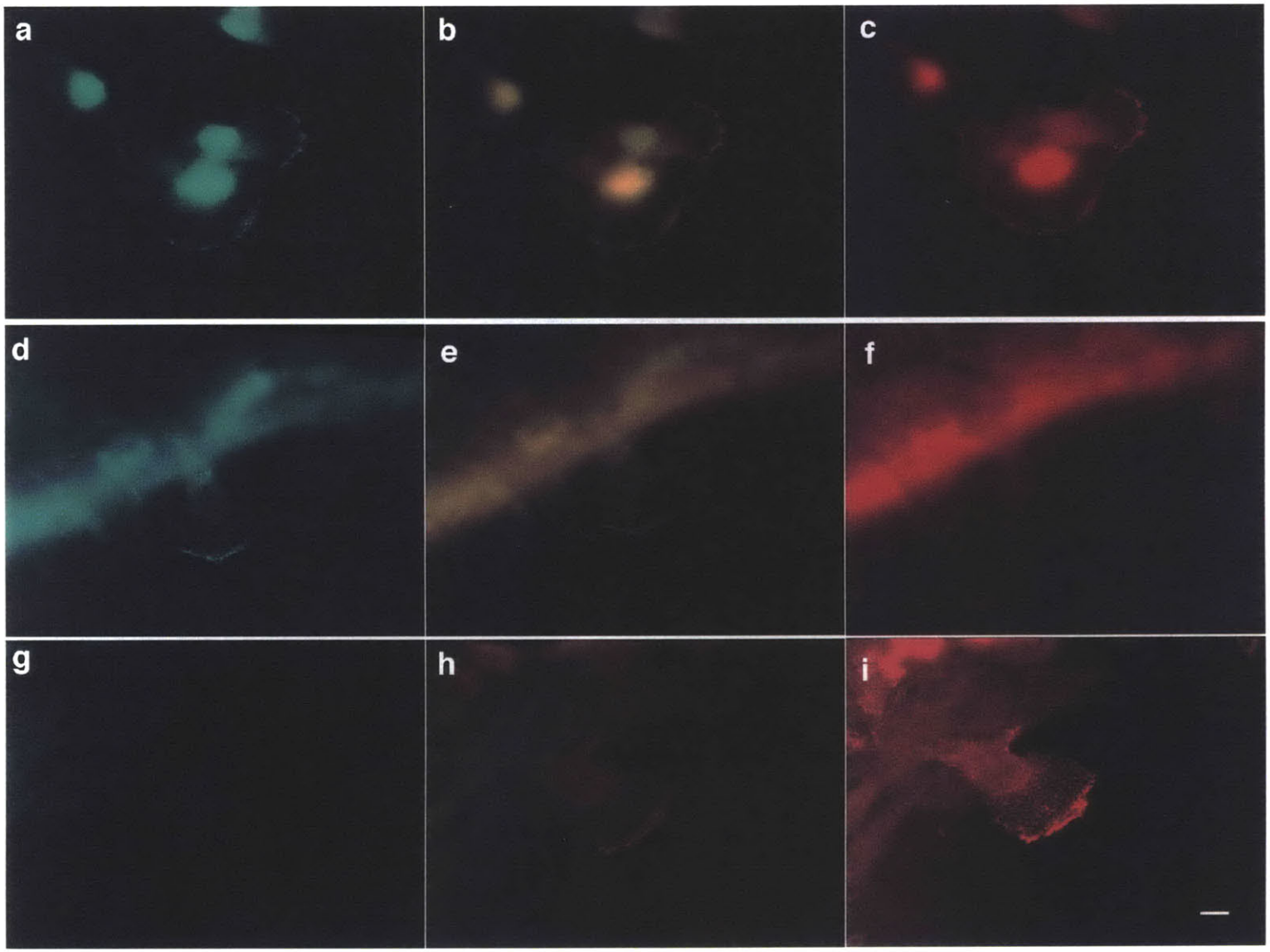
a
b
c
d
e
f
g
h
i

Figure 2-17: Endogenous layilin is in ruffles. Ruffling NIL8 cells are shown stained with (a-c) peptide-depleted anti-layilin antiserum and (d,g,j) affinity-purified anti-layilin antiserum. Cells were double-labelled with (c,f) phalloidin and (i,l) anti-talin. Arrowheads highlight peripheral and leading edge ruffles. Arrows (g-l) indicate focal contacts, which stain with anti-talin but not anti-layilin antibodies. Layilin signals in the nucleus and midbody are probably artifacts. Bar = 10 microns.

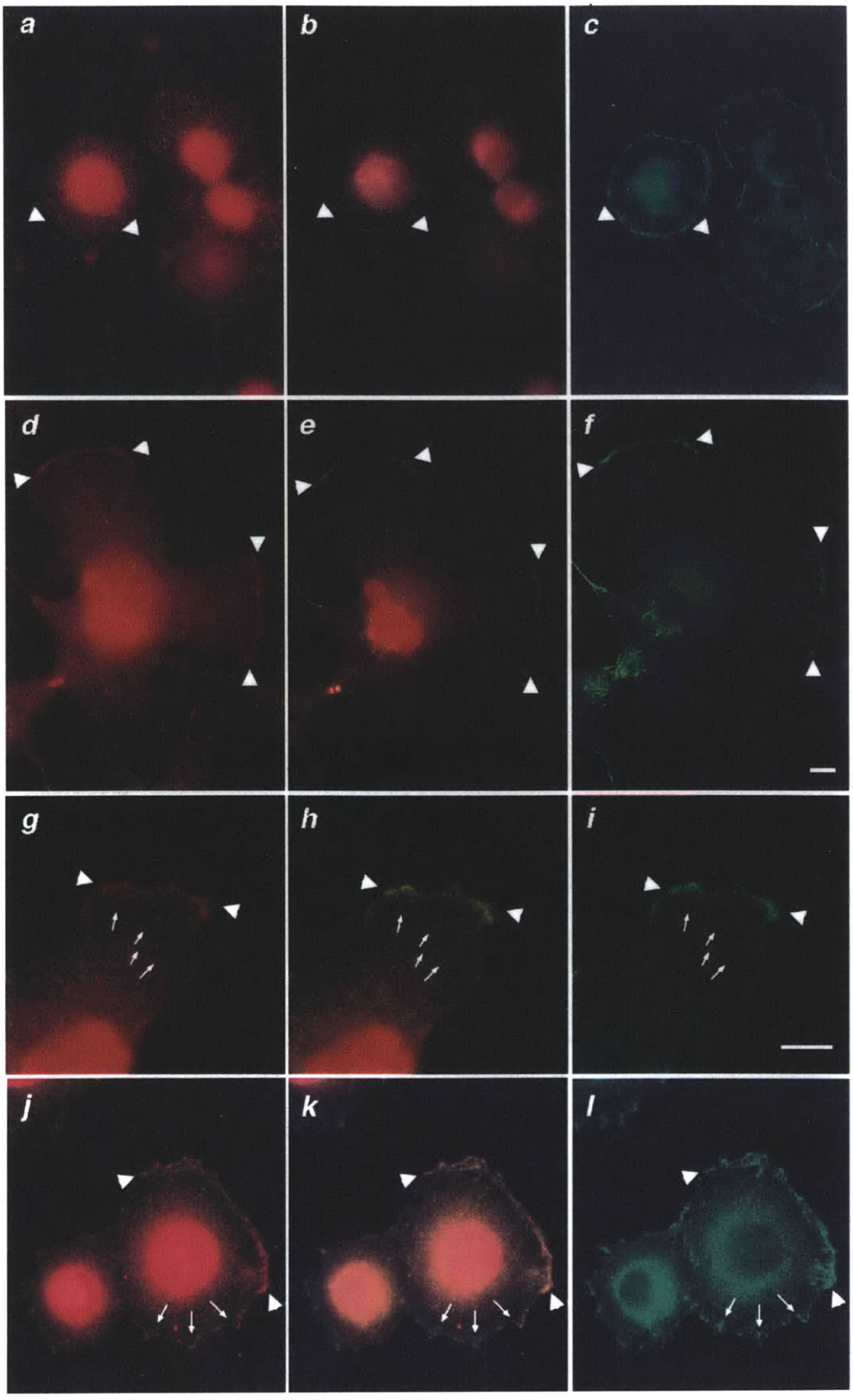
a
b
c
d
e
f
g
h
i
j
k
l

Figure 2-18: Layilin is not concentrated in the uropod of polarized mouse T-cells. Primary mouse T-cells stimulated with recombinant RANTES develop a flat leading edge and a rounded dorsal projection called the uropod. CD43 (c) and members of the ERM family (e) are concentrated in the uropod. ERM proteins can also be seen in the leading edge of this cell. Layilin does not preferentially localize in the uropod (d, f). Secondary FITC-anti-mouse (a) and peptide-depleted anti-layilin antiserum (b) are included as negative controls. Bar = 5 microns.

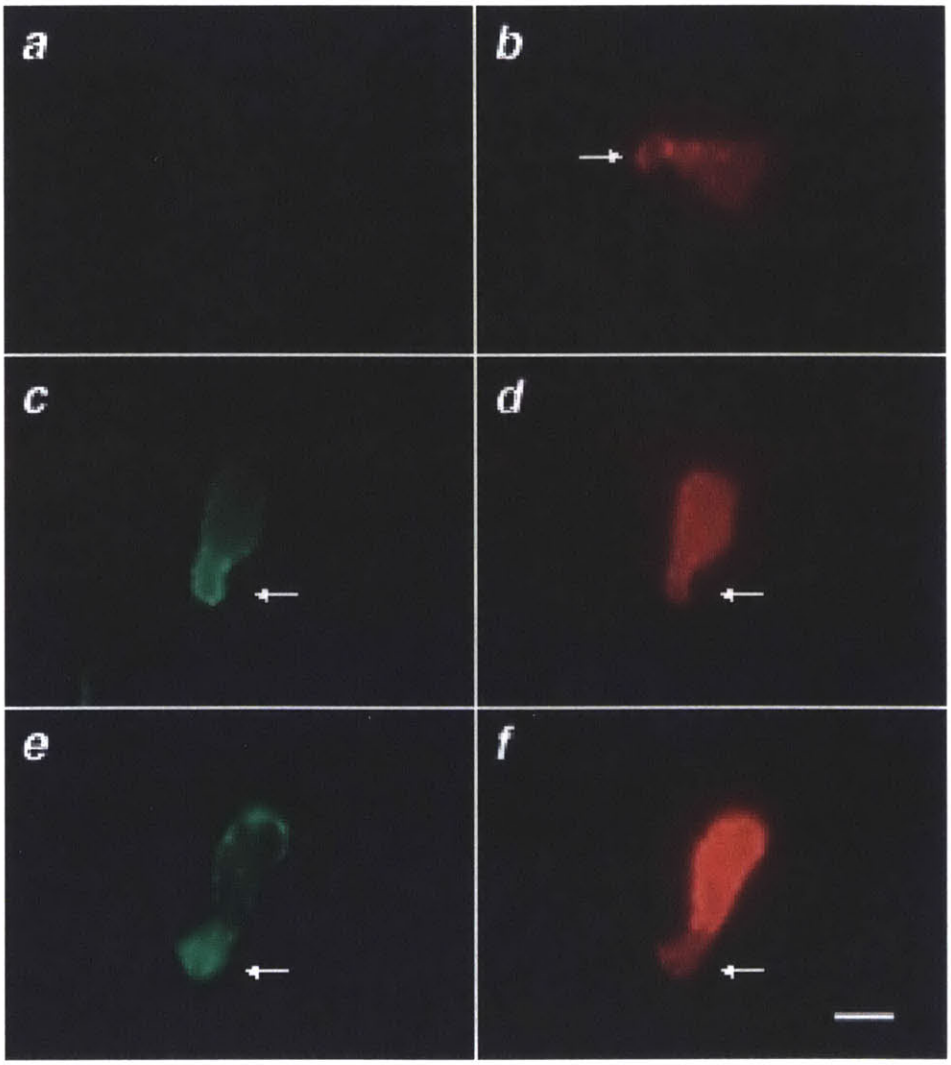
a
b
c
d
e
f

Figure 2-19: GST-layilin binds talin in cell extracts. (A) GST fusion proteins containing portions of the layilin cytoplasmic domain were immobilized on agarose and mixed with a CHO cell detergent lysate. Each fusion protein contains the layilin amino acids indicated, except (LH23)x3 which has 3 copies of the amino acid motif spanning layilin amino acids 343 to 352. Samples in which binding took place in the presence of a layilin-derived peptide (+LC20) or a control HA-epitope peptide (+HA) are indicated. An arrowhead indicates the position of talin and an arrow indicates a prominent proteolytic fragment. After washing, the agarose beads were boiled in gel loading buffer and the released material analysed by western blotting for talin. The lanes containing proteins bound by GST fusions of fibronectin EIIIB (FN EIIIB) or layilin are overloaded approximately 13-fold relative to the total lysate lane.
(B) Talin-layilin binding was assayed in the presence of 50 μM acidic phospholipids as shown. The GST-(LH23)x3 fusion protein bound talin equally well in the absence or presence of these phospholipids. The GST-FN control did not bind talin, nor did either GST fusion bind to vinculin under the conditions tested. PS, phosphatidyl-serine.

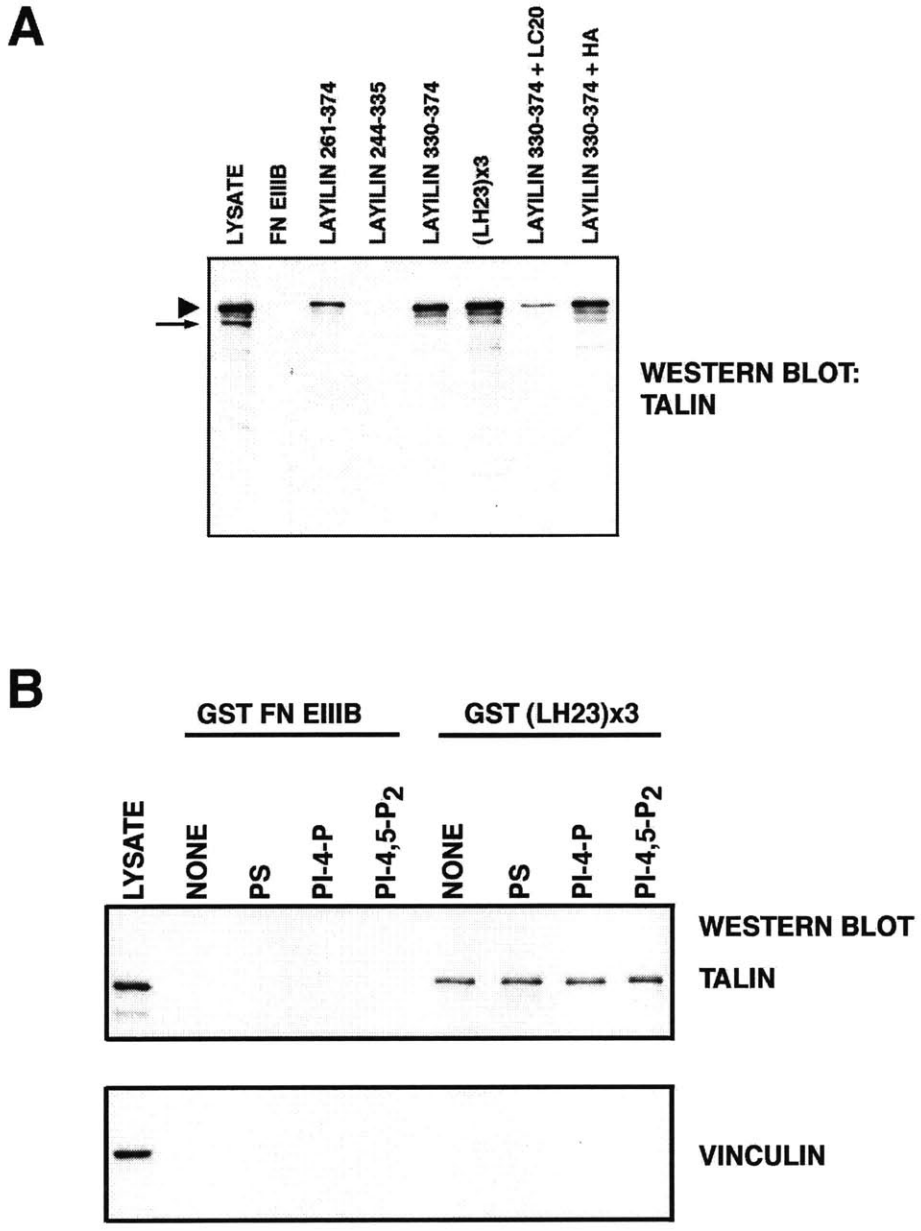
A
LYSATE
FN EIIIB
LAYILIN 261-374
LAYILIN 244-335
LAYILIN 330-374
(LH23)x3
LAYILIN 330-374 + LC20
LAYILIN 330-374 + HA
WESTERN BLOT:
TALIN
B
GST FN EIIIB
GST (LH23)x3
LYSATE
NONE
PS
PI-4-P
PI-4,5-P2
NONE
PS
PI-4-P
PI-4,5-P2
WESTERN BLOT
TALIN
VINCULIN

Figure 2-20: GST-talin binds layilin in cell extracts. (A) Glutathione agarose preloaded with GST fusions containing either FN EIIIB or the indicated amino acids of chicken talin was incubated with a CHO cell detergent lysate, washed, and boiled in gel loading buffer. Proteins released from the beads were detected by western blotting for FAK (top panel) and layilin (bottom panel). The lanes containing proteins bound by GST fusions to chicken talin and fibronectin EIIIB are overloaded approximately 25-fold relative to the total lysate lane.

(B) Glutathione agarose preloaded with GST fusions containing various fragments of chicken talin was incubated with detergent lysates of NIL8 cells expressing HA-tagged layilin or HA-tagged layilin lacking a cytoplasmic domain, washed, and boiled in gel loading buffer. Proteins released from the beads were detected by western blotting for the HA-epitope tag. GST-talin fusion proteins containing amino acids 280-435 bind HA-tagged layilin in extracts of NIL114 cells (solid arrowhead, top panel). The GST-talin 1-435 fusion was overloaded, resulting in the increased signal shown. In contrast, HA-layilin Δcyto does not bind GST-talin fusions above background (open arrowhead, bottom panel). Asterisks indicate background signal from the GST-fusion proteins which migrate near the HA-layilin Δcyto band. Lanes containing material bound to GST fusions are overloaded approximately 20-fold relative to the total lysate lane.

(C) Negative controls indicate that FAK binding is specific for GST-talin and that tensin, alpha-actinin, and beta-tubulin do not bind GST-talin. Glutathione agarose preloaded with GST-talin or GST-FN fusions were incubated with NIH3T3 cell lysates, washed and bound material eluted with binding buffer containing steps of increasing NaCl concentration. Eluted protein was analysed by western blotting with antibodies to the indicated proteins. Bound material was overloaded 20-fold relative to the lysates.

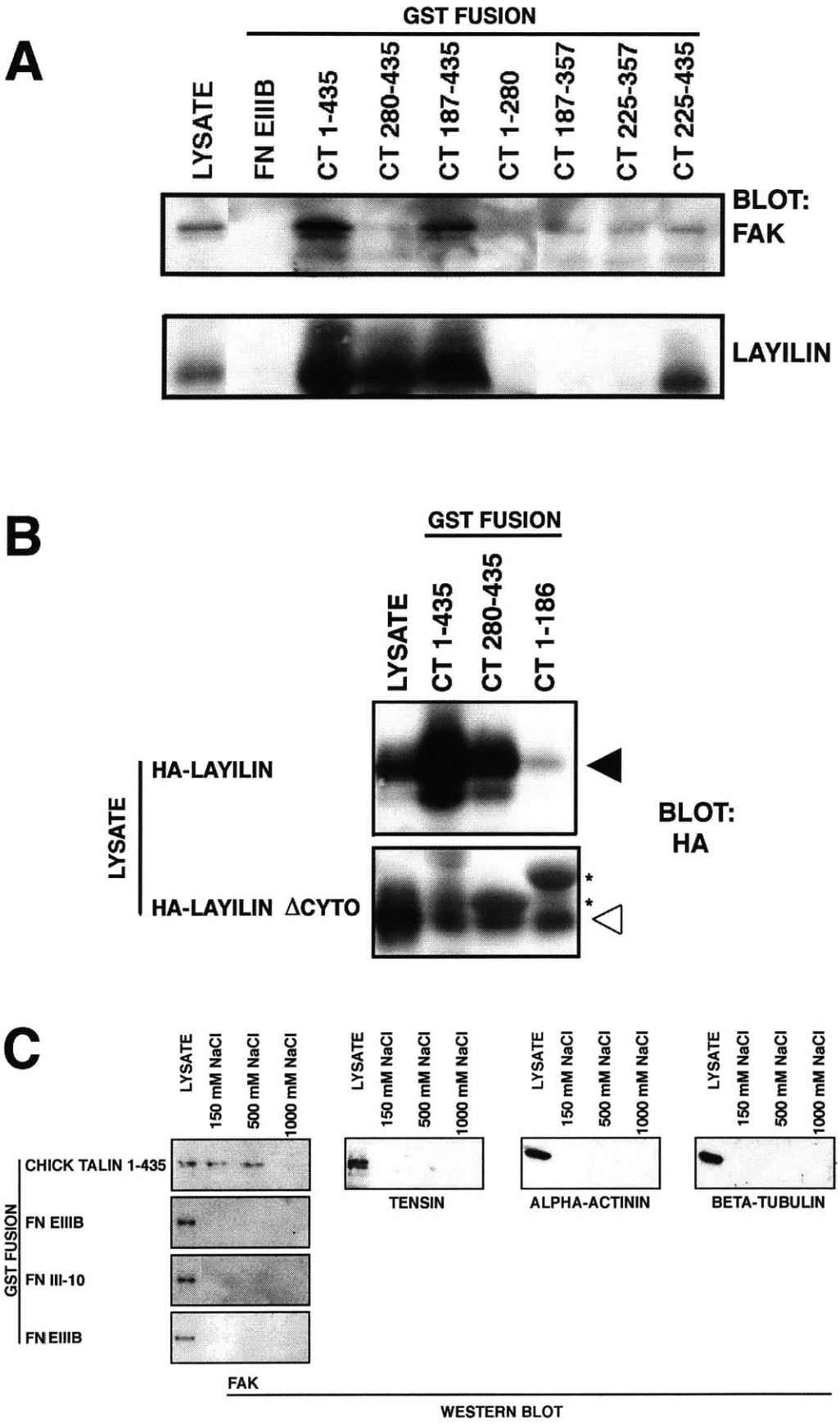
A
GST FUSION
LYSATE
FN EIIIB
CT 1-435
CT 280-435
CT 187-435
CT 1-280
CT 187-357
CT 225-357
CT 225-435
BLOT:
FAK
LAYILIN
B
GST FUSION
LYSATE
CT 1-435
CT 280-435
CT 1-186
LYSATE
HA-LAYILIN
HA-LAYILIN ΔCYTO
BLOT:
HA
C
LYSATE
150 mM NaCl
500 mM NaCl
1000 mM NaCl
GST FUSION
CHICK TALIN 1-435
FN EIIIB
FN III-10
FN EIIIB
FAK
TENSIN
ALPHA-ACTININ
BETA-TUBULIN
WESTERN BLOT

Figure 2-21: Interaction between layilin and radixin. (A) Nickel-Sepharose preloaded with bacterially-expressed his-tagged radixin N-terminal domain was mixed with a CHO cell detergent lysate, washed, and bound material eluted by boiling in gel loading buffer. His-tagged radixin N-terminal domain bound layilin whereas radixin C-terminal fragment and his-tagged full-length radixin do not bind layilin above the background levels seen with unloaded nickel-Sepharose (beads alone lane). GST-CT 1-435 and 2 GST-FN fusion were assayed in parallel as positive and negative controls, respectively.
(B) Purified GST-layilin(261-374) binds to purified his-tagged radixin N-terminal domain. Soluble GST-layilin(261-374) or GST alone was incubated with the indicated his-tagged radixin fragments, complexes were captured on nickel-Sepharose, washed, bound material released by boiling in gel loading buffer and analysed by western blotting with anti-GST antibodies. Arrow, GST-layilin.
(C) Layilin and radixin C-terminal fragment exhibit mutually exclusive binding to radixin N-terminal fragment. GST-layilin(261-374) was incubated with his-tagged radixin N-terminal fragment in the presence of increasing amounts of his-tagged radixin C-terminal fragment. An anti-GST western blot shows bound GST-layilin (top panel), and an anti-radixin blot shows C-terminal fragment levels in the same samples (bottom panel).
(D) His-tagged full length radixin was incubated with GST-layilin (261-374) in the absence or presence of 15 or 50 micromolar PI-4-P. Bound GST-layilin was detected by western blotting with anti-GST.

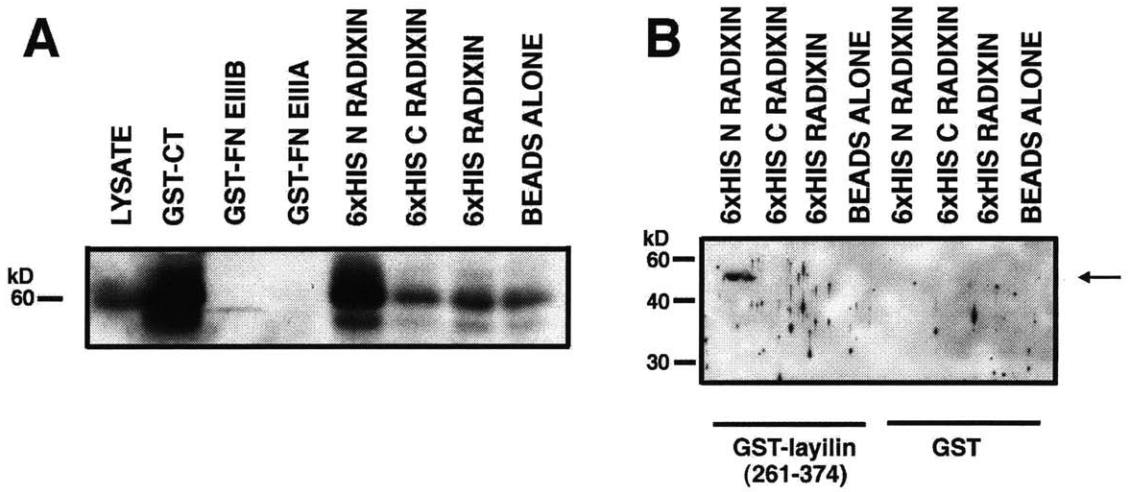
A
LYSATE
GST-CT
GST-FN EIIIB
GST-FN EIIIA
6xHIS N RADIXIN
6xHIS C RADIXIN
6xHIS RADIXIN
BEADS ALONE
kD
60
B
6xHIS N RADIXIN
6xHIS C RADIXIN
6xHIS RADIXIN
BEADS ALONE
6xHIS N RADIXIN
6xHIS C RADIXIN
6xHIS RADIXIN
BEADS ALONE
kD
60
40
30
GST-layilin
(261-374)
GST
C
C RADIXIN
GST-LAYILIN
C RADIXIN
D
PIP μM
0 15 50
kD
90
70
60
40
30

Chapter 3

Strategies to identify layilin function

"Arrogance – the besetting sin of some young academicians – almost always inhibits the discovery process and personal advancement. They have 'an answer to everything and are astonished at nothing.'"

T.B. Lawrence

Introduction

In the previous chapter, the discovery and basic cell-biological characterization of layilin, a new talin-binding protein, was described. Here I relate efforts to uncover the function of this protein. My efforts were guided by models laid out in the discussion of the previous chapter, and I decided to focus on layilin's potential role in cell motility because the role of talin in cell migration has been well documented. In contrast, talin's role in phagocytosis, although suggested by talin's presence in phagocytic cups, still awaits demonstration. In addition, the identification of an integral membrane protein specific and necessary for migration in a variety of cell types would be a significant advance. Such a molecule would be an obvious target for new drugs to treat metastatic cancer. This would also be of great interest because cell motility is necessary for wound healing, inflammation and immunity. Similarly, cell migrations constitute fundamental steps in development, ranging from gastrulation and neural crest deployment to axonal guidance.

Despite the broad significance of cell motility, no surface proteins have been shown to be dedicated specifically to this process. The role of some surface proteins in motility is complex. Integrins are required for fibroblast movement, presumably by providing traction, and hence a counterforce for movement (Palecek et al., 1997). However, integrin-mediated adhesion can be sufficiently strong to reduce motility, presumably by simply anchoring cells tightly to the extracellular matrix. Hence, motility peaks when cell-matrix interactions are of moderate strength and is reduced if adhesion is either too strong or too weak. Some experiments suggest that the hyaluronic acid receptor, CD44, mediates migration but the precise role of CD44 in this process has not been elucidated (Sherman et al., 1994). One ruffle-specific membrane protein is detected by the monoclonal antibody YF-169, although the antigen has not been cloned (Hasegawa, 1993). I have been unable to obtain the antibody in order to ascertain whether or not this 55 kD cell-surface protein is layilin.

To address the role of layilin in cell motility I adopted two general strategies. I tested the effect of a candidate dominant negative form of layilin on migration, and I generated cell lines expressing antisense layilin transcripts. My choice of dominant negative protein was influenced by the observation that membrane-anchored β1-integrin cytoplasmic domain inhibited spreading and cell adhesion (LaFlamme et al., 1994; Lukashev et al., 1994; Smilenov

et al., 1994). Cells stably transfected with chimeras consisting of the extracellular and transmembrane domains of heterologous receptors fused to the cytoplasmic domain of β1-integrin adhere more poorly than do cells expressing truncated IL2R lacking most of its cytoplasmic domain. However, this effect was quite subtle and was not appreciated until the cell lines had been studied extensively (LaFlamme et al., 1992; LaFlamme et al., 1994) In one case, the inhibitory effect was revealed only when cytoskeletal reorganization was stimulated by LPA (Smilenov et al., 1994). It is possible that these chimeric receptors exerted a subtle inhibitory effect on cell adhesion because the membrane anchored cytoplasmic domain, which was shown to be concentrated in focal adhesions, retained some function by serving as a membrane-binding site for cytoskeletal proteins. To avoid this potential difficulty in a layilin dominant negative, a cytosolic rather than membrane-bound version of the layilin cytoplasmic domain was tested.

One alternative dominant negative (which was not tested) would consist of the layilin extracellular and transmembrane domains fused to an irrelevant cytoplasmic domain or a stop-transfer sequence only. This form of layilin might be expected to compete with the full-length polypeptide for binding to hypothetical extracellular ligands. However, absent any data pertaining to the biochemical function of the extracellular domain, I felt it wisest to pursue first the cytoplasmic domain. Data presented in the previous chapter show that this region of layilin binds to talin and hence has at least one specific potential mechanism for interfering with cell motility. Moreover, if such a dominant negative were effective, ablation of the talin-binding sites in the dominant negative could be used to test the mechanism and to show specificity.

Expression of antisense layilin transcripts is also described. This method has been used with mixed results to deplete cells of specific polypeptides. Talin and ERM proteins offer two successful applications of this technology (Takeuchi et al., 1994b; Albigès-Rizo et al., 1995). A cell line with inducible antisense talin expression, AT22, has 20% of normal talin protein levels as assessed by metabolic labeling and immunoprecipitation. These cells have slowed initial rates of adhesion and spreading, but at late timepoints they resemble wild-type cells (Albigès-Rizo et al., 1995). The use of an inducible system lessens the likelihood that the phenotype of these cells is a clone-specific artifact, although the report would be greatly strengthened by the study of several independent clones. In another study, antisense oligonucleotides were used to reduce the amounts of ezrin, radixin, and moesin in two cell

types tested (Takeuchi et al., 1994b). Each oligonucleotide was shown to be specific for the appropriate member of this protein family, and treatment with the mixture of oligonucleotides resulted in significant reduction in all three polypeptides (discussed in chapter 1).

Materials and Methods

Microinjection experiments

Preparation of GST-fusion proteins: Bacterial fusion proteins for microinjection were prepared as described in Chapter 2. After proteins were bound to GSH-agarose and washed as described, fusion proteins were washed once with elution buffer (50 mM Tris pH 7.5, 1 mM PMSF, 9 TIU/ml aprotinin, 5 micrograms/ml leupeptin) and then eluted three times for 30 minutes each at room temperature with one bed volume of elution buffer containing 10 mM reduced glutathione. The first eluted fraction was dialyzed overnight at 4°C against three changes of microinjection buffer (75 mM KCl, 10 mM KPO_4, 0.1% β-ME) and stored at 4°C until use. Immediately before loading microinjection needles, fusion proteins were adjusted to 1 mg/ml and spun for 30 minutes at room temperature in an airfuge at 100,000 x g to remove particulate debris.

Microinjection and processing of cells: FN-coated coverslips containing confluent monolayers of NIL8 cells were prepared as described in chapter 2. On the day of injection, coverslips were transferred to 10 cm dishes containing 20 mls of warm PBS+Ca/Mg and half the cells removed with a rubber cell scraper. The margin of the wound was found using an inverted microscope and, as the coverslip was held in place with forceps, 1 or 2 short scratches were made in the coverslip approximately on the edge of the wound. Typically these marks were 10-20 cell diameters in length and paralleled the long axis of the wound. Due to the difficulty in placing the pen point precisely at the edge of the wound, markings were frequently offset by up to 10 cell diameters from the actual edge of the wound. For this reason, the marks indicated the approximate edge of the wound. Cells were returned to individual wells in a fresh 24-well dish loaded with 1 ml of media containing 5% serum. Cells were used after 2-3 hours of incubation at 37°C/5% CO_2. At this timepoint most of the cells at the wound edge appear healthy, and between 10-30% of cells have become polarized with a single lamellipodium extending into the denuded area. Eppendorf femtotips were loaded with about 1 microliter of bacterially-expressed GST fusion protein prepared as described above. The needle concentration of fusion protein was 1 mg/ml. Coverslips were transferred to an open-topped stage chamber containing warm medium, and the chamber was placed on the stage of a Nikon Diaphot 300. A loaded needle was attached to a stage-mounted Eppendorf micromanipulator (model number 5171),

and cells were microinjected by positioning the needle above the perinuclear region and then lowering the needle into the cell. As soon as the cell membrane underwent noticeable deformation, or a crescent-shaped clear zone began to form around the nucleus, the needle was raised out of the cell. On average about 30 cells were injected per coverslip. After microinjection, coverslips were returned to a 37°C/5% CO_2 incubator for 20-24 hours. Cells were fixed and processed for immunofluorescence as described in chapter 2. Anti-GST antibodies were used to detect injected cells.

Generation of inducible GFP-fusion protein cell lines

Constructs: A subclone of the layilin cDNA encoding the cytoplasmic domain from amino acid 261-374 was made by PCR with primers LECTF2 and LECTR3. The PCR product was digested with BstYI, rendered blunt with Klenow fragment, digested with AvaI and then ligated into EcoRV/XhoI-digested pBluescript SK- to produce the plasmid MB145. An EcoRI/KpnI fragment from MB145 was ligated into EcoRI/KpnI-digested pEGFP-C2 (Clontech) which generated a construct which encodes an in-frame fusion between GFP and layilin cytoplasmic domain with layilin C-terminal to GFP. This construct was digested with NheI and blunted with Klenow, digested with BamHI and ligated into pTRE (Clontech) which had been partially digested with XmnI and completely digested with BamHI. The resulting construct places the GFP-layilin chimera under the control of a tet/VP16 hybrid transcriptional activator. The same strategy was used to make plasmid MB168, a construct placing GFP under the transcriptional control of tet/VP16. To make GFP-FRNK (MB170), a pBluescript subclone of chicken FAK was digested with NdeI, blunted with Klenow, digested with SalI, and ligated into MB168 which had been partially digested with EcoRI and completely digested with SalI.

Electroporation: CHO AA8 cells were purchased from Clontech. These cells are stable transfectants which produce the chimeric transcriptional regulator tet/VP16. This fusion protein binds to tet-repressor binding sites and activates transcription only in the absence of tetracycline and related antibiotics (such as doxycycline). CHO AA8 cells were electroporated according to manufacturer's instructions using a Biorad Gene Pulser. Briefly, DNA was prepared by ethanol precipitating 10 micrograms of the tet-regulated plasmid with 1 microgram of pTK-Hyg (containing a constitutively-expressed selectable marker) and resuspending in 20

microliters of sterile PBS. Sub-confluent CHO AA8 cells were suspended by treatment with trypsin/EDTA, washed, and adjusted to 10^7 cells/ml. Cells and DNA were mixed, electroporated, and allowed to recover for 10 minutes at room temperature. Aliquots containing 2.5% and 12.5% of the total cells were plated on 15 cm dishes in medium containing doxycycline and G418. Forty-eight hours later hygromycin B was added to final concentration of 400 micrograms/ml. Eighteen days later clones were recovered using cloning rings and trypsin.

FACS analysis and sorting: Cells were released with trypsin/EDTA or EDTA alone (as CHO AA8 cells were found to be easily released from tissue culture plastic by pipetting), washed once in PBS, and resuspended in PBS containing 0.5 mg/ml propidium iodide (PI) to a final concentration of between 1 and $5x10^6$ cells/ml. For expression analysis, a region containing PI-negative cells was defined and 10,000 events were collected on a Becton-Dickinson FACScan using standard settings. To clone by FACS, mixed clones known to contain a population of GFP-positive cells were induced to express the GFP-fusion protein by growth in the absence of antibiotic for four days. Cells were released as described above and sorted on a FACStar plus. Sorted clones were reanalyzed at a later date to verify that the desired population of cells had been purified.

Western analysis of protein expression in GFP-expressing cells: For timecourse experiments, $5x10^4$ cells were distributed to each well of a 6-well plate in medium containing antibiotic (uninduced conditions). At the appropriate time, the media was replaced with media lacking antibiotics to induce expression of the fusion proteins. At the endpoint, cells were rinsed in PBS and lysed in RIPA buffer. Protein concentrations were determined using the Micro-BCA kit, and an equal mass of each lysate was assayed by western blotting with antibodies against layilin or GFP (Clontech).

Generation of tetracycline-regulated antisense-expressing cell lines

Constructs: Inserts for antisense-expressing constructs were derived from the plasmids MB112 and MB93. MB93 consists of the layilin cDNA cloned into pBluescript. The vector-derived EcoRI site in MB93 was ablated by digestion with EcoRI, Klenow blunting, and self-

ligation. The resulting plasmid, MB108, was digested with HincII and a synthetic oligonucleotide containing an EcoRI site was inserted. The result is plasmid MB112, and the linker adds 4 in-frame amino acids to the layilin lectin homology domain. To make the 350 bp antisense insert, MB112 was digested with EcoRI and BamHI, and the insert was ligated into EcoRI/BamHI-cut pTRE. The 600 bp antisense insert was made by digesting MB93 with XmnI and BamHI, and ligating the insert into EcoRI-cut, blunted, BamHI-cut pTRE.

Analysis of cell lines: Cell lines were electroporated and cloned as described above except that limiting dilution was used instead of FACS cloning to subclone positive cell lines. Timecourse analysis was performed as described for GFP-expressing cell lines. Total RNA was harvested from 6-well dishes essentially as described in chapter 2 except volumes were scaled to accommodate fewer cells. Northern blots were performed as described in chapter 2.

Transwell migration assay

GFP-fusion protein expression was induced by plating $7.5x10^4$ cells on 10cm tissue culture dishes plus or minus doxycycline. After three days of induction, phase photomicrographs were recorded on Kodak T160 film using a Nikon Diaphot microscope. The next day, cells were released with warm versene, pelleted, and resuspended in medium containing 0.5 % BSA, 1% serum, and doxycycline for uninduced samples. Falcon transwell migration chambers were used as inserts in 24-well plates. Migration chambers were prepared by coating the underside with 10 micrograms/ml human plasma fibronectin in PBS+Ca/Mg for at least an hour at 37°C/5% CO_2 and then washing with PBS+Ca/Mg. Media containing 0.5 % BSA, 1% serum, and doxycycline (for uninduced samples) was added to the bottom of each well. Cells were adjusted to 10^6 cells/ml and 100 microliters gently pipetted into the top of a Falcon transwell migration chamber. Cells were returned to a 37°C/5% CO_2 incubator for 6 hours. During this time, the remaining cells from each sample were analyzed by FACS as described above. Transwell chambers were then quickly rinsed three times in PBS+Ca/Mg and cells remaining on the upper surface of the chamber were wiped off with a cotton-tipped swab. Cells were simultaneously fixed and stained for two minutes in 2% ethanol/1% crystal violet/100 mM borate pH 9.0 and then rinsed three times with distilled water. Stained cells were air-dried

overnight and then bound dye was released with 10% acetic acid. Absorbance at 600 nm was determined for each sample. Four to six chambers were assayed per cell line and condition.

Results

Effect of GST-layilin cytoplasmic domain fusion protein on cell migration

Microinjection of fusion proteins has been used to demonstrate function for various cytoskeleton associated proteins found in focal contacts (Hemmings et al., 1996; Gilmore and Romer, 1996; Nix and Beckerle, 1997). I microinjected NIL8 cells with bacterially-expressed GST-fusion proteins in an effort to disrupt layilin activity and reveal a role for layilin in cell motility. Cells were plated on FN-coated coverslips at high density in 0.5% serum overnight to generate confluent monolayers of extremely flat, well spread NIL8 cells. Half of each coverslip was denuded by scraping with a rubber scraper, and the position of the wound edge was marked by gently scoring the coverslip with a diamond-tipped pen. Two hours later the majority of cells on the edge of the wound were observed migrating into the cleared region of the coverslip. The cells on each coverslip were microinjected with one of three proteins: GST alone, GST fused to the layilin cytoplasmic domain (amino acids 261-374), and GST fused to a C-terminal fragment of focal adhesion kinase (FRNK). After microinjection, cells were incubated overnight, fixed and stained with anti-GST antibodies to detect injected cells. Cells were counted as being at the base if they were still approximately equal to the position of the wound edge after overnight incubation. Cells scored as leading edge cells were those which remained ahead of all other cells such that no cell could be seen between them and the denuded region. Cells between the base and leading edge cells were scored as being in the pack.

Examination of approximately 300 cells each microinjected with either GST or GST-layilin(261-374) revealed no difference in the distribution of cells between the leading edge, the pack, and the baseline (figure 3-1A). In contrast, microinjection of GST-FRNK displaced cells from the leading edge to the migrating pack, suggesting that this fusion protein inhibited motility (figure 3-1B). In this experiment, although 150 cells were initially microinjected, only 50 were detected when cells were counted the next day. It is possible that the GST-FRNK fusion protein disrupts adhesion in some cells sufficiently that they do not remain attached when coverslips were processed for immunofluorescence. The cells which remained may have been injected with slightly less fusion protein, or may have been larger cells to begin with and hence experienced a lower final intracellular concentration of fusion protein. Alternatively, the fusion protein may only prevent re-adhesion of cells, perhaps after they round during cell

division, in which case the remaining cells might have been lost once they underwent mitosis. It is also possible that this fusion protein is toxic to NIL8 cells.

Effect of GFP-layilin cytoplasmic domain fusion protein on cell migration

The microinjection experiments described above allowed examination of a relatively small number of cells. To assess migration in large populations of cells, CHO cells expressing a candidate dominant-negative form of layilin, a green-fluorescent-protein layilin cytoplasmic domain (amino acids 261-374) fusion protein, were generated. Fusion protein production is under the control of a tetracycline-regulated promoter such that it is expressed in the absence of antibiotics and repressed in the presence of tetracycline or doxycycline. This strategy was chosen to prevent loss of cell lines due to potential physiological effects or toxicity of the fusion protein. Several positive cell lines were recovered and found to express a fusion protein of appropriate molecular weight which reacts with anti-layilin antibodies. Timecourse analysis of fusion protein expression indicated that fusion protein levels increased with time and that endogenous layilin levels were unaffected by GFP-layilin expression (figure 3-2). FACS analysis of these cell lines confirmed time-dependent increase in GFP signal at least up to 45 hours (figure 3-3). This analysis also revealed that the cloned cell lines consisted of two population of cells, those that expressed the GFP-fusion and those that did not. Cells were sorted by FACS and positive and negative cell populations examined for GFP by FACS (figure 3-4). Figure 3-4 shows that after FACS sorting, a population of positive cells was obtained; these cells have remained positive thereafter, suggesting that differences in GFP expression observed in the original clones were due to multiple clonal origins. The sorted cell lines were returned to culture in the presence of doxycycline to repress expression of the GFP-fusion proteins. These FACS-sorted cell lines were used for subsequent experiments.

Expression of GFP-layilin cytoplasmic domain had no effect on CHO cell morphology as assessed by phase microscopy. Induced transfected cell lines resembled both uninduced transfectants and uninduced and induced vector-only transfectants (figure 3-5, panels a-d). Cells are spindle shaped and appear adherent but somewhat refractile, indicating that cells are not well spread. As a positive control, CHO cells with tetracycline-regulated GFP-FRNK were created in parallel with GFP-layilin (261-374) cells. Induction of the GFP-FRNK protein correlated with the appearance of significant numbers of round, weakly adherent cells (figure

3-5, panels e-f). This is consistent with the presumed adhesion-disrupting effect of the GST-FRNK fusion discussed above and with published effects of GST-FRNK (Gilmore and Romer, 1996). Again the persistence of some adherent cells in these cultures may result from variability in fusion protein levels or could reflect the requirement that cells detach, for instance during mitosis, to allow for the dominant-negative effect.

Subcellular localization of the fusion proteins was followed with the GFP tag and compared to actin cytoskeleton. GFP alone exhibits diffuse cytoplasmic localization in addition to some nuclear localization (figure 3-6a). GFP-layilin cytoplasmic domain fusions appear similar to GFP alone except that small actin-rich ruffles also contain GFP-layilin (figure 3-6, panel c-d). In some cases, similar signal was seen in GFP-only cells, making interpretation of the ruffle signal difficult. It is probable that sufficient levels of any GFP fusion protein in the cytoplasm can result in some ruffle signal; however, ruffle signal was seen in cells which did not exhibit high all-over GFP signal (e.g. figure 3-6c). GFP-FRNK localized to the cytoplasm and nucleus, and also became concentrated in focal contacts which align with the ends of actin stress fibers (arrows, figure 3-6 panel e-f). Most GFP-FRNK expressing cells were rounded, and in these cells bright green fluorescence was evident throughout the cell body.

The GFP-layilin cytoplasmic domain fusion protein appears to have the same talin-binding ability as does endogenous layilin. GFP-layilin cytoplasmic domain was able to bind to bacterially-expressed GST-CT 1-435 fusion protein immobilized on agarose beads (figure 3-7). The fusion protein which bound to GST-CT 1-435 was recognized by antibodies directed against both GFP and layilin, indicating that the fusion protein is generally intact (figure 3-7). Moreover, the anti-layilin antibody recognizes an epitope at the C-terminus of the cytoplasmic domain adjacent to the talin-binding site.

The effect of GFP-layilin cytoplasmic domain expression on cell motility was assessed in a transwell migration assay. In this assay, cells are placed on one side of a semi-porous membrane and allowed to cross the membrane. Two clones of GFP-layilin-expressing cell lines were assayed and found to exhibit no net effect on cell motility in this assay (figure 3-8). In different experiments, induction of GFP-layilin expression was found either to increase or decrease migration by up to 30% in these cell lines. Similar results were found with cells containing the expression vector alone. Varying the length of the incubation did not reveal an

effect of GFP-layilin expression although net migration increased with time, as expected. In contrast to the results with GFP-layilin cytoplasmic domain, GFP-FRNK expression consistently caused a 60% decrease in migration in three cell lines examined (two are shown in figure 3-8). This result indicates that differences in migration can be detected in this assay.

Attempts to reduce layilin protein levels by expression of layilin antisense transcripts

Two layilin antisense expression vectors were constructed which drive the expression of transcripts of 600 and 350 nucleotides, respectively. Two were made to increase the likelihood of success, and both were designed to overlap the proposed start of translation. Stably-transfected cell lines were assayed by Northern blotting for inducible antisense expression, and 32 of 52 clones were judged to be positive. The three most strongly-expressing clones of each type were followed-up by timecourse analysis of antisense expression (figure 3-9). Antisense expression increased with time over the 62 hours assayed. Clone 123-23 also produced an aberrantly large transcript of unknown origin. In a parallel timecourse, protein from the same six clones was prepared and western blotted with anti-layilin antibodies. Layilin levels appeared unaffected (figure 3-10, bottom panel). The same lanes were blotted with antibodies against the focal contact protein vinculin as a loading control (figure 3-10, top panel). The slight variations in layilin levels parallel changes in vinculin levels, indicating that they result from minor differences in gel loading.

As previously discussed, FACS analysis indicated that primary clones of GFP-layilin expressing cells were a mix of positive and negative cells. Similar presence of negative cells in the antisense clones could mask down-regulation of layilin protein by antisense expression. To reduce the likelihood of this, the six antisense clones described above were subcloned by limiting dilution. Eighty-one clones were recovered and layilin protein levels assayed by western blotting at a single time point under induced and uninduced conditions. Thirty of the eighty-one subclones were judged to exhibit at least a two-fold decrease in layilin protein; four examples are shown in figure 3-11A. These clones were expanded and assayed for layilin protein levels in a timecourse study. None of 10 clones retested showed any changes in layilin protein levels upon induction of the antisense transcript (four examples are shown in figure 3-11B).

Discussion

Dominant negative approaches

This chapter describes efforts to test the hypothesis presented in the previous chapter that layilin plays a role in cell migration. Two implementations of a dominant-negative strategy (injection of GST-fusion proteins and expression of GFP-fusion proteins) and attempts to make layilin-deficient cells by antisense expression did not generate data to support this theory. It is impossible to interpret these negative results as evidence against this model because other plausible explanations for the data exist. This and previous dominant-negative experiments are motivated by the belief that expression of an appropriate fragment of a protein which exhibits some but not all biochemical activities of the intact molecule may perturb the function of endogenous protein. In this case, I hypothesized that the cytoplasmic domain of layilin serves as a membrane docking site for talin. I reasoned that the presence of excess layilin cytoplasmic domain which was not anchored to the membrane could bind talin and prevent its interaction with endogenous membrane-associated layilin cytoplasmic domain. This dominant-negative also could sequester unknown layilin cytoplasmic domain-binding partners or prevent their association with the plasma membrane.

Microinjection of GST-layilin cytoplasmic domain and expression of GFP-layilin cytoplasmic domain were used to test this idea. In *in vitro* wounding experiments, cells microinjected with GST-layilin cytoplasmic domain migrated equally well into the wound as did cells injected with control GST protein. In contrast, cells injected with GST-FRNK were somewhat inhibited in their migration relative to control GST-injected cells, consistent with previous studies (Gilmore and Romer, 1996). I detected reduced numbers of GST-FRNK injected NIL8 cells after 22 hours of incubation (66% of injected cells were lost), suggesting that this fusion protein also disrupts adhesion, possibly as cells re-attach to the substrate after dividing. This observation is supported strongly by the disruptive effect on cell adhesion of expression of GFP-FRNK fusion protein in CHO cells. In contrast, Gilmore and Romer (1996) reported that BALB/c 3T3 and HUVEC cells microinjected or bead-loaded with GST-FRNK respread normally. It is possible that chicken FAK has a stronger effect on cell adhesion in the hamster cells lines analyzed here than in the human and mouse cells reported previously. However, Gilmore and Romer (1996) found a slightly greater effect on cell motility than did I,

suggesting that species differences do not account for the observed differences, unless the effects of FRNK on cell adhesion and motility are mediated by distinct mechanisms.

There are several explanations for the failure of the GST-layilin fusion protein to produce an effect on cell migration. First, my hypothesis that layilin functions in cell migration may be incorrect. Alternative models for layilin function were discussed in the previous chapter. There is a large soluble pool of talin in the cytoplasm, and only a small fraction of talin is incorporated into cytoskeleton. Hence, a large amount of layilin fusion protein might be required in order to effectively titrate out talin, and I may not have achieved these levels in my microinjection experiments. A typical microinjection introduces an estimated 10^{-13} liters per cell; using a 1 mg/ml solution this corresponds to about 10^{-13} grams of injected protein (Graessmann et al., 1980). Assuming there are 10^{-10}-10^{-9} grams of total protein per cell, the injected protein constitutes between 0.01-0.1% of the total cellular protein, or about 1 to 10 times the abundance of a protein of average abundance. At the low end of this range, only a potent dominant negative is likely to be successful. Moreover, microinjected fusion protein may be subject to proteolysis. Antibodies directed against both the layilin cytoplasmic domain and GST stain microinjected cells at the endpoint of the assay, revealing diffusely localized protein and indicating that at least enough fusion protein remains sufficient to be detected by immunofluorescence. This could be substantially less than was microinjected.

The layilin-talin interaction might be disrupted in cells by microinjecting layilin-derived peptides, such as LC20, which compete binding of talin to GST-layilin *in vitro* (figure 2-19A). Peptides could be microinjected to higher molar concentrations than were achieved for GST fusions because of the peptides' relatively small size. Performance of injected cells in the wound migration model should be compared to that of cells microinjected with a scrambled peptide. However, even the higher concentration of peptides achievable, probably on the order of 10-25 fold greater than that of the GST-fusions used, may be insufficient to titrate talin. An alternative would be to microinject peptides derived from the membrane-proximal half of the layilin cytoplasmic domain. While no biochemical activity has been associated with this segment of layilin, it does contain three copies of one of the internal repeated motifs (LH1), the presence of which may be indicative of function. This hypothesis is consistent with the

observation that this region of the layilin cytoplasmic domain is conserved in the putative human homolog (discussed in chapter 2, figure 2-4D).

Inducible expression of GFP-layilin cytoplasmic domain offered some advantages over microinjection. Larger numbers of cells were tested in migration assays, producing more representative data. FACS analysis allowed an estimation of the heterogeneity of expression levels, which were considerable, varying over two logs within the positive population of cells. Western blotting revealed that the GFP-layilin fusion protein was present in significant excess over endogenous layilin, however, making the possibility that there was insufficient dominant-negative to compete with endogenous layilin an unlikely interpretation. This observation does not rule out the possibility that there were inadequate amounts of fusion protein to titrate all potential layilin-binding sites on talin or other binding partners. Moreover, GFP-layilin fusions may also substitute for endogenous layilin as an adaptor between talin and unknown proteins. If we learn that layilin is involved in cellular processes other than migration, it will be of great interest to see whether these reagents and methods effectively inhibit layilin function in other assays.

Attempts to generate layilin-negative cells via antisense expression

The ineffectiveness of the initial antisense-expressing clones is most likely the result of impure cell clones. These cell lines were cloned in parallel with the GFP-expressing cells, and the latter were proven by FACS analysis to be mixed clones. Upon subcloning it became evident that 31/81 subclones or an average of ~38% of cells in the initial clones expressed the antisense transcript. Hence the primary clones consisted of ~62% non-expressing cells. Assuming the antisense had the effect of reducing protein levels by ~80%, then the band on a western blot would appear (62%×100%+38%×20%=) ~70% as intense as a control band. This may be within the variability observed in the assay or too small a difference to reliably detect by chemiluminescence.

Immediately after subcloning, numerous individual subclones exhibited down-regulation of layilin protein levels when cultured under conditions that induce antisense expression. This effect was lost after two additional passages in culture, and might result from antisense-negative cells taking over the cultures. Non-expressing cells which arise spontaneously may have a growth advantage over layilin-deficient cells, or perhaps cells which

down-regulate layilin die due to an absolute requirement for layilin. Transcription of endogenous layilin may also increase to offset the effects of antisense expression. However, Northern analysis showed that antisense transcripts are produced in vast excess over endogenous transcripts, making the latter hypothesis unlikely.

The finding that antisense suppression of layilin protein appears to be unsustainable in CHO cells is promising. It is unclear why this effect was observed only immediately after subcloning, but it is possible that expression of the antisense transcript under non-induced conditions was deleterious. Although an inducible expression system was chosen to avoid loss of the desired cell population, FACS and western analysis of GFP-expressing cell lines revealed that the system does give rise to some background expression even under uninduced conditions. Antisense transcripts were not detected in uninduced cells, but this observation was made in clones which appear to have been mixed (that is, prior to limiting dilution), thereby leading to an underestimate of the background expression levels in those cells that were positive. The best solution to this potential pitfall is transient expression of antisense transcripts, which could be achieved by high efficiency infection with retroviral vectors or by treatment of cells with antisense oligonucleotides (Marcus-Sekura et al., 1987). If effective, either method would result in populations of cells which have significantly reduced layilin protein levels. In addition to their utility in the transwell migration assay, these cells could be compared with cells treated with control retrovirus or sense oligonucleotides in a range of assays for potential layilin functions.

Figure 3-1: Microinjected GST-FRNK fusion protein inhibits cell migration while microinjected GST-layilin (261-374) does not.

(A) Percent of cells scored as stationary (base), as migrated a maximal amount (front), or as migrated an intermediate amount (pack) are shown with open bars for cells injected with GST and filled bars for cells injected with GST-layilin (261-374). Chi-squared analysis indicates that samples are not significantly different ($p=0.91$).

(B) As in A, above, except filled bars represent cells injected with GST-FRNK. Chi-squared analysis indicates that samples are significantly different ($p=0.046$). As an internal control, GST samples from the experiments shown in A were compared with those from panel B by chi-squared analysis and found not to be significantly different ($p=0.61$).

A

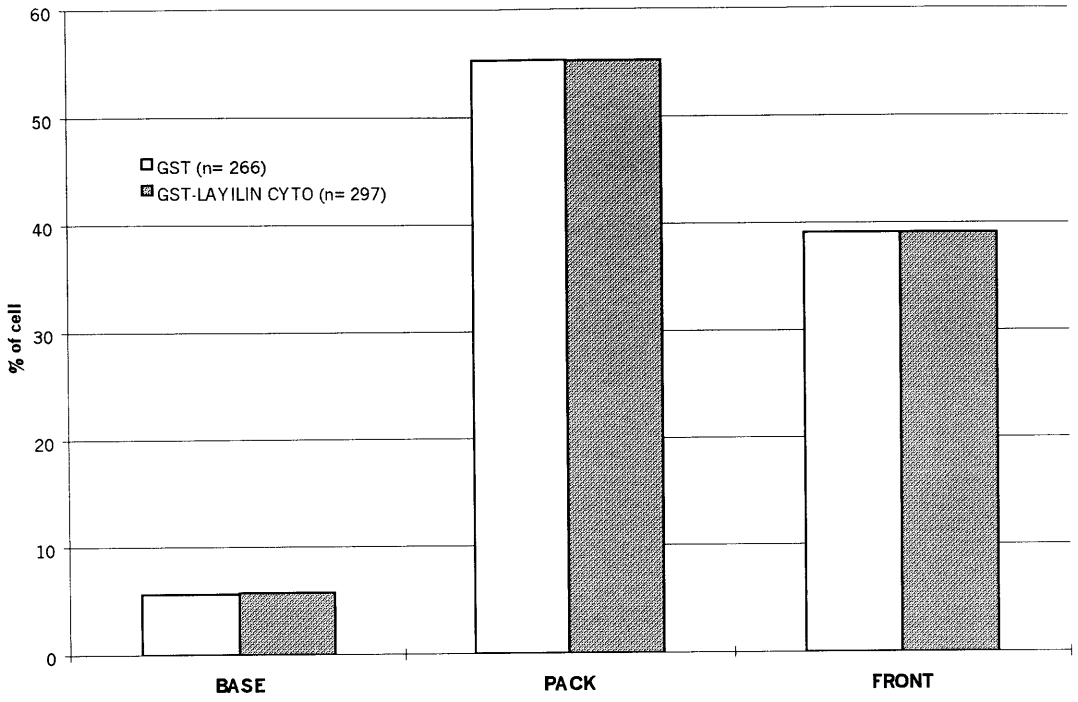
60
50
40
30
20
10
0
% of cell
GST (n= 266)
GST-LAYILIN CYTO (n= 297)
BASE
PACK
FRONT

B

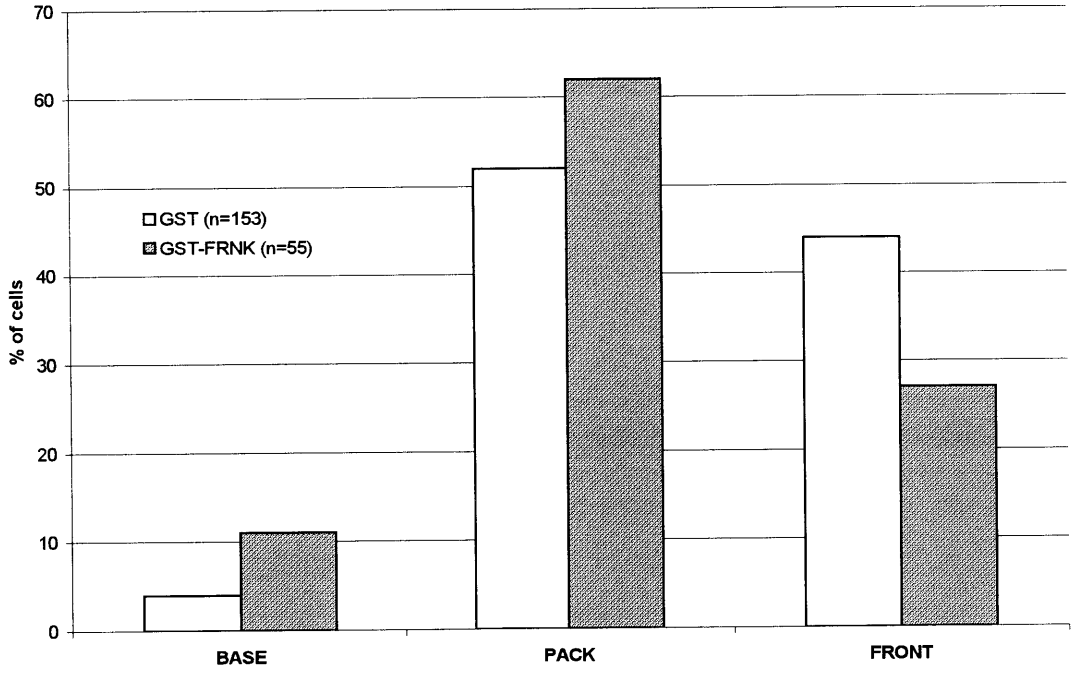
70
60
50
40
30
20
10
0
% of cells
GST (n=153)
GST-FRNK (n=55)
BASE
PACK
FRONT

Figure 3-2: Western analysis of GFP-layilin expression in stably-transfected CHO AA8 cells (clone 162-18). Endogenous layilin (arrowhead) and GFP-layilin (261-374) fusion protein (arrow) are shown for cells induced for the lengths of time indicated. Short and long exposures of the same gel are shown. Note a small amount of fusion protein is evident in the uninduced cells that is not seen in the vector-only transfectants (compare time=0 hours for both sets of lanes). The lanes for the vector-only sample are overloaded relative to the lanes from the GFP-layilin cell line (compare the background band migrating at the bottom of the gel in the long exposure). The same cells were analysed by FACS (figure 3-3).

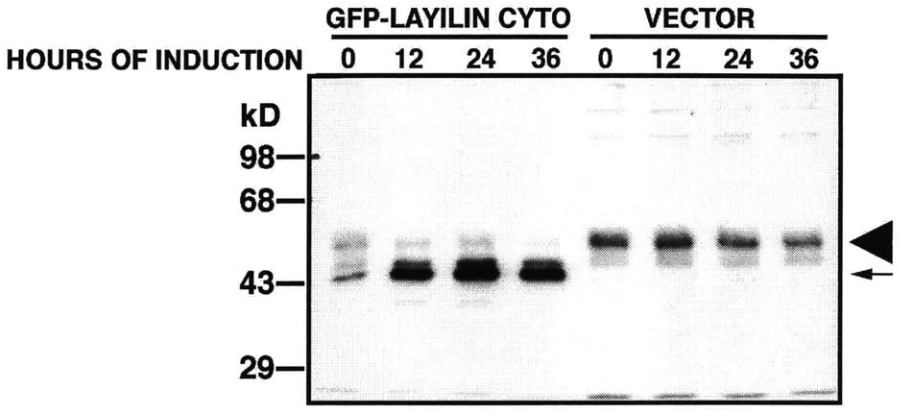

WESTERN BLOT: LAYILIN

Exposure: 30 seconds

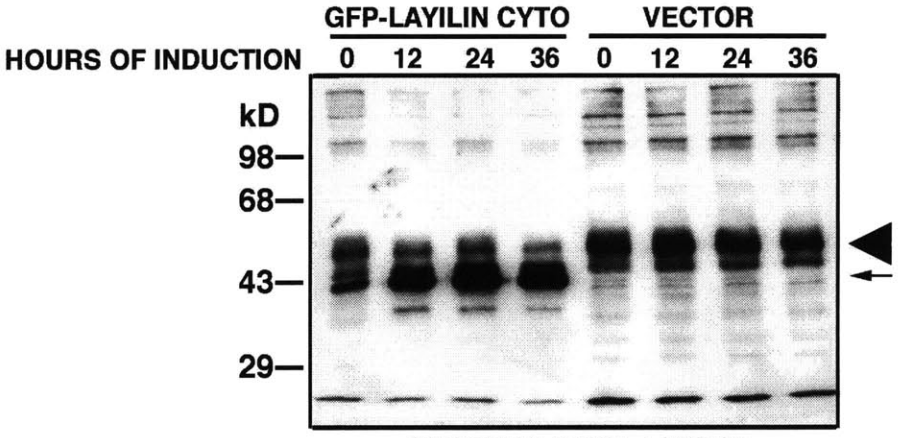

WESTERN BLOT: LAYILIN

Exposure: 5 minutes

Figure 3-3: Timecourse FACS analysis of GFP-layilin expression in live cells. Green fluorescence was measured from samples induced for the number of hours shown. The traces in the left hand column are from cells tranfected with the vector alone, and the right hand data are from a stable transfectant expressing GFP-layilin (261-374), clone 162-18. The mean fluorescence intensity (MFI) for each sample is shown in each histogram. Note that uninduced clone 162-18 has a four-fold greater MFI than does the vector only clone at any timepoint. Two fluorescence peaks are evident in the 45 hour timepoint; the left peak corresponds to the position of the uninduced cells. Cells from the first three timepoints were subsequently lysed and analysed by western (figure 3-2).

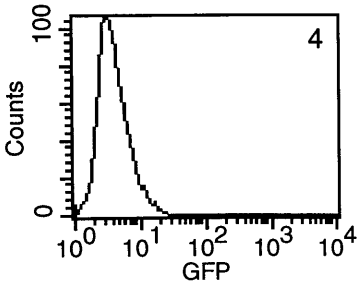

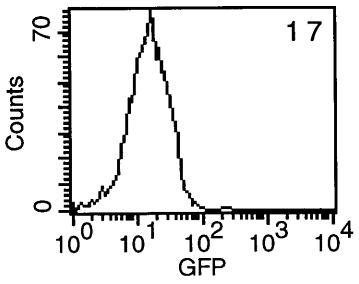

0 hours

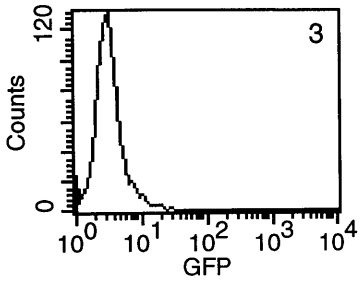

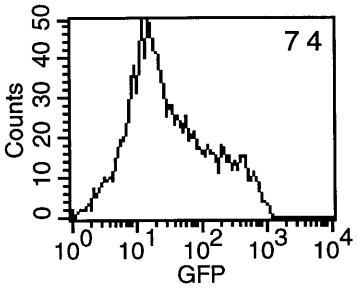

12 hours

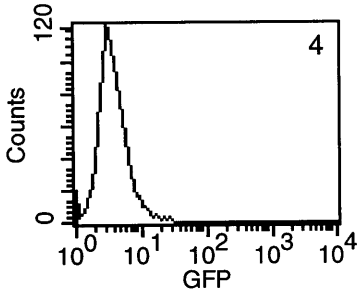

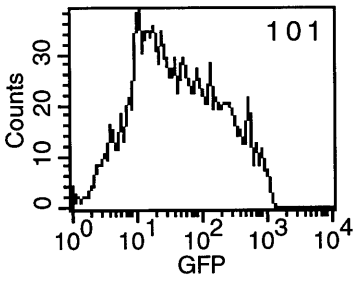

24 hours

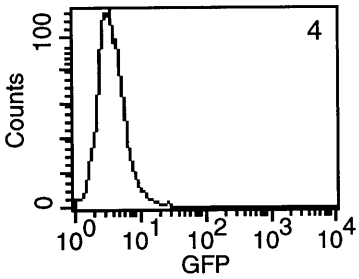

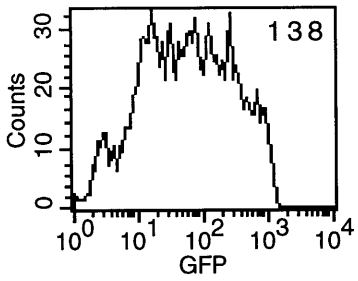

36 hours

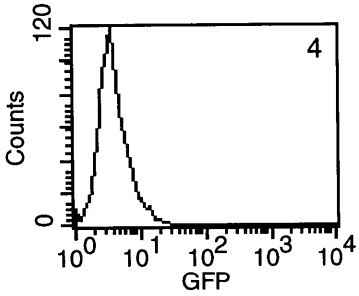

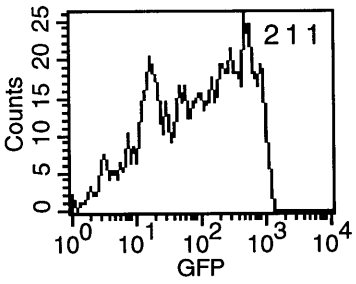

45 hours

Vector

GFP-layilin

Figure 3-4: FACS analysis of FACS-sorted cell lines. (A) Vector transformed cells, (B) GFP-layilin (261-374) clone 162-12, (C) GFP-layilin (261-374) clone 162-18, (D) GFP-FRNK clone 170-14, (E) GFP-FRNK clone 170-15. Left column, uninduced cells; right column, cells induced for four days. The MFI is shown in each histogram.

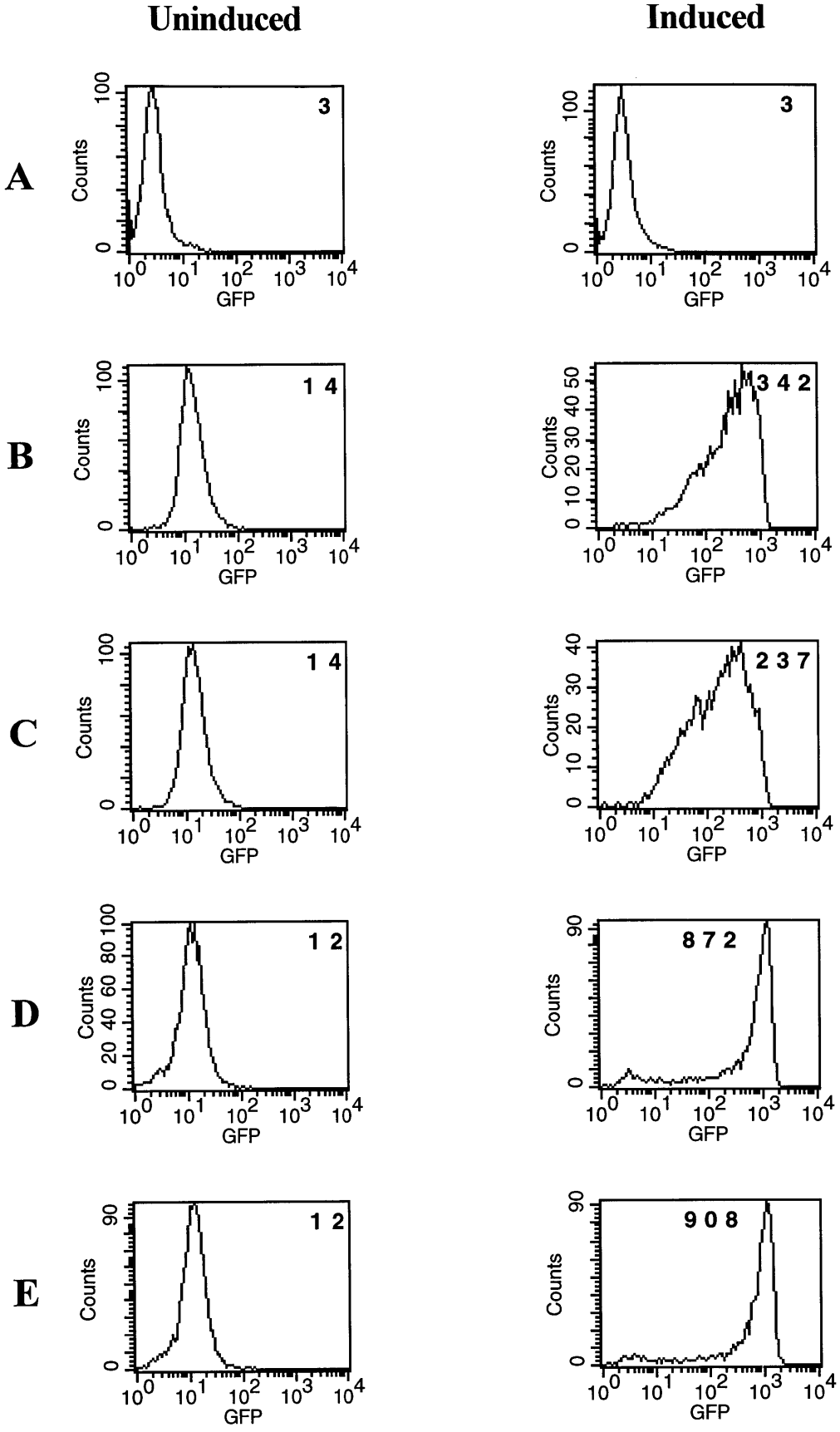
Uninduced
Induced
A
B
C
D
E
Counts
GFP
3
3
1 4
3 4 2
1 4
2 3 7
1 2
8 7 2
1 2
9 0 8

Figure 3-5: Expression of GFP-layilin (261-374) has no effect on cell morphology; expression of GFP-FRNK causes cell rounding. Phase micrographs of live cells stably transfected with (a,b) vector, (c,d) GFP-layilin (261-374), (e,f) GFP-FRNK. Cells are shown uninduced (a,c,e) and after 3 days of induction (b,d,f). Bar = 10 microns.

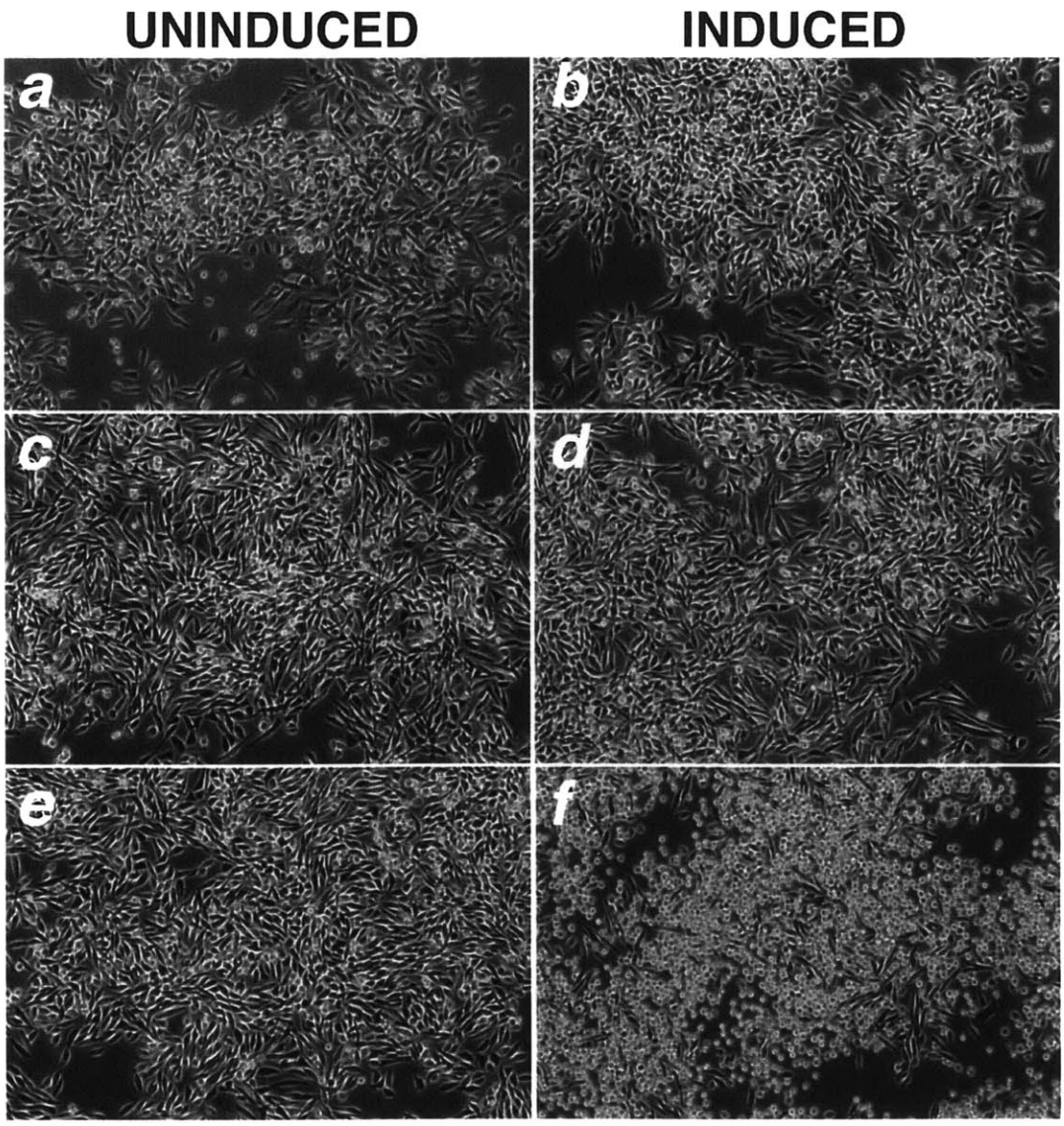
UNINDUCED
INDUCED
a
b
c
d
e
f

Figure 3-6: Subcellular localization of GFP fusion proteins. Although CHO cells rarely produce prominent ruffles akin to those made by NIL8 cells, GFP-layilin (261-374) is seen in modest, actin-containing ruffles which are sometimes found at a cell's leading edge (arrows, c and d). GFP alone is also detectable in some small ruffles as well (arrows, a and b). Cells expressing high amounts of GFP-FRNK are rounded up (arrowheads, e and f). FRNK localizes to focal contacts (arrows) in moderate and low expressing cells such as the one spread cell in e. Bar = 10 microns.

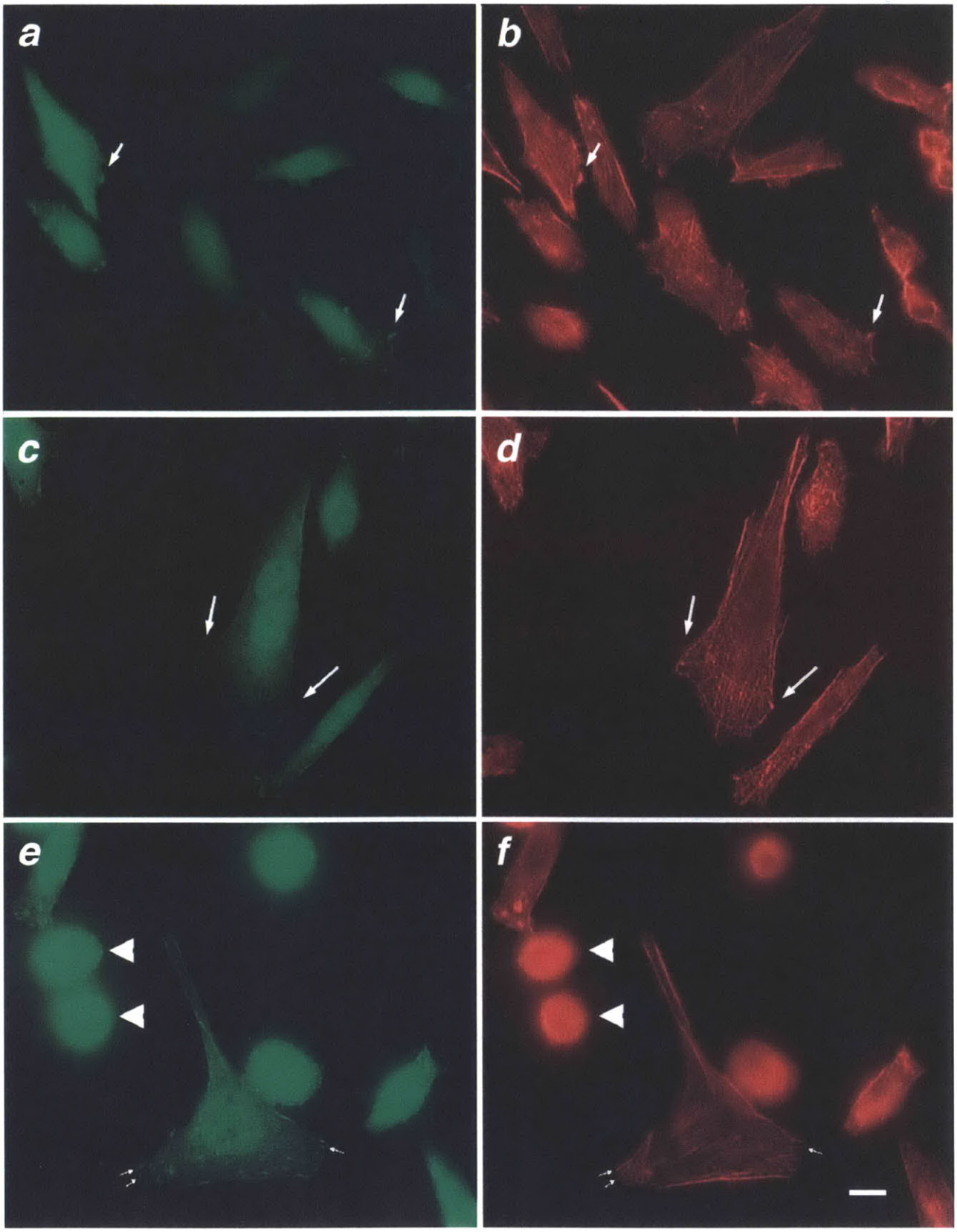
a
b
c
d
e
f

Figure 3-7: GFP-layilin (261-374) binds to GST-CT (1-435) *in vitro*. Lanes + lysate: detergent lysates from induced CHO AA8 cells expressing GFP-layilin were incubated with glutathione agarose preloaded with either GST-CT (1-435) or a control GST fusion (LH3), washed, and the bound material released by boiling in sample buffer. Lanes - lysate were processed in parallel except cells were omitted. Immunoblotting the same filter sequentially with antibodies to GFP (left panel) and layilin (right panel) indicates that the GFP-layilin fusion binds to GST-CT(1-435). The five bands marked in the layilin western blot are as follows: 1, endogenous layilin; 2 and 5, cross-reacting contaminants in the GST CT (1-435) fusion prep, 3, GFP-layilin; 4, breakdown product of GFP-layilin. Note that the lysate itself contains only bands 1, 3 and 4. The GST-fusion protein alone (- lysate) has only bands 2 and 5. The sample in which lysate was mixed with GST-CT (1-435) has all five bands, indicating that GST-CT (1-435) binds both endogenous and GFP-layilin. Moreover, the GFP-layilin breakdown product (band 4) also binds talin head, suggesting it consists of the C-terminal portion of the fusion protein. Evidently the portion of GFP which has been cleaved contains the epitope for the anti-GFP antibody used in this experiment as this band is not seen in the GFP immunoblot.

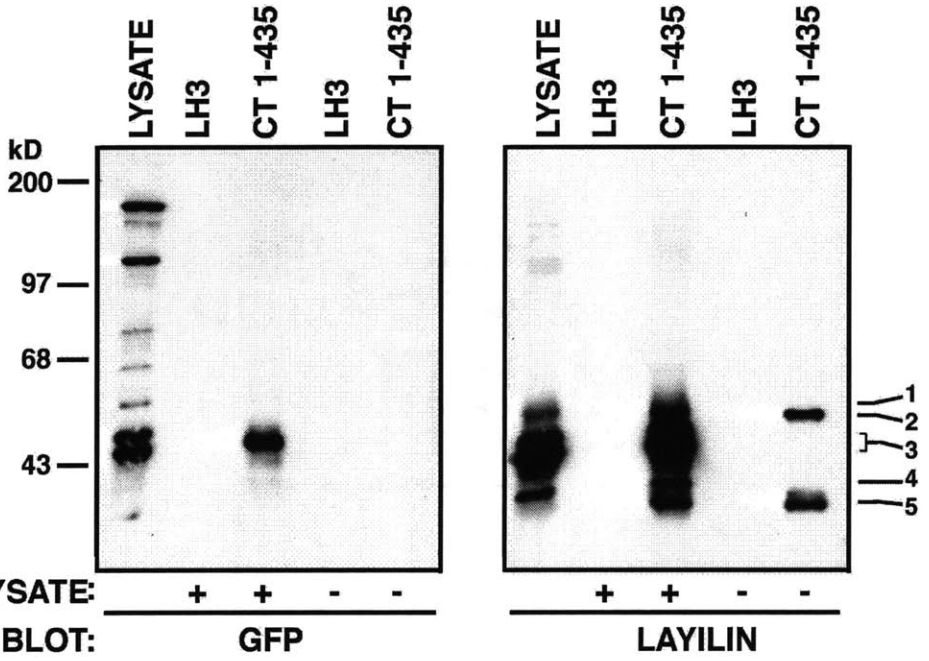
LYSATE
LH3
CT 1-435
LH3
CT 1-435
LYSATE
LH3
CT 1-435
LH3
CT 1-435
kD
200
97
68
43
1
2
3
4
5
LYSATE:
+ + - -
+ + - -
WESTERN BLOT:
GFP
LAYILIN

Figure 3-8: Effects of GFP-layilin (261-374) and GFP-FRNK expression on CHO migration in a transwell assay. The samples shown in figure 3-4 were used in this assay. Migrating cells were quantitated after a 6 hour incubation. GFP-layilin (261-374) has no consistent effect on motility whereas GFP-FRNK inhibits migration by 60-70%. One standard deviation is shown. p values were determined using a two-tailed student's t-test with equal variance.

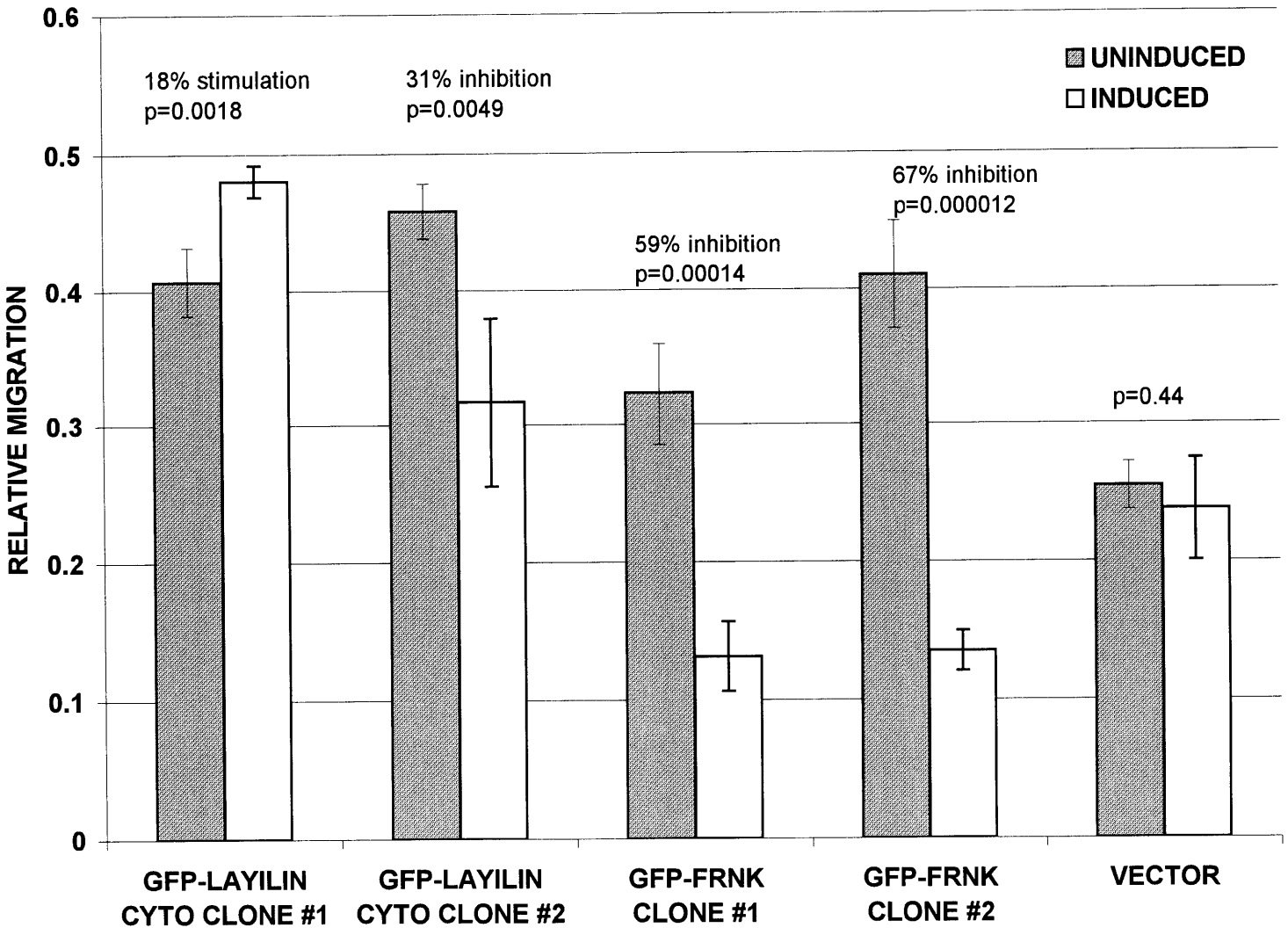
0.6
0.5
0.4
0.3
0.2
0.1
0
RELATIVE MIGRATION
UNINDUCED
INDUCED
18% stimulation
p=0.0018
31% inhibition
p=0.0049
59% inhibition
p=0.00014
67% inhibition
p=0.000012
p=0.44
GFP-LAYILIN CYTO CLONE #1
GFP-LAYILIN CYTO CLONE #2
GFP-FRNK CLONE #1
GFP-FRNK CLONE #2
VECTOR

Figure 3-9: Northern analysis of total RNA from stably-transfected CHO AA8 cells expressing layilin antisense transcripts. Cell lines were cultured in uninducing conditions or were induced by withdrawal of doxycycline for the number of hours indicated. Antisense transcripts are undetectable in uninduced samples, while correctly sized transcripts (arrowheads) show time-dependent increase in expression. Clones 123-15, 123-23, and 123-26 express antisense transcripts with 600 nt of overlap with layilin, and clones 124-1, 124-5, and 124-29 make antisense transcripts with 350 nt of overlap with layilin. Clone 123-23 also produces an abberantly large transcript (arrow). The endogenous layilin transcript is not detectable in this exposure.

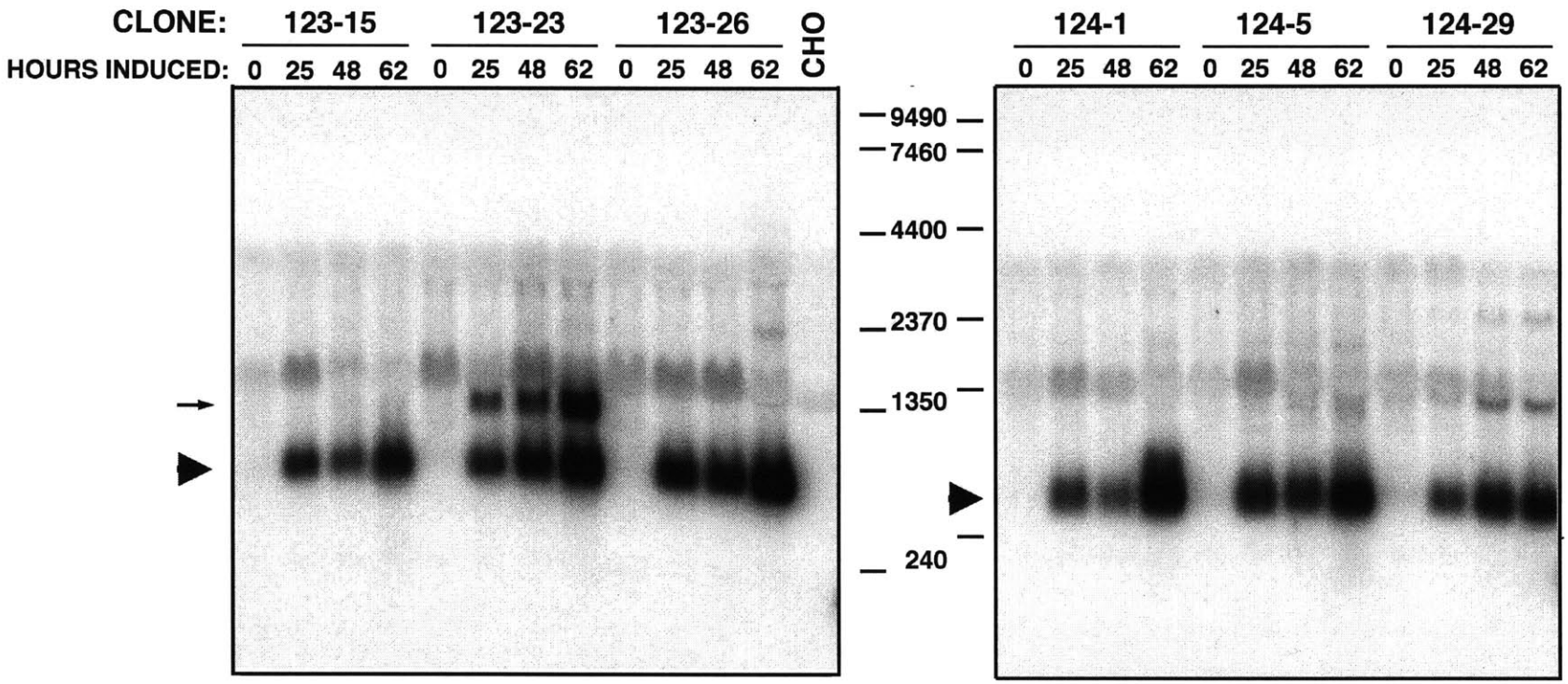
CLONE:
123-15
123-23
123-26
CHO
124-1
124-5
124-29
HOURS INDUCED:
0 25 48 62 0 25 48 62 0 25 48 62
0 25 48 62 0 25 48 62 0 25 48 62
9490
7460
4400
2370
1350
240

Figure 3-10: Layilin antisense expression has no effect on layilin protein levels. No change in layilin protein levels are evident in western analysis of protein made from stably-transfected CHO AA8 cells expressing layilin antisense transcript (bottom panel). Cell lines were cultured in uninducing conditions or were induced by withdrawal of doxycycline for the number of hours indicated. These samples were prepared in parallel with the samples shown in figure 3-9. An equal mass of protein was loaded in each lane; even loading is confirmed by western blotting with anti-vinculin antibodies (top panel).

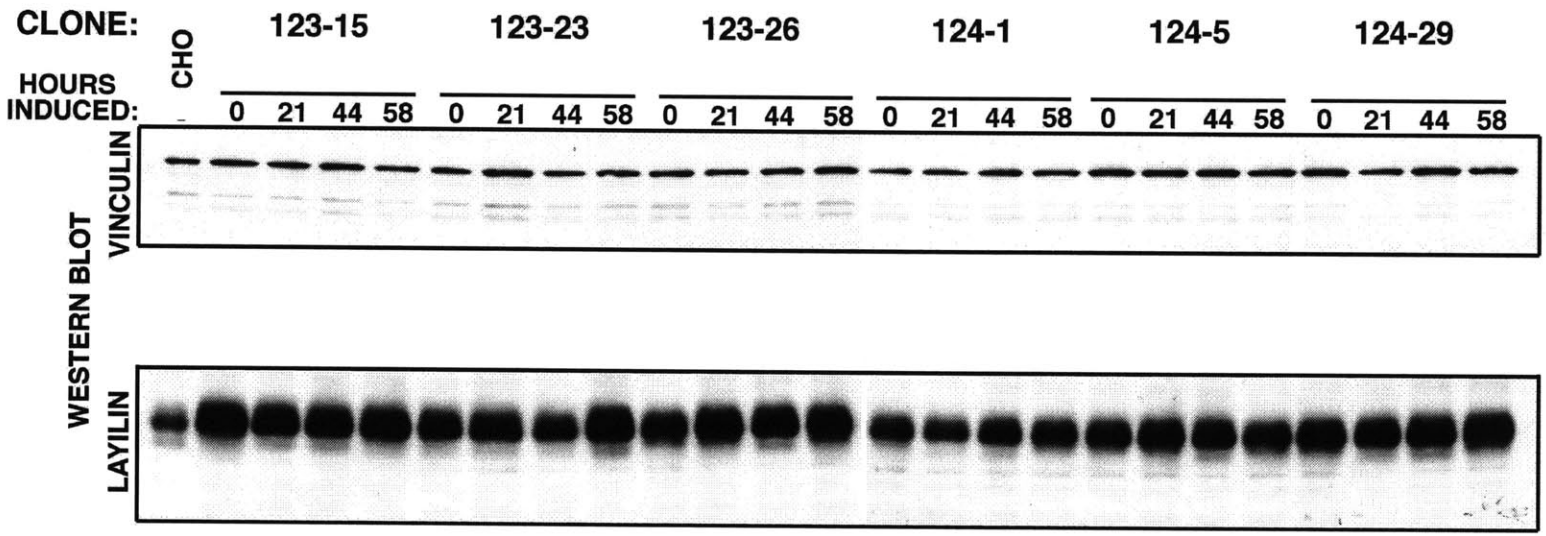
CLONE:
CHO
123-15
123-23
123-26
124-1
124-5
124-29
HOURS INDUCED:
0 21 44 58 0 21 44 58 0 21 44 58 0 21 44 58 0 21 44 58 0 21 44 58
WESTERN BLOT
VINCULIN
LAYILIN

Figure 3-11: Subcloned layilin antisense cell lines lose the ability to suppress layilin protein production. (A) Immediately after cloning, several subclones appear to suppress layilin levels. Layilin protein levels from four subclones grown under inducing (+) or non-inducing (-) culture conditions for 3 days were assayed by western blotting (bottom panel). The top panel is a loading control indicating that vinculin levels in the same lanes are unaffected by antisense expression. Each of these four clones appears to have at least a two-fold reduction in layilin protein levels after induction of the antisense transcipt. (B) Timecourse analysis of layilin protein levels in the same clones as in (A) after two additional passages in culture. Western blotting reveals that layilin levels are now insensitive to antisense expression even after 87 hours of induction (bottom panel). The top panel is a loading control.

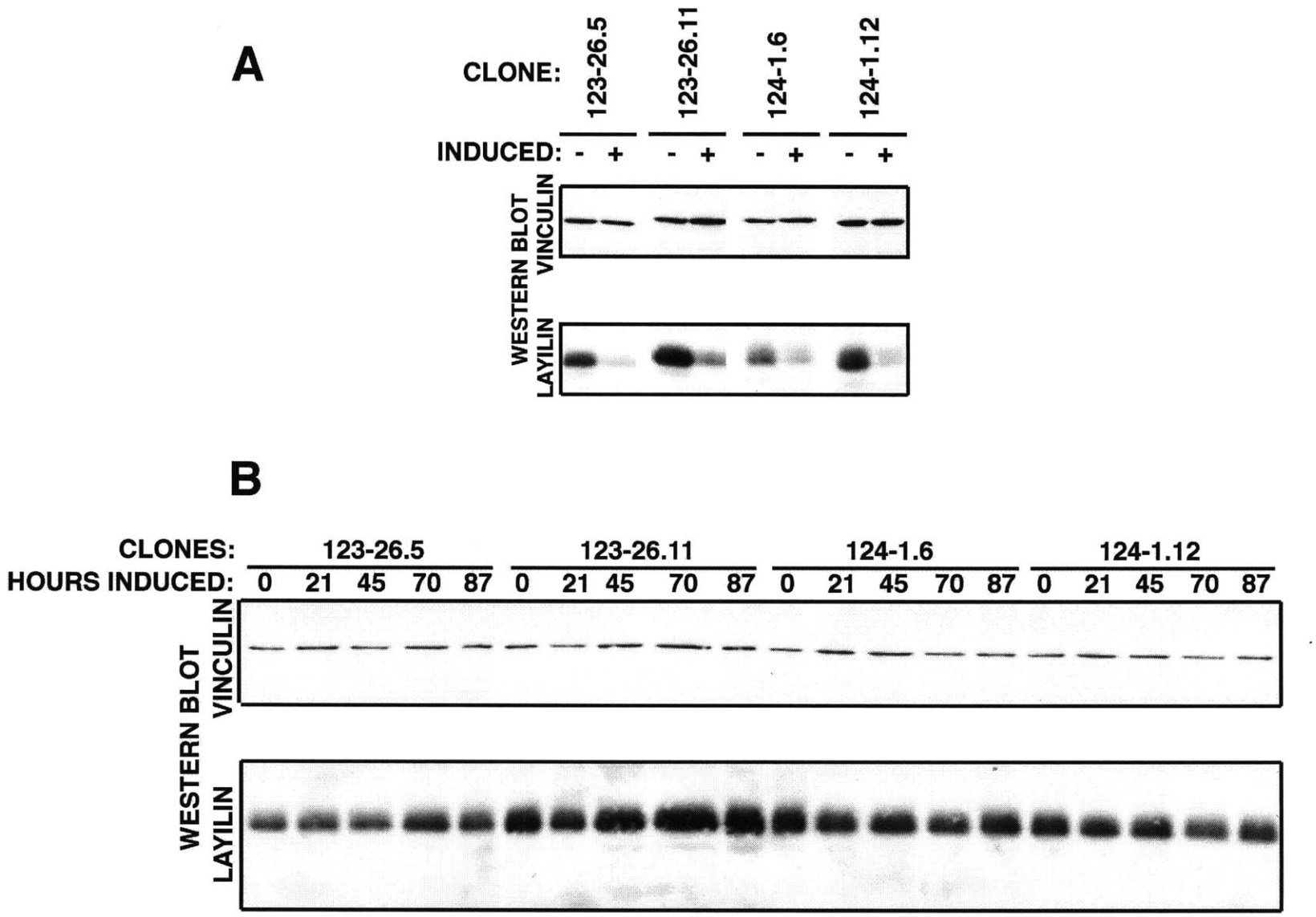
A
CLONE:
123-26.5
123-26.11
124-1.6
124-1.12
INDUCED: - + - + - + - +
WESTERN BLOT
VINCULIN
LAYILIN
B
CLONES:
123-26.5
123-26.11
124-1.6
124-1.12
HOURS INDUCED: 0 21 45 70 87 0 21 45 70 87 0 21 45 70 87 0 21 45 70 87
WESTERN BLOT
VINCULIN
LAYILIN

Chapter 4

Future directions

Identifying function

The discovery of layilin, like that of any new protein, raises a host of questions such as the function of layilin, its potential carbohydrate or glycoprotein ligands, its integration into rac signaling pathways, and other biochemical characteristics of the cytoplasmic domain. Answering these questions will not be a trivial task; while biochemical interactions of focal contact proteins are readily observed, the biological functions of several (such as zyxin, MENA, syndecan-4 and tensin) remain elusive. Because of their ability to bind to one or more other cytoskeletal proteins, these molecules generally have been thought to be structural proteins. Although such conclusions are reasonable, they merit experimental demonstration. Likewise the sensible proposal that layilin is a membrane-binding site for talin must be confirmed by demonstrating that disrupting this interaction or depriving cells of layilin has consequences for cell physiology or morphology. In the discussion of chapter 3, I have proposed ways to extend dominant-negative and antisense approaches. Additional routes to layilin function are mapped below.

An alternative but related dominant-negative strategy to that discussed in chapter 3 is expression of partial layilin cytoplasmic domains. Such proteins in theory would function by binding to a subset of layilin ligands and frustrating their interaction, normally mediated by layilin, with other proteins. It is possible that the dominant negative GFP fusion containing the intact layilin cytoplasmic domain, described in chapter 3, simply substitutes for endogenous layilin, serving as an adaptor linking talin to one or more other cytoskeletal proteins. If this were the case, then a fusion protein containing a partial layilin cytoplasmic domain, for example, only a talin-binding site, might be effective in disrupting a complex between talin and an unknown partner because it could bind to one but not both proteins. Partial cytoplasmic domain dominant negatives may be most effective if concentrated at the membrane either in the context of truncated layilin or as a fusion with heterologous extracellular and transmembrane domains. If such an inhibitor proved potent, inducible or transient expression may be preferable to stable expression. This would minimize loss of cell lines due to potential deleterious effects of the dominant negative and would reduce selection of cells with compensatory changes in expression of endogenous layilin or its binding partners.

Microinjection of peptides containing only part of the layilin cytoplasmic domain may also achieve the desired effect.

Assuming the layilin CRD-homologous sequence is a functional carbohydrate-binding domain, layilin's biological role could be uncovered by reagents which disrupt ligand binding. I believe this general approach is likely to be fruitful. Identification of a specific glycoprotein ligand, if one exists, would facilitate creation of reagents which disrupt its binding to layilin. Even without this knowledge, generation of monoclonal antibodies directed against the lectin domain might result in function-blocking antibodies independent of the nature of a putative ligand. Hence this would be a more general approach than an alternative, which is to identify carbohydrate ligands (discussed below) that would compete with endogenous ligands for layilin binding. Both types of reagents would be useful in a relatively broad spectrum of assays, including spreading and migration, which might be used to probe layilin function. If the 55 kD YF-169 antigen described by Hasegawa (1993) is layilin, the monoclonal antibody directed against it may prove helpful.

Layilin function might be addressed by inactivating the gene by homologous recombination. Although this time-consuming and expensive approach would undoubtedly yield valuable insights into the role of layilin during development, it is not clear that this is the best strategy to find the cell biological function of a protein. Heterozygous ES cell clones should be used both to create heterozygous mice, which can be bred to determine the phenotype, if any, of layilin-deficient mice, and as the basis for double-null ES cell lines. Depending on the phenotype of layilin-null mice, null ES cells may be a more useful reagent with which to investigate the cell biological function of layilin. The membrane dynamics (or other properties) of homozygous null ES cell clones can be studied, and these cells also can be used to make both embryoid bodies and chimeric animals in order to generate other null cell types. If transfection of wild-type layilin rescues the phenotype (whatever it may be) of layilin-null cells, the significance of talin binding may be addressed by transfecting mutant layilins lacking or mutated in one or more LH2/LH3 repeats, those used to bind talin *in vitro*.

Identifying ligands

The search for ligands of the putative lectin domain should include both carbohydrate ligands and potential glycoprotein ligands. The former will reveal at least one aspect of the

protein's biochemical function and will serve as the basis for development of useful inhibitors, whereas the latter could provide considerable insight into the biological roles of layilin. Soluble chimeric CRD domains fused to the constant region (Fc) of immunoglobulin heavy chains have been produced for E-, P-, and L-selectin as well as for the link module of CD44 (Aruffo et al., 1990; Watson et al., 1990; Aruffo et al., 1991; Moore et al., 1992; Levinovitz et al., 1993). Each has been used to identify candidate ligands, and some have been used as if they were antibodies in immunohistochemistry to detect ligand-enriched cell types in tissue sections (Imai et al., 1991; Lasky et al., 1992; Spertini et al., 1996). Two criteria can be applied to sort candidate ligands for a C-type lectin, Ca^{2+}-dependence and carbohydrate-dependence of binding. These Ig chimeras can be used to affinity-purify candidate ligands from surface- or metabolically-labeled cell extracts and binding can be assessed for calcium-dependence and sensitivity to glycosidases. Control chimeras should include the Fc fusion partner alone as well as a layilin CRD with one or a few mutations in amino acids known to be required for ligand binding by other CRDs (discussed in chapter 2). These controls should allow identification of good candidate ligands. Co-localization of layilin with a potential ligand in cells and tissues will enhance confidence that a genuine ligand has been identified. Ultimately, a demonstration that interference with each molecule or specific disruption of their binding gives rise to identical or overlapping effects will be the best evidence of their functional interaction *in vivo*.

I also have proposed that layilin may mediate uptake of glycoprotein ligands during phagocytosis. In this case it may recognize a broad array of glycosylated species rather than a discrete few. This would be revealed during efforts to affinity isolate ligands by recovery of a ladder of bands or even a smear of specifically bound material. Under these circumstances it would be most appropriate to identify the carbohydrate ligand rather than individual glycoprotein ligands.

Soluble bacterially-expressed CRDs have been used to characterize the interaction of lectins with their carbohydrate ligands (Ghrayeb et al., 1984; Weis et al., 1991a; Kohda et al., 1996). In these cases purification of the CRD from bacteria has exploited a sugar-affinity step which requires foreknowledge of at least one carbohydrate ligand. Layilin's carbohydrate preferences might be discovered by passing cell lysates over various immobilized sugars, such as a column matrix, washing, eluting with EDTA or soluble sugars and assaying for layilin by

western blotting. Absent that knowledge, these bacterially-expressed CRDs could be purified by conventional biochemical methods. Since they offer no particular advantage over CRD-Ig fusions, this approach should be considered a second choice in case expression or protein-A affinity purification of layilin-Ig chimeras proves impossible.

In addition to their utility as an affinity reagent to isolate candidate glycoprotein ligands, recombinant CRDs can be used to screen combinatorial carbohydrate libraries to directly select sugar ligands. Solid phase synthesis of such libraries greatly facilitates recovery and identification of ligands (Liang et al., 1996). Although these binding partners will likely not represent physiological sugar ligands, they may be effective antagonists. Further screening of carbohydrate libraries built by varying one or more initial positive sugar structures could be used to optimize a candidate ligand, hence enhancing its potential as an inhibitor.

Cytoplasmic domain functions

The roles of layilin and talin in membrane ruffles and during cell motility might be clarified by further characterization of interactions between them and other molecules known to regulate ruffling and/or motility. The recent report of association between vav and talin stimulates the speculation that in other cell types talin may bind to other guanine nucleotide exchange factors (Fischer et al., 1998). Similar observations have been reported for ERM proteins (Takahashi et al., 1998). Tiam-1, which stimulates ruffling in fibroblasts, contains rac exchange factor activity and has two PDZ domains, either of which could bind the layilin cytoplasmic domain. A complex consisting of talin, Tiam-1 and layilin would be analogous to that composed of band 4.1, p55, and glycophorin (Marfatia et al., 1994).

The search for other layilin cytoplasmic domain-binding partners may further inform our understanding of layilin function. In particular, it will be of interest to learn what, if any, proteins associate with the long LH1 repeats. Since a LexA/layilin cytoplasmic domain fusion gives rise to constitutive activation of reporters, baits made from subfragments of the cytoplasmic domain will have to be used if this approach is taken. In addition, further study of the spectrum of band 4.1 superfamily members which can bind layilin may indicate the breadth of layilin's role in anchoring actin cytoskeleton at the cell membrane. Finally, several serine, threonine and tyrosine residues in the cytoplasmic domain could be subject to phosphorylation, and analysis of this possible modification and its correlation with spreading or migration may

lead to the discovery of regulatory mechanisms for layilin function. Interestingly, the minimal talin-binding site (E**S**GFVXNDI**Y**) contains two potential phosphorylation sites.

Appendix A

Integrin two-hybrid studies

"No one yet has been able to produce wheat without chaff. Not even...such transcendent spirits as Abraham Lincoln can produce a history which does not in large part rest on a foundation of tedium and detail – and even sheer drudgery.

P. Graham

Introduction

Given the varied physiological changes induced in cells by adhesion to ECM, the β1 integrin chain common to major matrix receptors is a likely candidate for transducing signals which lead to these effects (Hynes, 1992). Chimeras containing only the β1 integrin cytoplasmic domain fused to heterologous transmembrane and extracellular domains are sufficient, when clustered, to mimic adhesion-induced phosphorylation of FAK (Akiyama et al., 1994). Various approaches to identifying integrin-associated signaling molecules have yielded few clues, however, as no consistent results have been obtained in co-immunoprecipitation or affinity purification studies. I applied a novel method for finding protein-protein interactions, the yeast two-hybrid screen, in the hope of advancing our understanding of this interesting question. Since these experiments were done some data has emerged suggesting that adhesion signaling is not exclusively mediated by integrin cytoplasmic domains (Berditchevski et al., 1997a; Wary et al., 1998).

Materials and Methods

Yeast two-hybrid assay

Construction of plasmids: Integrin cytoplasmic domain fragments were generated by PCR using the chicken β1 integrin cDNA pECE/1DT as a template and CBR1 as a reverse primer. CBR1 is situated downstream of the stop codon. Forward primers CBF1, CBF2, and CBF3 were used to amplify sequences starting at amino acids 758, 756, and 729 respectively. To make 757/804 A4K, two overlapping oligonucleotides, A5KF and A5KR, were annealed, filled-in with Klenow fragment, and denatured. This denatured mixture was used as a primer as described above. These fragments were digested with EcoRI and NcoI and ligated into EcoRI/NcoI-digested, phosphatase-treated pEG202. In addition a fusion containing amino acids 763/804 was made by digesting pECE/1DT with BspHI and EcoRI, blunting with Klenow fragment and ligating the product into pEG202 which had been digested with EcoRI, treated with calf intestinal acid phosphatase and rendered blunt with Klenow fragment.

Primer sequences:

CBR1	GGCACCATGGGACCTC
CBF1	TCGCGAATTCCTACTGATGATCATTCAT
CBF2	TAGTGGCGCCGAATTCTGGAAACTACTGATGATC
CBF3	GATCGAATTCCCTAGTGGCCCTGAC
A5KF	GATCGAATTCGGCGCCGCGGCCGCAAAAGCCGCAGCAGCCAAGGCAGCGGC
A5KR	CCTGTCATGAATGATCATTAATAATTTGGCGGCCGCTGCCTTGGCTGCTGC

Yeast manipulations: See chapter 2 for yeast culture techniques. Immunostaining of yeast was performed essentially as described (Solomon et al., 1992).

Results

Several chicken β1 integrin cytoplasmic domain segments were fused to either LexA or B42, transformed into yeast and assayed for expression by western, nuclear entry by immunostaining and transcriptional repression, and for interaction with FAK and talin fragments. As shown in figure A-1A, three LexA integrin fusions are expressed in yeast and the same bands react with both anti-LexA and anti-β1 integrin antibodies, suggesting the fusion proteins are intact. In figure A-1B expression of two LexA/talin fusions spanning the carboxy-terminal domain of talin and a LexA/FAK fusion encoding all of FAK is shown. In a transcriptional repression assay designed to assess nuclear entry and DNA binding by LexA fusions, the LexA/β1 fusion suppresses transcription by about 50% compared to essentially 100% repression achieved by either LexA alone or the LexA/max fusion protein. These data suggest that the LexA/β1 fusion either does not efficiently translocate into the yeast nucleus or cannot bind DNA once it enters. Yeast were immunostained with either anti-LexA to detect a LexA/max fusion or anti-β1 integrin to detect a LexA/integrin fusion and counter stained with DAPI to highlight the nucleus (figure A-3). The LexA/max is present in tight spots which colocalize with the brightest DAPI signal , whereas the LexA/β1 fusion is diffuse throughout the cytoplasm (compare panels b and d in figure A-3). This indicates that the fusion does not become efficiently concentrated in the nucleus. These observations may explain the negative results obtained when these LexA/β1 integrin fusions were assayed for interaction with several talin and FAK "fish". Both proteins have been reported to bind the cytoplasmic domain of β1 integrin. Several variations of the integrin cytoplasmic domain were assayed, including several varied N-terminal endpoints (amino acids 756, 758, and 763), the transmembrane and cytoplasmic domain together (starting at a.a. 729), and one construct in which three copies of a repeat (AAAK) predicted to form an α-helix was inserted between LexA and the integrin cytoplasmic domain. The last construct was intended to mimic the presentation of the cytoplasmic domain in the context of an intact integrin. The integrin binding site within FAK is reported to reside between amino acids 1-127, so this fragment was tested alone and in the context of full-length FAK (1/1052) (Schaller et al., 1995). In addition, I found that a LexA/FAK (1/1052) fusion protein gave rise to constitutive leucine prototrophy and blue color on X-gal such that this is not a suitable bait. In addition, several B42/β1 fusions were

constructed consisting of the β1 integrin cytoplasmic domain fused to a different fusion partner. Among the 69 pairs of bait and fish shown in figure A-4 tested, only the positive control pair LexA/max and B42/MXI1 gave a positive result.

Discussion

Although these data suggest that the β1 integrin cytoplasmic domain is a poor two-hybrid bait due to inefficient nuclear localization, several groups subsequently have recovered integrin-binding partners using this approach (Shattil et al., 1995; Hannigan et al., 1996; Kolanus et al., 1996; Chang et al., 1997; Liliental and Chang, 1998). In fact, Hannigan et al. (1996), using the same two-hybrid system and a similar segment of β1 integrin to that I used, reported identical transcriptional repression data (50% suppression) as I obtained (figure A-2). Hence, either my interpretation of these controls was overly pessimistic, or the kinase cloned by Hannigan et al. (1996) is an intriguing artifact (or both). In addition, Chang et al. (1997) detected an interaction using a β1 integrin bait similar to those I tested, although these authors did not specify results of their transcriptional repression assay. Hence, small differences in their bait may account for differing results. It is also possible that my LexA fusions would have been adequate for a library screen had I attempted one. However, the best data available at that time suggested that the LexA/β1 integrin fusions were not functional baits and as such no screen was performed. It will be interesting to see which of the several integrin-associated proteins identified in two-hybrid screens prove to be relevant to cell adhesion.

Figure A-1: (A) Western blots of yeast lysates showing expression of LexA/β1 integrin baits. Left panel: anti-LexA blot; right panel, same blot reprobed with anti-β1 integrin antiserum 363. A LexA/Max fusion and untransformed yeast are included as controls. (B) Western blot showing expression of two LexA/talin fusions and the LexA/FAK(1/1052) fusion.

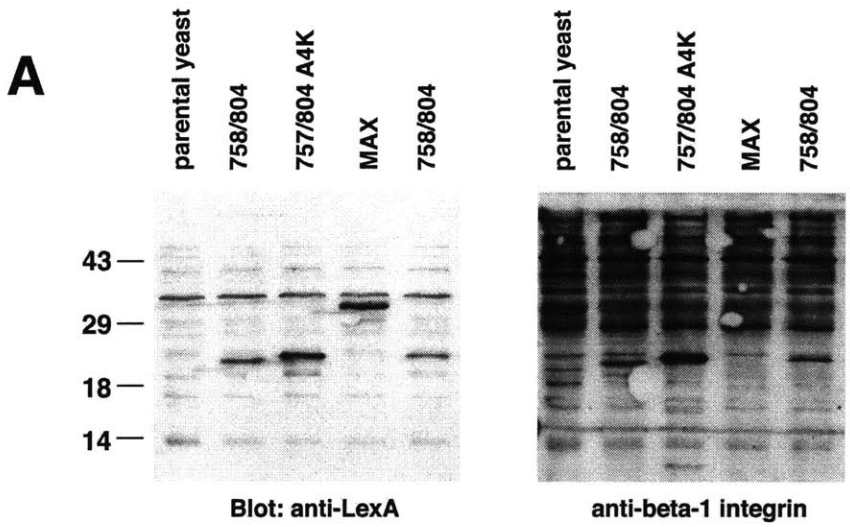
A
parental yeast
758/804
757/804 A4K
MAX
758/804
43
29
18
14
Blot: anti-LexA
parental yeast
758/804
757/804 A4K
MAX
758/804
anti-beta-1 integrin

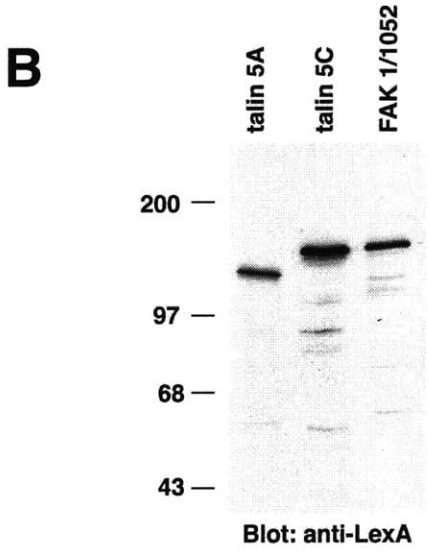
B
talin 5A
talin 5C
FAK 1/1052
200
97
68
43
Blot: anti-LexA

Figure A-2: Quantitation of β-galactosidase activity in yeast strain EGY40 in the absence or presence of the LexA-β1 integrin bait. Each bar represents the average of two samples. Comparison of LexA-β1 and control strains under induced conditions shows a 2-fold repression of β-galactosidase activity in the presence of the LexA-β1 integrin fusion. LexA alone and LexA/Max are shown as positive controls.

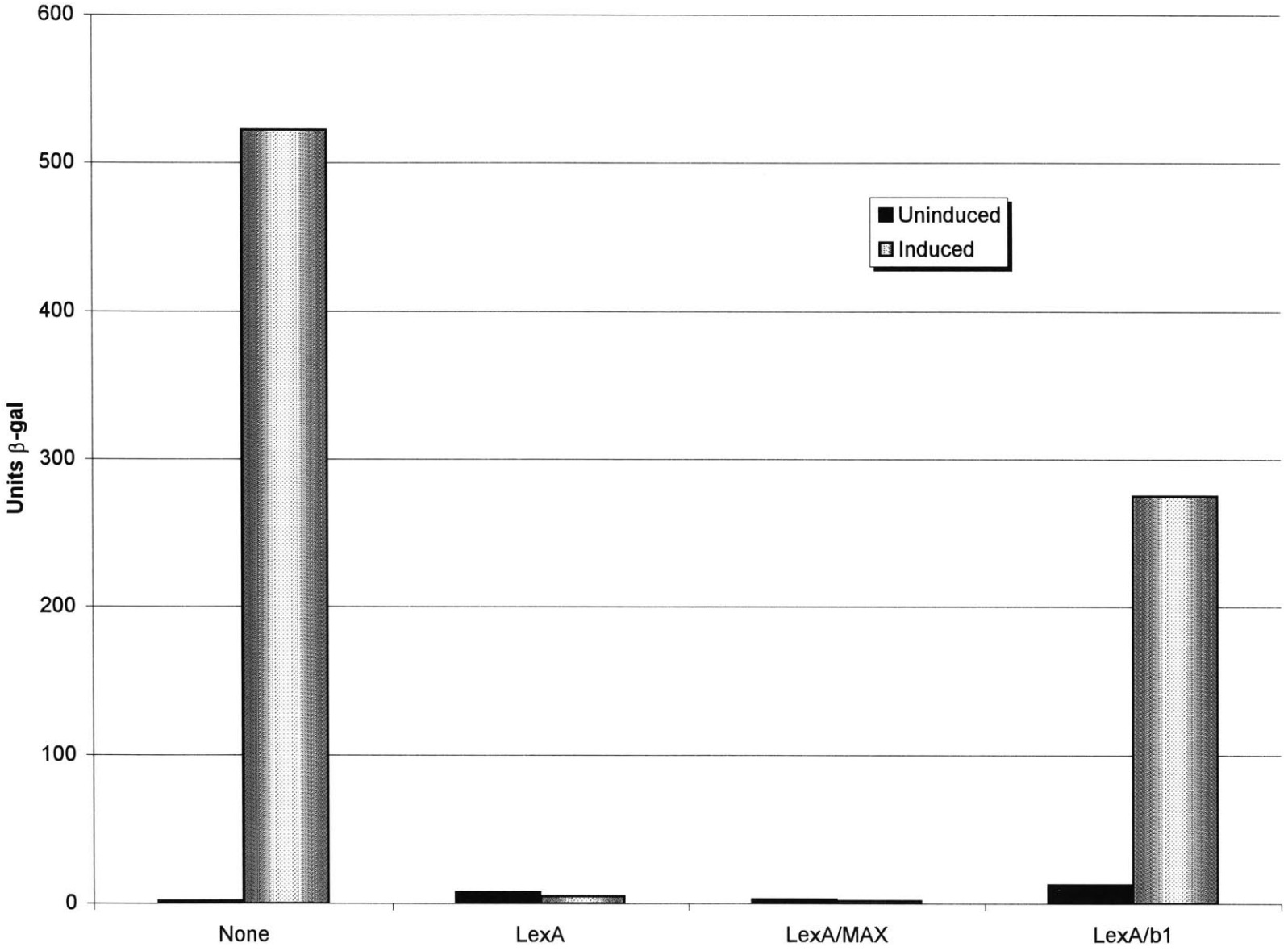
600
500
400
300
200
100
0
Units β-gal
Uninduced
Induced
None
LexA
LexA/MAX
LexA/b1

Figure A-3: Immunolocalization of LexA/Max (a and b) and LexA/β1 integrin (c and d) in yeast. Cells were double stained with DAPI (a and c) and anti-LexA (b) or anti-β1 integrin (d). Note the LexA/Max colocalizes with the DAPI nuclear signal while the integrin signal is seen throughout the cell.

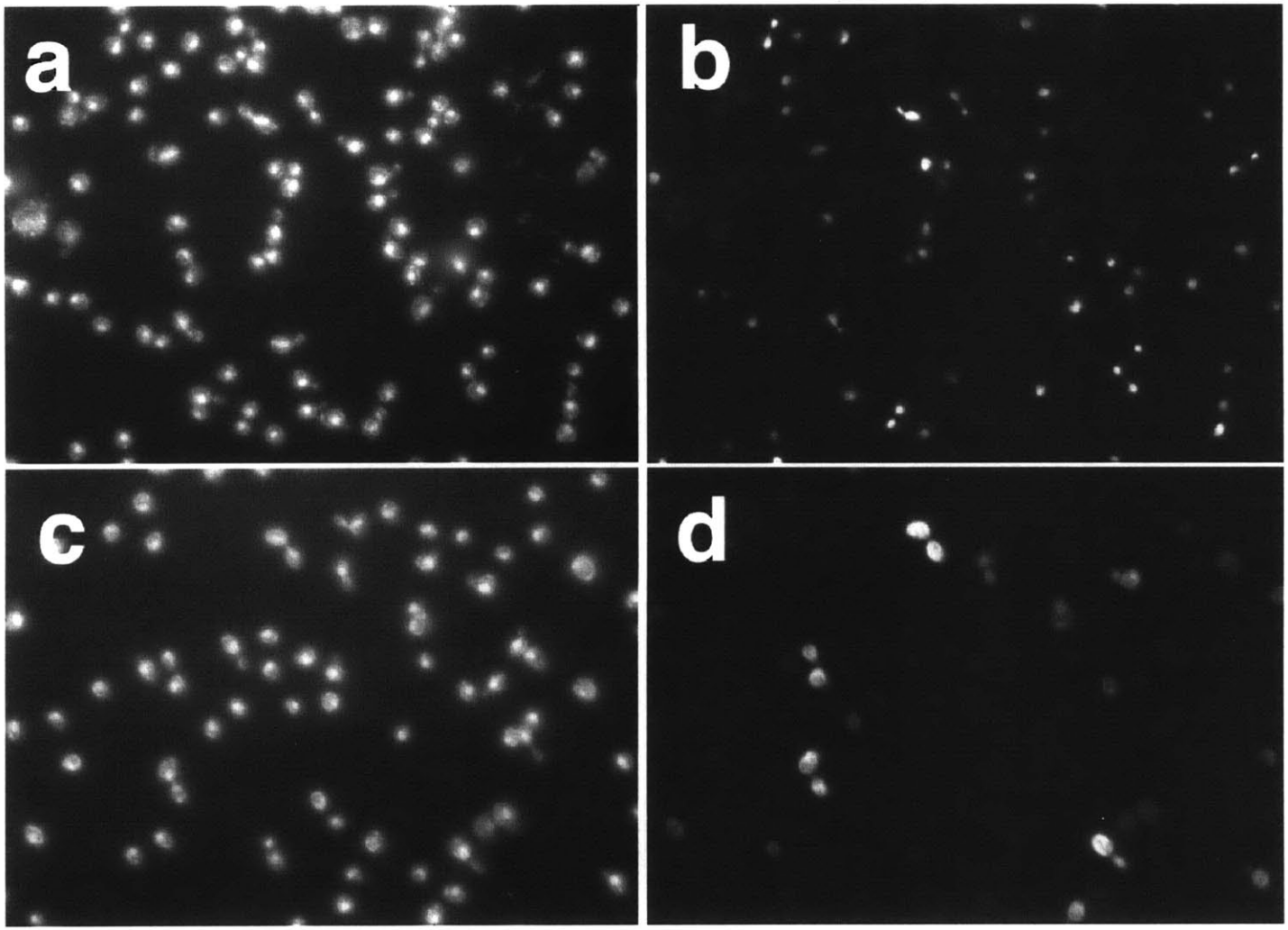
a
b
c
d

Figure A-4: Interactions among integrin bait and fish fusions with putative positive controls. Growth on leucine-deficient plates and/or blue color when grown on X-gal is indicated with a plus (+) whereas no growth or blue color is indicated with a minus (-). Note that LexA/FAK1/1052 activates reporters even when cotransformed in yeast with the vector alone.

FISH→ BAIT↓	Vector	MXI1	FAK 1/1052	FAK 1/127	FAK 127/1052	β1 729/804	β1 756/804	β1 758/804	β1 A4K 757/804	Talin 5A	Talin 5C	Talin 9B
Vector	-	-	-	-	-	-	-	-	-	-	-	-
MAX	-	+	-	-	-	-	-	-	-	-	-	-
β1 729/804	-	-	-	-	-					-	-	-
β1 756/804	-	-		-	-							
β1 758/804	-	-		-	-							
β1 763/804	-	-		-	-							
β1 A4K 757/804	-	-		-	-							
FAK 1/1052	+	+					+	+	+			
Talin 1/435	-	-	-	-	-							
Talin 9B	-	-				-	-					
Talin 5A	-	-				-	-	-	-			
Talin 5C	-	-				-	-	-	-			

Appendix B

Layilin, a novel talin-binding transmembrane protein homologous with C-type lectins, is localized in membrane ruffles

Layilin, A Novel Talin-binding Transmembrane Protein Homologous with C-type Lectins, is Localized in Membrane Ruffles

Mark L. Borowsky and Richard O. Hynes

Howard Hughes Medical Institute, Center for Cancer Research and Department of Biology, Massachusetts Institute of Technology, Cambridge, Massachusetts 02139

Abstract. Changes in cell morphology and motility are mediated by the actin cytoskeleton. Recent advances in our understanding of the regulators of microfilament structure and dynamics have shed light on how these changes are controlled, and efforts continue to define all the structural and signaling components involved in these processes. The actin cytoskeleton-associated protein talin binds to integrins, vinculin, and actin. We report a new binding partner for talin that we have named layilin, which contains homology with C-type lectins, is present in numerous cell lines and tissue extracts, and is expressed on the cell surface. Layilin colocalizes with talin in membrane ruffles, and is recruited to membrane ruffles in cells induced to migrate in in vitro wounding experiments and in peripheral ruffles in spreading cells. A ten–amino acid motif in the layilin cytoplasmic domain is sufficient for talin binding. We have identified a short region within talin's amino-terminal 435 amino acids capable of binding to layilin in vitro. This region overlaps a binding site for focal adhesion kinase.

Key words: layilin • talin • ruffles • C-type lectin • focal adhesion kinase (FAK)

CELL shape and movement form the basis for fundamental developmental events such as gastrulation, tubule formation, and morphogenesis. The actin cytoskeleton plays a significant role in these processes because it is a major determinant of cell shape, and is essential for cell motility. Furthermore, interactions of actin filaments with the cell membrane are necessary both for changes in and maintenance of cell morphology. Our understanding of membrane–cytoskeleton linkages has been advanced significantly with the recognition of various proteins as adaptors between integral membrane proteins and the actin cytoskeleton. Proteins of the band 4.1 superfamily, band 4.1, talin, ezrin/radixin/moesin (ERM)[1], and merlin, the product of the neurofibromatosis type 2 tumor suppressor gene, perform this function in many cell types (Tsukita et al., 1997). Band 4.1 confers mechanical stability to red blood cells by attaching the spectrin and actin cytoskeletons to glycophorin or the erythrocyte anion exchanger (band 3) in the erythrocyte membrane (Bennett and Gilligan, 1993). Talin plays an essential role in integrin-mediated cell matrix adhesion by binding to integrin cytoplasmic domains, focal adhesion kinase (FAK), actin, and the actin-binding protein vinculin (Burridge and Mangeat, 1984; Horwitz et al., 1986; Chen et al., 1995; Hemmings et al., 1996; Knezevic et al., 1996). ERM proteins contribute to microvillar structure, function in cell adhesion, and bind to actin and sites on the plasma membrane; ERMs have been reported to bind to the cytoplasmic domains of several transmembrane proteins, including CD44, CD43, ICAM-2, and ICAM-3 (Algrain et al., 1993; Takeuchi et al., 1994; Tsukita et al., 1994; Turunen et al., 1994; Helander et al., 1996; Serrador et al., 1997; Yonemura et al., 1998).

Talin, ERMs, merlin, and band 4.1 have a similar overall domain structure, and are proposed to function by the same mechanism. They are related by sequence homology in the amino-terminal domain, which is proposed to contain their membrane-binding sites (Rees et al., 1990). ERMs can bind CD44, CD43, and ICAM-2 via their NH_2-terminal domains, and band 4.1 interacts with both glycophorin C and band 3 through its NH_2-terminal domain (Jöns and Drenckhahn, 1992; Yonemura et al., 1998). The NH_2-terminal domains of merlin and ERMs also associate with NHE-RF, which may link them indirectly to the

Address all correspondence to R.O. Hynes, Massachusetts Institute of Technology, 77 Massachusetts Avenue, E17-227, Cambridge, MA 02139. Tel.: (617) 253-6422. Fax: (617) 253-8357. E-mail: rohynes@mit.edu

1. *Abbreviations used in this paper*: CRD, carbohydrate-recognition domains; ERM, ezrin/radixin/moesin; GST, glutathione-S-transferase; nt, nucleotide.

membrane by binding to one or more Na^+-H^+ exchanger isoforms (Reczek et al., 1997; Murthy et al., 1998). In addition to the sequence homology in their NH_2-terminal domains, talin and ERMs have a central domain predicted to be mostly α-helical and demonstrating actin-binding activity, while this region of band 4.1 binds spectrin (Ungewickell et al., 1979; Rees et al., 1990; McLachlan et al., 1994). With these biochemical activities, band 4.1 family members could link membrane and cytoskeleton by binding to each simultaneously.

Talin, which is expressed in essentially all adherent cell types, is found at sites of cell-matrix adhesion (such as focal contacts), leading edge ruffles of migratory cells, at sites of phagocytosis in macrophages, and at cell–cell contacts of T cells (Burridge and Connell, 1983; Burn et al., 1988; Greenberg et al., 1990; DePasquale and Izzard, 1991; Kreitmeier et al., 1995). These are also sites where integrin cell adhesion receptors are found. While integrins are clearly associated with the leading edge of some types of motile cells, it is unclear whether they are located in dorsal ruffling membrane sheets, in the ventral-most base of the leading edge, or both (Schmidt et al., 1993; Lawson and Maxfield, 1995; Lee and Jacobson, 1997). Talin's importance in adhesion and migration has been demonstrated in experiments that interfere with talin function or expression. Injection of anti-talin antibodies disrupts cell adhesion and migration, and downregulation of talin protein levels by expression of anti-sense talin RNA reduces the rate of cell spreading (Nuckolls et al., 1992; Albigès-Rizo et al., 1995). Talin's role as a membrane–cytoskeleton linker in focal contacts has been characterized in detail; a short peptide derived from the β1-integrin cytoplasmic domain can block the association of talin with integrins, and three actin-binding domains and three vinculin-binding sites have been mapped in talin (Tapley et al., 1989; Hemmings et al., 1996). Interestingly, the integrin-, three vinculin-, and two of the three actin-binding sites in talin are all found within the carboxy-terminal 190-kD calpain tail fragment of talin (Horwitz et al., 1986; Gilmore et al., 1993; Hemmings et al., 1996). Microinjected talin tail fragment localizes to focal contacts, suggesting that the known integrin-, vinculin-, and actin-binding sites account for talin's membrane–cytoskeleton linking role in focal contacts (Nuckolls et al., 1990). In contrast, talin's role in membrane ruffles has not been elucidated, although it seems reasonable to project that, as in focal contacts, it connects F-actin to an unknown site on the plasma membrane.

While the tail fragment can account for talin's role in focal adhesions, the role of talin's 47-kD amino-terminal calpain cleavage product (talin head, amino acids 1–435) is not known. An examination of talin protein sequence from highly divergent organisms reveals that talin's NH_2-terminal domain is the most well-conserved region within the sequence. For instance, *Caenorhabditis elegans* and *Dictyostelium discoideum* talins are 78 and 66% similar to mouse talin within the head domain, but only 59 and 46% similar to mouse talin overall (Kreitmeier et al., 1995; Moulder et al., 1996). This highly conserved segment also contains talin's homology to band 4.1. While this sequence conservation suggests that some conserved function exists for the talin head domain, experimental analyses have given varied results. Nuckolls et al. found that a small fraction of microinjected talin 47-kD domain fragment incorporated into focal contacts, while most was diffusely localized in cells. The injected protein had no effect on cytoskeletal morphology, cell spreading, or adhesion. However, injected talin tail protein was targeted to focal contacts, and also exhibited ectopic localization at cell–cell junctions where full-length talin is not normally found, suggesting that talin head may enhance targeting to focal contacts or mask other binding sites within talin's tail domain (Nuckolls et al., 1990). In contrast, microinjected glutathione-S-transferase (GST)-talin 47-kD fragment colocalized with actin filaments and disrupted stress fibers in a majority of cells (Hemmings et al., 1996). Similarly, we found that cells transiently overexpressing talin head were not spread and appeared poorly adherent (M.L. Borowsky and R.O. Hynes, unpublished results). Bolton and colleagues generated two anti-talin monoclonal antibodies that, when microinjected into human foreskin fibroblasts, disrupt actin stress fibers, and when injected into chick embryo fibroblasts, significantly inhibit cell migration (Bolton et al., 1997). One of these monoclonal antibodies recognizes an epitope in the talin 47-kD fragment, and the other binds a site at the extreme COOH terminus of talin.

While the talin head domain appears to play an important role in cell motility and morphology, no specific mechanism has been proposed to explain these observations. Based on the sequence similarity between talin's NH_2-terminal domain and band 4.1, we hypothesized that the conserved talin head domain contained an additional membrane-binding site for talin. In a two-hybrid screen we have identified a previously unknown type I integral membrane protein that interacts with talin head, is expressed in all adherent cell lines analyzed, and colocalizes with talin in membrane ruffles. A short motif present in the cytoplasmic domain of this protein is sufficient for talin head binding. We believe this protein represents a membrane-binding site for talin in ruffles, while integrins anchor talin in focal contacts.

Materials and Methods

Yeast Two-hybrid Screen

Plasmid construction. Manipulation of DNA was performed according to standard molecular biological protocols (Sambrook et al., 1989). Unless otherwise stated, restriction enzymes and DNA-modifying enzymes were purchased from New England Biolabs Inc. (Beverly, MA). A pBluescript subclone of a talin cDNA encoding amino acids 1–435 (clone A14) was made by partially digesting a chicken talin cDNA with NcoI, digesting with PstI, and cloning the product into pBluescript SK- that had been digested with NcoI and PstI. To make the LexA fusion bait, clone A14 was digested with SacI and EcoRV, the ends were polished with T4 DNA polymerase, and the appropriate fragment was ligated into pEG202 that had been digested with EcoRI and rendered blunt (Gyuris et al., 1993). A pJG4-5 subclone of layilin lacking a cytoplasmic domain was made by inserting a synthetic oligonucleotide (2STOPS: CGGTTAATGATCATTAACCG) with two in-frame stop codons into the 3′ PvuII site in the longest partial layilin cDNA isolated in the two-hybrid screen (Gyuris et al., 1993). A pJG4-5 subclone of layilin cytoplasmic domain was made by ligating a PvuII/XhoI layilin cDNA fragment into pJG4-5 that had been digested with EcoRI, Klenow-blunted, and digested with XhoI. A plasmid encoding LexA fused to the type-II TGFβR cytoplasmic domain was the gift of Dr. R. Weinberg (Massachusetts Institute of Technology).

Library screen. The two-hybrid library screen was performed as previously described using the CHO cDNA library pVPCHO (gift of Dr. V.

Prasad, Albert Einstein Medical College; Gyuris et al., 1993). EGY48 containing the LexA-talin bait and the beta-galactosidase (β-gal) reporter plasmid pSH18-34 was transformed with DNA prepared from two pools of pVPCHO library that contained ~7.5×10^4 and 8.2×10^4 recombinants. Yeast transformants were pooled and frozen in aliquots, and their plating efficiency was determined. About 10^6 yeast transformants were plated on synthetic complete medium containing raffinose and galactose as carbon sources, but lacking histidine, leucine, tryptophan, and uracil. 48–96 h later, 244 yeast colonies were picked and assayed for blue color on medium containing X-gal (Boehringer Mannheim Corp., Indianapolis, IN). Plasmid DNA was recovered from 40 double-positive (leu^+, $lacZ^+$) colonies, and candidate interactors were sorted into classes based on AluI and HaeIII restriction digestion patterns of the library inserts (Hoffman and Winston, 1987; Gyuris et al., 1993). After retesting representative interactors of each class with negative control baits, 30 of the original 40 clones were deemed worthy of further study. Based on partial sequence data, these 30 candidates were determined to comprise three cDNAs (Epicentre PCR sequencing kit, Epicentre Technologies, Madison, WI).

Anchored PCR. Primers internal to the longest layilin cDNA recovered from pVPCHO (LECTF1: TGGACAGATGGGAGCACAT; and LECTR1: GGAATTCCCCACTTTCTGAAGGGTTC) were used to screen pools of a CHO cDNA library subcloned in pcDNA I (gift of Dr. M. Krieger, Massachusetts Insititute of Technology) for the presence of our interactor cDNA (Guo et al., 1994). A fragment of the layilin cDNA was amplified from a positive pool using a 3′ primer within the cDNA (LECTR1), and a 5′ primer complementary to the T7 promoter present in the vector (T7P: TAATACGACTCACTATAGG), subcloned into pBluescript, sequenced, and found to encode an open reading frame continuous with and overlapping that in the cDNA cloned from pVPCHO. The open reading frame encoded by the PCR product completed the C-type lectin homology present in the original pVPCHO isolate, contained a suitable start codon, and so was deemed likely to be the genuine 5′ end of the cDNA.

Northern analysis. CHO RNA was prepared by acid phenol extraction as previously described (Chomczynski and Sacchi, 1987) Poly-A^+ RNA was isolated essentially as described (Bradley et al., 1988). In brief, 20 × 15-cm dishes of nearly confluent CHO cells were trypsinized, pooled, pelleted, and washed with PBS. The cells were resuspended in 20 ml of proteinase K solution (200 μg/ml proteinase K, 0.5% SDS, 100 mM NaCl, 20 mM Tris, pH 7.5, 1 mM EDTA), lysed with 3× 25-s cycles in a Polytron homogenizer (Brinkmann Instruments, Waterbury, NY), and incubated for 90 min at 37°C. The NaCl concentration was brought to 500 mM, and 200 mg of oligo dT cellulose (as a suspension in high salt buffer [0.1% SDS, 500 mM NaCl, 20 mM Tris, pH 7.5, 1 mM EDTA]; Pharmacia Biotech, Inc., Piscataway, NJ) was added per 10^9 cells. After mixing for 2 h at room temperature, the oligo dT cellulose was washed twice in batch with high-salt buffer, and was poured as a column in a 1-ml syringe plugged at the bottom with sterile glass wool. The resulting column was washed with 10-column volumes of high-salt buffer and then eluted with 4-column bed volumes of low salt buffer (0.05% SDS, 20 mM Tris pH 7.5, 1 mM EDTA). The four fractions were pooled, heated to 65°C for 5 min, cooled on ice, brought to a final NaCl concentration of 0.5 M, and incubated with a fresh aliquot of oligo dT cellulose for 30 min at RT. Washes, column building, elutions, and rebinding were repeated as above twice for a total of three rounds of selection on oligo dT cellulose. On the last cycle, four 300-μl fractions of poly-A^+ RNA were eluted in low-salt buffer and ethanol-precipitated overnight at −20°C. RNA was pelleted, washed with 70% ethanol, and resuspended in 50 μl of diethylpyrocarbonate-treated water. Samples were electrophoresed on 1% agarose/formaldehyde gels, transferred to Hybond-N nitrocellulose (Amersham Life Science, Inc., Arlington Heights, IL), cross-linked in a Stratagene stratalinker (Stratagene, La Jolla, CA), prehybridized for 2 h at 57.5°C in Church-Gilbert buffer (1 mM EDTA, 500 mM Na_2HPO_4 pH 7.2, 7% SDS, 1% BSA), hybridized overnight at 57.5°C in Church-Gilbert buffer containing 10^6 cpm of random-primed layilin probe, washed twice at room temperature in 2× SSC/0.1% SDS and twice at 55°C in 0.2× SSC/0.1% SDS, and then exposed on X-OMAT AR film (Eastman Kodak Co., Rochester, NY) with an intensifying screen at −80°C (Alwine et al., 1977).

Preparation of Polyclonal Anti-layilin Antisera

A synthetic oligopeptide consisting of a cysteine followed by the carboxy-terminal 20 amino acids of layilin (LC20: CSPDRMGRSKESGWVENEIYY) was purchased from the Massachusetts Institute of Technology Biopolymer Facility, conjugated to keyhole limpet hemocyanin as previously described, and sent to Covance (Denver, PA) for production of rabbit antisera (Marcantonio and Hynes, 1988).

Affinity purification. A thiopropyl-Sepharose 6B (Pharmacia Biotech, Inc.) column with covalently-coupled LC20 was washed sequentially with 15 ml of 10 mM Tris, pH 7.5 under gravity flow, 100 mM glycine, pH 2.5 at 25 ml/h, 10 mM Tris, pH 7.5 at 25 ml/h. Ammonium sulphate–precipitated antiserum was applied to the column at 20 ml/h. The flow rate was increased to 25 ml/h, and the eluate recirculated on the column for 30 min so that the antiserum ran over the column a total of three times. On the last cycle, the depleted serum was collected and saved for use as a control for the affinity-purified antiserum. The column was washed at 25 ml/h with 30 ml of 10 mM Tris pH 7.5, and then at 30 ml of 500 mM NaCl in 10 mM Tris pH 7.5. Antibody was eluted in 1.2-ml fractions with 100 mM glycine pH 2.5 into 1.5-ml microcentrifuge tubes preloaded with 1 M Tris, pH 8.0 sufficient to neutralise the glycine.

GST Fusion Binding

Plasmid construction. The GST-chicken talin 1-435 fusion (GST-CT) was made by ligating a BamHI/EcoRI fragment from chicken talin clone A14 into BamHI/EcoRI-digested pGEX-2T (Pharmacia Biotech Inc.). Deletions within this region of talin were made by either digesting this construct with appropriate enzymes, or by generating PCR products within it. Specifically, to make GST-CT 280-435, GST-CT was cut with BglII and BamHI, blunted with Klenow, and religated. To generate GST-CT 1-280, GST-CT was cut with BglII and EcoRI, blunted with Klenow, and religated. To create GST-CT 186-435, GST-CT was cut with ClaI and BamHI, blunted with Klenow, and religated. The insert for GST-CT 186-357 was derived from GST-CT 186-435 using PCR with a primer starting at the codon for amino acid 357 (CTR1: CGAATTCGATGTTGGTCAGGCTCC) and a primer in the vector (pGEX1: TTGCAGGGCTGGCAAGC). The insert for GST-CT 225-435 was synthesized by PCR using a primer starting at the codon for amino acid 225 (CTF1: CGGATCCGGCTCCCACCCCGTC) and a primer in the vector (pGEX2: GCTGCATGTGTCAGAGG). A PCR product encoding amino acids 225–357 was produced using the primers CTF1 and CTR1. Each PCR product was digested with BamHI and EcoRI and ligated into BamHI/EcoRI-digested pGEX-2T. To make the GST-layilin cytoplasmic domain fusion containing amino acids 261–374, a pBluescript subclone of layilin cDNA was made that extends from the 3′ XhoII site to the 3′ end of the cDNA, with the XhoII site blunted and ligated to the pBluescript EcoRV site, and the 3′ end of the layilin cDNA cloned into the pBluescript XhoI site. The construct was digested with EcoRI and XhoI, and the appropriate fragment was cloned into EcoRI/XhoI-cut pGEX-5X-1 (Pharmacia Biotech Inc.). The GST-layilin 244–335 fusion was made by amplifying the cDNA encoding those amino acids with primers LECTF2 (GGAATTCTCAGCTGCATGTTGGGTT) and LECTR1, digesting the PCR product with EcoRI, and subcloning the fragment into EcoRI-digested, phosphatase-treated pGEX-5X-1. The GST-layilin 330–374 fusion was made by amplifying a pBluescript subclone of the layilin cDNA with a 5′ primer starting with the codon for amino acid 330 (LECTF3: GGAATTCAACCCTTCAGAAAGTGGGTT) and T7P. The PCR product was digested with EcoRI and XhoI, and the resulting fragment was ligated into pGEX-5X-1 that had been digested with EcoRI and XhoI. The GST-(LH23)×3 fusion was made by self-ligation of a double-stranded oligomer consisting of top-strand LH23T (GATCCTTGAGAGTGGATTTGTGACCAATGACATTTATGA) and bottom-strand LH23B (GATCTCATAAATGTCATTGGTCACAAATCCACTCTCAAG), digestion with BamHI and BglII, and ligation of the resulting multimerized oligomer into pGEX-5X-1 that had been digested with BamHI and treated with shrimp alkaline phosphatase (Boehringer Mannheim Corp.). All GST-talin and GST-layilin fusion protein constructs were confirmed by sequence analysis. The GST-fibronectin (FN) EIIIB construct has been previously described (Peters et al., 1995).

Affinity isolation. Detergent lysates of CHO, NIL8, or their transfected derivatives were made by scraping and pooling cells, washing with Tris wash buffer (50 mM Tris, pH 7.5, 150 mM NaCl, 1 mM $MgCl_2$, 1 mM $CaCl_2$), and then lysing on ice for 20 min with 1 ml of lysis buffer (0.1% TX-100, 0.3 M sucrose, 50 mM Tris, pH 7.5, 100 mM KCl, 1 mM $CaCl_2$, 2.5 mM $MgCl_2$, 1 mM PMSF, 9 TIU/ml aprotinin, 5 μg/ml leupeptin) per 10^7 cells. The lysate was centrifuged at 13,000 *g* for 10 min at 4°C, and was then precleared with 500 μl of packed glutathione-agarose (preequilibrated in lysis buffer) per ml of lysate for 30 min at 4°C. For peptide-blocking experiments, 5 mg/ml peptide in PBS was added to a final concentration of 1 mg/ml to the cleared lysate, and the mixture was incubated on ice for 20 min. 500 μl of cleared lysate was added to 50 μl of glutathione-agarose preloaded with each GST-fusion protein, and was ro-

tated end-over-end for 1 h at 4°C. The samples were centrifuged briefly, the supernatants were removed, and the glutathione-agarose pellets were washed four times with 500 μl lysis buffer without detergent. The glutathione-agarose pellets were then boiled for 10 min in an equal volume of 1× gel loading buffer, and were analyzed by Western blotting (Towbin et al., 1979).

Preparation of Tissue Lysates

Organs dissected from an adult female mouse were washed twice with cold PBS, resuspended in an equal volume of homogenization buffer (100 mM NaCl, 10 mM Tris, pH 7.5, 1 mM EDTA, 1 mM PMSF, 9 TIU/ml aprotinin, 5 μg/ml leupeptin), and homogenized on ice with an electric grinder (Kontes, Vineland, NJ) in 1.5-ml microcentrifuge tubes. An equal volume of 2× RIPA buffer (1× RIPA: 1% Triton X-100, 1% sodium deoxycholate, 0.1% SDS, 158 mM NaCl, 10 mM Tris, pH 7.5, 1 mM EGTA, 1 mM PMSF, 9 TIU/ml aprotinin, 5 μg/ml leupeptin) was added, and samples were vortexed, incubated on ice for 60 min, boiled for 10 min, spun at 13,000 *g* at 4°C for 10 min, and assayed for total protein using a detergent-compatible protein assay (Bio-Rad Laboratories, Hercules, CA). An equal mass of each sample was analyzed by Western blotting.

Avidin Depletion

Three 10-cm dishes of nearly confluent CHO cells (10^7 cells) were washed with PBS, and cells were released with versene (0.02% EDTA, PBS, phenol red), pooled, washed twice with PBS, and diluted to a density of 5×10^6/ml with PBS. The sample was divided into two parts, and DMSO containing 10 mg/ml EZ-Link sulfo-NHS-LC-biotin (Pierce Chemical Co., Rockford, IL) was added to one half of the sample while DMSO alone was added to the other half, and cells were rocked gently for 60 min at room temperature (Isberg and Leong, 1990). Cells were washed three times with 1 ml of Tris wash buffer, lysed in 1.5 ml RIPA buffer, sheared through a 26-gauge needle to reduce viscosity, and spun for 10 min at 4°C and 13,000 *g* to remove insoluble debris. Two 1-ml syringes plugged with glass wool were packed with 200 μl of Immunopure Immobilized Monomeric Avidin (Pierce Chemical Co.), poured as a 33% slurry, and prepared according to the manufacturer's instructions. The columns were loaded with 200 μl of biotin-labeled or mock-labeled lysate and capped and incubated at room temperature for 76 min, and then PBS was applied to each column as three 200-μl fractions were collected. Equal volumes of each eluted fraction were analyzed by Western blotting.

Surface Labeling and Immunoprecipitation

RIPA lysates from surface-biotinylated CHO cells were prepared as described above. Lysate from 8×10^5 cells was mixed with 50 μl of protein A Sepharose CL-4B (as a 1:1 slurry in RIPA buffer; Pharmacia Biotech Inc.), 1 μl of anti-layilin antiserum or control serum, and 1 mg of heat-inactivated BSA in RIPA buffer in a total volume of 450 μl. After incubating at 4°C overnight with end-over-end mixing, the Sepharose was washed five times with 1 ml RIPA buffer. Each sample was divided into two parts, and one part was treated with peptide N-glycosidase F (PNGase F) according to the manufacturer's instructions (New England Biolabs Inc.). Samples were boiled for 10 min in 1× gel loading buffer, spun for 10 min at 13,000 *g* at room temperature, electrophoresed on 7.5% acrylamide gels, and transferred to nitrocellulose filters. Filters were blocked overnight at 4°C in blocking buffer (5% non-fat dry milk reconstituted in PBS/0.1% Tween-20), rinsed twice, and then washed once for 5 min with PBS/0.1% Tween-20, incubated for 45 min at room temperature with HRP-streptavidin (Amersham Life Science, Inc., Arlington Heights, IL) diluted 1:2,000 in PBS/0.1% Tween-20, rinsed twice, and then washed once for 15 min in PBS/0.1% Tween-20, followed by 5 × 10-min washes in PBS/0.1% Tween-20. Bands were detected using chemiluminescence (NEN™ Life Science Products, Boston, MA).

Generation of Cell Lines Expressing Epitope-tagged Layilin

A hemagglutinin (HA)-tagged version of layilin was made by inserting a synthetic EcoRI linker (New England Biolabs Inc.) into the 5′ PvuII site in the layilin cDNA. An oligonucleotide encoding the sequence EFYPY-DVPDYASPEF was ligated into the EcoRI linkered form of layilin, and this construct was confirmed by DNA sequencing (Wilson et al., 1984). The tagged layilin cDNA was transferred into the expression vector pLEN-neo, and the resulting construct transfected into cells using standard calcium-phosphate protocols.

Immunofluorescence

Adherent NIL8 cells were released with trypsin/EDTA, plated on glass coverslips coated with 5 μg/ml human plasma fibronectin (Beckton Dickinson, Bedford, MA), and incubated for 15 min to detect ruffles in spreading cells, overnight to obtain well-spread cells, or several days to achieve high cell density for in vitro wounding experiments. Spreading cells were stained before fixation and permeabilization, although identical staining patterns were observed when staining was performed on fixed and permeabilized cells. Otherwise, cells were stained after fixation and permeabilization as follows. Coverslips were washed three times in PBS, fixed for 10 min in 4% paraformaldehyde in PBS, washed as above, permeabilized for 10 min in 1% Brij 99 (Fluka, Ronkonkoma, NY) in PBS, washed as above, blocked with 10% normal goat serum (NGS, Vector Labs, Inc., Burlingame, CA) in PBS for 30 min at 37°C, incubated with primary antibody diluted in 10% NGS/PBS for 30 min at 37°C, washed as above, incubated with fluorescently labeled secondary antibodies (Biosource International, Camarillo, CA), and fluorescently labeled phalloidin (Sigma Chemical Co.) as appropriate for 30 min at 37°C, washed as above, rinsed once in water, and mounted in gelvatol (Monsanto, St. Louis, MO) containing DABCO (Sigma Chemical Co.) to prevent fading. For peptide-blocking experiments, antibodies were preincubated on ice with an appropriate peptide at 1 mg/ml for at least 30 min. Antibodies were used at the following dilutions: anti-layilin, 1:200; TD77 (anti-talin), 1:100; 12CA5 (anti-HA-tag), 1:2,000; secondary antibodies, 1:200; phalloidin, 1:5,000. Monoclonal antibody TD77 was the gift of Dr. D.R. Critchley, University of Leicester (Bolton et al., 1997). Stained cells were viewed on a Zeiss Axiophot, and immunofluorescent images were recorded on film (Eastman Kodak Co., Rochester, NY) except for Fig. 7, *g*, *h*, and *i*, which were recorded digitally on an Axioplan 2 (Carl Zeiss Inc., Thornwood, NY) equipped with a CCD camera (Photometrics, Tucson, AZ) and IPLab Spectrum software (Signal Analytics, Vienna, VA). For wounding experiments, confluent monolayers grown on fibronectin-coated coverslips were scraped under warm PBS with a rubber policeman to remove approximately half of the monolayer, and were then returned to a 37°C/5% CO_2 incubator for 45–90 min until prominent phase-dark ruffles were observed (Nuckolls et al., 1992).

Results

Identification of a Talin-head-binding Partner by a Yeast Two-hybrid Screen

Given talin's homology to other members of the band 4.1 superfamily, we hypothesized that talin's NH_2-terminal domain, like those of band 4.1 and ERM proteins, would bind to an integral membrane protein. Since previous biochemical efforts to find such a talin-head-binding protein yielded no candidates, we used a LexA-based yeast two-hybrid system to find talin-head-binding proteins (our unpublished results; Nuckolls et al., 1990; Gyuris et al., 1993). We generated a LexA-talin fusion protein containing the band 4.1-homologous region of chicken talin (amino acids 1–435). This fusion protein is expressed in yeast, and neither alone nor when coexpressed with the B42 acidic transcriptional activator, activated either the leu2 or β-gal reporter genes (data not shown). In a yeast transciptional repression assay we found that the LexA-talin fusion protein downregulates reporter gene expression by fourfold, indicating that our talin bait enters the nucleus and binds to LexA binding sites (Gyuris et al., 1993; data not shown). We screened approximately 10^6 yeast colonies representing about 10^5 cDNAs from a CHO cDNA library with this LexA-talin head bait, and picked 40 colonies that displayed both leucine prototrophy and the ability to activate a lacZ reporter. After grouping the 40 cDNAs into classes based on Alu and HaeIII restriction patterns, we recov-

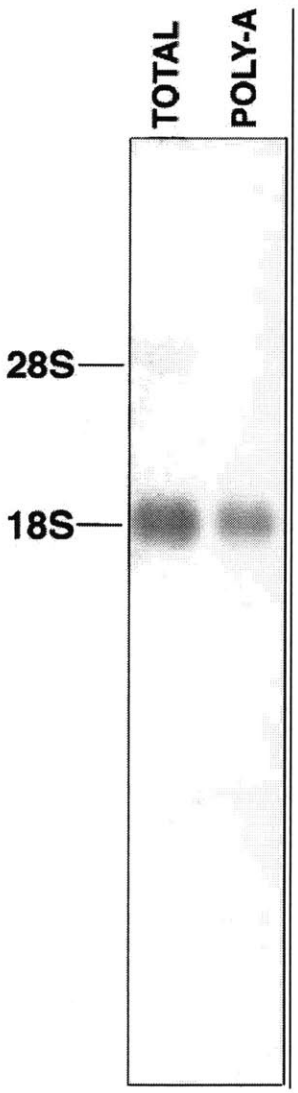

Figure 1. Northern blot analysis of CHO total and poly-A^+ RNA. 5 μg of CHO total RNA or 1 μg of CHO poly-A^+ RNA were analyzed for expression of a gene encoding a candidate talin-interacting protein. The single detectable transcript is highly enriched in the poly-A^+ RNA. The lane showing total RNA was exposed for 15 d and that showing poly-A^+ RNA for 2 d. The positions of the 18S (1874 nt) and 28S (4718 nt) ribosomal RNAs are indicated for size reference.

ered representative cDNAs from each class and retested them with the LexA-talin-head bait and a panel of four negative control LexA-fusion protein baits (LexA-max, LexA-bicoid, LexA-sec16p, LexA-TGFβR; Zervos et al., 1993; Espenshade et al., 1995). We recovered 30 cDNAs comprising a total of three genes that reproduced leucine prototrophy and β-gal activation when cotransformed into yeast with the talin bait, but not with the negative controls. Of these 30 cDNAs, 25 were overlapping fragments of a previously unidentified cDNA. We cloned the 5′ end of the cDNA encoding this candidate talin-interacting protein from a pcDNA-CHO library using anchored PCR with a primer based on our novel cDNA (Guo et al., 1994). Probes derived from the resulting 1,747-bp cDNA detected a single 1,800 nucleotide (nt) band in CHO RNA (Fig. 1).

The cDNA contains an open reading frame predicted to encode a 374–amino acid protein of an estimated molecular mass of 43 kD (Fig. 2 *a*). The protein has an amino-terminal signal sequence and predicted cleavage site typical of a secreted or transmembrane protein, a 130–amino acid domain with significant homology to C-type lectin carbohydrate-recognition domains (CRD), a 30–amino acid hydrophobic span suggestive of a transmembrane domain, and a 120–amino acid COOH-terminal domain containing three novel repeated motifs and two YXXΦ motifs similar to those known to allow AP-2–mediated recycling of some transmembrane proteins (von Heijne, 1986; Letourneur and Klausner, 1992; Drickamer, 1993). We named this protein *layilin* based on the sequence LAYILI found in its putative transmembrane domain.

Since talin is a cytosolic protein, a physiologically relevant interaction between layilin and talin must be mediated by layilin's putative cytoplasmic domain. Each of the seven independent layilin cDNAs recovered and sequenced contains the cytoplasmic domain of layilin, suggesting that the layilin cytoplasmic domain is sufficient for talin binding. We confirmed this by testing the cytoplasmic domain and the extracellular and transmembrane domains separately in the two-hybrid assay. The layilin cytoplasmic domain alone (amino acids 244–374) conferred leucine prototrophy and activated the LacZ reporter whereas the largest B42-fusion, which contains most of the rest of layilin (amino acids 92–244), did not (data not shown).

A comparison of layilin's C-type lectin homologous sequences with the CRDs of two known C-type lectins is shown in Fig. 2 *b*. Layilin contains 14/14 residues found in all carbohydrate-binding C-type lectins, and an additional 18/20 highly conserved residues (Drickamer, 1993). One of the two nonconserved residues, V141, corresponds to an oxygen-containing residue that coordinates one of two calcium ions bound by some C-type lectins (Weis et al., 1991). However, not all lectins use this calcium-binding site, and the absence of an oxygen-containing side chain at position 141 suggests that layilin lacks this second calcium-binding site (Graves et al., 1994). Interestingly, layilin contains a 5–amino acid insertion relative to the mannose-binding protein CRD (amino acids 148–152 of layilin; Fig. 2 *b*, *underline*), which is of the same size and at the identical position as an insertion found in the E-selectin CRD. The inserted sequences in the E-selectin CRD form a loop that projects into the ligand-binding pocket, and mutation of these sequences disrupts selectin-mediated adhesion (Graves et al., 1994). Layilin contains an additional 7–amino acid insertion adjacent to the 5–amino acid insertion that may form part of the same loop (Fig. 2 *b*, *double underline*). Layilin shares ~40% amino acid similarity with all other CRDs examined; the presence of a selectin-like insertion raises the possibility that layilin may bind to ligand in a manner similar to selectins. Layilin also differs from other CRDs by inserting 7 amino acids relative to the mannose-binding protein CRD (amino acids 102–108 of layilin, Fig. 2 *b*, *broken underline*). This insertion falls in sequences that form the first of four large calcium-binding loops in other CRDs, and is distal to the proposed ligand-binding, site. The 45 amino acids between the CRD and the putative transmembrane domain are rich in negatively charged amino acids (11/45), prolines (7/45), and S/T residues that may serve as O-linked carbohydrate attachment sites (10/45). These characteristics are suggestive of an elongated stalk that projects the CRD away from the plasma membrane.

Potential human and pig layilin homologues present in the expressed sequence tag (EST) database indicate con-

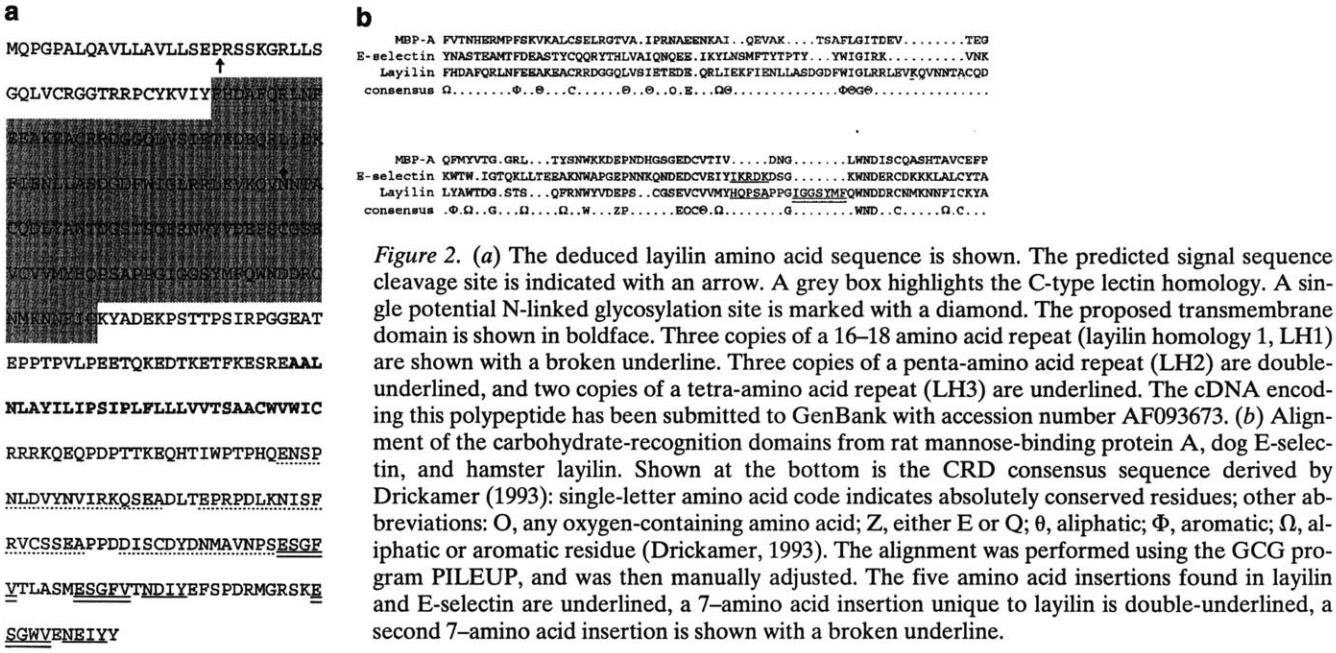

Figure 2. (*a*) The deduced layilin amino acid sequence is shown. The predicted signal sequence cleavage site is indicated with an arrow. A grey box highlights the C-type lectin homology. A single potential N-linked glycosylation site is marked with a diamond. The proposed transmembrane domain is shown in boldface. Three copies of a 16–18 amino acid repeat (layilin homology 1, LH1) are shown with a broken underline. Three copies of a penta-amino acid repeat (LH2) are double-underlined, and two copies of a tetra-amino acid repeat (LH3) are underlined. The cDNA encoding this polypeptide has been submitted to GenBank with accession number AF093673. (*b*) Alignment of the carbohydrate-recognition domains from rat mannose-binding protein A, dog E-selectin, and hamster layilin. Shown at the bottom is the CRD consensus sequence derived by Drickamer (1993): single-letter amino acid code indicates absolutely conserved residues; other abbreviations: O, any oxygen-containing amino acid; Z, either E or Q; θ, aliphatic; Φ, aromatic; Ω, aliphatic or aromatic residue (Drickamer, 1993). The alignment was performed using the GCG program PILEUP, and was then manually adjusted. The five amino acid insertions found in layilin and E-selectin are underlined, a 7–amino acid insertion unique to layilin is double-underlined, a second 7–amino acid insertion is shown with a broken underline.

servation among different species of some layilin sequence features. First, the pig EST (accession no. AA063669) encodes a protein that includes most of the layilin CRD. This potential homologue is 80% identical and 88% similar to hamster layilin, and includes the insertions discussed above. In addition, both hamster and pig layilin sequences contain the sequence EPS in a motif that has some value in predicting the carbohydrate specificity of CRDs; CRDs containing the sequence EPN generally bind mannose or glucose while those with the sequence QPD tend to bind galactose sugars (Drickamer, 1992). We cannot make any prediction based on the sequence EPS found in layilin. The second candidate layilin homologue is encoded by two human ESTs (accession nos. AA447940 and AA384314), and overlaps the layilin cytoplasmic domain. The 92–amino acid hypothetical human protein is 73% identical and 83% similar to hamster layilin, and contains three copies of the long repeat and a single copy of each of the short cytoplasmic domain motifs. Alignment of the human and hamster cytoplasmic domains reveals that the human version lacks the COOH-terminal 20 amino acids, precisely those used in our peptide antigen. This may explain our inability to detect layilin protein in human cell lines with our antibody (see below).

Layilin Protein is Widely Expressed in Cells and Tissues

We raised a polyclonal antiserum directed against a keyhole limpet hemocyanin-conjugated peptide corresponding to the 20 carboxy-terminal amino acids of layilin, and affinity-purified it against the immobilized peptide. Both the serum and affinity-purified antibodies detect a cluster of bands migrating at ~55 kD in detergent lysates of CHO cells, while the serum depleted over the peptide column did not detect any specific bands (Fig. 3 *a*, compare lanes *3* and *5* with lane *4*). Fig. 3 *a* also shows that the bands detected by the anti-layilin antiserum are competed by the layilin-derived peptide (compare lane *1* with lane *2*). In cells transfected with an HA-tagged layilin cDNA, the anti-HA monoclonal antibody 12CA5 detects a similar cluster of bands that migrate slightly more slowly, presumably because of the presence of the HA tag; the anti-layilin antiserum detects the same bands (data not shown).

To find out whether layilin, like talin, is expressed in a variety of cell lines and cell types, we screened several cultured cell lines and mouse tissues for the presence of layilin protein. Our antiserum detected an immunoreactive protein of approximately the same size as hamster layilin in each cell line tested, except the human cell line K562 (Fig. 3 *b*). These bands were efficiently competed in the presence of the layilin-derived peptide LC20 (data not shown). The cross-reacting band in three rat cell lines tested migrated slightly faster than the band in hamster cell lysates, indicating a molecular weight difference of ~4 kD. This result could represent differential glycosylation (see below) or a deletion or alteration in the polypeptide itself. We observed a significantly weaker signal in COS cells, indicating either that these cells express less layilin protein or that the monkey antigen does not cross-react with our antibody as well as rodent layilins. Our inability to detect layilin-reactive protein in human cells might be explained by the sequence of the candidate human layilin homologue described above. We found detectable levels of layilin in most of the 12 mouse tissues analyzed by Western blotting (Fig. 3 *c*). Layilin was most abundant in the ovary, and was readily detectable in most other solid tissues assayed. These observations indicate that layilin, like talin, is widely expressed in adherent cell types both in vitro and in vivo.

GST-talin-head Fusions Bind Layilin and FAK

To confirm and characterize further the interaction between talin and layilin, we tested the ability of GST fusion

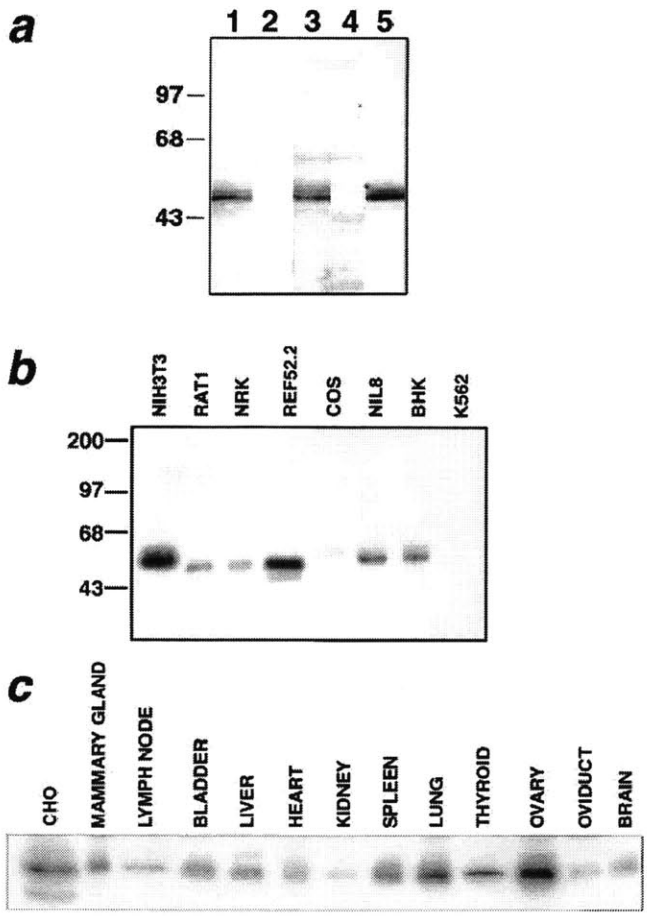

Figure 3. Expression of layilin protein in cells and tissues. (*a*) A rabbit polyclonal antiserum was raised against a synthetic peptide comprising the COOH-terminal 20 amino acids of layilin and used to Western blot a lysate of CHO cells. Lane *1*, immune serum; lane *2*, immune serum preincubated with 1 mg/ml layilin peptide; lane *3*, immune serum; lane *4*, immune serum after depletion over immobilized layilin peptide; lane *5*, affinity-purified antibody eluted from the immobilized layilin peptide. The position and size in kilodaltons of molecular weight standards are shown. (*b*) Western blot with affinity-purified anti-layilin antiserum of mouse, rat, monkey, hamster, and human cell lines. Specifically reacting bands in rat cell lines migrate slightly faster than do the prevalent immunoreactive species in monkey, mouse and hamster. NRK, normal rat kidney; REF, rat embryo fibroblast. The position and size in kD of molecular weight standards are shown. 5 μg of lysate were loaded per lane. (*c*) Organs were dissected from a healthy adult female mouse, homogenized, and lysed in gel-loading buffer. 10 μg of each lysate were loaded per lane, and were blotted for layilin. Total CHO protein is included to indicate the position of layilin.

proteins containing either talin or layilin sequences to bind layilin or talin, respectively, in detergent extracts from CHO cells. In each experiment, samples were assayed by Coomassie staining to ensure equal loading of GST fusion proteins. GST-layilin fusions containing amino acids 261–374 and 330–374 of the layilin cytoplasmic domain retained a fraction of intact talin in CHO detergent lysates, whereas a GST-layilin fusion containing amino acids 244–335 and a negative control GST-fusion containing a fibronectin type III repeat (GST-FN EIIIB) did not (Fig. 4 *a*). Moreover, the GST-layilin fusions distinguished between the full-length talin protein and a prominent proteolytic fragment present in the lysate by binding to only the full-length talin polypeptide. These observations indicate that the minimal talin binding site is within amino acids 330–374. This region of layilin includes three copies of the motif ESG(F/W)V (LH2) and two N(D/E)IY repeats (LH3), with each LH3 repeat adjacent to an LH2 repeat (Fig. 2 *a*). Talin binds to a GST fusion protein containing 1 or 3 copies of a tandem array of the LH2+LH3 repeats found at amino acids 243–252 of layilin (Fig. 4 *a* and data not shown). In addition, a synthetic peptide (LC20) derived from the COOH-terminal 20 amino acids of layilin and containing one copy of the LH2+LH3 module, blocks binding of talin to GST-layilin 330–374 (Fig. 4 *a*). In contrast to LC20, an unrelated peptide containing the HA epitope does not block binding of talin to the GST-layilin fusion protein (Fig. 4 *a*). These observations confirm that talin binds layilin through one or more LH23 motifs.

Fig. 4 *b* (*bottom*) shows that glutathione-agarose preloaded with a GST fusion protein containing amino acids 1–435 of talin (GST-CT 1–435), the same talin fragment used in our LexA-talin head bait, binds layilin in CHO extracts, whereas glutathione-agarose loaded with equal amounts of a control GST-fibronectin fusion protein does not. The GST-CT fusion also binds HA-tagged layilin in extracts prepared from NIL8 cells expressing epitope-tagged layilin. Using the monoclonal 12CA5 to detect the epitope tag, we found that GST-talin fusions that include amino acids 280–435 can specifically retain HA-tagged layilin from a cell lysate (Fig. 4 *c*).

We used our GST-talin fusion protein to determine if other focal contact proteins bound to talin head. We examined the material bound to the talin and control fibronectin GST-fusions for the presence of other focal contact proteins, and found that FAK bound to talin's NH_2-terminal domain (Fig. 4 *b*, *top*). This confirms and extends previous reports of an interaction between FAK and talin (Chen et al., 1995; Zheng et al., 1998). We did not detect any binding of α-actinin, vinculin, tensin, paxillin, tubulin, or β1-integrin to GST-CT 1–435 or to GST-FN EIIIB (data not shown). We used this assay to map the sequences within talin head sufficient for layilin and FAK binding (Fig. 4, *b* and *c*). Layilin bound to each GST-talin fusion containing at least amino acids 280–435. FAK bound well to GST-fusions that include amino acids 186–435. Shorter fusions overlapping amino acids 225–357 and a fusion protein containing only amino acids 225–357 of talin bound FAK weakly. Hence, amino acids 225–357 contain a minimal FAK-binding site, and amino acids 280–435 constitute the smallest layilin-binding site tested. The FAK binding site maps entirely within talin's band 4.1 homologous domain, and the layilin-binding site overlaps this region while including more COOH-terminal talin sequences. The fact that these binding sites are distinguishable confirms the specificity of each interaction.

Layilin is a Glycoprotein Expressed on the Cell Surface

The presence of a putative signal sequence and transmembrane domain suggested that layilin would be found on the

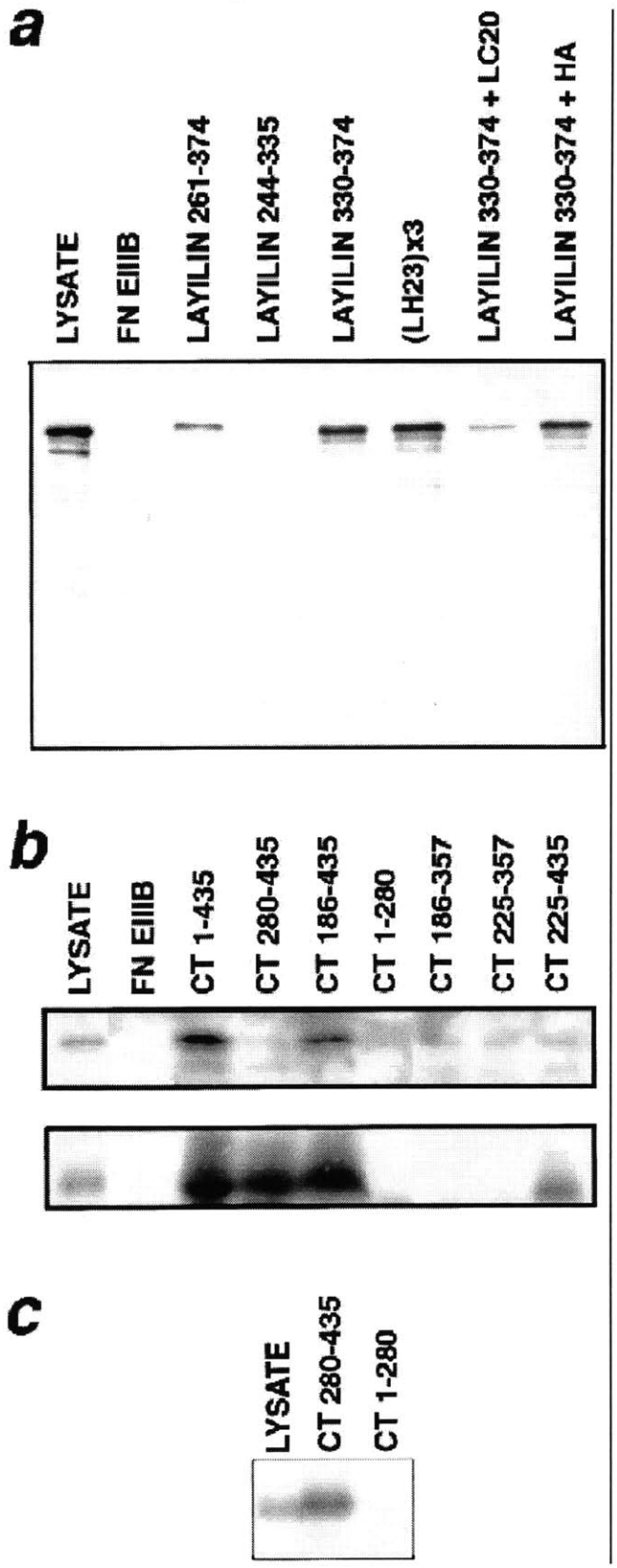

Figure 4. (*a*) GST fusion proteins containing portions of the layilin cytoplasmic domain were immobilized on agarose and mixed with a CHO cell detergent lysate. Each fusion protein contains the layilin amino acids indicated, except (LH23)×3, which has three copies of the amino acid motif spanning layilin amino acids 243–252. After washing, the agarose beads were boiled in gel-loading buffer, and the released material was analyzed by Western blotting for talin. The lanes containing proteins bound by GST fusions of fibronectin EIIIB (FN EIIIB) or layilin are overloaded approximately 13-fold relative to the total lysate lane. (*b*) Glutathione agarose preloaded with GST fusions containing either FN EIIIB or the indicated amino acids of chicken talin was incubated with a CHO cell detergent lysate, washed, and boiled in gel-loading buffer. Proteins released from the beads were detected by Western blotting for focal adhesion kinase (FAK, *top*) or layilin (*bottom*). The lanes containing proteins bound by GST fusions to chicken talin and fibronectin EIIIB are overloaded approximately 25-fold relative to the total lysate lane. (*c*) Glutathione agarose preloaded with GST fusions containing various fragments of chicken talin was incubated with a detergent lysate of NIL8 cells expressing HA-tagged layilin, washed, and boiled in gel-loading buffer. Proteins released from the beads were detected by Western blotting for the HA-epitope tag. Lanes containing material bound to GST fusions are overloaded approximately 20-fold relative to the total lysate lane.

cell surface. We tested this hypothesis by immunoprecipitation from surface-labeled CHO cell lysates. The anti-layilin antiserum immunoprecipitates from lysates of surface-biotinylated CHO cells a 55-kD band whose size is in good agreement with the band we detected by Western blotting of whole cell lysates with the same antibody (Fig. 5 *a*, lane *3*; Fig. 3 *a*, lanes *1*, *3*, and *5*; similar results were obtained with NIL8 hamster fibroblasts, data not shown). Peptide-depleted serum does not immunoprecipitate any surface-labeled material from biotin-labeled CHO cells, and the 55-kD band precipitated by the antiserum can be competed by preincubating the affinity-purified antiserum with a layilin-derived peptide (Fig. 5 *a*, lane *1*, and data not shown). We found that the surface-labeled band immunoprecipitated by anti-layilin antiserum is sensitive to treatment with PNGase F, indicating the presence of N-linked carbohydrates (Fig. 5 *a*, compare lanes *3* and *4*; Maley et al., 1989). The anti-HA epitope monoclonal 12CA5 immunoprecipitates a similarly sized, surface-labeled, PNGase F–sensitive band from both CHO and NIL8 cells expressing HA-tagged layilin (data not shown). Western blotting of CHO cell lysates treated with PNGase F shows a similar shift in the mobility of the band detected by anti-layilin antiserum, confirming that we are observing the same band by both surface label and Western blotting, and indicating that most of the cellular pool of layilin is glycosylated (Fig. 5 *b*). PNGase F-treated layilin migrates slightly slower than predicted based on its deduced amino acid sequence (51 vs. 43 kD); this discrepancy may reflect additional posttranslational modifications to layilin, such as O-linked glycosylation, or may simply reflect aberrant electrophoretic migration.

We used accessibility to a membrane nonpermeable biotinylation reagent to assess the proportion of total layilin present on the cell surface. A population of CHO cells was divided into two parts: one was surface-labeled with sulfo-NHS-LC-biotin while the other was subjected to the same surface-labeling protocol in parallel without adding biotin. Lysates made from these two samples were applied to identical columns of immobilized avidin to capture any proteins that reacted with the surface-labeling reagent,

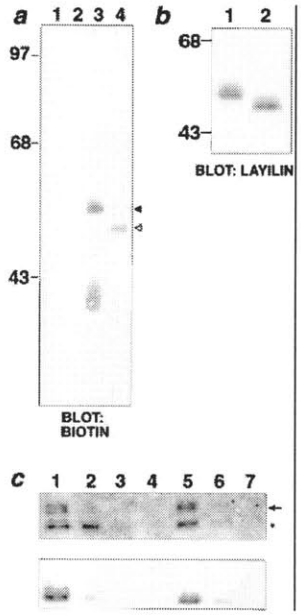

Figure 5. Layilin is a glycoprotein expressed on the cell surface. (*a*) CHO cells were surface-labeled with biotin, lysed in RIPA buffer, immunoprecipitated with either peptide-depleted (lanes *1* and *2*) or affinity-purified (lanes *3* and *4*) anti-layilin antiserum, and labeled bands were detected with HRP-streptavidin. Samples in lanes *2* and *4* were treated with PNGase F to remove N-linked carbohydrates. The position of the layilin band is marked with a solid arrowhead before PNGase F treatment, and with an open arrowhead after PNGase F treatment. The position and size in kD of molecular mass standards are shown. (*b*) A detergent lysate of CHO cells was treated with (lane *2*) or without (lane *1*) PNGase F to remove N-linked sugars, Western-blotted, and probed with affinity-purified anti-layilin antiserum. Note that essentially all the layilin present in the lysate is PNGase F-sensitive. The position and size in kD of molecular weight standards are shown. (*c*) Layilin is predominantly found on the cell surface. CHO cells were surface-labeled with biotin (lanes *2–4*) or mock surface-labeled without biotin (lanes *5–7*), lysed, and passed over an avidin column to remove labeled material. The first three fractions eluted from each column (lanes *2–4* and *5–7*) were analyzed by Western blotting for β1-integrin and layilin. When assayed for β1-integrin (*top*), the lysate (lane *1*) contains two bands: the upper band (*arrow*) represents mature β1-integrin; the lower band (*asterisk*) is an intracellular precursor. Biotin selectively labels the mature (*top*) band without affecting the precursor form of β1 (compare lanes *2* and *5*, *top*), indicating the reagent does not have access to the cells' interior. The same fractions (*bottom*) reveal that most layilin, like mature β1-integrin, is biotin-labeled (compare lanes *2* and *5*, *bottom*). All lanes were loaded with equivalent fractions of the cell lysate.

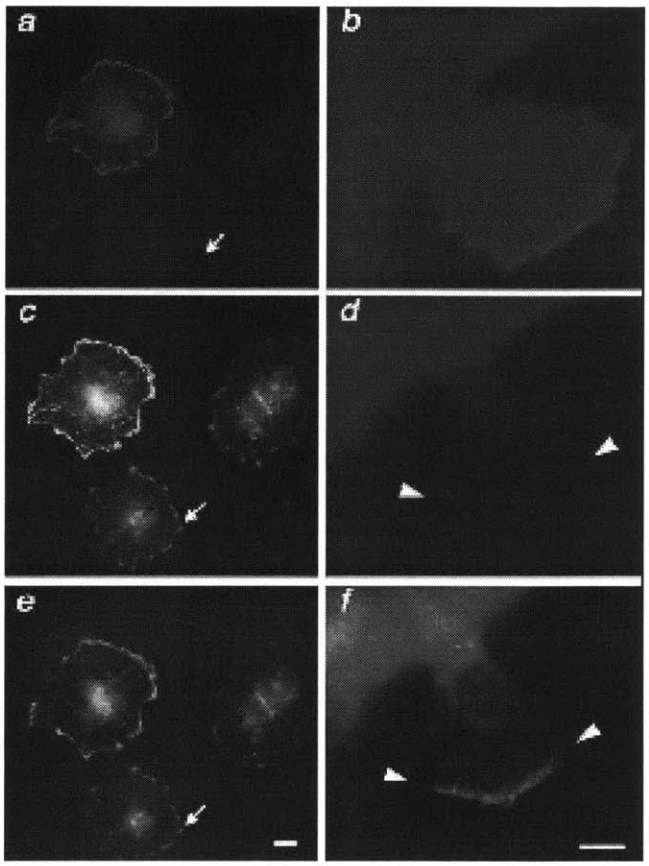

Figure 6. Localization of HA-tagged layilin in spreading (*a*, *c*, and *e*) or migrating (*b*, *d*, and *f*) NIL8 hamster cells. Cells spreading on a fibronectin matrix (*a*, *c*, and *e*) contain peripheral ruffles that stain for both HA-layilin (*a*) and phalloidin (*e*). Yellow ruffles in the double exposure (*c*) show the extent of overlap of staining. Migrating NIL8 cells also contain layilin-rich ruffles at their leading edges (*b*, *d*, and *f*). Cells shown are stained with 12CA5 in the presence of 1 mg/ml LC20 (*b*), 12CA5 in the presence of 1 mg/ml HA peptide (*d*), and the same cell as in *d* double-stained with affinity-purified anti-layilin antiserum (*f*). Bar, 10 μm.

thereby depleting surface proteins from the extracts. The flow-throughs from these columns were then analyzed by Western blotting for β1-integrin and layilin (Fig. 5 *c*). The integrin control indicates that the avidin column efficiently removed all of the mature surface-expressed β1-integrin (Fig. 5 *c*, *arrow*) from the labeled lysates (lanes *2–4*) without affecting the amount of precursor β1-integrin (which is not expressed on the surface; Fig. 5 *c*, *asterisk*). In contrast, the avidin column did not deplete either form of β1-integrin from mock-labeled lysates (Fig. 5 *c*, lanes *5–7*). By assaying the same fractions for layilin, we found that the majority of layilin was depleted in the biotin-treated sample when compared with the unbiotinylated control, indicating that most layilin protein is on the cell surface (Fig. 5 *c*, *bottom*; compare lanes *2–4* with lanes *5–7*).

Layilin Localization

We chose to analyze layilin subcellular distribution in NIL8 hamster fibroblasts because they have a well-articulated actin cytoskeleton that has been extensively characterized (Mautner and Hynes, 1977; Hynes and Destree, 1978). To confirm the specificity of our observations, we examined the distribution of both HA-tagged and endogenous layilin. In NIL8 cells stably transfected with an HA epitope–tagged version of layilin, 12CA5, the monoclonal antibody directed against the HA epitope tag, stains ruffling membranes in both spreading and migrating cells (Fig. 6, *a–f*). 15 min after plating on fibronectin-coated coverslips, NIL8 cells have a rim of F-actin filaments around the cell edge (Fig. 6 *e*). Spreading cells expressing HA-tagged layilin exhibit strong staining that colocalizes with phalloidin signal at the cell periphery (Fig. 6, *a*, *c*, and *e*). As an internal control, we examined nonexpressing cells in the same field; these cells have ruffles as assessed by phalloidin staining, but show no 12CA5 signal in the ruffles, indicating that 12CA5 staining produces little or no background in NIL8 cells (Fig. 6, *a*, *c*, and *e*, *arrows*).

The leading edges of migrating cells also contain actin- and talin-rich ruffles. To assess layilin localization in these

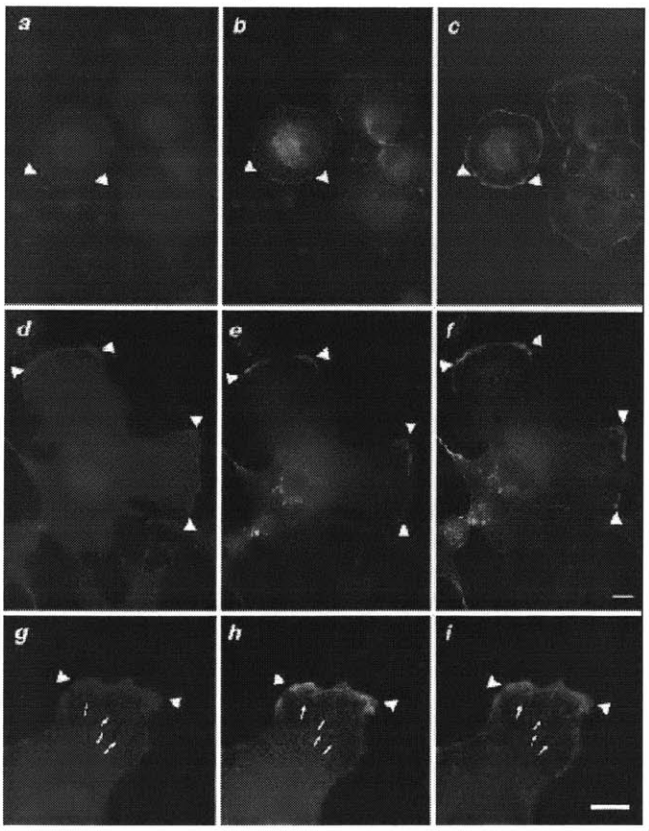

Figure 7. Endogenous layilin is in membrane ruffles. Cells are shown stained with peptide-depleted anti-layilin antiserum (*a*), affinity-purified anti-layilin antiserum (*d* and *g*), phalloidin (*c* and *f*), and anti-talin (*i*). *b*, *e*, and *h* are double exposures of *a* and *c*, *d* and *f*, and *g* and *i*. Layilin antibodies stain membrane ruffles (*arrowheads*) which also contain talin (*i*) and actin (*f*). The talin monoclonal stains both ruffles (*h* and *i*, *arrowheads*) and focal contacts (*h* and *i*, *arrows*), while the layilin antiserum stains ruffles but not focal contacts (*g* and *h*). Bar, 10 μm.

ruffles, we stimulated cells to migrate by wounding confluent monolayers with a rubber cell scraper, and examined the distribution of epitope-tagged layilin in cells migrating into the wound. 45–90 min after wounding, we observed lamellipodia with phase-dark ruffles on 10–30% of cells adjacent to the region cleared of cells. We detected HA-tagged layilin in these leading edge ruffles formed by migrating cells (Fig. 6, *b*, *d*, and *f*). This HA signal is competed by a peptide containing the HA epitope, but not by an unrelated peptide (LC20), demonstrating the specificity of the observed staining (Fig. 6, *b* and *d*). The cell in Fig. 6 *d* is double-stained with the polyclonal anti-layilin antiserum in Fig. 6 *f* to show that the cell has a layilin-positive ruffle at its leading edge.

We next examined the distribution of endogenous layilin in untransfected NIL8 cells. Our affinity-purified polyclonal anti-layilin antiserum stains the leading edge of migrating cells and peripheral ruffles of spreading cells (Fig. 7). Signals in the nucleus and the midbody are probably artifacts of the antiserum as we saw no nuclear or midbody staining with 12CA5 in cells expressing HA-tagged layilin (Fig. 6 and data not shown). Furthermore, our biochemical analysis, which suggests that layilin is predominantly on the cell surface, is inconsistent with the presence of significant levels of layilin in the nucleus (Fig. 5 *c*).

We compared the distribution of endogenous layilin with that of F-actin in NIL8 cells that were grown overnight on fibronectin-coated coverslips. The cell shown in Fig. 7, *d–f* is extending two lamellipodia at right angles to one another, each showing strong layilin staining at its leading edge. Phalloidin staining confirms that F-actin is also concentrated in these structures (Fig. 7 *f*). The cell shown in Fig. 7, *d–f*) has recently divided, and has not yet formed actin stress fibers characteristic of a well-spread cell. However, we did not observe specific stress-fiber staining with the anti-layilin antiserum in well-spread cells exhibiting prominent stress fibers (data not shown). Control anti-layilin antiserum was depleted of layilin immunoreactivity by preincubation of immune serum on a column containing immobilized layilin peptide (Fig. 3 *a*). In contrast to the affinity-purified anti-layilin antiserum, the depleted serum does not stain peripheral actin-rich ruffles (Fig. 7, *a–c*).

Colocalization of Layilin with Talin in Ruffles

We used double-label immunofluorescence to see whether layilin colocalizes with talin in focal contacts or membrane ruffles. We induced leading edges in NIL8 cells by scraping monolayer cultures. The resulting ruffles show strong staining with the anti-talin monoclonal TD77, confirming earlier reports of talin in ruffling membranes (Fig. 7 *i*; Burridge and Connell, 1983; DePasquale and Izzard, 1991; Bolton et al., 1997). In the same cells, talin is also readily seen in focal contacts arrayed behind the leading edge (Fig. 7, *h* and *i*, *arrows*). Layilin staining is clearly visible in the same ruffles that contain talin, but is not evident in focal contacts (Fig. 7 *g*, *arrows*). The coincidence of talin and layilin staining in these cells is indicated by yellow staining in the merged image of layilin and talin immunofluorescence, while the green focal contacts confirm that talin, but not layilin, is found in focal contacts (Fig. 7 *h*). Overall, we found essentially identical subcellular distribution in ruffles of both endogenous and HA-tagged layilin. The layilin signal colocalizes with both talin and phalloidin staining found in peripheral ruffles, but not with stress fibers or focal contacts (Fig. 7 and data not shown).

Discussion

Talin was discovered as a component of focal contacts and the leading edge of migrating cells, but the molecular basis of its role in ruffles is unknown (Burridge and Connell, 1983). Similarly, the significance of talin's band 4.1 homology, initially observed when the talin cDNA was reported (Rees et al., 1990), has not been revealed. The discovery of layilin, an integral membrane protein found in ruffles that binds to talin's band 4.1 homologous domain, confirms the hypothesis of Rees et al. that this domain of talin contains a membrane-binding site, and suggests a specific function for talin in the leading edge of migrating cells as an adaptor between the membrane and F-actin. A role for talin in migration was initially suggested by its subcellular localization in ruffles, and was demonstrated by the inhibitory

effect of microinjecting anti-talin antibodies into cells along the edge of a wound (Nuckolls et al., 1992; Bolton et al., 1997). Microinjecting a monoclonal antibody (TA205) that recognizes a fusion protein containing amino acids 139–433 within talin head domain also inhibits cell motility, further implicating this talin fragment in cell motility (Bolton et al., 1997). The monoclonal antibody TA205 recognizes a GST-talin fusion containing amino acids 1–186, placing the epitope between amino acids 139 and 186 (our unpublished observations); we have identified binding sites for both FAK and layilin adjacent to this antibody binding site, which may account for its inhibitory activity (Fig. 4). Talin's role in the dynamic aspects of membrane–cytoskeletal junctions in vertebrate cells is underscored by the observation that localized disruption of talin in neuronal growth cones prevents formation of new membrane extensions (Sydor et al., 1996). By binding to integrins and layilin, two types of transmembrane proteins with distinct subcellular distributions, talin may be able to distinguish between the relatively static membrane–cytoskeletal connections in focal contacts and the highly dynamic membrane–actin linkages in ruffles. How the talin–layilin interaction is regulated by or contributes to the control of membrane–cytoskeleton associations is the subject of ongoing investigations.

Models for Layilin Function

Given the colocalization of layilin with talin and the observed binding between them, layilin is a good candidate for a membrane-binding site for talin in ruffles. We observe colocalization of both epitope-tagged and endogenous layilin with talin in actin-rich membrane ruffles (Figs. 6 and 7). Bacterially expressed GST-talin fusion proteins bound layilin in cell lysates, and, in parallel experiments, GST-layilin cytoplasmic domain fusions bound talin in cell lysates (Fig. 4). These results, in addition to our initial finding that talin and layilin interact in a yeast two-hybrid assay, are consistent with a direct interaction between the two proteins. Layilin contains significant homology to proteins with C-type lectin activity. Carbohydrate recognition domains have been found in both type I (NH_2 terminus extracellular) and type II (NH_2 terminus cytoplasmic) single-pass transmembrane proteins (Drickamer and Taylor, 1993). Known type I C-type lectins fall into two functional groups: cell–cell adhesion molecules of the selectin family, and endocytic receptors such as the macrophage mannose receptor. This observation, combined with our initial characterization of the layilin protein, leads us to suggest two general models for layilin function.

In the first model, layilin acts in cell migration by anchoring to the membrane talin, which in turn binds F-actin. This chain of interactions may transmit force from actin to the membrane, resulting in its characteristic deformation into ruffles. In this scenario, layilin may serve simply as a talin docking site, or it could be an early-acting adhesion molecule that binds extracellular matrix, nucleating the formation of focal contact precursors at the cell periphery. In this case, layilin would be functioning analogously to selectins, which mediate transient adhesion between rolling leukocytes and the endothelium followed by tight integrin-mediated adhesion. However, whereas selectins mediate cell adhesion in specialized cells of the immune system, we hypothesize that layilin performs fundamental cell adhesion tasks common to most cells because layilin and talin are present in many different tissues (Fig. 3). Layilin would thus form transient adhesion sites between ruffles and extracellular matrix that are refined into focal contacts after integrin recruitment. This could occur in both spreading and migrating cells. Talin, which can bind both layilin and integrins, may provide continuity between the two types of cell–matrix linkages as transient layilin-containing structures mature into integrin-containing focal adhesions. Integrin extracellular matrix receptors are known to be signaling as well as adhesion receptors, and if layilin encounters matrix early in the process of cell adhesion it may also signal. The three internally repeated motifs in the layilin cytoplasmic domain are potential binding sites for cytoskeletal or signaling molecules in addition to talin. Conservation of these motifs in hamster and human layilins suggests that they are of importance, and we have shown that two of these repeats form a binding-site for talin (Fig. 4).

It is interesting to note that the C-type lectin CRD is structurally homologous to another carbohydrate-binding domain, the link module (Kohda et al., 1996). Link modules are found in a variety of carbohydrate-binding proteins, including CD44, one of the proteins reported to bind to the NH_2-terminal domain of ERMs (Tsukita et al., 1994). CD44 has also been proposed to function in cell migration and tumor metastasis (Sherman et al., 1994). It is notable that several members of the band 4.1 superfamily interact with the cytoplasmic domain of carbohydrate-binding molecules with roles in migration and adhesion.

In a second model, layilin may function as an endo- or phagocytic receptor, similar to some other C-type lectins such as the macrophage mannose receptor (Drickamer and Taylor, 1993). This model is suggested by the observation that talin is present in phagocytic cups in macrophages and at sites of uptake of some bacterial pathogens (Greenberg et al., 1990; Finlay et al., 1991; Finlay et al., 1992; Young et al., 1992; Love et al., 1998). In addition, the layilin cytoplasmic domain contains two YXXΦ motifs (YNVI, YDNM; Fig. 2 *a*). These motifs are similar to sequences that mediate clathrin-dependent endocytosis of other membrane proteins by binding to the μ2 chain of the AP-2 adaptor complex (Ohno et al., 1995; Marks et al., 1997). Layilin may act simply by binding to and internalizing ligands bearing an appropriate carbohydrate moiety, or it may have additional functions in recruitment or stabilization of cytoskeleton in phagocytic ruffles. Alternatively, talin might stabilize a complex consisting of layilin and its bound ligand during uptake. Again, we would postulate that, given its widespread expression pattern in tissues, layilin participates in some general mode of uptake not limited to macrophages or other professional phagocytes. These two models, adhesion and uptake, are not mutually exclusive, however, and we are currently engaged in experiments to confirm or rule out either possibility.

Implications for the Band 4.1 Superfamily

The band 4.1 superfamily members merlin and ezrin/radixin/

moesin are present in membrane ruffles, and downregulation of ERM proteins by treating cells with antisense oligonucleotides results in reduced cell adhesion (Takeuchi et al., 1994; Henry et al., 1995). This defect may be causal or may be a secondary consequence of reduced cell spreading. We are investigating the possible interaction of layilin with ERM proteins and other members of the band 4.1 superfamily found in ruffles. Previous reports of binding between band 4.1 family members and membrane proteins implicate clustered basic residues as binding sites for band 4.1 and ERMs. Jöns and Drenckhahn (1992) found that band 4.1 binds to the basic sequence LRRRY in the cytoplasmic domain of the erythrocyte anion exchanger, one band 4.1 membrane docking site in red blood cells. Marfatia and colleagues showed that mutation of three membrane-proximal basic residues in the glycophorin C cytoplasmic domain abrogates binding in vitro between protein 4.1 and peptides derived from glycophorin C (Hemming et al., 1995; Marfatia et al., 1995). Recently, Yonemura et al. (1998) identified short basic sequences in CD44, CD43, and ICAM-2 that appear to mediate binding to ERM proteins (Legg and Isacke, 1998; Yonemura et al., 1998). Interestingly, as shown in Fig. 4, talin binds to ten amino acids derived from two repeated motifs within the layilin cytoplasmic domain. This binding site does not contain the membrane proximal or any other stretch of basic residues in layilin, demonstrating another mode of binding between band 4.1 family members and integral membrane proteins.

The interaction of band 4.1 with glycophorin C is enhanced in the presence of polyphosphoinositides (Anderson and Marchesi, 1985). A mechanism for this regulation is suggested by studies on ERM proteins demonstrating binding between ERM head and tail domains that is reversed in the presence of acidic phospholipids (Gary and Bretscher, 1995; Magendantz et al., 1995; Hirao et al., 1996). Although no such regulated head–tail interaction has been described for talin, talin's NH_2-terminal domain has been reported to bind some phospholipids under conditions of low ionic strength (Niggli et al., 1994). In addition, talin undergoes a conformational change from a globular structure to an elongated rod in response to changes in salt concentration, which may represent a transition from a closed to an open form of the protein with different abilities to bind talin-binding partners (Molony et al., 1987; Winkler et al., 1997). We would have circumvented this mode of regulation with our recombinant LexA- and GST-fusion proteins that contain only talin head. Recent reports that ERM localization and head–tail association can be influenced by phosphorylation of ERMs suggest a potential mode of talin regulation that is consistent with observed talin phosphorylation (Pasquale et al., 1986; Turner et al., 1989; Beckerle, 1990; Bertagnolli et al., 1993; Tidball and Spencer, 1993; Matsui et al., 1998; Shaw et al., 1998). It will be of interest to determine whether talin binding to layilin or FAK is regulated by either phospholipid binding or talin phosphorylation.

In conclusion, we have uncovered novel functions for the talin head domain analogous with those of the homologous NH_2-terminal domains of other band 4.1 family members: interaction with layilin in ruffles, and FAK binding. This talin domain therefore acts both as a membrane linker and in signal transduction, while the tail of talin binds a different membrane anchor (integrins) and forms links to the cytoskeleton.

We wish to thank the Brent, Prasad, Krieger, Kaiser, and Weinberg labs for providing valuable two-hybrid materials. We are grateful to Michael DiPersio for providing the talin-head subclones A14 and GST-CT 1–435, and to David Critchley for providing the monoclonal antibodies TD77 and TA205. Thanks to Ed Clark, Michael DiPersio, Sheila Francis, and Frank Solomon for their insightful comments on the manuscript.

This work was supported by a grant from the National Cancer Institute (RO1 CA17007) and by the Howard Hughes Medical Institute. M. Borowsky received support from an NIGMS Predoctoral Training Grant to the Massachusetts Institute of Technology Biology Department, and R.O. Hynes is an Howard Hughes Medical Institute Investigator.

Received for publication 20 June 1998 and in revised form 1 September 1998.

References

Albigès-Rizo, C., P. Frachet, and M.R. Block. 1995. Down regulation of talin alters cell adhesion and the processing of the α5β1 integrin. *J. Cell Sci.* 108: 3317–3329.

Algrain, M., O. Turunen, A. Vaheri, D. Louvard, and M. Arpin. 1993. Ezrin contains cytoskeleton and membrane binding domains accounting for its proposed role as a membrane-cytoskeleton linker. *J. Cell Biol.* 120:129–139.

Alwine, J.C., D.J. Kemp, and G.R. Stark. 1977. Method for detection of RNAs in agarose gels by transfer to diazobenzyloxymethyl-paper and hybridization with DNA probes. *Proc. Natl. Acad. Sci. USA.* 74:5350–5354.

Anderson, R.A., and V.T. Marchesi. 1985. Regulation of the association of membrane skeletal protein 4.1 with glycophorin by a polyphosphoinositide. *Nature.* 318:295–298.

Beckerle, M.C. 1990. The adhesion plaque protein, talin, is phosphorylated in vivo in chick embryo fibroblasts exposed to a tumor-promoting phorbol ester. *Cell Regul.* 1:227–236.

Bennett, V. and D.M. Gilligan. 1993. The spectrin-based membrane skeleton and micron-scale organization of the plasma membrane. *Annu. Rev. Cell Biol.* 9:27–66.

Bertagnolli, M.E., S.J. Locke, M.E. Hensler, P.F. Bray, and M.C. Beckerle. 1993. Talin distribution and phosphorylation in thrombin-activated platelets. *J. Cell Sci.* 106:1189–1199.

Bolton, S.J., S.T. Barry, H. Mosley, B. Patel, B.M. Jockusch, J.M. Wilkinson, and D.R. Critchley. 1997. Monoclonal antibodies recognizing the N- and C-terminal regions of talin disrupt actin stress fibers when microinjected into human fibroblasts. *Cell Motil. Cytoskelet.* 36:363–376.

Bradley, J.E., G.A. Bishop, T. St. John, and J.A. Frelinger. 1988. A simple, rapid method for the purification of Poly A+ RNA. *Biotechniques.* 6:114–116.

Burn, P., A. Kupfer, and S.J. Singer. 1988. Dynamic membrane-cytoskeletal interactions: Specific association of integrin and talin arises in vivo after phorbol ester treatment of peripheral blood lymphocytes. *Proc. Natl. Acad. Sci. USA.* 85:497–501.

Burridge, K., and L. Connell. 1983. A new protein of adhesion plaques and ruffling membranes. *J. Cell Biol.* 97:359–367.

Burridge, K., and P. Mangeat. 1984. An interaction between vinculin and talin. *Nature.* 308:744–746.

Chen, H.-C., P.A. Appeddu, J.T. Parsons, J.D. Hildebrand, M.D. Schaller, and J.-L. Guan. 1995. Interaction of focal adhesion kinase with cytoskeletal protein talin. *J. Biol. Chem.* 270:16995–16999.

Chomczynski, P., and N. Sacchi. 1987. Single-step method of RNA isolation by acid guanidium thiocyanate-phenol-chloroform extraction. *Anal. Biochem.* 162:156–159.

DePasquale, J., and C. Izzard. 1991. Accumulation of talin in nodes at the edge of the lamellipodium and separate incorporation into adhesion plaques at focal contacts in fibroblasts. *J. Cell Biol.* 113:1351–1359.

Drickamer, K. 1992. Engineering galactose-binding activity into a C-type mannose-binding protein. *Nature.* 360:183–186.

Drickamer, K. 1993. Ca2+-dependent carbohydrate-recognition domains in animal proteins. *Curr. Opin. Struct. Biol.* 3:393–400.

Drickamer, K., and M.E. Taylor. 1993. Biology of animal lectins. *Annu. Rev. Cell Biol.* 9:237–264.

Espenshade, P., R. Gimeno, E. Holzmacher, P. Teung, and C. Kaiser. 1995. Yeast SEC16 gene encodes a multidomain vesicle coat protein that interacts with Sec23p. *J. Cell Biol.* 131:311–324.

Finlay, B.B., I. Rosenshine, M.S. Donnenberg, and J.B. Kaper. 1992. Cytoskeletal composition of attaching and effacing lesions associated with enteropathogenic *Escherichia coli* adherence to HeLa cells. *Infect. Immun.* 60: 2541–2543.

Finlay, B.B., S. Ruschkowski, and S. Dedhar. 1991. Cytoskeletal rearrangements accompanying *Salmonella* entry into epithelial cells. *J. Cell Sci.* 99:

283–296.
Gary, R., and A. Bretscher. 1995. Ezrin self-association involves binding of an N-terminal domain to a normally masked C-terminal domain that includes the F-actin binding site. *Mol. Biol. Cell.* 6:1061–1075.
Gilmore, A.P., C. Wood, V. Ohanian, P. Jackson, B. Patel, D.J.G. Rees, R.O. Hynes, and D.R. Critchley. 1993. The cytoskeletal protein talin contains at least two distinct vinculin binding domains. *J. Cell Biol.* 122:337–347.
Graves, B.J., R.L. Crowther, C. Chandran, J.M. Rumberger, S. Li, K.-S. Huang, D.H. Presky, P.C. Familletti, B.A. Wolitzky, and D.K. Burns. 1994. Insight into E-selectin/ligand interaction from the crystal structure and mutagenesis of the lec/EGF domains. *Nature.* 367:532–538.
Greenberg, S., K. Burridge, and S.C. Silverstein. 1990. Colocalization of F-actin and talin during Fc receptor-mediated phagocytosis in mouse macrophages. *J. Exp. Med.* 172:1853–1856.
Guo, Q., E. Vasile, and M. Krieger. 1994. Disruptions in golgi structure and membrane traffic in a conditional lethal mammalian cell mutant are corrected by ε-COP. *J. Cell Biol.* 125:1213–1224.
Gyuris, J., E.A. Golemis, H. Chertkov, and R. Brent. 1993. Cdi1, a human G1 and S phase protein phosphatase that associates with Cdk2. *Cell.* 75:791–803.
Helander, T.S., O. Carpen, O. Turunen, P.E. Kovanen, A. Vaheri, and T. Timonen. 1996. ICAM-2 redistributed by ezrin as a target for killer cells. *Nature.* 382:265–268.
Hemming, N.J., D.J. Anstee, M.A. Staricoff, M.J.A. Tanner, and N. Mohandas. 1995. Identification of the membrane attachment sites for protein 4.1 in the human erythrocyte. *J. Biol. Chem.* 270:5360–5366.
Hemmings, L., D.J.G. Rees, V. Ohanian, J.J. Bolton, A.P. Gilmore, B. Patel, H. Priddle, J.E. Trevithick, R.O. Hynes, and D.R. Critchley. 1996. Talin contains three actin-binding sites each of which is adjacent to a vinculin-binding site. *J. Cell Sci.* 109:2715–2726.
Henry, M.D., C. Gonzalez Agosti, and F. Solomon. 1995. Molecular dissection of radixin: distinct and interdependent functions of the amino- and carboxy-terminal domains. *J. Cell Biol.* 129:1007–1022.
Hirao, M., N. Sato, T. Kondo, S. Yonemura, M. Monden, T. Sasaki, Y. Takai, S. Tsukita, and S. Tsukita. 1996. Regulation mechanism of ERM (ezrin/radixin/moesin) protein/plasma membrane association: possible involvement of phosphatidylinositol turnover and rho-dependent signaling pathway. *J. Cell Biol.* 135:37–51.
Hoffman, C.S., and F. Winston. 1987. A ten-minute DNA preparation from yeast efficiently releases autonomous plasmids for transformation of *Escherichia coli*. *Gene.* 57:267–272.
Horwitz, A., K. Duggan, C. Buck, M.C. Beckerle, and K. Burridge. 1986. Interaction of plasma membrane fibronectin receptor with talin–a transmembrane linkage. *Nature.* 320:531–533.
Hynes, R.O., and A.T. Destree. 1978. Relationships between fibronectin (LETS protein) and actin. *Cell.* 15:875–886.
Isberg, R.R., and J.M. Leong. 1990. Multiple β1 chain integrins are receptors for invasin, a protein that promotes bacterial penetration into mammalian cells. *Cell.* 60:861–871.
Jöns, T., and D. Drenckhahn. 1992. Identification of the binding interface involved in linkage of cytoskeletal protein 4.1 to the erythrocyte anion exchanger. *EMBO (Eur. Mol. Biol. Organ.) J.* 11:2863–2867.
Knezevic, I., T.M. Leisner, and S.C.-T. Lam. 1996. Direct binding of the platelet integrin $\alpha_{IIb}\beta_3$ (GPIIb-IIIa) to talin. *J. Biol. Chem.* 271:16416–16421.
Kohda, D., C.J. Morton, A.A. Parkar, H. Hatanaka, F.M. Inagaki, I.D. Campbell, and A.J. Day. 1996. Solution structure of the link module: a hyaluronan-binding domain involved in extracellular matrix stability and cell migration. *Cell.* 86:767–775.
Kreitmeier, M., G. Gerisch, C. Heizer, and A. Muller-Taubenberger. 1995. A talin homologue of *Dictyostelium* rapidly assembles at the leading edge of cells in response to chemoattractant. *J. Cell Biol.* 129:179–188.
Lawson, M.A., and F.R. Maxfield. 1995. Ca2+- and calcineurin-dependent recycling of an integrin to the front of migrating neutrophils. *Nature.* 377:75–79.
Lee, J., and K. Jacobson. 1997. The composition and dynamics of cell-substratum adhesions in locomoting fish keratocytes. *J. Cell Sci.* 110:2833–2844.
Legg, J.W., and C.M. Isacke. 1998. Identification and functional analysis of the ezrin-binding site in the hyaluronan receptor, CD44. *Curr. Biol.* 8:705–708.
Letourneur, F., and R.D. Klausner. 1992. A novel di-leucine motif and a tyrosine-based motif independently mediate lysosomal targeting and endocytosis of CD3 chains. *Cell.* 69:1143–1157.
Love, D.C., M.M. Kane, and D.M. Mosser. 1998. *Leishmania amazonensis*: The phagocytosis of amastigotes by macrophages. *Exp. Parasitol.* 88:161–171.
Magendantz, M., M.D. Henry, A. Lander, and F. Solomon. 1995. Interdomain interactions of radixin in vitro. *J. Biol. Chem.* 270:25324–25327.
Maley, F., R.B. Trimble, A.L. Tarentino, and T.H. Plummner. 1989. Characterization of glycoproteins and their associated oligosaccharides through the use of endoglycosidases. *Anal. Biochem.* 180:195–204.
Marcantonio, E.E., and R.O. Hynes. 1988. Antibodies to the conserved cytoplasmic domain of the integrin β1 subunit react with proteins in vertebrates, invertebrates, and fungi. *J. Cell Biol.* 106:1765–1772.
Marfatia, S.M., R.A. Lue, D. Branton, and A.H. Chishti. 1995. Identification of the protein 4.1 binding interface on glycophorin C and p55, a homologue of the *Drosophila discs-large* tumor suppressor protein. *J. Biol. Chem.* 270:715–719.
Marks, M.S., H. Ohno, T. Kirchhausen, and J.S. Bonifacino. 1997. Protein sorting by tyrosine-based signals: adapting to the Ys and wherefores. *Trends Cell Biol.* 7:124–128.
Matsui, T., M. Maeda, Y. Doi, S. Yonemura, M. Amano, K. Kaibuchi, S. Tsukita, and S. Tsukita. 1998. Rho-kinase phosphorylates COOH-terminal threonines in ezrin/radixin/moesin (ERM) proteins and regulates their head-to-tail association. *J. Cell Biol.* 140:647–657.
Mautner, V., and R.O. Hynes. 1977. Surface distribution of LETS protein in relation to the cytoskeleton of normal and transformed cells. *J. Cell Biol.* 75: 743–768.
McLachlan, A.D., M. Stewart, R.O. Hynes, and D.J.G. Rees. 1994. Analysis of repeated motifs in the talin rod. *J. Mol. Biol.* 235:1278–1290.
Molony, L., D. McCaslin, J. Abernethy, B. Paschal, and K. Burridge. 1987. Properties of talin from chicken gizzard smooth muscle. *J. Biol. Chem.* 262: 7790–7795.
Moulder, G.L., M.M. Huang, R.H. Waterston, and R.J. Barstead. 1996. Talin requires β-integrin, but not vinculin, for its assembly into focal adhesion-like structures in the nematode *Caenorhabditis elegans*. *Mol. Biol. Cell.* 7:1181–1193.
Murthy, A., C. Gonzalez-Agosti, E. Cordero, D. Pinney, C. Candia, F. Solomon, J. Gusella, and V. Ramesh. 1998. NHE-RF, a regulatory cofactor for Na+-H+ exchange, is a common interactor for merlin and ERM (MERM) proteins. *J. Biol. Chem.* 273:1273–1276.
Niggli, V., S. Kaufmann, W.H. Goldmann, T. Weber, and G. Isenberg. 1994. Identification of functional domains in the cytoskeletal protein talin. *Eur. J. Biochem.* 224:951–957.
Nuckolls, G.H., L.H. Romer, and K. Burridge. 1992. Microinjection of antibodies against talin inhibits the spreading and migration of fibroblasts. *J. Cell Sci.* 102:753–762.
Nuckolls, G.H., C.E. Turner, and K. Burridge. 1990. Functional studies of the domains of talin. *J. Cell Biol.* 110:1635–1644.
Ohno, H., J. Stewart, M.-C. Fournier, H. Bosshart, I. Rhee, S. Miyatake, T. Saito, A. Gallusser, T. Kirchhausen, and J.S. Bonifacino. 1995. Interaction of tyrosine-based sorting signals with clathrin-associated proteins. *Science.* 269: 1872–1875.
Pasquale, E.B., P.A. Maher, and S.J. Singer. 1986. Talin is phosphorylated on tyrosine in chicken embryo fibroblasts transformed by Rous sarcoma virus. *Proc. Natl. Acad. Sci. USA.* 83:5507–5511.
Peters, J.H., J.E. Trevithick, P. Johnson, and R.O. Hynes. 1995. Expression of the alternatively spliced EIIIB segment of fibronectin. *Cell Adh. Comm.* 3:67–89.
Reczek, D., M. Berryman, and A. Bretscher. 1997. Identification of EBP50: a PDZ-containing phosphoprotein that associates with members of the ezrin-radixin-moesin family. *J. Cell Biol.* 139:169–179.
Rees, D.J.G., S.E. Ades, S.J. Singer, and R.O. Hynes. 1990. Sequence and domain structure of talin. *Nature.* 347:685–689.
Sambrook, J., E.F. Fritsch, and T. Maniatis. 1989. Molecular Cloning. Cold Spring Harbor Laboratory Press, Plainview, NY.
Schmidt, C.E., A.F. Horwitz, D.A. Lauffenburger, and M.P. Sheetz. 1993. Integrin-cytoskeletal interactions in migrating fibroblasts are dynamic, asymmetric, and regulated. *J. Cell Biol.* 123:977–991.
Serrador, J.M., J.L. Alonso-Lebrero, M.A. del Pozo, H. Furthmayr, R. Schwartz-Albiez, J. Calvo, F. Lozano, and F. Sánchez-Madrid. 1997. Moesin interacts with the cytoplasmic region of intercellular adhesion molecule-3 and is redistributed to the uropod of T lymphocytes during cell polarization. *J. Cell Biol.* 138:1409–1423.
Shaw, R.J., M. Henry, F. Solomon, and T. Jacks. 1998. RhoA-dependent Phosphorylation and relocalization of ERM proteins into apical membrane/actin protrusions in fibroblasts. *Mol. Biol. Cell.* 9:403–419.
Sherman, L., J. Sleeman, P. Herrlich, and H. Ponta. 1994. Hyaluronate receptors: key players in growth, differentiation, migration and tumor progression. *Curr. Opin. Cell Biol.* 6:726–733.
Sydor, A.M., A.L. Su, F.-S. Wang, A. Xu, and D.G. Jay. 1996. Talin and Vinculin Play Distinct Roles in Filopodial Motility in the Neuronal Growth Cone. *J. Cell Biol.* 134:1197–1207.
Takeuchi, K., N. Sato, H. Kasahara, N. Funayama, A. Nagafuchi, S. Yonemura, S. Tsukita, and S. Tsukita. 1994. Perturbation of cell adhesion and microvilli formation by antisense oligonucleotides to ERM family members. *J. Cell Biol.* 125:1371–1384.
Tapley, P., A. Horwitz, C. Buck, K. Duggan, and L. Rohrschneider. 1989. Integrins isolated from Rous sarcoma virus-transformed chicken embryo fibroblasts. *Oncogene.* 4:325–333.
Tidball, J.G., and M.J. Spencer. 1993. PDGF stimulation induces phosphorylation of talin and cytoskeletal reorganization in skeletal muscle. *J. Cell Biol.* 123:627–635.
Towbin, H., T. Staehelin, and J. Gordon. 1979. Electrophoretic transfer of proteins from polyacrylamide gels to nitrocellulose sheets: Procedure and some applications. *Proc. Natl. Acad. Sci. USA.* 76:4350–4354.
Tsukita, S., K. Oishi, N. Sato, J. Sagara, A. Kawai, and S. Tsukita. 1994. ERM family members as molecular linkers between the cell surface glycoprotein CD44 and actin-based cytoskeletons. *J. Cell Biol.* 126:391–401.
Tsukita, S., S. Yonemura, and S. Tsukita. 1997. ERM (ezrin/radxin/moesin) family: from cytoskeleton to signal transduction. *Curr. Opin. Cell Biol.* 9:70–75.
Turner, C.E., F.M. Pavalko, and K. Burridge. 1989. The role of phosphorylation and limited proteolytic cleavage of talin and vinculin in the disruption of focal adhesion integrity. *J. Biol. Chem.* 264:11938–11944.

Turunen, O., T. Wahlstrom, and A. Vaheri. 1994. Ezrin has a COOH-terminal actin-binding site that is conserved in the ezrin protein family. *J. Cell Biol.* 126:1445–1453.

Ungewickell, E., P.M. Bennett, R. Calvert, V. Ohanian, and W.B. Gratzer. 1979. In vitro formation of a complex between cytoskeletal proteins of the human erythrocyte. *Nature.* 280:811–814.

von Heijne, G. 1986. A new method for predicting signal sequence cleavage sites. *Nucleic Acids Res.* 14:4683–4690.

Weis, W.I., R. Kahn, R. Fourme, K. Drickamer, and W.A. Hendrickson. 1991. Structure of the calcium-dependent lectin domain from a rat mannose-binding protein determined by MAD phasing. *Science.* 254:1608–1615.

Wilson, I.A., H.L. Niman, R.A. Houghten, A.R. Cherenson, M.L. Connolly, and R.A. Lerner. 1984. The structure of an antigenic determinant in a protein. *Cell.* 37:767–778.

Winkler, J., H. Lunsdorf, and B. Jockusch. 1997. Energy-filtered electron microscopy reveals that talin is a highly flexible protein composed of a series of globular domains. *Eur. J. Biochem.* 243:430–436.

Yonemura, S., M. Hirao, Y. Doi, N. Takahashi, T. Kondo, S. Tsukita, and S. Tsukita. 1998. Ezrin/radixin/moesin (ERM) proteins bind to a positively charged amino acid cluster in the juxta-membrane cytoplasmic domain of CD44, CD43, and ICAM-2. *J. Cell Biol.* 140:885–895.

Young, V.B., S. Falkow, and G.K. Schoolnik. 1992. The invasin protein of *Yersinia enterocolitica*: Internalization of invasin-bearing bacteria by eukaryotic cells is associated with reorganization of the cytoskeleton. *J. Cell Biol.* 116: 197–207.

Zervos, A.S., J. Gyuris, and R. Brent. 1993. Mxi1, a protein that specifically interacts with Max to bind Myc-Max recognition sites. *Cell.* 72:223–232.

Zheng, C., X. Zheng, C.Z. Bian, C. Guo, A. Akbay, L. Warner, and J.-L. Guan. 1998. Differential regulation of Pyk2 and Focal Adhesion Kinase (FAK). *J. Biol. Chem.* 273:2384–2389.

Literature Cited

Agre, P., Casella, J. F., Zinkham, W. H., McMillan, C., and Bennett, V. (1985). Partial deficiency of erythrocyte spectrin in hereditary spherocytosis. Nature *314*, 380-3.

Akiyama, S. K., Yamada, S. S., Yamada, K. M., and LaFlamme, S. E. (1994). Transmembrane signal transduction by integrin cytoplasmic domains expressed in single-subunit chimeras. J Biol Chem *269*, 15961-4.

Albigès-Rizo, C., Frachet, P., and Block, M. R. (1995). Down regulation of talin alters cell adhesion and the processing of the α5β1 integrin. J. Cell Sci. *108*, 3317-3329.

Algrain, M., Turunen, O., Vaheri, A., Louvard, D., and Arpin, M. (1993). Ezrin contains cytoskeleton and membrane binding domains accounting for its proposed role as a membrane-cytoskeleton linker. J. Cell Biol. *120*, 129-139.

Ali, I. U., Mautner, V., Lanza, R., and Hynes, R. O. (1977). Restoration of normal morphology, adhesion and cytoskeleton in transformed cells by addition of a transformation-sensitive surface protein. Cell *11*, 115-26.

Alloisio, N., Morle, L., Bachir, D., Guetarni, D., Colonna, P., and Delaunay, J. (1985). Red cell membrane sialoglycoprotein beta in homozygous and heterozygous 4.1(-) hereditary elliptocytosis. Biochim Biophys Acta *816*, 57-62.

Alwine, J. C., Kemp, D. J., and Stark, G. R. (1977). Method for detection of RNAs in agarose gels by transfer to diazobenzyloxymethyl-paper and hybridization with DNA probes. Proc. Natl. Acad. Sci. USA *74*, 5350-5354.

Amano, M., Ito, M., Kimura, K., Fukata, Y., Chihara, K., Nakano, T., Matsuura, Y., and Kaibuchi, K. (1996). Phosphorylation and activation of myosin by rho-associated kinase (rho-kinase). J. Biol. Chem. *271*, 20246-20249.

Amano, M., Chihara, K., Kimura, K., Fukata, Y., Nakamura, N., Matsuura, Y., and Kaibuchi, K. (1997). Formation of actin stress fibers and focal adhesions enhanced by Rho-kinase. Science *275*, 1308-11.

An, X. L., Takakuwa, Y., Nunomura, W., Manno, S., and Mohandas, N. (1996). Modulation of band 3-ankyrin interaction by protein 4.1. Functional implications in regulation of erythrocyte membrane mechanical properties. J Biol Chem *271*, 33187-91.

Anderson, R. A., and Lovrien, R. E. (1981). Erythrocyte membrane sidedness in lectin control of the Ca2+- A23187-mediated diskocyte ↔ echinocyte conversion. Nature *292*, 158-61.

Anderson, R. A., and Lovrien, R. E. (1984). Glycophorin is linked by band 4.1 protein to the human erythrocyte membrane skeleton. Nature *307*, 655-8.

Anderson, R. A., and Marchesi, V. T. (1985). Regulation of the association of membrane skeletal protein 4.1 with glycophorin by a polyphosphoinositide. Nature *318*, 295-8.

Arber, S., Barbayannis, F. A., Hanser, H., Schneider, C., Stanyon, C. A., Bernard, O., and Caroni, P. (1998). Regulation of actin dynamics through phosphorylation of cofilin by LIM-kinase. Nature *393*, 805-809.

Arrieumerlou, C., Donnadieu, E., Brennan, P., Keryer, G., Bismuth, G., Cantrell, D., and Trautmann, A. (1998). Involvement of phosphoinositide 3-kinase and Rac in membrane ruffling induced by IL-2 in T cells. Eur J Immunol *28*, 1877-85.

Aruffo, A., Stamenkovic, I., Melnick, M., Underhill, C. B., and Seed, B. (1990). CD44 is the principal cell surface receptor for hyaluronate. Cell *61*, 1303-1313.

Aruffo, A., Kolanus, W., Walz, G., Fredman, P., and Seed, B. (1991). CD62/P-selection recognition of myeloid and tumor cell sulfatides. Cell *67*, 35-44.

Assoian, R. K. (1997). Anchorage-dependent cell cycle progression. J Cell Biol *136*, 1-4.

Aubry, J. P., Pochon, S., Graber, P., Jansen, K. U., and Bonnefoy, J. Y. (1992). CD21 is a ligand for CD23 and regulates IgE production. Nature *358*, 505-7.

Aubry, J. P., Pochon, S., Gauchat, J. F., Nueda-Marin, A., Holers, V. M., Graber, P., Siegfried, C., and Bonnefoy, J. Y. (1994). CD23 interacts with a new functional extracytoplasmic domain involving N-linked oligosaccharides on CD21. J Immunol *152*, 5806-13.

Ayscough, K. (1998). In vivo functions of actin-binding protiens. Curr. Opin. Cell Biol. *10*, 102-111.

Azuma, T., Witke, W., Stossel, T. P., Hartwig, J. H., and Kwiatkowski, D. J. (1998). Gelsolin is a downstream effector of rac for fibroblast motility. Embo J *17*, 1362-70.

Beckerle, M. C., Burridge, K., DeMartino, G. N., and Croall, D. E. (1987). Colocalization of calcium-dependent protease II and one of its substrates at sites of cell adhesion. Cell *51*, 569-77.

Beckerle, M. C., Miller, D. E., Bertagnolli, M. E., and Locke, S. J. (1989). Activation-dependent redistribution of the adhesion plaque protein, talin, in intact human platelets. J. Cell Biol. *109*, 3333-3346.

Beckerle, M. C. (1990). The adhesion plaque protein, talin, is phosphorylated in vivo in chick embryo fibroblasts exposed to a tumor-promoting phorbol ester. Cell Reg. *1*, 227-236.

Belkin, A. M., and Koteliansky, V. E. (1987). Interaction of iodinated vinculin, metavinculin and alpha-actinin with cytoskeletal proteins. FEBS Lett *220*, 291-4.

Bennett, V., and Stenbuck, P. J. (1979). The membrane attachment protein for spectrin is associated with band 3 in human erythrocyte membranes. Nature *280*, 468-73.

Bennett, V. (1992). Ankyrins. Adaptors between diverse plasma membrane proteins and the cytoplasm. J Biol Chem *267*, 8703-6.

Bennett, V., and Gilligan, D. M. (1993). The spectrin-based membrane skeleton and micron-scale organization of the plasma membrane. Annu. Rev. Cell Biol. *9*, 27-66.

Berditchevski, F., Bazzoni, G., and Hemler, M. E. (1995). Specific association of CD63 with the VLA-3 and VLA-6 integrins. J Biol Chem *270*, 17784-90.

Berditchevski, F., Zutter, M., and Hemler, M. (1996). Characterization of novel complexes on the cell surface between integrins and proteins with 4 transmembrane domains (TM4 protiens). Mol. Biol. Cell *7*, 193-207.

Berditchevski, F., Tolias, K. F., Wong, K., Carpenter, C. L., and Hemler, M. E. (1997a). A novel link between integrins, transmembrane-4 superfamily proteins (CD63 and CD81), and phosphatidylinositol 4-kinase. J Biol Chem *272*, 2595-8.

Berditchevski, F., Chang, S., Bodorova, J., and Hemler, M. E. (1997b). Generation of monoclonal antibodies to integrin-associated proteins. Evidence that alpha3beta1 complexes with EMMPRIN/basigin/OX47/M6. J Biol Chem *272*, 29174-80.

Bernard, O., Ganiatsas, S., Kannourakis, G., and Dringen, R. (1994). Kiz-1, a protein with LIM zinc finger and kinase domains, is expressed mainly in neurons. Cell Growth Differ *5*, 1159-71.

Berryman, M., Franck, Z., and Bretscher, A. (1993). Ezrin is concentrated in the apical microvilli of a wide variety of epithelial cells whereas moesin is found primarily in endothelial cells. J Cell Sci *105*, 1025-43.

Bertagnolli, M. E., Locke, S. J., Hensler, M. E., Bray, P. F., and Beckerle, M. C. (1993). Talin distribution and phosphorylation in thrombin-activated platelets. J. Cell Sci. *106*, 1189-1199.

Birgbauer, E., and Solomon, F. (1989). A marginal band-associated protein has properties of both microtubule- and microfilament-associated proteins. J Cell Biol *109*, 1609-20.

Bolton, S. J., Barry, S. T., Mosley, H., Patel, B., Jockusch, B. M., Wilkinson, J. M., and Critchley, D. R. (1997). Monoclonal antibodies recognizing the N- and C-terminal regions of talin disrupt actin stress fibers when microinjected into human fibroblasts. Cell Motil. Cytoskeleton *36*, 363-376.

Borowsky, M. L., and Hynes, R. O. (1998). Layilin, a novel talin-binding transmembrane protein homologous with C-type lectins, is localized in membrane ruffles. J. Cell Biol. *143*, 429-442.

Bradley, J. E., Bishop, G. A., St. John, T., and Frelinger, J. A. (1988). A simple, rapid method for the purification of Poly A+ RNA. Biotechniques *6*, 114-116.

Bretscher, A. (1983). Purification of an 80,000-dalton protein that is a component of the isolated microvillus cytoskeleton, and its localization in nonmuscle cells. J Cell Biol *97*, 425-32.

Bretscher, A. (1989). Rapid phosphorylation and reorganization of ezrin and spectrin accompany morphological changes induced in A-431 cells by epidermal growth factor. J Cell Biol *108*, 921-30.

Brindle, N., Holt, M., Davies, J., Price, C., and Critchley, D. (1996). The focal-adhesion vasodilator-stimulated phosphoprotein (VASP) binds to the proline-rich domain in vinculin. Biochemical Journal *318*, 753-757.

Brown, M. C., Perrotta, J. A., and Turner, C. E. (1996). Identification of LIM3 as the principal determinant of paxillin focal adhesion localization and characterization of a novel motif on paxillin directing vinculin and focal adhesion kinase binding. J Cell Biol *135*, 1109-23.

Burn, P., Kupfer, A., and Singer, S. J. (1988). Dynamic membrane-cytoskeletal interactions: Specific association of integrin and talin arises in vivo after phorbol ester treatment of peripheral blood lymphocytes. Proc. Natl. Acad. Sci. USA *85*, 497-501.

Burridge, K., and Feramisco, J. R. (1981). Non-muscle alpha-actinins are calcium-sensitive actin-binding proteins. Nature *294*, 565-7.

Burridge, K. (1981). Are stress fibres contractile? Nature *294*, 691-2.

Burridge, K., and Connell, L. (1983). A new protein of adhesion plaques and ruffling membranes. J. Cell Biol. *97*, 359-367.

Burridge, K., and Mangeat, P. (1984). An interaction between vinculin and talin. Nature *308*, 744-746.

Burridge, K., Turner, C. E., and Romer, L. H. (1992). Tyrosine phosphorylation of paxillin and pp125FAK accompanies cell adhesion to extracellular matrix: a role in cytoskeletal assembly. J Cell Biol *119*, 893-903.

Burridge, K., and Chrzanowska-Wodnicka, M. (1996). Focal adhesions, contractility, and signaling. Annu Rev Cell Dev Biol *12*, 463-518.

Cary, L., Chang, J., and Guan, J. (1996). Stimulation of cell migration by overexpression of focal adhesion kinase and its association with Src and Fyn. J. Cell Sci. *109*, 1787-1794.

Cary, L. A., Han, D. C., Polte, T. R., Hanks, S. K., and Guan, J. L. (1998). Identification of p130Cas as a mediator of focal adhesion kinase-promoted cell migration. J Cell Biol *140*, 211-21.

Chadwick, C. M., Ellison, J. E., and Garrod, D. R. (1984). Dual role for Dictyostelium contact site B in phagocytosis and developmental size regulation. Nature *307*, 646-7.

Chang, D. D., Wong, C., Smith, H., and Liu, J. (1997). ICAP-1, a novel beta1 integrin cytoplasmic domain-associated protein, binds to a conserved and functionally important NPXY sequence motif of beta1 integrin. J Cell Biol *138*, 1149-57.

Chasis, J. A., and Mohandas, N. (1992). Red blood cell glycophorins. Blood *80*, 1869-79.

Chen, H. C., and Guan, J. L. (1994). Association of focal adhesion kinase with its potential substrate phosphatidylinositol 3-kinase. Proc Natl Acad Sci U S A *91*, 10148- 52.

Chen, Q., Kinch, M. S., Lin, T. H., Burridge, K., and Juliano, R. L. (1994). Integrin-mediated cell adhesion activates mitogen-activated protein kinases. J Biol Chem *269*, 26602-5.

Chen, H.-C., Appeddu, P. A., Parsons, J. T., Hildebrand, J. D., Schaller, M. D., and Guan, J.-L. (1995). Interaction of focal adhesion kinase with cytoskeletal protein talin. J. Biol. Chem. *270*, 16995-16999.

Chihara, K., Amano, M., Nakamura, N., Yano, T., Shibata, M., Tokui, T., Ichikawa, H., Ikebe, R., Ikebe, M., and Kaibuchi, K. (1997). Cytoskeletal rearrangements and transcriptional activation of c-fos serum response element by Rho-kinase. J Biol Chem *272*, 25121-7.

Chomczynski, P., and Sacchi, N. (1987). Single-step method of RNA isolation by acid guanidium thiocyanate-phenol-chloroform extraction. Anal. Biochem. *162*, 156-159.

Chong, L. D., Traynor-Kaplan, A., Bokoch, G. M., and Schwartz, M. A. (1994). The small GTP-binding protein Rho regulates a phosphatidylinositol 4-phosphate 5-kinase in mammalian cells. Cell *79*, 507-13.

Chrzanowska-Wodnicka, M., and Burridge, K. (1996). Rho-stimulated contractility drives the formation of stress fibers and focal adhesions. J. Cell Biol. *133*, 1403-1415.

Clark, E. A., and Brugge, J. S. (1993). Redistribution of activated pp60c-src to integrin-dependent cytoskeletal complexes in thrombin-stimulated platelets. Mol Cell Biol *13*, 1863-71.

Clark, E., and Hynes, R. (1996). Ras activation is necessary for integrin-mediated activation of extracellular signal-regulated kinase 2 and cytosolic phospholipase A2 but not for cytoskeletal organization. J. Biol. Chem. *271*, 14814-14818.

Clark, E., and Hynes, R. (1997). 1997 Keystone symposium on signal transduction by cell adhesion receptors. Biochim Biophys Acta *1333*, R9-R16.

Clark, E. A., King, W. G., Brugge, J. S., Symons, M., and Hynes, R. O. (1998). Integrin-mediated signals regulated by members of the rho family of GTPases. J Cell Biol *142*, 573-86.

Cohen, A. R., Wood, D. F., Marfatia, S. M., Walther, Z., Chishti, A. H., and Anderson, J. M. (1998). Human CASK/LIN-2 binds syndecan-2 and protein 4.1 and localizes to the basolateral membrane of epithelial cells. J Cell Biol *142*, 129-38.

Crawford, A. W., and Beckerle, M. C. (1991). Purification and characterization of zyxin, an 82,000-dalton component of adherens junctions. J Biol Chem *266*, 5847-53.

Crawford, A. W., Michelsen, J. W., and Beckerle, M. C. (1992). An interaction between zyxin and alpha-actinin. J Cell Biol *116*, 1381-93.

Crespo, P., Schuebel, K. E., Ostrom, A. A., Gutkind, J. S., and Bustelo, X. R. (1997). Phosphotyrosine-dependent activation of Rac-1 GDP/GTP exchange by the vav proto-oncogene product. Nature *385*, 169-72.

Damsky, C. H., Knudsen, K. A., Bradley, D., Buck, C. A., and Horwitz, A. F. (1985). Distribution of the cell substratum attachment (CSAT) antigen on myogenic and fibroblastic cells in culture. J Cell Biol *100*, 1528-39.

Debant, A., Serra-Pagès, C., Seipel, K., O'Brien, S., Tang, M., Park, S. H., and Streuli, M. (1996). The multidomain protein Trio binds the LAR transmembrane tyrosine phosphatase, contains a protein kinase domain, and has separate rac-specific and rho-specific guanine nucleotide exchange factor domains. Proc Natl Acad Sci U S A *93*, 5466- 71.

DeClue, J. E., and Martin, G. S. (1987). Phosphorylation of talin at tyrosine in Rous sarcoma virus-transformed cells. Mol. Cell. Biol. *7*, 371-378.

del Pozo, M. A., Sánchez-Mateos, P., Nieto, M., and Sánchez-Madrid, F. (1995). Chemokines regulate cellular polarization and adhesion receptor redistribution during lymphocyte interaction with endothelium and extracellular matrix. Involvement of cAMP signaling pathway. J Cell Biol *131*, 495-508.

den Bakker, M. A., Riegman, P. H., Hekman, R. A., Boersma, W., Janssen, P. J., van der Kwast, T. H., and Zwarthoff, E. C. (1995). The product of the NF2 tumour suppressor gene localizes near the plasma membrane and is highly expressed in muscle cells. Oncogene *10*, 757-63.

DePasquale, J., and Izzard, C. (1991). Accumulation of talin in nodes at the edge of the lamellipodium and separate incorporation into adhesion plaques at focal contacts in fibroblasts. J. Cell Biol. *113*, 1351-1359.

Dharmawardhane, S., Sanders, L. C., Martin, S. S., Daniels, R. H., and Bokoch, G. M. (1997). Localization of p21-activated kinase 1 (PAK1) to pinocytic vesicles and cortical actin structures in stimulated cells. J Cell Biol *138*, 1265-78.

Dike, L. E., and Farmer, S. R. (1988). Cell adhesion induces expression of growth-associated genes in suspension-arrested fibroblasts. Proc Natl Acad Sci U S A *85*, 6792-6.

DiPersio, C. M., Hodivala-Dilke, K. M., Jaenisch, R., Kreidberg, J. A., and Hynes, R. O. (1997). alpha3beta1 Integrin is required for normal development of the epidermal basement membrane. J Cell Biol *137*, 729-42.

Dold, F. G., Sanger, J. M., and Sanger, J. W. (1994). Intact alpha-actinin molecules are needed for both the assembly of actin into the tails and the locomotion of Listeria monocytogenes inside infected cells. Cell Motil Cytoskeleton (CRD) *28*, 97-107.

Drickamer, K. (1992). Engineering galactose-binding activity into a C-type mannose-binding protein. Nature *360*, 183-186.

Drickamer, K. (1993). Ca2+-dependent carbohydrate-recognition domains in animal proteins. Curr. Opin. Struct. Biol. *3*, 393-400.

Drickamer, K., and Taylor, M. E. (1993). Biology of animal lectins. Annu. Rev. Cell Biol. *9*, 237-264.

Edwards, K. A., Montague, R. A., Shepard, S., Edgar, B. A., Erikson, R. L., and Kiehart, D. P. (1994). Identification of Drosophila cytoskeletal proteins by induction of abnormal cell shape in fission yeast. Proc Natl Acad Sci U S A *91*, 4589- 93.

Espenshade, P., Gimeno, R., Holzmacher, E., Teung, P., and Kaiser, C. (1995). Yeast SEC16 gene encodes a multidomain vesicle coat protein that interacts with Sec23p. J. Cell Biol. *131*, 311-324.

Finlay, B. B., Ruschkowski, S., and Dedhar, S. (1991). Cytoskeletal rearrangements accompanying *Salmonella* entry into epithelial cells. J. Cell Sci. *99*, 283-296.

Finlay, B. B., Rosenshine, I., Donnenberg, M. S., and Kaper, J. B. (1992). Cytoskeletal composition of attaching and effacing lesions associated with enteropathogenic *Escherichia coli* adherence to HeLa cells. Infect. Immun. *60*, 2541-2543.

Fischer, K.-D., Kong, Y.-Y., Nishina, H., Tedford, K., Marengère, L. E. M., Kozieradzki, I., Sasaki, T., Starr, M., Chan, G., Gardener, S., Nghiem, M. P., Bouchard, D., Barbacid, M., Bernstein, A., and Penninger, J. M. (1998). Vav is a regulator of cytoskeletal reorganization mediated by the T-cell receptor. Curr. Biol. *8*, 554-562.

Fox, J. E. B., Goll, D. E., Reynolds, C. C., and Phillips, D. R. (1985). Identification of two proteins (actin-binding protein and P235) that are hydrolyzed by endogenous Ca2+-dependenct protease during platelet aggregation. J. Biol. Chem. *260*, 1060-1066.

Fox, J. E. (1993). The platelet cytoskeleton. Thromb Haemost *70*, 884-93.

Franck, Z., Gary, R., and Bretscher, A. (1993). Moesin, like ezrin, colocalizes with actin in the cortical cytoskeleton in cultured cells, but its expression is more variable. J Cell Sci *105*, 219-31.

Frosch, P. M., Frosch, M., Pfister, T., Schaad, V., and Bitter-Suermann, D. (1991). Cloning and characterisation of an immunodominant major surface antigen of Echinococcus multilocularis. Mol Biochem Parasitol *48*, 121-30.

Fuchs, E., and Cleveland, D. W. (1998). A structural scaffolding of intermediate filaments in health and disease. Science *279*, 514-9.

Fukata, Y., Kimura, K., Oshiro, N., Saya, H., Matsuura, Y., and Kaibuchi, K. (1998). Association of the myosin-binding subunit of myosin phosphatase and moesin: dual regulation of moesin phosphorylation by Rho-associated kinase and myosin phosphatase. J Cell Biol *141*, 409-18.

Funayama, N., Nagafuchi, A., Sato, N., Tsukita, S., and Tsukita, S. (1991). Radixin is a novel member of the band 4.1 family. J Cell Biol *115*, 1039-48.

Gary, R., and Bretscher, A. (1995). Ezrin self-association involves binding of an N-terminal domain to a normally masked C-terminal domain that includes the F-actin binding site. Mol Biol Cell *6*, 1061-75.

Geiger, B. (1979). A 130K protein from chicken gizzard: its localization at the termini of microfilament bundles in cultured chicken cells. Cell *18*, 193-205.

Gertler, F. B., Niebuhr, K., Reinhard, M., Wehland, J., and Soriano, P. (1996). Mena, a relative of VASP and Drosophila Enabled, is implicated in the control of microfilament dynamics. Cell *87*, 227-39.

Ghrayeb, J., Kimura, H., Takahara, M., Hsiung, H., Masui, Y., and Inouye, M. (1984). Secretion cloning vectors in Escherichia coli. Embo J *3*, 2437-42.

Giancotti, F., and Ruoslahti, E. (1990). Elevated levels of the $\alpha 5\beta 1$ fibronectin receptor suppresses the transformed phenotype of Chinese hamster ovary cells. Cell *60*, 849-59.

Gilmore, A. P., Jackson, P., Waites, G. T., and Critchley, D. R. (1992). Further characterization of the talin-binding site in the cytoskeletal protein vinculin. J. Cell Sci. *103*, 719-731.

Gilmore, A. P., Wood, C., Ohanian, V., Jackson, P., Patel, B., Rees, D. J. G., Hynes, R. O., and Critchley, D. R. (1993). The cytoskeletal protein talin contains at least two distinct vinculin binding domains. J. Cell Biol. *122*, 337-347.

Gilmore, A. P., and Burridge, K. (1996). Regulation of vinculin binding to talin and actin by phosphatidyl-inositol-4-5-bisphosphate. Nature *381*, 531-5.

Gilmore, A. P., and Romer, L. H. (1996). Inhibition of focal adhesion kinase (FAK) signaling in focal adhesions decreases cell motility and proliferation. Mol. Biol. Cell *7*, 1209-1224.

Gonzalez-Agosti, C., Xu, L., Pinney, D., Beauchamp, R., Hobbs, W., Gusella, J., and Ramesh, V. (1996). The merlin tumor suppressor localizes preferentially in membrane ruffles. Oncogene *13*, 1239-1247.

Goslin, K., Birgbauer, E., Banker, G., and Solomon, F. (1989). The role of cytoskeleton in organizing growth cones: a microfilament-associated growth cone component depends upon microtubules for its localization. J Cell Biol *109*, 1621-31.

Gould, K., Bretscher, A., Esch, F., and Hunter, T. (1989). cDNA cloning and sequencing of the protein-tyrosine kinase substrate, ezrin, reveals homology to band 4.1. EMBO J. *8*, 4133-42.

Graessmann, A., Graessman, M., and Mueller, C. (1980). Microinjection of early SV40 DNA fragments and T antigen. Meth. Enz. *65*, 816-825.

Graves, B. J., Crowther, R. L., Chandran, C., Rumberger, J. M., Li, S., Huang, K.-S., Presky, D. H., Familletti, P. C., Wolitzky, B. A., and Burns, D. K. (1994). Insight into E-selectin/ligand interaction from the crystal structure and mutagenesis of the lec/EGF domains. Nature *367*, 532-538.

Greenberg, S., Burridge, K., and Silverstein, S. C. (1990). Colocalization of F-actin and talin during Fc receptor-mediated phagocytosis in mouse macrophages. J. Exp. Med. *172*, 1853-1856.

Grinstein, S., Woodside, M., Waddell, T. K., Downey, G. P., Orlowski, J., Pouyssegur, J., Wong, D. C., and Foskett, J. K. (1993). Focal localization of the NHE-1 isoform of the Na+/H+ antiport: assessment of effects on intracellular pH. Embo J *12*, 5209-18.

Grootjans, J. J., Zimmermann, P., Reekmans, G., Smets, A., Degeest, G., Durr, J., and David, G. (1997). Syntenin, a PDZ protein that binds syndecan cytoplasmic domains. Proc Natl Acad Sci U S A *94*, 13683-8.

Gu, M. X., York, J. D., Warshawsky, I., and Majerus, P. W. (1991). Identification, cloning, and expression of a cytosolic megakaryocyte protein-tyrosine-phosphatase with sequence homology to cytoskeletal protein 4.1. Proc Natl Acad Sci U S A *88*, 5867-71.

Guadagno, T. M., and Assoian, R. K. (1991). G1/S control of anchorage-independent growth in the fibroblast cell cycle. J Cell Biol *115*, 1419-25.

Guadagno, T. M., Ohtsubo, M., Roberts, J. M., and Assoian, R. K. (1993). A link between cyclin A expression and adhesion-dependent cell cycle progression. Science *262*, 1572-5.

Guan, J. L., Trevithick, J. E., and Hynes, R. O. (1991). Fibronectin/integrin interaction induces tyrosine phosphorylation of a 120-kDa protein. Cell Regul *2*, 951-64.

Guan, J. L., and Shalloway, D. (1992). Regulation of focal adhesion-associated protein tyrosine kinase by both cellular adhesion and oncogenic transformation. Nature *358*, 690-2.

Guo, Q., Vasile, E., and Krieger, M. (1994). Disruptions in golgi structure and membrane traffic in a conditional lethal mammalian cell mutant are corrected by ε-COP. J. Cell Biol. *125*, 1213-1224.

Guthrie, C., and Fink, G. R. (1991). Guide to yeast genetics and molecular biology, Volume 194 (San Diego, CA: Academic Press, Inc.).

Gyuris, J., Golemis, E. A., Chertkov, H., and Brent, R. (1993). Cdi1, a human G1 and S phase protein phosphatase that associates with Cdk2. Cell *75*, 791-803.

Habets, G. G., Scholtes, E. H. M., Zuydgeest, D., van der Kammem, R. A., Stam, J. C., Berns, A., and Collard, J. G. (1994). Identification of an invasion-inducing gene, tiam1, that encodes a protein with homology to GDP-GTP exchangers for rho-like proteins. Cell *77*, 537-549.

Hanks, S. K., Calalb, M. B., Harper, M. C., and Patel, S. K. (1992). Focal adhesion protein-tyrosine kinase phosphorylated in response to cell attachment to fibronectin. Proc Natl Acad Sci U S A *89*, 8487- 91.

Hannigan, G. E., Leung-Hagesteijn, C., Fitz-Gibbon, L., Coppolino, M. G., Radeva, G., Filmus, J., Bell, J. C., and Dedhar, S. (1996). Regulation of cell adhesion and anchorage-dependent growth by a new beta 1-integrin-linked protein kinase. Nature *379*, 91-6.

Hart, M. J., Eva, A., Evans, T., Aaronson, S. A., and Cerione, R. A. (1991). Catalysis of guanine nucleotide exchange on the CDC42Hs protein by the dbl oncogene product. Nature *354*, 311-4.

Hartwig, J. H., and Stossel, T. P. (1976). Interactions of actin, myosin, and an actin-binding protein of rabbit pulmonary macrophages. III. Effects of cytochalasin B. J Cell Biol *71*, 295-303.

Hartwig, J. H., Bokoch, G. M., Carpenter, C. L., Janmey, P. A., Taylor, L. A., Toker, A., and Stossel, T. P. (1995). Thrombin receptor ligation and activated Rac uncap actin filament barbed ends through phosphoinositide synthesis in permeabilized human platelets. Cell *82*, 643-53.

Hasegawa, T. (1993). Production of a unique antibody specific for membrane ruffles and its use to characterize the behavior of two distinct types of ruffles. J Cell Biol *120*, 1439-48.

Helander, T. S., Carpen, O., Turunen, O., Kovanen, P. E., Vaheri, A., and Timonen, T. (1996). ICAM-2 redistributed by ezrin as a target for killer cells. Nature *382*, 265-268.

Hemming, N. J., Anstee, D. J., Staricoff, M. A., Tanner, M. J., and Mohandas, N. (1995). Identification of the membrane attachment sites for protein 4.1 in the human erythrocyte. J Biol Chem *270*, 5360-6.

Hemmings, L., Rees, D. J. G., Ohanian, V., Bolton, J. J., Gilmore, A. P., Patel, B., Priddle, H., Trevithick, J. E., Hynes, R. O., and Critchley, D. R. (1996). Talin contains three actin-binding sites each of which is adjacent to a vinculin-binding site. J. Cell Sci. *109*, 2715-2726.

Henry, M. D., Gonzalez Agosti, C., and Solomon, F. (1995). Molecular dissection of radixin: distinct and interdependent functions of the amino- and carboxy-terminal domains. J Cell Biol *129*, 1007-22.

Heraud, J.-M., Racaud-Sultan, C., Gironcel, D., Albiges-Rizo, C., Giacomini, T., Roques, S., Martel, V., Breton-Douillon, M., Perrett, B., and Chap, H. (1998). Lipid products of phosphoinositide 3-kinase and phosphatidylinositol 4', 5' -biphosphate are both required for ADP-dependent platelet spreading. J. Biol. Chem. *273*, 17817-17823.

Hildebrand, J. D., Schaller, M. D., and Parsons, J. T. (1993). Identification of sequences required for the efficient localization of the focal adhesion kinase, pp125FAK, to cellular focal adhesions. J Cell Biol *123*, 993-1005.

Hildebrand, J. D., Schaller, M. D., and Parsons, J. T. (1995). Paxillin, a tyrosine phosphorylated focal adhesion- associated protein binds to the carboxyl terminal domain of focal adhesion kinase. Mol Biol Cell *6*, 637-47.

Hirao, M., Sato, N., Kondo, T., Yonemura, S., Monden, M., Sasaki, T., Takai, Y., Tsukita, S., and Tsukita, S. (1996). Regulation mechanism of ERM (ezrin/radixin/moesin) protein/plasma membrane association: possible involvement of phosphatidylinositol turnover and Rho-dependent signaling pathway. J Cell Biol *135*, 37-51.

Hoffman, C. S., and Winston, F. (1987). A ten-minute DNA preparation from yeast efficiently releases autonomous plasmids for transformation of *Escherichia coli*. Gene *57*, 267-272.

Hooshmand-Rad, R., Claesson-Welsh, L., Wennstrom, S., Yokote, K., Siegbahn, A., and Heldin, C. H. (1997). Involvement of phosphatidylinositide 3'-kinase and Rac in platelet-derived growth factor-induced actin reorganization and chemotaxis. Exp Cell Res *234*, 434-41.

Horwitz, A., Duggan, K., Buck, C., Beckerle, M. C., and Burridge, K. (1986). Interaction of plasma membrane fibronectin receptor with talin -- a transmembrane linkage. Nature *320*, 531-533.

Hotchin, N. A., and Hall, A. (1995). The assembly of integrin adhesion complexes requires both extracellular matrix and intracellular rho/rac GTPases. J Cell Biol *131*, 1857-65.

Hsueh, Y. P., Yang, F. C., Kharazia, V., Naisbitt, S., Cohen, A. R., Weinberg, R. J., and Sheng, M. (1998). Direct interaction of CASK/LIN-2 and syndecan heparan sulfate proteoglycan and their overlapping distribution in neuronal synapses. J Cell Biol *142*, 139-51.

Huttenlocher, A., Palecek, S. P., Lu, Q., Zhang, W., Mellgren, R. L., Lauffenburger, D. A., Ginsberg, M. H., and Horwitz, A. F. (1997). Regulation of cell migration by the calcium-dependent protease calpain. J Biol Chem *272*, 32719-22.

Hynes, R. O. (1987). Integrins: a family of cell surface receptors. Cell *48*, 549-54.

Hynes, R. O. (1992). Integrins: versatility, modulation, and signaling in cell adhesion. Cell *69*, 11-25.

Hynes, R. O., and Lander, A. D. (1992). Contact and adhesive specificities in the associations, migrations, and targeting of cells and axons. Cell *68*, 303-22.

Ilic, D., Furuta, Y., Kanazawa, S., Takeda, N., Sobue, K., Nakatsuji, N., Nomura, S., Fujimoto, J., Okada, M., Yamamoto, T., and Alzawa, S. (1995). Reduced cell motility and enhanced focal adhesion contact formation in cells from FAK-deficient mice. Nature *377*, 539-544.

Imai, Y., Singer, M. S., Fennie, C., Lasky, L. A., and Rosen, S. D. (1991). Identification of a carbohydrate-based endothelial ligand for a lymphocyte homing receptor. J Cell Biol *113*, 1213-21.

Ingber, D. E., Prusty, D., Frangioni, J. V., Cragoe, E. J., Jr., Lechene, C., and Schwartz, M. A. (1990). Control of intracellular pH and growth by fibronectin in capillary endothelial cells. J Cell Biol *110*, 1803-11.

Isberg, R. R., and Leong, J. M. (1990). Multiple β1 chain integrins are receptors for invasin, a protein that promotes bacterial penetration into mammalian cells. Cell *60*, 861-871.

Jaken, S., Leach, K., and Klauck, T. (1989). Association of type 3 protein kinase C with focal contacts in rat embryo fibroblasts. J Cell Biol *109*, 697-704.

Janmey, P. A., Iida, K., Yin, H. L., and Stossel, T. P. (1987). Polyphosphoinositide micelles and polyphosphoinositide-containing vesicles dissociate endogenous gelsolin-actin complexes and promote actin assembly from the fast-growing end of actin filaments blocked by gelsolin. J Biol Chem *262*, 12228-36.

Janmey, P. A., and Stossel, T. P. (1987). Modulation of gelsolin function by phosphatidylinositol 4,5- bisphosphate. Nature *325*, 362-4.

Janmey, P. A., and Stossel, T. P. (1989). Gelsolin-polyphosphoinositide interaction. Full expression of gelsolin-inhibiting function by polyphosphoinositides in vesicular form and inactivation by dilution, aggregation, or masking of the inositol head group. J Biol Chem *264*, 4825-31.

Johnson, R. P., and Craig, S. W. (1994). An intramolecular association between the head and tail domains of vinculin modulates talin binding. J Biol Chem *269*, 12611-9.

Johnson, R. P., and Craig, S. W. (1995a). F-actin binding site masked by the intramolecular association of vinculin head and tail domains. Nature *373*, 261-4.

Johnson, R. P., and Craig, S. W. (1995b). The carboxy-terminal tail domain of vinculin contains a cryptic binding site for acidic phospholipids. Biochem Biophys Res Commun *210*, 159- 64.

Jones, P., Jackson, P., Price, G. J., Patel, B., Ohanion, V., Lear, A. L., and Critchley, D. R. (1989). Identification of a talin binding site in the cytoskeletal protein vinculin. J Cell Biol *109*, 2917-27.

Joneson, T., McDonough, M., Bar-Sagi, D., and Van Aelst, L. (1996). RAC regulation of actin polymerization and proliferation by a pathway distinct from Jun kinase. Science *274*, 1374-6.

Jöns, T., and Drenckhahn, D. (1992). Identification of the binding interface involved in linkage of cytoskeletal protein 4.1 to the erythrocyte anion exchanger. EMBO J. *11*, 2863-2867.

Kalomiris, E. L., and Bourguignon, L. Y. (1988). Mouse T lymphoma cells contain a transmembrane glycoprotein (GP85) that binds ankyrin. J Cell Biol *106*, 319-27.

Kaplan, K. B., Bibbins, K. B., Swedlow, J. R., Arnaud, M., Morgan, D. O., and Varmus, H. E. (1994). Association of the amino-terminal half of c-src with focal adhesions alters their properties and is regulated by phosphorylation of tyrosine 527. EMBO J. *13*, 4745-4756.

Kaplan, K. B., Swedlow, J. R., Morgan, D. O., and Varmus, H. E. (1995). c-Src enhances the spreading of src-/- fibroblasts on fibronectin by a kinase-independent mechanism. Genes Dev *9*, 1505-17.

Kaufmann, S., Piekenbrock, T., Goldmann, W. H., Barmann, M., and Isenberg, G. (1991). Talin binds to actin and promotes filament nucleation. FEBS Lett *284*, 187-91.

Keely, P. J., Westwick, J. K., Whitehead, I. P., Der, C. J., and Parise, L. V. (1997). Cdc42 and Rac 1 induce integrin-mediated cell motility and invasiveness through PI(3)K. Nature *390*, 632-636.

Kimura, K., Ito, M., Amano, M., Chihara, K., Fukata, Y., Nakafuku, M., Yamamori, B., Feng, J., Nakano, T., Okawa, K., Iwamatsu, A., and Kaibuchi, K. (1996). Regulation of myosin phosphatase by rho and rho-associated kinase (rho-kinase). Science *273*, 245-248.

Klemke, R. L., Leng, J., Molander, R., Brooks, P. C., Vuori, K., and Cheresh, D. A. (1998). CAS/Crk coupling serves as a "molecular switch" for induction of cell migration. J Cell Biol *140*, 961-72.

Kohda, D., Morton, C. J., Parkar, A. A., Hatanaka, H., Inagaki, F. M., Campbell, I. D., and Day, A. J. (1996). Solution structure of the link module: a hyaluronan-binding domain involved in extracellular matrix stability and cell migration. Cell *86*, 767-775.

Kolanus, W., Nagel, W., Schiller, B., Zeitmann, L., Godar, S., Stockinger, H., and Seed, B. (1996). αLβ2 integrin/LFA-1 binding to ICAM-1 induced by cytohesin-1, a cytoplasmic regulatory molecule. Cell *86*, 233-242.

Kornberg, L. J., Earp, H. S., Turner, C. E., Prockop, C., and Juliano, R. L. (1991). Signal transduction by integrins: increased protein tyrosine phosphorylation caused by clustering of beta 1 integrins. Proc Natl Acad Sci U S A *88*, 8392-6.

Kornberg, L., Earp, H. S., Parsons, J. T., Schaller, M., and Juliano, R. L. (1992). Cell adhesion or integrin clustering increases phosphorylation of a focal adhesion-associated tyrosine kinase. J Biol Chem *267*, 23439-42.

Kotani, H., Takaishi, K., Sasaki, T., and Takai, Y. (1997). Rho regulates association of both the ERM family and vinculin with the plasma membrane in MDCK cells. Oncogene *14*, 1705-13.

Kreitmeier, M., Gerisch, G., Heizer, C., and Muller-Taubenberger, A. (1995). A talin homologue of *Dictyostelium* rapidly assembles at the leading edge of cells in response to chemoattractant. J. Cell Biol. *129*, 179-188.

Kupfer, A., Singer, S. J., and Dennert, G. (1986). On the mechanism of unidirectional killing in mixtures of two cytotoxic T lymphocytes. Unidirectional polarization of cytoplasmic organelles and the membrane-associated cytoskeleton in the effector cell. J Exp Med *163*, 489-98.

LaFlamme, S. E., Akiyama, S. K., and Yamada, K. M. (1992). Regulation of fibronectin receptor distribution. J Cell Biol *117*, 437-47.

LaFlamme, S. E., Thomas, L. A., Yamada, S. S., and Yamada, K. M. (1994). Single subunit chimeric integrins as mimics and inhibitors of endogenous integrin functions in receptor localization, cell spreading and migration, and matrix assembly. J Cell Biol *126*, 1287-98.

Lamarche, N., Tapon, N., Stowers, L., Burbelo, P. D., Aspenström, P., Bridges, T., Chan, J., and Hall, A. (1996). Rac and Cdc42 induce actin polymeriazation and G1 cell cycle progression independently of $p65^{PAK}$ and the JNK/SAPK MAP kinase cascade. Cell *87*, 519-529.

Lamb, R. F., Ozanne, B. W., Roy, C., McGarry, L., Stipp, C., Mangeat, P., and Jay, D. G. (1997). Essential functions of ezrin in maintenance of cell shape and lamellipodial extension in normal and transformed fibroblasts. Curr Biol *7*, 682-8.

Lankes, W. T., and Furthmayr, H. (1991). Moesin: a member of the protein 4.1-talin-ezrin family of proteins. Proc Natl Acad Sci USA *88*, 8297- 301.

Lasky, L. A., Singer, M. S., Dowbenko, D., Imai, Y., Henzel, W. J., Grimley, C., Fennie, C., Gillett, N., Watson, S. R., and Rosen, S. D. (1992). An endothelial ligand for L-selectin is a novel mucin-like molecule. Cell *69*, 927-38.

Lauffenburger, D., and Horwitz, A. (1996). Cell migration: a physically integrated molecular process. Cell *84*, 359-369.

Legg, J. W., and Isacke, C. M. (1998). Identification and functional analysis of the ezrin-binding site in the hyaluronan receptor, CD44. Curr. Biol. *8*, 705-708.

Lemmon, M. A., Ferguson, K. M., and Schlessinger, J. (1996). PH domains: diverse sequences with a common fold recruit signaling molecules to the cell surface. Cell *85*, 621-4.

Letourneur, F., and Klausner, R. D. (1992). A novel di-leucine motif and a tyrosine-based motif independently mediate lysosomal targeting and endocytosis of CD3 chains. Cell *69*, 1143-1157.

Leung, T., Chen, X.-Q., Manser, E., and Lim, L. (1996). The p160 RhoA-binding kinase ROKα is a member of a kinase family and is involved in the reorganization of the cytoskeleton. Mol. Cell. Biol. *16*, 5313-5327.

Levinovitz, A., Muhlhoff, J., Isenmann, S., and Vestweber, D. (1993). Identification of a glycoprotein ligand for E-selectin on mouse myeloid cells. J Cell Biol *121*, 449-59.

Lewis, J. M., and Schwartz, M. A. (1995). Mapping in vivo associations of cytoplasmic proteins with integrin beta 1 cytoplasmic domain mutants. Mol Biol Cell *6*, 151-60.

Liang, R., Yan, L., Loebach, J., Ge, M., Uozumi, Y., Sekanina, K., Horan, N., Gildersleeve, J., Thompson, C., Smith, A., Biswas, K., Still, W. C., and Kahne, D. (1996). Parallel synthesis and screening of a solid phase carbohydrate library. Science *274*, 1520-2.

Liliental, J., and Chang, D. D. (1998). Rack1, a receptor for activated protein kinase C, interacts with integrin beta subunit. J Biol Chem *273*, 2379-83.

Litchfield, D. W., and Ball, E. H. (1986). Phosphorylation of the cytoskeletal protein talin by protein kinase C. Biochem Biophys Res Commun *134*, 1276- 83.

Love, D. C., Kane, M. M., and Mosser, D. M. (1998). *Leishmania amazonensis:* The phagocytosis of amastigotes by macrophages. Experimental Parasitology *88*, 161-171.

Lue, R. A., Marfatia, S. M., Branton, D., and Chishti, A. H. (1994). Cloning and characterization of hdlg: the human homolog of the *Drosophila* discs large tumor suppressor binds to protein 4.1. Proc. Natl. Acad. Sci. USA *91*, 9818-9822.

Lue, R. A., Brandin, E., Chan, E. P., and Branton, D. (1996). Two independent domains of hDlg are sufficient for subcellular targeting: the PDZ1-2 conformational unit and an alternatively spliced domain. J Cell Biol *135*, 1125-37.

Lukashev, M. E., Sheppard, D., and Pytela, R. (1994). Disruption of integrin function and induction of tyrosine phosphorylation by the autonomously expressed beta 1 integrin cytoplasmic domain. J Biol Chem *269*, 18311-4.

Luna, E. J., and Hitt, A. L. (1992). Cytoskeleton-plasma membrane interactions. Science *258*, 955-964.

Magendantz, M., Henry, M. D., Lander, A., and Solomon, F. (1995). Interdomain interactions of radixin in vitro. J Biol Chem *270*, 25324-7.

Maley, F., Trimble, R. B., Tarentino, A. L., and Plummner, T. H. (1989). Characterization of glycoproteins and their associated oligosaccharides through the use of endoglycosidases. Anal. Biochem. *180*, 195-204.

Marcus-Sekura, C. J., Woerner, A. M., Shinozuka, K., Zon, G., and Quinnan, G. V., Jr. (1987). Comparative inhibition of chloramphenicol acetyltransferase gene expression by antisense oligonucleotide analogues having alkyl phosphotriester, methylphosphonate and phosphorothioate linkages. Nucleic Acids Res *15*, 5749-63.

Marfatia, S. M., Lue, R. A., Branton, D., and Chishti, A. H. (1994). In vitro binding studies suggest a membrane-associated complex between erythroid p55, protein 4.1, and glycophorin C. J Biol Chem *269*, 8631-4.

Marfatia, S. M., Lue, R. A., Branton, D., and Chishti, A. H. (1995). Identification of the protein 4.1 binding interface on glycophorin C and p55, a homologue of the Drosophila discs-large tumor suppressor protein. J Biol Chem *270*, 715-9.

Marfatia, S. M., Cabral, J. H. M., Lin, L., Hough, C., Bryant, P. J., Stolz, L., and Chishti, A. H. (1996). Modular organization of the PDZ domains in the human discs-large protein suggests a mechanism for coupling PDZ domain-binding proteins to ATP and the membrane cytoskeleton. J. Cell Biol. *135*, 753-766.

Marfatia, S. M., Morais-Cabral, J. H., Kim, A. C., Byron, O., and Chishti, A. H. (1997). The PDZ domain of human erythrocyte p55 mediates its binding to the cytoplasmic carboxyl terminus of glycophorin C. Analysis of the binding interface by in vitro mutagenesis. J Biol Chem *272*, 24191-7.

Marks, M. S., Ohno, H., Kirchhausen, T., and Bonifacino, J. S. (1997). Protein sorting by tyrosine-based signals: adapting to the Ys and wherefores. Trends Cell Biol. *7*, 124-128.

Martin, M., Andreoli, C., Sahuquet, A., Montcourrier, P., Algrain, M., and Mangeat, P. (1995). Ezrin NH2-terminal domain inhibits the cell extension activity of the COOH-terminal domain. J Cell Biol *128*, 1081-93.

Matsui, T., Amano, M., Yamamoto, T., Chihara, K., Nakafuku, M., Ito, M., Nakano, T., Okawa, K., Iwamatsu, A., and Kaibuchi, K. (1996). Rho-associated kinase, a novel serine/threonine kinase, as a putative target for the small GTP binding protein rho. EMBO J. *15*, 2208-2216.

Matsui, T., Maeda, M., Doi, Y., Yonemura, S., Amano, M., Kaibuchi, K., Tsukita, S., and Tsukita, S. (1998). Rho-kinase phosphorylates COOH-terminal threonines in ezrin/radixin/moesin (ERM) proteins and regulates their head-to-tail association. J. Cell Biol. *140*, 647-657.

McClain, D. A., Maness, P. F., and Edelman, G. M. (1978). Assay for early cytoplasmic effects of the src gene product of Rous sarcoma virus. Proc Natl Acad Sci U S A *75*, 2750-4.

McLachlan, A. D., Stewart, M., Hynes, R. O., and Rees, D. J. G. (1994). Analysis of repeated motifs in the talin rod. J. Mol. Biol. *235*, 1278-1290.

McNamee, H. P., Ingber, D. E., and Schwartz, M. A. (1993). Adhesion to fibronectin stimulates inositol lipid synthesis and enhances PDGF-induced inositol lipid breakdown. J Cell Biol *121*, 673-8.

Michiels, F., Habets, G. G. M., Stam, J. C., van der Kammem, R. A., and Collard, J. G. (1995). A role for rac in tiam1-induced membrane ruffling and invasion. Nature *375*, 338-340.

Michiels, F., Stam, J. C., Hordijk, P. L., van der Kammem, R. A., Ruuls-Van Stalle, L., Feltkamp, C. A., and Collard, J. G. (1997). Regulated membrane localization of Tiam1, mediated by the NH2-terminal pleckstrin homology domain, is required for rac-dependent membrane ruffling and c-jun NH2-terminal kinase activation. J. Cell Biol. *137*, 387-398.

Milam, L. M. (1985). Electron microscopy of rotary shadowed vinculin and vinculin complexes. J Mol Biol *184*, 543-5.

Miyamoto, S., Akiyama, S. K., and Yamada, K. M. (1995a). Synergistic roles for receptor occupancy and aggregation in integrin transmembrane function. Science *267*, 883-5.

Miyamoto, S., Teramoto, H., Coso, O. A., Gutkind, J. S., Burbelo, P. D., Akiyama, S. K., and Yamada, K. M. (1995b). Integrin function: molecular hierarchies of cytoskeletal and signaling molecules. J Cell Biol *131*, 791-805.

Mizuno, K., Okano, I., Ohashi, K., Nunoue, K., Kuma, K., Miyata, T., and Nakamura, T. (1994). Identification of a human cDNA encoding a novel protein kinase with two repeats of the LIM/double zinc finger motif. Oncogene *9*, 1605-12.

Molony, L., McCaslin, D., Abernethy, J., Paschal, B., and Burridge, K. (1987). Properties of talin from chicken gizzard smooth muscle. J. Biol. Chem. *262*, 7790-7795.

Moore, K. L., Stults, N. L., Diaz, S., Smith, D. F., Cummings, R. D., Varki, A., and McEver, R. P. (1992). Identification of a specific glycoprotein ligand for P-selectin (CD62) on myeloid cells. J Cell Biol *118*, 445-56.

Moulder, G. L., Huang, M. M., Waterston, R. H., and Barstead, R. J. (1996). Talin requires β-integrin, but not vinculin, for its assembly into focal adhesion-like structures in the nematode *Caenorhabditis elegans*. Mol. Biol. Cell *7*, 1181-1193.

Muguruma, M., Matsumura, S., and Fukazawa, T. (1990). Direct interactions between talin and actin. Biochem Biophys Res Commun *171*, 1217- 23.

Murthy, A., Gonzalez-Agosti, C., Cordero, E., Pinney, D., Candia, C., Solomon, F., Gusella, J., and Ramesh, V. (1998). NHE-RF, a regulatory cofactor for Na+-H+ exchange, is a common interactor for merlin and ERM (MERM) proteins. J. Biol. Chem. *273*, 1273-1276.

Nelson, W. J., and Veshnock, P. J. (1987). Ankyrin binding to (Na+ + K+)ATPase and implications for the organization of membrane domains in polarized cells. Nature *328*, 533-6.

Niewöhner, J., Weber, I., Maniak, M., Muller-Taubenberger, A., and Gerisch, G. (1997). Talin-null cells of *Dictyostelium* are strongly defective in adhesion to particle and substrate surfaces and slightly impaired in cytokinesis. J. Cell Biol. *138*, 349-61.

Niggli, V., Kaufmann, S., Goldmann, W. H., Weber, T., and Isenberg, G. (1994). Identification of functional domains in the cytoskeletal protein talin. Eur. J. Biochem. *224*, 951-957.

Nix, D. A., and Beckerle, M. C. (1997). Nuclear-cytoplasmic shuttling of the focal contact protein, zyxin: a potential mechanism for communication between sites of cell adhesion and the nucleus. J Cell Biol *138*, 1139-47.

Nobes, C. D., and Hall, A. (1995). Rho, rac, and cdc42 GTPases regulate the assembly of multimolecular focal complexes associated with actin stress fibers, lamellipodia, and filopodia. Cell *81*, 53-62.

Nuckolls, G. H., Turner, C. E., and Burridge, K. (1990). Functional studies of the domains of talin. J. Cell Biol. *110*, 1635-1644.

Nuckolls, G. H., Romer, L. H., and Burridge, K. (1992). Microinjection of antibodies against talin inhibits the spreading and migration of fibroblasts. J. Cell Sci. *102*, 753-762.

Nunomura, W., Takakuwa, Y., Tokimitsu, R., Krauss, S. W., Kawashima, M., and Mohandas, N. (1997). Regulation of CD44-protein 4.1 interaction by Ca2+ and calmodulin. Implications for modulation of CD44-ankyrin interaction. J Biol Chem *272*, 30322-8.

Ohno, H., Stewart, J., Fournier, M.-C., Bosshart, H., Rhee, I., Miyatake, S., Saito, T., Gallusser, A., Kirchhausen, T., and Bonifacino, J. S. (1995). Interaction of tyrosine-based sorting signals with clathrin-associated proteins. Science *269*, 1872-1875.

Okano, I., Hiraoka, J., Otera, H., Nunoue, K., Ohashi, K., Iwashita, S., Hirai, M., and Mizuno, K. (1995). Identification and characterization of a novel family of serine/threonine kinases containing two N-terminal LIM motifs. J Biol Chem *270*, 31321-30.

Otey, C. A., Pavalko, F. M., and Burridge, K. (1990). An interaction between alpha-actinin and the beta 1 integrin subunit in vitro. J Cell Biol *111*, 721-9.

Otto, J. J. (1983). Detection of vinculin-binding proteins with an 125I-vinculin gel overlay technique. J Cell Biol *97*, 1283-7.

Palecek, S. P., Loftus, J. C., Ginsberg, M. H., Lauffenburger, D. A., and Horwitz, A. F. (1997). Integrin-ligand binding properties govern cell migration speed through cell-substratum adhesiveness. Nature *385*, 537-40.

Palecek, S. P., Huttenlocher, A., Horwitz, A. F., and Lauffenburger, D. A. (1998). Physical and biochemical regulation of integrin release during rear detachment of migrating cells. J Cell Sci *111*, 929-40.

Parsons, J. T., Schaller, M. D., Hildebrand, J., Leu, T. H., Richardson, A., and Otey, C. (1994). Focal adhesion kinase: structure and signalling. J Cell Sci Suppl *18*, 109-13.

Pascual, J., Castresana, J., and Saraste, M. (1997). Evolution of the spectrin repeat. Bioessays *19*, 811-7.

Pasquale, E. B., Maher, P. A., and Singer, S. J. (1986). Talin is phosphorylated on tyrosine in chicken embryo fibroblasts transformed by Rous sarcoma virus. Proc Natl Acad Sci U S A *83*, 5507-11.

Pasternack, G. R., Anderson, R. A., Leto, T. L., and Marchesi, V. T. (1985). Interactions between protein 4.1 and band 3. An alternative binding site for an element of the membrane skeleton. J Biol Chem *260*, 3676-83.

Pavalko, F. M., and Burridge, K. (1991). Disruption of the actin cytoskeleton after microinjection of proteolytic fragments of alpha-actinin. J Cell Biol *114*, 481-91.

Peters, J. H., Trevithick, J. E., Johnson, P., and Hynes, R. O. (1995). Expression of the alternatively spliced EIIIB segment of fibronectin. Cell Adh. Comm. *3*, 67-89.

Pfaff, M., Liu, S., Erle, D. J., and Ginsberg, M. H. (1998). Integrin beta cytoplasmic domains differentially bind to cytoskeletal proteins. J Biol Chem *273*, 6104-9.

Pietromonaco, S. F., Simons, P. C., Altman, A., and Elias, L. (1998). Protein kinase C-theta phosphorylation of moesin in the actin-binding sequence. J Biol Chem *273*, 7594-603.

Pollack, R., Osborn, M., and Weber, K. (1975). Patterns of organization of actin and myosin in normal and transformed cultured cells. Proc Natl Acad Sci U S A *72*, 994-8.

Polte, T. R., and Hanks, S. K. (1997). Complexes of focal adhesion kinase (FAK) and Crk-associated substrate (p130(Cas)) are elevated in cytoskeleton-associated fractions following adhesion and Src transformation. Requirements for Src kinase activity and FAK proline-rich motifs. J Biol Chem *272*, 5501-9.

Potter, D. A., Tirnauer, J. S., Janssen, R., Croall, D. E., Hughes, C. N., Fiacco, K. A., Mier, J. W., Maki, M., and Herman, I. M. (1998). Calpain regulates actin remodeling during cell spreading. J Cell Biol *141*, 647-62.

Priddle, H., Hemmings, L., Monkley, S., Woods, A., Patel, B., Sutton, D., Dunn, G., Zicha, D., and Critchley, D. (1998). Disruption of the talin gene compromises focal adhesion assembly in undifferentiated but not differentiated embryonic stem cells. J. Cell Biol. *142*, 1121-1133.

Quesenberry, M. S., and Drickamer, K. (1992). Role of conserved and nonconserved residues in the Ca2+-dependent carbohydrate-recognition domain of a rat mannose-binding protein. J. Biol. Chem. *267*, 10831-10841.

Reczek, D., Berryman, M., and Bretscher, A. (1997). Identification of EBP50: a PDZ-containing phosphoprotein that associates with members of the ezrin-radixin-moesin family. J. Cell Biol. *139*, 169-179.

Reczek, D., and Bretscher, A. (1998). The carboxyl-terminal region of EBP50 binds to a site in the amino-terminal domain of ezrin that is masked in the dormant molecule. J Biol Chem *273*, 18452-8.

Rees, D. J. G., Ades, S. E., Singer, S. J., and Hynes, R. O. (1990). Sequence and domain structure of talin. Nature *347*, 685-689.

Reid, M. E., Takakuwa, Y., Conboy, J., Tchernia, G., and Mohandas, N. (1990). Glycophorin C content of human erythrocyte membrane is regulated by protein 4.1. Blood *75*, 2229-34.

Reinhard, M., Halbrugge, M., Scheer, U., Wiegand, C., Jockusch, B. M., and Walter, U. (1992). The 46/50 kDa phosphoprotein VASP purified from human platelets is a novel protein associated with actin filaments and focal contacts. Embo J *11*, 2063-70.

Reinhard, M., Giehl, K., Abel, K., Haffner, C., Jarchau, T., Hoppe, V., Jockusch, B. M., and Walter, U. (1995). The proline-rich focal adhesion and microfilament protein VASP is a ligand for profilins. Embo J *14*, 1583-9.

Ren, R., Mayer, B. J., Cicchetti, P., and Baltimore, D. (1993). Identification of a ten-amino acid proline-rich SH3 binding site. Science *259*, 1157-61.

Retta, S. F., Balzac, F., Ferraris, P., Belkin, A. M., Fassler, R., Humphries, M. J., De Leo, G., Silengo, L., and Tarone, G. (1998). beta1-integrin cytoplasmic subdomains involved in dominant negative function. Mol Biol Cell *9*, 715-31.

Richardson, A., and Parsons, T. (1996). A mechanism for regulation of the adhesion-associated protein tyrosine kinase pp125FAK. Nature *380*, 538-40.

Ridley, A. J., and Hall, A. (1992). The small GTP-binding protein rho regulates the assembly of focal adhesions and actin stress fibers in response to growth factors. Cell *70*, 389-99.

Ridley, A. J., Paterson, H. F., Johnston, C. L., Diekmann, D., and Hall, A. (1992). The small GTP-binding protein rac regulates growth factor-induced membrane ruffling. Cell *70*, 401-10.

Rodriguez Fernandez, J. L., Geiger, B., Salomon, D., Sabanay, I., Zoller, M., and Ben-Ze'ev, A. (1992). Suppression of tumorigenicity in transformed cells after transfection with vinculin cDNA. J Cell Biol *119*, 427-38.

Rodriguez-Viciana, P., Warne, P. H., Khwaja, A., Marte, B. M., Pappin, D., Das, P., Waterfield, M. D., Ridley, A., and Downward, J. (1997). Role of phosphoinositide 3-OH kinase in cell transformation and control of the actin cytoskeleton by Ras. Cell *89*, 457-67.

Rohrschneider, L., and Rosok, M. J. (1983). Transformation parameters and pp60src localization in cells infected with partial transformation mutants of Rous sarcoma virus. Mol Cell Biol *3*, 731-46.

Rouleau, G. A., Merel, P., Lutchman, M., Sanson, M., Zucman, J., Marineau, C., Hoang-Xuan, K., Demczuk, S., Desmaze, C., Plougastel, B., Pulst, S., Lenior, G., Bijlsma, E., Fashold, R., Dumanski, J., de Jong, P., Parry, D., Eldrige, R., Aurias, A., Delattre, O., and Thomas, G. (1993). Alteration in a new gene encoding a putative membrane-organizing protein causes neuro-fibromatosis type 2. Nature *363*, 515-21.

Sadler, I., Crawford, A. W., Michelsen, J. W., and Beckerle, M. C. (1992). Zyxin and cCRP: two interactive LIM domain proteins associated with the cytoskeleton. J Cell Biol *119*, 1573-87.

Sainio, M., Zhao, F., Heiska, L., Turunen, O., den Bakker, M., Zwarthoff, E., Lutchman, M., Rouleau, G. A., Jaaskelainen, J., Vaheri, A., and Carpen, O. (1997). Neurofibromatosis 2 tumor suppressor protein colocalizes with ezrin and CD44 and associates with actin-containing cytoskeleton. J Cell Sci *110*, 2249-60.

Saitoh, A., Takiguchi, K., Tanaka, Y., and Hotani, H. (1998). Opening-up of liposomal membranes by talin. Proc Natl Acad Sci U S A *95*, 1026-31.

Salgia, R., Li, J. L., Lo, S. H., Brunkhorst, B., Kansas, G. S., Sobhany, E. S., Sun, Y., Pisick, E., Hallek, M., Ernst, T., and et al. (1995). Molecular cloning of human paxillin, a focal adhesion protein phosphorylated by P210BCR/ABL. J Biol Chem *270*, 5039-47.

Sambrook, J., Fritsch, E. F., and Maniatis, T. (1989). Molecular Cloning, Second Edition (Cold Spring Harbor, NY: Cold Spring Harbor Laboratory Press).

Saras, J., and Heldin, C.-H. (1996). PDZ domains bind carboxy-terminal sequences of target proteins. Trends Biochem. Sci. *21*, 455-458.

Sato, N., Funayama, N., Nagafuchi, A., Yonemura, S., Tsukita, S., and Tsukita, S. (1992). A gene family consisting of ezrin, radixin and moesin. Its specific localization at actin filament/plasma membrane association sites. J Cell Sci *103*, 131-43.

Saunders, S., and Bernfield, M. (1988). Cell surface proteoglycan binds mouse mammary epithelial cells to fibronectin and behaves as a receptor for interstitial matrix. J. Cell Biol. *106*, 423-430.

Schaller, M. D., Borgman, C. A., Cobb, B. S., Vines, R. R., Reynolds, A. B., and Parsons, J. T. (1992). pp125FAK a structurally distinctive protein-tyrosine kinase associated with focal adhesions. Proc Natl Acad Sci U S A *89*, 5192-6.

Schaller, M. D., Borgman, C. A., and Parsons, J. T. (1993). Autonomous expression of a noncatalytic domain of the focal adhesion-associated protein tyrosine kinase pp125FAK. Mol Cell Biol *13*, 785-91.

Schaller, M. D., Otey, C. A., Hildebrand, J. D., and Parsons, J. T. (1995). Focal adhesion kinase and paxillin bind to peptides mimicking beta integrin cytoplasmic domains. J Cell Biol *130*, 1181-7.

Schiestl, and Gietz (1989). High efficiency transformation of yeast cells using single stranded nucleic acid as a carrier. Current Genetics *16*, 339-346.

Schlaepfer, D. D., Hanks, S. K., Hunter, T., and van der Geer, P. (1994). Integrin-mediated signal transduction linked to Ras pathway by GRB2 binding to focal adhesion kinase. Nature *372*, 786-91.

Scoles, D. R., Huynh, D. P., Morcos, P. A., Coulsell, E. R., Robinson, N. G., Tamanoi, F., and Pulst, S. M. (1998). Neurofibromatosis 2 tumour suppressor schwannomin interacts with betaII-spectrin. Nat Genet *18*, 354-9.

Sells, M. A., Knaus, U. G., Bagrodia, S., Ambrose, D. M., Bokoch, G. M., and Chernoff, J. (1997). Human p21-activated kinase (Pak1) regulates actin organization in mammalian cells. Curr Biol *7*, 202-10.

Serrador, J. M., Nieto, M., Alonso-Lebrero, J. L., del Pozo, M. A., Calvo, J., Furthmayr, H., Schwartz-Albiez, R., Lozano, F., González-Amaro, R., Sánchez-Mateos, P., and Sánchez-Madrid, F. (1998). CD43 interacts with moesin and ezrin and regulates its redistribution to the uropods of T lymphocytes at the cell-cell contacts. Blood *91*, 4632-4644.

Shattil, S. J., O'Toole, T., Eigenthaler, M., Thon, V., Williams, M., Babior, B. M., and Ginsberg, M. H. (1995). Beta 3-endonexin, a novel polypeptide that interacts specifically with the cytoplasmic tail of the integrin beta 3 subunit. J Cell Biol *131*, 807-16.

Shaw, R. J., Henry, M., Solomon, F., and Jacks, T. (1998). RhoA-dependent phosphorylation and relocalization of ERM proteins into apical membrane/actin protrusions in fibroblasts. Mol. Biol. Cell *9*, 403-419.

Sherman, L., Sleeman, J., Herrlich, P., and Ponta, H. (1994). Hyaluronate receptors: key players in growth, differentiation, migration and tumor progression. Curr. Opin. Cell Biol. *6*, 726-733.

Shuster, C. B., and Herman, I. M. (1995). Indirect association of ezrin with F-actin: isoform specificity and calcium sensitivity. J Cell Biol *128*, 837-48.

Smilenov, L., Briesewitz, R., and Marcantonio, E. E. (1994). Integrin beta 1 cytoplasmic domain dominant negative effects revealed by lysophosphatidic acid treatment. Mol Biol Cell *5*, 1215-23.

Smith, D. B., and Johnson, K. S. (1988). Single-step purification of polypeptides expressed in *Escherichia coli* as fusions with glutathione *S*-transferase. Gene *67*, 31-40.

Solomon, F., Connell, L., Kirkpatrick, D., Praitis, V., and Weinstein, B. (1992). Methods for studying the yeast cytoskeleton (Oxford: Oxford University Press), pp. 197-221.

Spertini, O., Cordey, A. S., Monai, N., Giuffrè, L., and Schapira, M. (1996). P-selectin glycoprotein ligand 1 is a ligand for L-selectin on neutrophils, monocytes, and CD34+ hematopoietic progenitor cells. J Cell Biol *135*, 523-31.

Sydor, A. M., Su, A. L., Wang, F.-S., Xu, A., and Jay, D. G. (1996). Talin and vinculin play distinct roles in filopodial motility in the neuronal growth cone. J. Cell Biol. *134*, 1197-1207.

Takahashi, K., Sasaki, T., Mammoto, A., Takaishi, K., Kameyama, T., Tsukita, S., and Takai, Y. (1997). Direct interaction of the Rho GDP dissociation inhibitor with ezrin/radixin/moesin initiates the activation of the Rho small G protein. J Biol Chem *272*, 23371-5.

Takahashi, K., Sasaki, T., Mammoto, A., Hotta, I., Takaishi, K., Imamura, H., Nakano, K., Kodama, A., and Takai, Y. (1998). Interaction of radixin with Rho small G protein GDP/GTP exchange protein Dbl. Oncogene *16*, 3279-3284.

Takeuchi, K., Kawashima, A., Nagafuchi, A., and Tsukita, S. (1994a). Structural diversity of band 4.1 superfamily members. J Cell Sci *107*, 1921-8.

Takeuchi, K., Sato, N., Kasahara, H., Funayama, N., Nagafuchi, A., Yonemura, S., Tsukita, S., and Tsukita, S. (1994b). Perturbation of cell adhesion and microvilli formation by antisense oligonucleotides to ERM family members. J Cell Biol *125*, 1371-84.

Tapley, P., Horwitz, A., Buck, C., Duggan, K., and Rohrschneider, L. (1989). Integrins isolated from Rous sarcoma virus-transformed chicken embryo fibroblasts. Oncogene *4*, 325-333.

Tchernia, G., Mohandas, N., and Shohet, S. B. (1981). Deficiency of skeletal membrane protein band 4.1 in homozygous hereditary elliptocytosis. Implications for erythrocyte membrane stability. J Clin Invest *68*, 454-60.

Thomas, S. M., Soriano, P., and Imamoto, A. (1995). Specific and redundant roles of Src and Fyn in organizing the cytoskeleton. Nature *376*, 267-71.

Tidball, J. G., O'Halloran, T., and Burridge, K. (1986). Talin at myotendinous junctions. J Cell Biol *103*, 1465-72.

Tidball, J. G., and Spencer, M. J. (1993). PDGF stimulation induces phosphorylation of talin and cytoskeletal reorganization in skeletal muscle. J. Cell Biol. *123*, 627-635.

Tominaga, T., and Barber, D. (1998). Na-H exchange acts downstream of rhoA to regulate integrin-induced cell adhesion and spreading. Mol. Biol. Cell *9*, 2287-2303.

Towbin, H., Staehelin, T., and Gordon, J. (1979). Electrophoretic transfer of proteins from polyacrylamide gels to nitrocellulose sheets: Procedure and some applications. Proc. Natl. Acad. Sci. USA *76*, 4350-4354.

Tranqui, L., and Block, M. R. (1995). Intracellular processing of talin occurs within focal adhesions. Experimental Cell Research *217*, 149-156.

Trofatter, J. A., MacCollin, M. M., Rutter, J. L., Murrell, J. R., Duyao, M. P., Parry, D. M., Eldridge, R., Kley, N., Menon, A. G., Pulaski, K., Haase, V., Ambrose, C., Munroe, D., Bove, C., J., H., Martuza, R., MacDonald, M., Seizinger, B., Short, M., Buckler, A., and Gusella, J. (1993). A novel moesin-, ezrin-, radixin-like gene is a candidate for the neurofibromatosis 2 tumor suppressor. Cell *72*, 791-800.

Tsukita, S., Hieda, Y., and Tsukita, S. (1989). A new 82-kD barbed end-capping protein (radixin) localized in the cell-to-cell adherens junction: purification and characterization. J Cell Biol *108*, 2369-82.

Tsukita, S., Oishi, K., Sato, N., Sagara, J., Kawai, A., and Tsukita, S. (1994). ERM family members as molecular linkers between the cell surface glycoprotein CD44 and actin-based cytoskeletons. J Cell Biol *126*, 391-401.

Turner, C. E., and Burridge, K. (1989). Detection of metavinculin in human platelets using a modified talin overlay assay. Eur. J. Cell Biol. *49*, 202-206.

Turner, C. E., Pavalko, F. M., and Burridge, K. (1989). The role of phosphorylation and limited proteolytic cleavage of talin and vinculin in the disruption of focal adhesion integrity. J. Biol. Chem. *264*, 11938-11944.

Turner, C. E., Glenney, J. R., Jr., and Burridge, K. (1990). Paxillin: a new vinculin-binding protein present in focal adhesions. J Cell Biol *111*, 1059-68.

Turner, C. E., Kramarcy, N., Sealock, R., and Burridge, K. (1991). Localization of paxillin, a focal adhesion protein, to smooth muscle dense plaques, and the myotendinous and neuromuscular junctions of skeletal muscle. Exp Cell Res *192*, 651-5.

Turner, C. E., and Miller, J. T. (1994). Primary sequence of paxillin contains putative SH2 and SH3 domain binding motifs and multiple LIM domains: identification of a vinculin and pp125Fak-binding region. J Cell Sci *107*, 1583-91.

Turunen, O., Wahlstrom, T., and Vaheri, A. (1994). Ezrin has a COOH-terminal actin-binding site that is conserved in the ezrin protein family. J. Cell Biol. *126*, 1445-1453.

Vercelli, D., Helm, B., Marsh, P., Padlan, E., Geha, R. S., and Gould, H. (1989). The B-cell binding site on human immunoglobulin E. Nature *338*, 649-51.

Vexler, Z., Symons, M., and Barber, D. (1996). Activation of Na^+-H^+ exchange is necessary for rhoA-induced stress formation. J. Biol. Chem. *271*, 22281-22284.

von Heijne, G. (1986). A new method for predicting signal sequence cleavage sites. Nuc. Acids Res. *14*, 4683-4690.

Vuori, K., Hirai, H., Aizawa, S., and Ruoslahti, E. (1996). Induction of p130CAS signaling complex formation upon integrin-mediated cell adhesion: a role for src family kinases. Mol. Cell. Biol. *16*, 2606-2613.

Wachsstock, D. H., Wilkins, J. A., and Lin, S. (1987). Specific interaction of vinculin with alpha-actinin. Biochem Biophys Res Commun *146*, 554- 60.

Wary, K. K., Mainiero, F., Isakoff, S. J., Marcantonio, E. E., and Giancotti, F. G. (1996). The adaptor protein Shc couples a class of integrins to the control of cell cycle progression. Cell *87*, 733-43.

Wary, K., Mariotti, A., Zurzolo, C., and Giancotti, F. (1998). A requirement for caveolin-1 and associated kinase fyn in integrin signaling and anchorage-dependent cell growth. Cell *94*, 625-634.

Watson, S. R., Imai, Y., Fennie, C., Geoffroy, J. S., Rosen, S. D., and Lasky, L. A. (1990). A homing receptor-IgG chimera as a probe for adhesive ligands of lymph node high endothelial venules. J Cell Biol *110*, 2221-9.

Weinman, E. J., Steplock, D., and Shenolikar, S. (1993). CAMP-mediated inhibition of the renal brush border membrane Na+-H+ exchanger requires a dissociable phosphoprotein cofactor. J. Clin. Invest. *92*, 1781-1786.

Weinman, E. J., Steplock, D., Wang, Y., and Shenolikar, S. (1995). Characterization of a protein cofactor that mediates protein kinase A regulation of the renal brush border membrane Na(+)- H+ exchanger. J Clin Invest *95*, 2143-9.

Weis, W. I., Crichlow, G. V., Murthy, H. M., Hendrickson, W. A., and Drickamer, K. (1991a). Physical characterization and crystallization of the carbohydrate-recognition domain of a mannose-binding protein from rat. J Biol Chem *266*, 20678-86.

Weis, W. I., Kahn, R., Fourme, R., Drickamer, K., and Hendrickson, W. A. (1991b). Structure of the calcium-dependent lectin domain from a rat mannose-binding protein determined by MAD phasing. Science *254*, 1608-1615.

Weis, W. I., Drickamer, K., and Hendrickson, W. A. (1992). Structure of a C-type mannose-binding protein complexed with an oligosaccharide. Nature *360*, 127-134.

Wennström, S., Hawkins, P., Cooke, F., Hara, K., Yonezawa, K., Kasuga, M., Jackson, T., Claesson-Welsh, L., and Stephens, L. (1994). Activation of phosphoinositide 3-kinase is required for PDGF-stimulated membrane ruffling. Curr. Biol. *4*, 385-393.

Westwick, J. K., Lambert, Q. T., Clark, G. J., Symons, M., Van Aelst, L., Pestell, R. G., and Der, C. J. (1997). Rac regulation of transformation, gene expression, and actin organization by multiple, PAK-independent pathways. Mol Cell Biol *17*, 1324-35.

Wilson, I. A., Niman, H. L., Houghten, R. A., Cherenson, A. R., Connolly, M. L., and Lerner, R. A. (1984). The structure of an antigenic determinant in a protein. Cell *37*, 767-778.

Winkler, J., Lunsdorf, H., and Jockusch, B. (1997). Energy-filtered electron microscopy reveals that talin is a highly flexible protein composed of a series of globular domains. Eur. J. Biochem. *243*, 430-436.

Woods, A., and Couchman, J. R. (1994). Syndecan 4 heparan sulfate proteoglycan is a selectively enriched and widespread focal adhesion component. Mol Biol Cell *5*, 183-92.

Workman, R. F., and Low, P. S. (1998). Biochemical analysis of potential sites for protein 4.1-mediated anchoring of the spectrin-actin skeleton to the erythrocyte membrane. J Biol Chem *273*, 6171-6.

Xing, Z., Chen, H. C., Nowlen, J. K., Taylor, S. J., Shalloway, D., and Guan, J. L. (1994). Direct interaction of v-Src with the focal adhesion kinase mediated by the Src SH2 domain. Mol Biol Cell *5*, 413-21.

Xu, L., Gonzalez-Agosti, C., Beauchamp, R., Pinney, D., Sterner, C., and Ramesh, V. (1998). Analysis of molecular domains of epitope-tagged merlin isoforms in Cos-7 cells and primary rat Schwann cells. Exp Cell Res *238*, 231-40.

Yang, N., Higuchi, O., Ohashi, K., Nagata, K., Wada, A., Kangawa, K., Nishida, E., and Mizuno, K. (1998). Cofilin phosphorylation by LIM-kinase 1 and its role in Rac mediated actin reorganization. Nature *393*, 809-812.

Yang, Q., and Tonks, N. K. (1991). Isolation of a cDNA clone encoding a human protein-tyrosine phosphatase with homology to the cytoskeletal-associated proteins band 4.1, ezrin, and talin. Proc Natl Acad Sci U S A *88*, 5949- 53.

Yao, X., Thibodeau, A., and Forte, J. G. (1993). Ezrin-calpain I interactions in gastric parietal cells. American Journal of Physiology, C36-C46.

Yonemura, S., Nagafuchi, A., Sato, N., and Tsukita, S. (1993). Concentration of an integral membrane protein, CD43 (leukosialin, sialophorin), in the cleavage furrow through the interaction of its cytoplasmic domain with actin-based cytoskeletons. J Cell Biol *120*, 437-49.

Yonemura, S., Hirao, M., Doi, Y., Takahashi, N., Kondo, T., Tsukita, S., and Tsukita, S. (1998). Ezrin/radixin/moesin (ERM) proteins bind to a positively charged amino acid cluster in the juxta-membrane cytoplasmic domain of CD44, CD43, and ICAM-2. J. Cell Biol. *140*, 885-895.

Young, V. B., Falkow, S., and Schoolnik, G. K. (1992). The invasin protein of *Yersinia enterocolitica:* Internalization of invasin-bearing bacteria by eukaryotic cells is associated with reorganization of the cytoskeleton. J. Cell Biol. *116*, 197-207.

Yun, C. H., Oh, S., Zizak, M., Steplock, D., Tsao, S., Tse, C. M., Weinman, E. J., and Donowitz, M. (1997). cAMP-mediated inhibition of the epithelial brush border Na+/H+ exchanger, NHE3, requires an associated regulatory protein. Proc Natl Acad Sci USA *94*, 3010-5.

Zachary, I., Sinnett-Smith, J., and Rozengurt, E. (1992). Bombesin, vasopressin, and endothelin stimulation of tyrosine phosphorylation in Swiss 3T3 cells. Identification of a novel tyrosine kinase as a major substrate. J Biol Chem *267*, 19031-4.

Zachary, I., Sinnett-Smith, J., Turner, C. E., and Rozengurt, E. (1993). Bombesin, vasopressin, and endothelin rapidly stimulate tyrosine phosphorylation of the focal adhesion-associated protein paxillin in Swiss 3T3 cells. J Biol Chem *268*, 22060-5.

Zervos, A. S., Gyuris, J., and Brent, R. (1993). Mxi1, a protein that specifically interacts with Max to bind Myc-Max recognition sites. Cell *72*, 223-232.

Zheng, C., Xing, Z., Bian, Z. C., Guo, C., Akbay, A., Warner, L., and Guan, J. L. (1998). Differential regulation of Pyk2 and focal adhesion kinase (FAK). The C-terminal domain of FAK confers response to cell adhesion. J Biol Chem *273*, 2384-9.